The impact of vaccination against rotavirus on viral faecal shedding, genetic stability and mucosal immune response in a cohort of infants in the UK

Thesis submitted in accordance with the requirements of the University of Liverpool for the degree of

Doctor of Philosophy

by

Ledicia Botas Pérez

September 2019

Department of Clinical Infection, Microbiology and Immunology
The Institute of Infection and Global Health
Faculty of Health and Life Sciences
The University of Liverpool

Division of Virology
The National Institute for Biological Standards and Control
The Medicines and Healthcare products Regulatory Agency

Abstract

Background: In July 2013, an oral live-attenuated monovalent human rotavirus G1P[8] vaccine, Rotarix®, was introduced into the United Kingdom's national immunisation programme as a two-dose regime. This vaccine is used widely on a global scale. Data on vaccine take have been reported through clinical trials assessing shedding at specific timepoints and immunogenicity by seroconversion. However, the longitudinal dynamics of shedding and mucosal antibody IgA response had not been studied. Clinical trials have also evaluated vaccine safety, however, other than reports of vaccine-related genetic variants from single-timepoints captured through clinical admissions, there is an unanswered question about genome-wide genetic stability in vaccinees.

Aims: The overarching hypothesis of this thesis was that immunisation with Rotarix® would result in an evolving quasispecies through replication in vaccinees generating high-frequency variants and modulated by the mucosal secretory IgA response. To test this, the aims were i) to assess Rotarix® shedding profiles in stool of a cohort of vaccinated infants, ii) to identify any vaccine and/or novel variants in shed virus and iii) to define the infants' RV-specific copro-IgA levels.

Methods: Stool samples from a cohort of vaccinated infants were collected longitudinally every other day throughout the vaccination period. Viral shedding was assessed through quantification of viral RNA extracted from faecal suspensions. Genetic variation was evaluated through next generation sequencing on an Illumina® platform, focusing on viral proteins with known function in viral entry or virulence: VP4, VP7, VP6 and NSP4. Total copro-IgA was measured using a commercial ELISA kit and RV-specific copro-IgA using an in-house ELISA.

Results: All infants shed vaccine virus in faeces and patterns defined four profiles ranging from early control of vaccine virus in stool to delayed control with continued virus shedding. The maximum shedding of vaccine virus was comparable to natural infection. Some single nucleotide polymorphisms identified at low frequency in the vaccine were identified at higher frequencies in vaccine recipients, suggesting that these minority variants in cell culture were selected in infants. Novel vaccine-derived variant loci were identified from stool as a result of replication in the host, suggesting a possible effect in cell tropism, host range or immune evasion.

Mutations in the outer capsid proteins VP4 and VP7 impacted on residues involved in receptor binding, trypsin cleavage, membrane fusion and neutralisation; a mutation in VP6 highlighted the importance of structural conservation of the inner capsid and all novel mutations in NPS4 suggested they may be relevant in *in vivo* infection. Rotavirus-specific copro-IgA differed between infants ranging from continual high levels through sporadic to no detection. High pre-vaccination specific copro-IgA levels in three infants were likely to originate from maternal antibody, although this did not appear to affect vaccine virus shedding. Three of eight infants were positive for RV-specific copro-IgA a year after vaccination, suggesting they were late immune responders or had had a recent subclinical rotavirus infection. Infants with positive RV-specific copro-IgA presented viral load control and those with protracted shedding presented undetectable or weak RV-specific copro-IgA levels.

Conclusions: Shedding of RV vaccine virus in vaccine recipients suggested active virus replication over several weeks and it fell within four broad profiles. Previously identified vaccine genetic variants increased in frequency and novel variants arose after replication in the gut. Infants who could not rapidly control shedding had a weak or undetectable RV-specific copro-IgA response and a higher number of high-frequency genetic variants detectable by the end of the vaccination period. By contrast, infants who controlled shedding and presented a strong RV-specific copro-IgA response had vaccine virus variants that decreased in frequency by the end of the vaccination period, suggesting Rotarix® is stable in vaccine recipients who present a robust and early RV-specific copro-IgA response.

Publications and presentations

The work preceding or within this PhD thesis is awaiting written publication or has been presented nationally and internationally as:

Publications

- **Botas-Perez, L.**, Mate, R., Bleazard, T., Preston, M.D., Mee, E.T., Fritzsche, M., Mitchell, J.L., Iturriza-Gómara, M., Rose, N.J. Longitudinal shedding and genetic stability of rotavirus RNA in infants vaccinated with Rotarix® in the UK. *In preparation*.
- Mitchell, J.L., **Botas-Perez, L.**, Wilson, H.M., Mate, R., Palor, M.C., Summersgill, E.N., Bleazard, T., Fritzsche, M., Rose, N.J. Shedding and genetic stability of PCV1 DNA in infants vaccinated with Rotarix® in the UK. *In preparation*
- Mitchell, J.L., Lui, Y., Preston, M.D., **Botas-Perez, L.**, Xuan, B., Du, J., Guo, T., Rose, N.J. (2019). Stability assessment of two monovalent rotavirus vaccines by next generation sequencing. *In preparation*.

Oral communications

- 'Faecal shedding of Rotarix®, sequence stability and copro-IgA levels in a cohort of UK vaccinees', Joint **6th European Rotavirus Vaccination** and **8th European Rotavirus Biology Meeting 2019** (Riga, Latvia, 23rd-25th April).
- 'Viral shedding and genetic stability of rotavirus vaccine virus in vaccinees in the UK', **7th European Rotavirus Biology Meeting 2017** (Cork, Ireland, 18th-21st June).

Posters

- 'Faecal shedding of Rotarix® vaccine virus and mucosal immunity to rotavirus in a cohort of vaccinees in the UK', **The London Infections & Immunity Symposium 2018** (Francis Crick Institute; London, 5th-6th November).

- ‘Assessment of rotavirus vaccine shed in a cohort of vaccinees in the UK’, **The Microbiology Society Annual Conference 2018** (Birmingham, 9th -12th April).

Acknowledgements

Foremost, I would like to thank the parents of study subjects who provided samples from their infants and the NIBSC for funding this project. I would like to express my gratitude to my supervisors Prof Miren Iturriza Gómara and Dr Nicola J. Rose, as well as Dr Jane L. Mitchell for their guidance.

My gratitude also goes to Dr Christina Bronowski for kindly providing quantitative polymerase chain reaction (qPCR) material (NSP2- and VP6-containing plasmids), and to Dr Edward T. Mee for guidance in qPCR optimization. I would like to thank Machela C. Palor, Dr Jane L. Mitchell and Emma N. Summersgill for PCV1 qPCR optimization and running of plates. I would also like to thank Dr Anna M. Pulawska-Czub and Dr Yann R. R. Le Duff for discussions on rotavirus specific copro-IgA ELISA optimization. I would like to thank Dr Jane L. Mitchell for training in vaccine viral extraction with the QIAamp® Viral RNA Mini Kit and in sequencing library preparation with the Nextera® XT DNA Library Preparation kit v2. I would also like to thank Dr Khuzwayo C. Jere and Miss Jenna M. Dawson for training in methods for dsRNA extraction from stool samples (Potgieter's adapted method) and RNA ScriptSeq™ library preparation, as well as Dr Javier Martín González, Dr Dimitra Klapsa and Dr Manasi Majumdar for dsRNA extraction from stool advice and sequencing tips. I am grateful to Dr Martin Fritzsche, Ryan K. Mate and Dr Thomas P. Bleazard, as well as to Dr Mark D. Preston, Nadine Holmes and Åsa Nordgren for sequencing library preparation and bioinformatic analysis. My gratitude goes again to Dr Edward T. Mee for help with Python scripting for sequencing data sorting. I would like to thank Dr Daniel Hungerford for advice on statistical analysis and Dr Daniel Kelly and Dr Nathan J. Meade for next generation sequencing (NGS) analysis advice. I would also like to thank Miguel Ángel Couce Couto for IT support outside the NIBSC.

At the NIBSC, I would like to thank Dr Isobel S. Okoye, Dr Simon A. Chanas, Emma N. Summersgill, Machela C. Palor and Hamish M. Wilson for everyday help in the lab. I would also like to thank Dr Edward T. Mee, Dr Cristina Santirso Margaretto and Dr Michael P. Nicoll for valuable advice on approach to experimental design, analysis and writing throughout the PhD. My gratitude also goes to Dr Sheila Govind, Harsha Siani and Martina Hadrovic-Sinthalapadi for

valuable practical and professional advice. A very special thanks to Dr Cristina Santirso Margaretto and Richard W. Holmes for strong support, encouragement and great sense of humour. Thank you to Amy I. Jacobs for sharing the PhD journey, as well to Roshan R. Mohit, Abigail A. Galea, Julia Georgiades, Dr Elaine E. Pegg, Sara Fabi, Dr Gianluigi De Benedetto and Dr Leandro Lo Cascio for lifts and/or encouragement and/or social time outside the lab and Italian meals, treats and puns.

At the University of Liverpool, my gratitude goes to Dr Naomi S. Coombs for PhD support, accommodation and entertainment in and around Liverpool, and to Ruth Russell at the London Campus Library for her effective help with being able to work at the library, printing and binding. Around London, I would like to thank Dr Laura Mosteo López, Dr Vanessa F. Formigo Pataia and Dr Stephane Bandeira Pedro de Farias for valuable PhD advice and support. My gratitude goes to the friends I found during my MSc: Evangelia D. Williams, Dr Laura Medrano González, Dr Manoja Sivakumar (nee Rasamanikkam) and Dr Lachrissa A. Burns for understanding, support and good times together. I would also like to thank Laura Homet Sangil and Gonzalo de Ana Rodríguez for inspiring determination and sharing our love for dance, which recharged me throughout the project. A big hug goes to Patricia L. Short and Herbert C. Short for treating me like a granddaughter, with love and encouragement. I would also like to thank John R. Miles, Simon C. King and Minnie "gatita" for providing a friendly and relaxed living space to write.

From BSc times, I would like to thank friends: Dr Allende Miguélez Crespo, María Becker Loyola, Marta Aramburu Núñez, María Caño Calle, Carolina Alonso Barragán, Itziar Villabona Rivas and Ana Suárez-Lledó Grande for celebrating the good. My gratitude goes to hometown friends: Dr Sonia Rico Alonso, Noemí López García, Marta Varela Porto and Adrián Ares Legaspi for thesis writing advice (Sonia), support and encouragement. From my hometown in Spain, a big thank you to Rodríguez-Corral-Infante family friends Juan, Miluca (Emilia), Ángeles (María de los Ángeles), Gilberto, Cristina, Iván, Pablo, Martín and Beltrán, as well as to Narda (M. Bernarda) Teijeiro Varela, for keeping a smile on my face with their updates. Last, I would also like to express my gratitude to my big family, especially to my uncle Luis A. Botas Piñón, to my aunt Gelis (María de los Ángeles) Botas Piñón, to my cousins José M. Salido Botas and Paloma Sabiote Botas and to my father, Javier A. Botas Piñón for their love, support and encouragement along the process.

I would like to dedicate this thesis to those who passed away before I was born or who have passed away throughout my life: Gumersinda D. Piñón Montero, Enrique Botas Blanco, M. Isabel García Rivas, Antonio J. Klett Caprani, Carlos F. Botas Piñón, Casílda Feal Rodríguez and M. Margarita Rivas Fernández, with a very especial dedication to my mother Alfonsina M. Pérez López. You live in our memories.

Volverán las oscuras golondrinas
en tu balcón sus nidos a colgar,
y otra vez con el ala a sus cristales
jugando llamarán.
Pero aquellas que el vuelo refrenaban
tu hermosura y mi dicha a contemplar,
aquellas que aprendieron nuestros nombres....
ésas... ¡no volverán!
Volverán las tupidas madreselvas
de tu jardín las tapias a escalar
y otra vez a la tarde aún más hermosas
sus flores se abrirán.
Pero aquellas cuajadas de rocío
cuyas gotas mirábamos temblar
y caer como lágrimas del día....
ésas... ¡no volverán!
Volverán del amor en tus oídos
las palabras ardientes a sonar,
tu corazón de su profundo sueño
tal vez despertará.
Pero mudo y absorto y de rodillas
como se adora a Dios ante su altar,
como yo te he querido..., desengáñate,
así... ¡no te querrán!

- Gustavo Adolfo Bécquer

"Nothing in life is to be feared, it is only to be understood. Now is the time to understand more, so that we may fear less."

- Marie Curie

Funding and sample donors

This project was funded by the National Institute for Biological Standards and Control (NIBSC): PhD studentship with the Live Viral Vaccines Group (Division of Virology).

Parents who voluntarily donated stool samples from their vaccinated infants were employed at the NIBSC.

Statement of originality

I, Ledicia Botas Pérez, declare that the work presented in this thesis is entirely my own except where appropriately referenced.

Stool samples collected from 2014 to 2015 were archived by Dr Jane Mitchell and then re-organised by me. Stool samples from 2016 to 2018 were archived by me.

For PCV1 viral load quantification, experimental design was performed by Dr Jane L. Mitchell, Machaela C. Palor and myself, based on previous published work by Dr Sarah Connaughton (nee Gilliland) (Gilliland *et al.*, 2012) and previous practical work carried out by Dr Jane L., Mitchell, Emma N. Summersgill and me. Extraction of material and qPCR assays to determine limit of detection were performed and run by me. Extraction of PCV1 from vaccine material was performed by Machaela C. Palor (using the QIAamp® DNA Mini Kit and the QIAamp® Viral RNA Mini Kit, which also extracts DNA (Jane Mitchell, personal communication)) under the supervision of Dr Jane L. Mitchell. Five plates (samples from 10 infants after dose 1, plus vaccine DNA extracted with the QIAamp® DNA Mini Kit) for PCV1 quantification were run by Machaela C. Palor and five plates (samples from 2 infants after dose 1 and from 12 infants after dose 2, plus vaccine DNA extracted with the QIAamp® Viral RNA Mini Kit) by Emma N. Summersgill. Data analysis was performed by me.

The NGS of Rotarix® vaccine material was developed and implemented at NIBSC by Dr Jane L. Mitchell. I contributed to the sequencing of vaccine material by performing extractions, primer-specific cDNA synthesis and PCR, sample pooling and quantification of repeats and library preparation for vaccine virus

harvest bulks and final fills; as well as by setting up and optimising a Rotarix® NSP2 vaccine-specific qPCR used in this and further work.

The sequencing library preparation using the Nextera® XT DNA reagent kit (Illumina®, MiSeq) and the RNA ScriptSeq™ v2 library preparation kit, and the sequencing runs were performed by Ryan K. Mate and Nadine Holmes, supervised by Dr Martin Fritzsche in the NGS team at the NIBSC. The bioinformatic analysis pipeline was designed by Dr Mark D. Preston and run by Dr Thomas P. Bleazard and Åsa Nordgren. The Python scripts used to sort sequencing data were written by Dr Edward T. Mee.

Excess material from nucleic acid extractions to measure viral loads and early rotavirus-specific RNA sequencing using the Nextera® XT DNA reagent kit (Illumina®, MiSeq) was also used to study PCV1 DNA sequence changes by Dr Jane Mitchell and Hamish Wilson (Mitchell, Botas-Perez, *et al.*, unpublished).

A subset of the excess faecal suspensions from copro-IgA quantification work (from 12 infants, individuals B to M) are currently being used to study intracellular anti-VP6 neutralising antibodies (NAbs) in collaboration with Dr Sarah L. Caddy at the MRC Cambridge. They may be used to study anti-VP6 transcription blockade antibodies or PCV1-specific copro-IgA levels.

A subset of the remaining aliquoted stool samples (from 12 infants, individuals B to M) are currently being used to study the microbiome (down to genus level) of infants vaccinated with Rotarix® throughout the month after first and second dose. This is a collaboration with Dr Gregory C. A. Amos and Dr Sjoerd Rijpkema in the Bacteriology Department at the NIBSC.

Yet unused aliquoted stool samples, faecal suspensions and/or nucleic acid extract (from 12 infants, individuals B to M) may be used in future studies at the NIBSC or elsewhere.

Table of contents

List of abbreviations

A	Adenine nucleotide or alanine amino acid
aa	Amino acid
AGE	Acute gastroenteritis
AGMK	African green monkey kidney
AID	Activation-induced cytidine deasminase
ANOVA	Analysis of variance
ALT	Alanine aminotransferase
APCs	Antigen-presenting cells
APRIL	A proliferation-inducing ligand
AST	Aspartate aminotransferase
AT	Ambient temperature
BAFF	B-cell activating factor
bp	Base pair
BCG	Bacille Calmette-Guérin
BCR	B-cell receptor
BLAST	Basic Local Alignment Search Tool
β-TrCP	Beta-transducin repeat containing E3 ubiquitin protein ligase
BWA	Burrows Wheeler Algorithm
C	Cytosine nucleotide or cysteine amino acid
°C	Degree centigrade
Ca^{2+}	Calcium ions
cap	Capsid
CD	Cluster of differentiation
CDC	Centers for Disease Control
cDNA	Complementary DNA
cds	Coding sequence
$CHCl_3$	Chloroform
CI	Confidence interval
cIgA	Copro-immunoglobulin A
CFTR	Cystic fibrosis transmembrane regulator
CPE	Cytopathic effect
Cq	Quantitation cycle
Ct	Cycle threshold
CV	Coefficient of variation
CXCL	Chemokine C-X-C motif ligand
D	Aspartic acid amino acid
DCs	Dendritic cells
DLP	Double-layered particle
DMEM	Dulbecco´s Modified Eagle Medium
DNA	Deoxyribonucleic acid
DNAse	Deoxyribonuclease
ΔRn	Differential of normalised reporter
dsRNA	Double-stranded ribonucleic acid
DTaP	Diphtheria, tetanus and pertussis
ECACC	European Collection of Authenticated Cell Cultures
EED	Environmental enteric dysfunction
eIF4G	Eukaryotic initiation factor 4G

E	Glutamic acid amino acid
ELISA	Enzyme-linked immunosorbent assay
EM	Electron microscopy
EMA	European Medicines Agency
ENS	Enteric nervous system
EPAR	European Assessment Reports
ER	Endoplasmic reticulum
F	Phenylalanine amino acid
FCS	Foetal calf serum
FcRI	Fragment crystallizable receptor I
FDA	Food and drug administration
FFU	Focus forming unit(s)
FUT2	Fucosyltransferase 2
G	Glycoprotein type or guanine nucleotide or glycine amino acid
GALT	Gut-associated lymphoid tissue
GAVI	Global alliance for vaccines and immunizatino
GE	Gastroenteritis
GI	Gastrointestinal
GSK	Glaxo SmithKline
H	Histidine amino acid
h	Hour
HBGA	Histo-blood group antigen
HBV	Hepatitis B vaccine
HEPES	4-(2-hydroxyethyl)-1-piperazineethanesulphonic acid
HF	High fidelity
Hib	*Haemophilus influenzae* type b
HIE	Human intestinal enteroid
HIV	Human immunodeficiency virus
HRP	Horseradish peroxidase
HS	High sensitivity
H_2SO_4	Sulfuric acid
Hsc70	Heat-shock protein 70
5-HT	5-hydroxytryptamine or serotonin
HTA	Human tissue act
HuMAC	Human Materials Advisory Committee
I	Isoleucine amino acid
IFN	Interferon
IFNAR1	IFN-α/β receptor
IgA	Immunoglobulin A
IgG	Immunoglobulin G
IκB	Inhibitor of nuclear factor-κB
IKK-ε	Inhibitor of NF-κB kinase subunit ε
IL	Interleukin
ILFs	Isolated lymphoid follicles
INN	International nonproprietary
IPV	Inactivated poliovirus vaccine
IRF	IFN regulatory factor
ISG	IFN stimulatory genes

ISRE	IFN-stimulated response element
U	Units
IVB	Immunization, Vaccines and Biologicals
JAK1	Janus kinase 1
K	Lysine amino acid
kDa	Kilo Dalton
L	Leucine amino acid
LLR	Lanzhou lamb rotavirus
LMICs	Low and middle-income countries
LoD	Limit of detection
LoQ	Limit of quantification
LP	Lamina propria
M	Molar or methionine amino acid
MA104	African green monkey kidney cells
MDA5	IFN-induced helicase C domain-containing protein 1 (or IFIH1)
MEM	Minimum Essential Medium
Men B	Meningococcal group B vaccine
Men C	Meningococcal group C vaccine
mg	Miligram
min	Minute
mL	Mililitre
mM	Milimolar
MMR	Measles, mumps and rubella
mRNA	Messenger RNA
µg	Microgram
µL	Microlitre
N	Asparagine amino acid
NAb	Neutralising antibody
NCDV	Neonatal calf diarrhoea virus
NF-κB	Nuclear factor κB
ng	Nanogram
NGS	Next generation sequencing
NIBSC	National Institute for Biological Standards and Control
NIH	National Institutes of Health
NIP	National immunisation programme
NK	Natural killer
Nm	Nanometre
NSP	Non-structural protein
nt	Nucleotide
NTP	Nucleoside triphosphate
NTPase	Nucleoside triphosphatase
OMCL	Official medicines control laboratory
OPV	Oral poliovirus vaccine
ORF	Open reading frame
ORS	Oral rehydration solution
OSU	Ohio State University
P	Proline amino acid
PABP	Poly(A)-binding protein
PATH	Programme for appropriate technology in health
PBS	Phosphate buffered saline

PCR	Polymerase chain reaction
PCV	Pneumococcal conjugate vaccine
PCV1	Porcine circovirus 1
PCV2	Porcine circovirus 2
PCV3	Porcine circovirus 3
pIgR	Polymeric immunoglobulin receptor
PK15	Porcine kidney cells
4PL	Four-parameter logistic curve
PMWS	Post weaning multisystemic wasting syndrome
POLYVAC	Vietnamese Center for Research and Production of Vaccines
Q	Glutamine amino acid
QC	Quality control
qPCR	Quantitative PCR
R	Arginine amino acid
R^2	Coefficient of determination
RdRp	RNA-dependent RNA polymerase
rep	Replicase
RER	Rough endoplasmic reticulum
RIG-1	ATP-dependent RNA helicase DDX58
RIX4414	Precursor to RV1 vaccine
RLR	(RIG-I)-like receptor
RNA	Ribonucleic acid
RNAse	Ribonuclease
RoVI	Rotavirus vaccine immunogenicity study
RRV	Rhesus rotavirus vaccine
RT-PCR	Reverse-transcription PCR
RV	Rotavirus
RVA	Rotavirus A
RVGE	Rotavirus gastroenteritis
s	Second
S	Serine amino acid
SC	Secretory component
sIgA	Secretory IgA
SNP	Single nucleotide polymorphism
ssDNA	Single-stranded DNA
ssRNA	Single-stranded RNA
STAT	Signal transducer and activator of transcription
T	Thymine nucleotide or threonine amino acid
TANK	TRAF family member-associated NF-κB activator
TBC	Tuberculosis
TBK1	TANK-binding kinase 1
TGF-β	Transforming growth factor β
Th	T helper
TLP	Tripled-layered particle
TLR	Toll-like receptor
TMB	3’,3’,5’,5’-tetramethylbenzidine liquid substrate
TNF	Tumour necrosis factor
TRAF	Tumour necrosis factor receptor-associated factor
Treg	T regulatory cells
TYK2	Non-receptor tyrosine kinase 2

UK	United Kingdom
UNICEF	United Nations International Children's Emergency Fund
USA	United States of America
UTR	Untranslated region
V	Valine amino acid
vDNA	Viral DNA
VCF	Variant calls format
VE	Vaccine efficacy
Veros	African green monkey kidney cells
vNA	Viral nucleic acid
VL	Viral load
VLPs	Virus-like particles
vNA	Viral nucleic acid
VP	Viral protein
vRNA	Viral RNA
W	Tryptophan amino acid
WHO	World Health Organization
WT	Wild-type (adjective) or wild type (subject)
Y	Tyrosine amino acid

List of figures

List of tables

Chapter 1: Introduction

1.1 Thesis overview

Wild-type (WT) rotavirus (RV) is transmitted via the faecal oral route and causes acute gastroenteritis (AGE) in children of less than five years of age; the only effective treatment is re-hydration therapy. Live-attenuated oral vaccines with high efficacy are available worldwide and rotavirus vaccination was incorporated into the UK national immunisation programme (NIP) in 2013. As a live virus replicating in infants, Rotarix® is likely to be shed in stool of vaccinees and to accumulate changes in sequence. These may lead to variants in the vaccine virus population with potential to revert to WT virus. Virus replication will generate an immune response in the host, which may be affected by the quasispecies in the virus population.

This thesis considers the profile of viral shedding of Rotarix® in stool of vaccinated infants and genetic changes in the vaccine virus throughout the vaccination period. Mucosal responses in the cohort are reviewed as anti-rotavirus copro-IgA levels.

1.2 Rotavirus

The first rotaviruses were detected by electron microscopy (EM) of material isolated from faeces of mice (Pappenheimer and Enders, 1947), monkeys (Adams and Kraft, 1963; Malherbe and Harwin, 1963) and cattle in 1969 (Mebus *et al.*, 1969a, 1969b). Human rotavirus was discovered in 1973 (Bishop *et al.*, 1973) in samples from diarrhoeic children, as the causative agent of AGE in infants (0-1 year-old) and children under 5 years of age.

1.2.1 Rotavirus structure

Rotavirus is a non-enveloped, double-stranded RNA (dsRNA) virus. The fully infectious virion is approximately 75 nm in diameter and triple layered, containing two concentric icosahedral capsids and a core (Fig. 1.1; Estes, 2001). The viral proteins are encoded on 11 segments (section 1.2.3). The external capsid is formed by proteins VP7 and VP4, defining serotypes G (glycoprotein) and P

(protease-sensitive) respectively, with icosahedral symmetry and 780 molecules of VP7 as Ca^{2+}-stabilised trimers and 180 molecules of VP4 as trimer spikes (Chen *et al.*, 2009; Settembre *et al.*, 2011). VP4 is composed of the subunits of VP5*, in contact with VP7 and VP6, and VP8*, known to interact with host cell receptors (Settembre *et al.*, 2011; Liu *et al.*, 2012). The internal capsid is formed by VP6, which presents T=13 icosahedral symmetry (each icosahedral asymmetric unit is composed of 13 proteins) and 780 molecules arranged as trimers, and defines groups or species A-J based on its antigenicity and accounts for 50% of the virion's mass (Prasad and Chiu, 1994; Thouvenin *et al.*, 2001; McClain *et al.*, 2010; Mladenova *et al.*, 2011; Settembre *et al.*, 2011; Matthijnssens *et al.*, 2012; Mihalov-Kovács *et al.*, 2015). VP6 interacts with VP4 and VP7 as well as with VP2 (Petitpas *et al.*, 1998; Mathieu *et al.*, 2001). The core is formed by VP2, with T=2 symmetry and 120 molecules as dimers (Lawton *et al.*, 1997). The non-structural proteins RNA-polymerase VP1 and RNA-capping enzyme VP3, as well as the 11 dsRNA gene segments associated with them lay within the core (Estrozi *et al.*, 2013; Periz *et al.*, 2013).

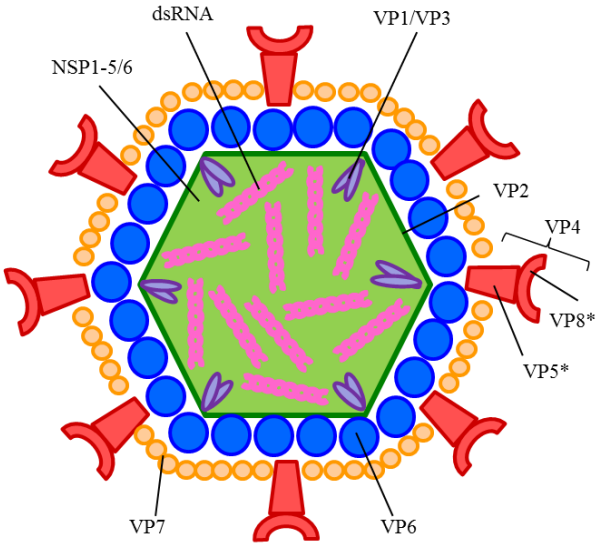

Fig. 1.1. Rotavirus A triple-layered virion. Outer capsid proteins VP7 in orange and VP4 in red. Inner capsid protein VP6 in blue and core protein VP2 in dark green. Non-structural proteins and dsRNA (in pink) within the core (light green). Adapted from Angel, Franco and Greenberg, 2007.

1.2.2 Classification and nomenclature

Rotaviruses belong to the *Reoviridae* family and comprise the genus *Rotavirus* within the family *Sedoreovirinae*.

Antigenicity and genetic variability of VP6 define groups or species of rotavirus, from A to J. Groups A, B, and C infect humans and animals and group A rotaviruses (RVA) are responsible for 90% of these infections (Kapikian, Hoshino and Chanock, 2001). Group B rotaviruses have been associated with adult rotavirus infection originally in China (Hung *et al.*, 1983, 1984) and subsequently in Asia (Kelkar and Zade, 2004; Lahon *et al.*, 2013). Group C rotaviruses have been associated with outbreaks in humans across all ages worldwide (Rodger, Bishop and Holmes, 1982; Nilsson *et al.*, 2002; Abid *et al.*, 2007; Doan *et al.*, 2016). The host range of groups D to J rotaviruses is restricted to non-human animals (Kapikian, Hoshino and Chanock, 2001) as seems the case for groups H to J (Wakuda *et al.*, 2011; Marthaler *et al.*, 2014; Molinari *et al.*, 2014; Mihalov-Kovács *et al.*, 2015; Bányai *et al.*, 2017) (see section 1.2.6).

The different strains of rotavirus are defined by their types G (VP7) and P (VP4) sequences. For rotavirus A (RVA), there exist at least 36 G types and 51 P types (Matthijnssens, Ciarlet, Rahman, *et al.*, 2008; Matthijnssens *et al.*, 2011; RCWG, 2018). Serotypes and genotypes are equivalent for G types, while multiple P genotypes are associated with certain P serotypes. G types are designated by genotype/serotype as *e.g. G1, G2, G3, etc.*, while P types are designated thus, *P1A[8]*, representing serotype *P1A* and genotype *[8]*. Due to the vast sequence diversity among the 11 RVA genome segments, a new nomenclature has been recently agreed relating genotypes to nucleotide sequence differences and assigning cut-off values for each of the segments's open reading frame (ORF). In summary, a one-letter code for each segment is followed by the number (x) of the corresponding genotype: Gx-P[x]-Ix-Rx-Cx-Mx-Ax-Nx-Tx-Ex-Hx (Matthijnssens, Ciarlet, Rahman, *et al.*, 2008; Matthijnssens *et al.*, 2011). The gold-standard strains in the study of rotavirus that present homology in animals are human Wa-like (G1P[8]; porcine-like), human DS-1 (G2P[4]; bovine-like) and AU-1-like (G3P[9]; feline-like) (Nakagomi *et al.*, 1990; Heiman *et al.*, 2008; Matthijnssens, Ciarlet, Heiman, *et al.*, 2008; McDonald, Matthijnssens, *et al.*, 2009).

1.2.3 Genome and proteins

Rotavirus A has a linear genome of 18,550 base pairs (bp), comprising 11 gene segments varying in size from 3,302 to 667 bp and encoding for six structural (VP1, VP2, VP3, VP4, VP6 and VP7) and six non-structural proteins (NSP1, NSP2, NSP3, NSP4, NSP5/6) (based on simian rotavirus A/strain SA11; Small *et al.*, 2007) (Fig. 1.2; Table 1.1). Ten segments are monocistronic, with segment 11 subject to leaky scanning and encoding NSP5 plus NSP6 as a second out-of-frame protein (Mattion *et al.*, 1991). The RVA gene segments contain 5′ and 3′ untranslated regions (UTRs) and a central ORF. The messenger ribonucleic acids (mRNAs) present a 5'-methylated cap structure, but no polyA tail at the 3' end, although there is a consensus sequence (5'-UGACC-3') conserved at the 3' end of all segments (Fig 1.3A) (Chizhikov and Patton, 2000).

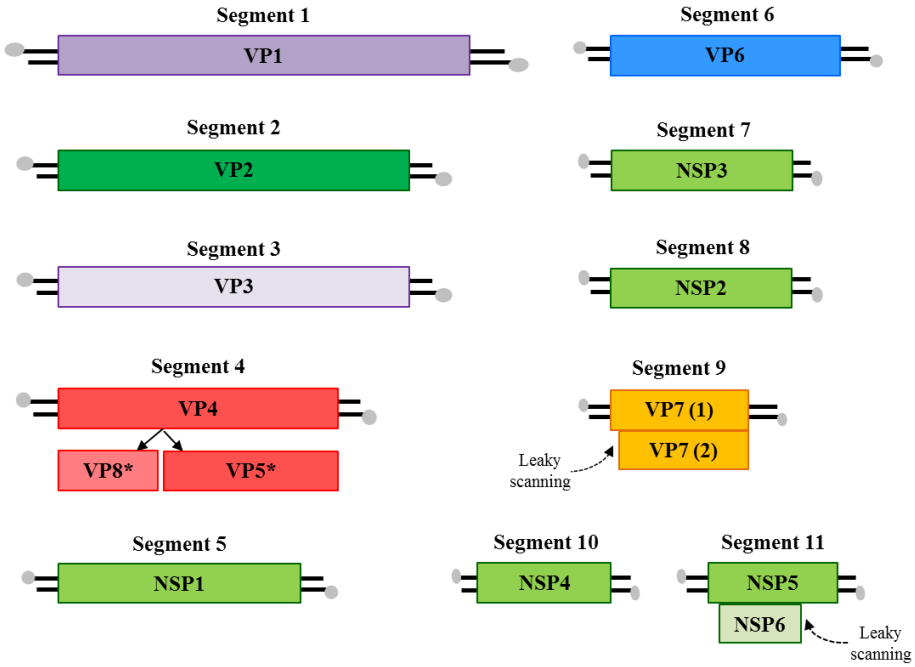

Fig. 1.2. Rotavirus gene segments and proteins. Gene segment with encoded protein name boxed in the ORF and 5’ methyl cap in grey. ORF, open reading frame. Adapted from ViralZone, 2013.

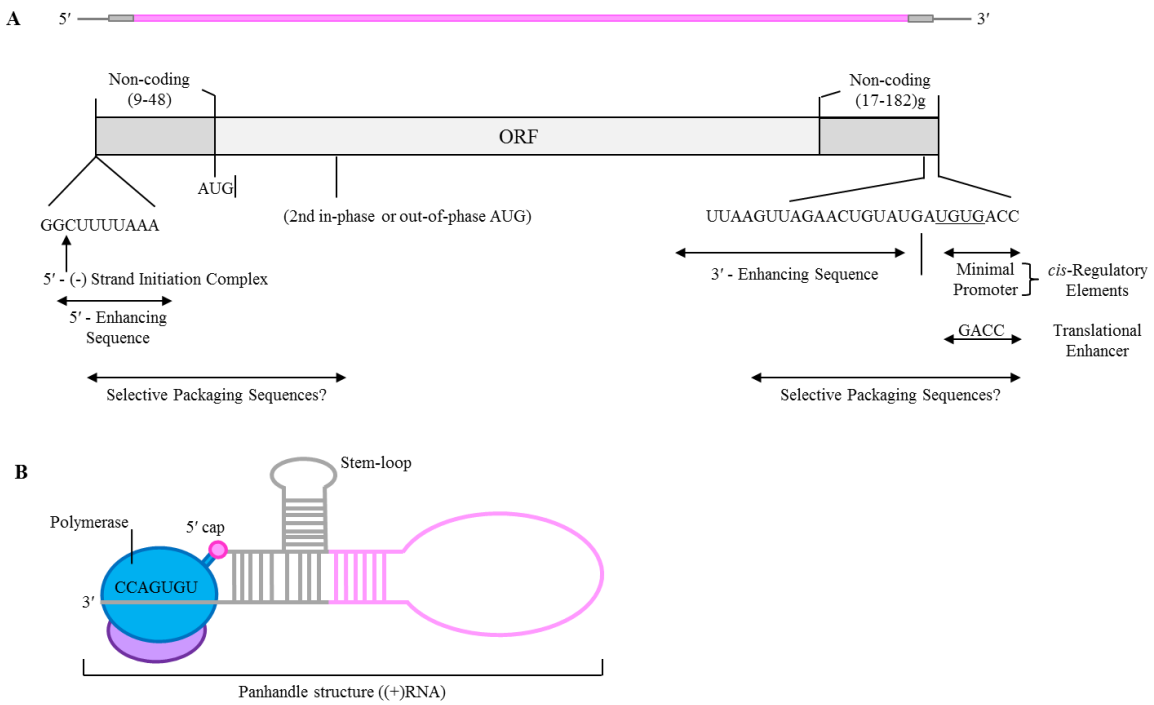

Fig. 1.3. Rotavirus genome. (A) Linear genome map. General structure of rotavirus gene segments. Rotavirus genes do not present a polyadenylation signal, are A+U rich and contain conserved consensus sequences at their 5′ and 3′ ends. Variation in conserved ends shown. The *cis*-regulatory elements of RV mRNA required for transcript replication in cell-free replication system shown (Patton *et al.*, 1996; Wentz, Patton and Ramig, 1996; Kearney *et al.*, 2004; Tortorici, Shapiro and Patton, 2006). The study of the 3′ variations indicated the minimal promoter as $RN_{05}CC$ (Kearney *et al.*, 2004). The non-coding regions are predicted to interact and stably base-pair to form a panhandle structure maybe stabilised by VP1 (Imai *et al.*, 1983; Patton *et al.*, 1996; Tortorici, Shapiro and Patton, 2006), and interactions between 3′ with NPS3 may promote viral mRNA translation (Vende *et al.*, 2002). 5′-GACC-3′ is a translation enhancer (Chizhikov and Patton, 2000). Reproduced from Estes, 2013, with permission from WK Health Book Copyright Clearance Center's RightsLink® order no. 4620900375548 (02/07/19). **(B) Folded genome.** Putative panhandle structure of one gene segment. The polymerase-capping enzyme complex (VP1-VP3) may be bound to the 3′- terminal sequence UGUGACC. A putative stem-loop may be an assortment and/or packaging signal. Reproduced from McDonald *et al.*, 2016, with permission from first author.

Table 1.1. Characteristics of rotavirus gene segments and proteins. The 11 rotavirus gene segments are listed, indicating length, encoded protein and protein molecular weight, location in virion and function. Figures are for RVA/Simian-tc/ZAF/SA11-H96/1958/G3P5B[2]. Initial of genotype name highlighted in bold. Ca^{2+}, calcium ions; eIF4G, eukaryotic initiation factor 4G; IFN, interferon; IRF, IFN regulatory factor; NTPase, nucleoside triphosphatase; PABP, poly(A)-binding protein; RdRp, RNA-dependent RNA polymerase. Adapted from (Small *et al.*, 2007; Matthijnssens, Ciarlet, Rahman, *et al.*, 2008).

Genome segment	Length (bp)	Encoded protein	Molecular weight (kDa)	Localization (copies)	Function	References
1	3,302	VP1	125	Core (12)	**RdRp**, RNA binding, interacts with VP2 and VP3	Estrozi *et al*., 2013; Rodríguez et al., 2014
2	2,639	VP2	102	**C**ore (120)	RNA binding, interacts with VP1	Lawton *et al*., 1997
3	2,591	VP3	98	Core (12)	RNA capping, guanilyl and **m**ethyltransferase, ssRNA binding, interacts with VP1	Rodríguez *et al*., 2014
4	2,362	VP4 (VP5*, VP8*)	88 (60, 28)	Outer capsid, spike protein (180)	P serotype, sensitive to trypsin (**p**rotease) cleavage for infectivity, neutralization antigen, hemagglutinin, cell attachment, phusion region, virulence determinant	Espejo, López and Arias, 1981; Estes, Graham and Mason, 1981; Chen *et al*., 2009; Settembre *et al*., 2011; Liu *et al*., 2012; Rodríguez *et al*., 2014
5	1,614	NSP1	58	Non-structural	Type I IFN response **a**ntagonist (IRF regulatory protein), RNA binding	
6	1,356	VP6	45	**I**nner capsid (780)	Group and subgroup antigen, hydrophobic trimer	Petitpas *et al*., 1998; Mathieu *et al*., 2001; Liu *et al*., 2012; Rodríguez *et al*., 2014
7	1,105	NSP3	36	Non-structural	**T**ranslation effector, cellular protein synthesis inactivation/translational control (PABP homologue, interacts with eIF4G), RNA binding	
8	1,059	NSP2	36	Non-structural	Viroplasm RNA binding, viral replication (**N**TPase), RNA packaging, interacts with NSP5	
9	1,062	VP7	37	Outer capsid (780)	Integral membrane **g**lyoprotein,G serotype, neutralization antigen, Ca^{2+} binding	Rodríguez *et al*., 2014
10	751	NSP4	20	Non-structural	Viral **e**nterotoxin, viral assembly, transmembrane glycoprotein	
11	667	NSP5/6	11/22	Non-structural	Accumulation in viroplasm, RNA binding, interacts with NSP2 and NSP6, protein kinase (p**h**osphoprotein) / Viroplasm protein, interacts with NSP5	

1.2.4 Rotavirus diversification

RNA virus populations, mutant spectra or quasispecies (Lauring and Andino, 2010) arise where an RNA polymerase lacking 3' exonuclease proofreading activity is encoded; such viruses undergo genetic drift at higher rates than do DNA viruses (Sanjuán *et al.*, 2010). Quasispecies comprise a collection of genomic variants co-evolving at the same time and within the same host, present at different relative frequencies, with a consensus sequence (or more than one) (Eigen and Schuster, 1977) that behave almost like a single variant. The high mutation rate arising from the viral RNA polymerase generates diversity, and the accumulation of point mutations may result in antigenic changes that impact on infectivity, fitness, pathogenesis and viral dissemination, thereby contributing to viral adaptation and survival (Crotty, Cameron and Andino, 2001; Paul, 2002; Vignuzzi *et al.*, 2006). Among the genetic variants that comprise the mutant spectra, minority variants may be selected throughout replication in the host (Moya, Holmes and González-Candelas, 2004). Substitution rates depend on the rate of mutation and the rate of replication and for RNA viruses they have been estimated around 1×10^{-3} substitutions per site and per year (Jenkins *et al.*, 2002). Different mutation rates occur for each of the rotavirus genome segments and strains, ranging from 5×10^{-5} bp/site/year for NSP5 (Blackhall, Fuentes and Magnusson, 1996), 8.7×10^{-4} bp/site/year for NSP2 of N1 genotype (Donker and Kirkwood, 2012), 5.8×10^{-4} bp/site/year for VP4 of human RV (Jenkins *et al.*, 2002), 1.6-1.8×10^{-3} bp/site/year for VP7 of G12 and G9 strains (Matthijnssens *et al.*, 2010) to 1.01×10^{-3} bp/site/year for NSP4 (Zeller *et al.*, 2015).

During recombination in non-segmented viruses, the polymerase copies the RNA template from one parental strain, switches template to use a different parental strain and generates a chimeric RNA molecule containing parts of sequence from each parent (McDonald *et al.*, 2016). It usually occurs at points of conserved sequence. Although unusual for RV, intragenotype recombination has been reported in several studies for strains of the same genotype in VP7 (G4, G1, G3), NSP2, NSP4 and NSP6 (Parra *et al.*, 2004; Phan *et al.*, 2007; Martínez-Laso *et al.*, 2009; Donker, Boniface and Kirkwood, 2011; Jere *et al.*, 2011). Rearrangements occur when there are partial duplications, deletions or insertions into coding or noncoding regions

(Pedley *et al.*, 1983; Hundley *et al.*, 1987; Tian *et al.*, 1993; Taniguchi, Kojima and Urasawa, 1996; Kirkwood, 2010).

Genetic reassortment of rotavirus occurs when segments from two parental viruses (from the same or different host species) are packaged together in new virions (in cells or *in vivo*), resulting in hybrid progeny (Fig. 1.4). It results in novel genetic and antigenic characteristics in the progeny, with theoretically up to 2^{11} progeny viruses with novel characteristics generated after co-infection by two different RVs being generated (Ramig, 1997). Recombination cannot occur between viruses belonging to different RV species, as the replicase complex cannot be substituted by those of other groups and the crucial 3' ends are particular to each RV species (McDonald, Aguayo, *et al.*, 2009; McDonald and Patton, 2011b). Compatibility between parental strains is determined by conserved packaging signals and the maintenance of RNA and protein interactions (McDonald *et al.*, 2016). Reassortment contributes to maintenance of the segmented genomic structure and it is the main mechanism of evolution and zoonotic transmission of RV (Martella *et al.*, 2010). There may also be direct transmission of rotavirus strains from an animal into a human host, with potential impact on human RV diversity and human health (Martella *et al.*, 2010).

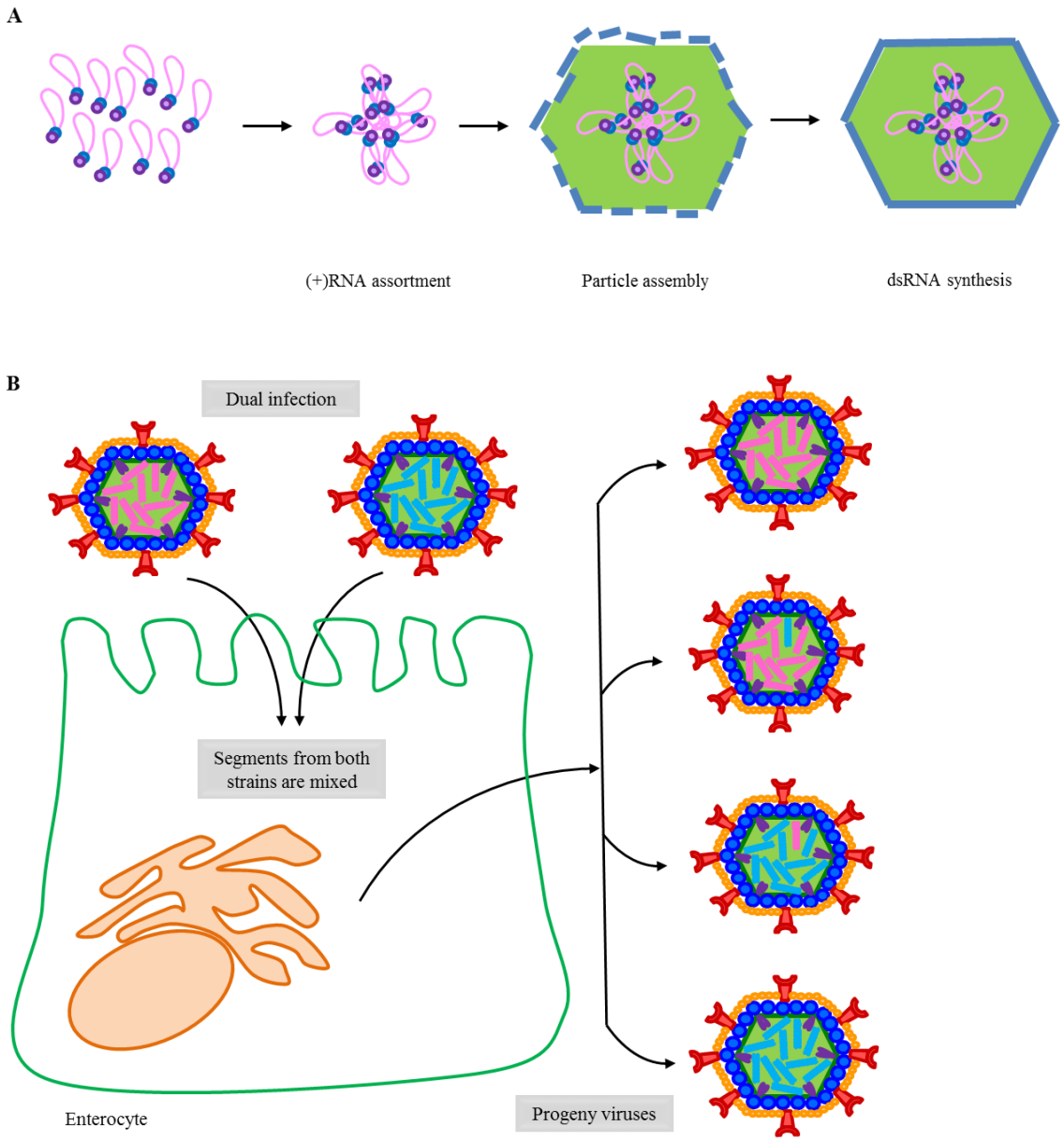

Fig. 1.4. Rotavirus assortment and reassortment. (A) Rotavirus A assortment and packaging. Each of the (+) RNAs is bound by a polymerase-capping enzyme complex (VP1-VP3). They pair up and form a supramolecular complex that is encapsidated by a virion particle that is forming. During encapsidation or immediately after, the (+) RNAs are converted into dsRNA genome segments by the polymerase, which functions while tethered to the viral capsid (not shown in this figure, although shown in Fig. 1.5). Reproduced from McDonald *et al.*, 2016, with permission from first author. **(B) Rotavirus reassortment.** Two different rotavirus strains infect the same enterocyte. The gene segments are mixed in replication in the cell, generating progeny viruses with the same genome as the parental viruses and with different genome segments from the parental viruses, hence, different strains.

1.2.5 Rotavirus replication cycle

Rotavirus is transmitted via the faecal-oral route, with as few as 10 virus particles required for transmission and an estimated infectious dose of 100-1000 rotavirus particles (Ward *et al.*, 1986). Rotavirus is shed in stool during infection and it can be transmitted via person-to person contact (Estes, 2001), as well as remain on fomites (Ansari, Springthorpe and Sattar, 1991; Butz *et al.*, 1993). Once inside the host, rotavirus resists the stomach acid secreted by parietal cells in infants, transiting through to the small intestine, where it infects mature enterocytes and enteroendocrine cells of the villi in the duodenum (Greenberg and Estes, 2009).

Trypsin in the gut lumen cleaves VP4 at amino acids 231, 241 and 247, as well as 259, 467 and 583, conserved in P serotypes of RVA, generating proteins VP5* and VP8* (Arias *et al.*, 1996; Crawford *et al.*, 2001). VP4 interacts with receptors containing N-acetylneuraminic acid (or sialic acid) and other glycans, such as those on histo-blood group antigens (HBGAs), via VP8* (López and Arias, 2004), which can perform the function of hemagglutinin (Weiner *et al.*, 1978; Yeung *et al.*, 1987), and with other receptors concentrated in lipid rafts, such as integrins and heat-shock protein 70 (Hsc70), via VP5* (Zárate *et al.*, 2000). HBGA receptors have been shown to be used by RV for attachment, the interaction depending on a functional fucosyltransferase 2 (FUT2) enzyme generating fucose (Lee *et al.*, 2018) and the *FUT2* gene variant determining susceptibility to infection (Nordgren *et al.*, 2014). Integrins α2β1, α*v*β3, αxβ2, α4β1 and other receptors, such as Hsc70 can act as receptors post-attachment (Coulson, Londrigan and Lee, 1997; Hewish, Takada and Coulson, 2000; Zárate *et al.*, 2004). Rotavirus also uses other hydrophobic domains/lipidic rafts to attach to the membrane. (López and Arias, 2004). The VP4 spikes undergo conformational changes (Wolf, Vo and Greenberg, 2011), where key hydrophobic domains previously hidden in a "post-penetration umbrella" shape are exposed on VP5* (Fig. 1.6) (Trask, McDonald and Patton, 2012). This allows penetration through the cell membrane by an as yet unknown mechanism likely to be direct penetration or receptor-mediated endocytosis (Gutierrez *et al.*, 2010). As calcium (Ca^{2+}) levels are low in endosomes, the outer capsid solubilises, producing dual-layered particles (DLPs) (Jayaram, Estes and Prasad, 2004).

Once in the cell, the DLPs remain in the cytoplasm, where the RNA undergoes transcription, translation and then replication in the viroplasm (a

specialised structure formed of cellular and viral proteins that recruit lipid droplet components for energy storage and transport in the cell) (Crawford *et al.*, 2017). The RNA-dependent RNA polymerase VP1, tethered to the inner surface of the virus core, recognises the antisense strand of the genomic RNA by a sequence-specific interaction with seven nucleotides UGUGACC or UGUGGCU located at the 3′ end, and synthesises the sense strand ssRNA (~mRNA) (Lu *et al.*, 2008). The mRNAs are capped at the 5′ end by VP3, a guanilyltransferase capping enzyme associated with the core, as a post-transcriptional modification that protects it from nuclease degradation (Figs. 1.3. B and 1.4. A) (Chen *et al.*, 1999). The dsRNA genome is not completely uncoated, thereby preventing activation of an antiviral state triggered by toll-like receptor recognition of dsRNA (Greenberg and Estes, 2009). The capped mRNA is translated in the cytoplasm. NSP1 blocks the cellular type I interferon (INFγ) response and it has been observed that the proteasome of infected cells degrades signaling components required for IFN production, like interferon-regulatory factor (IRF) and others necessary to respond to IFN secreted by neighbouring cells (Arnold, Barro and Patton, 2013). NSP3 binds to viral mRNAs in infected cells and impairs cellular protein synthesis by inactivating two translation initiation factors (Hu *et al.*, 2012). NSP3 is also a translation enhancer for viral proteins. NSP3 ejects poly(A)-binding protein (PABP) from the translation initiation factor eIF4F. PABP is required for efficient translation of transcripts with a 3' poly(A) tail, which is found on most host cell transcripts. Moreover, NSP3 inactivates eIF2 by stimulating its phosphorylation. Efficient translation of rotavirus mRNA, which lacks the 3' poly(A) tail, does not require either of these factors.

The mRNA is later replicated into dsRNA and packaged in cytoplasmic inclusions called viroplasms (Crawford and Desselberger, 2016). NSP2 and NSP5 are crucial in regulating translation and replication in the viroplasm (Hu *et al.*, 2012). The dsRNA cannot be packaged directly due to its large size. There are 12 transcription complexes available and it is not clear what role the extra complex plays in RV replication. The 11 different sense strand ssRNAs engage through *cis*-acting RNA elements into a supramolecular complex, which is encapsidated by VP2 during early viral assembly (McDonald and Patton, 2011a). Packaging/assortment signals are believed to be located within the 5' and 3' UTR sequences and are different for each of the segments and conserved in different strains of RVA (Trask,

McDonald and Patton, 2012). Rotavirus is believed to undergo an as yet unclear all-or-none packaging mechanism, not as yet elucidated (McDonald and Patton, 2011a; Desselberger *et al.*, 2013; Periz *et al.*, 2013). The synthesised DLPs bind NSP4, which functions as a rough endoplasmic reticulum (RER) receptor, and bud into the RER acquiring a transient envelope (Desselberger, 2014). Rotavirus matures in the RER by losing that envelope and assembling VP7 and VP4, to be then released as infectious virions by lysis or by Golgi-independent non-classical vesicular transport (epithelial cells), infecting neighbouring cells and enabling spread (Estes and Greenberg, 2013).

Viroplasms are formed within two hours post-infection and inclusion bodies within six to seven hours post-infection, with maximum yields at 10-12 h post-infection in AGMK cells (Ayala-Breton *et al.*, 2009).

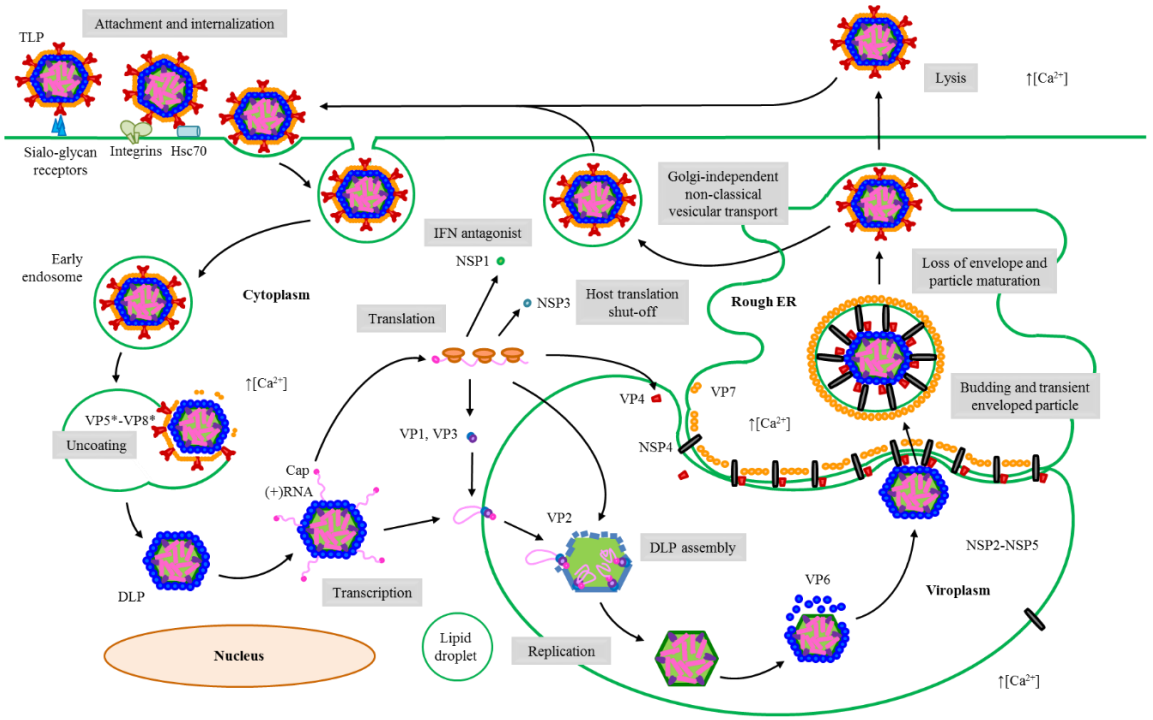

Fig. 1.5. Rotavirus replication cycle. The rotavirus triple-layered particle (TLP) attaches to host sialo-glycan receptors (histo-blood group antigen receptors) via the VP8* domain of VP4, followed by interaction of VP7 and the VP5* domain of VP4 with other receptors (integrins and Hsc70), concentrated in lipid rafts to mediate viral entry. Rotavirus can be internalised by several pathways: Clathrin-dependent or independent mechanisms and caveolin-independent endocytosis, mediated by the receptors. Lower levels of calcium in the early endosome trigger loss of the VP4 and VP7 layer and release the transcriptionally active double-layered particle (DLP) into the cytoplasm. Viral mRNA is used for transcription, translation and, when enough viral proteins have been produced, as a template for replication, being packaged into DLPs in the viroplasm (the viroplasm is a structure that uses components of lipid droplets and is formed of viral and cellular proteins). The formation of TLPs involves the binding of new DLPs to non-structural protein 4 (NSP4), acting as an endoplasmic reticulum (ER) receptor, followed by the budding of DLPs into ER. NPS4 also mediates increase of calcium in the cytoplasm from intracellular storage, acting as a viroporin. In the ER, proteins VP4 and VP7 are added onto the DLPs, transiently enveloped. Then, the envelope is lost, the virus particles mature and the progeny TLPs are released from cells through cell lysis or, in polarised epithelial cells, by a Golgi-independent non-classical vesicular transport mechanism. HSc70, heat-shock-protein 70. Adapted from López and Arias, 2004; Trask, McDonald and Patton, 2012; Estes & Greenberg, 2013; Desselberger, 2014; Crawford *et al.*, 2017, with permission from Nature Reviews Disease Primers Copyright Clearance Center's RightsLink® order no. 4620891497970 (02/07/19).

Fig. 1.6. Rotavirus outer capsid spike protein VP4 trypsin-mediated conformational change during entry. VP4 is formed by three VP5* subunits (in red) and two VP8* subunits (in grey). The hydrophobic domains of VP5* are highlighted in green and its coiled coils in blue. The pre-fusion state is stable, perturbed by trypsin cleavage of VP4 at amino acids 231, 241 and 247 (all arginine residues, simian rotavirus SA114S) (Arias *et al.*, 1996) as well as residues 259, 583 and 467, conserved in P serotypes of RVA (Crawford *et al.*, 2001) and resulting in dissociation of VP8*, extension of VP5* and penetration of the hydrophobic domain into the host cell membrane (pistachio). The stable post-fusion state generates a fold-back conformation of VP5*. It is unknown how membrane penetration occurs and whether VP5* is associated or dissociated from the viral particle. Its refolding may be triggered by VP7 dissociation (Yoder *et al.*, 2009; Trask *et al.*, 2010). Adapted and reproduced from Trask, McDonald and Patton, 2012, with permission from last author.

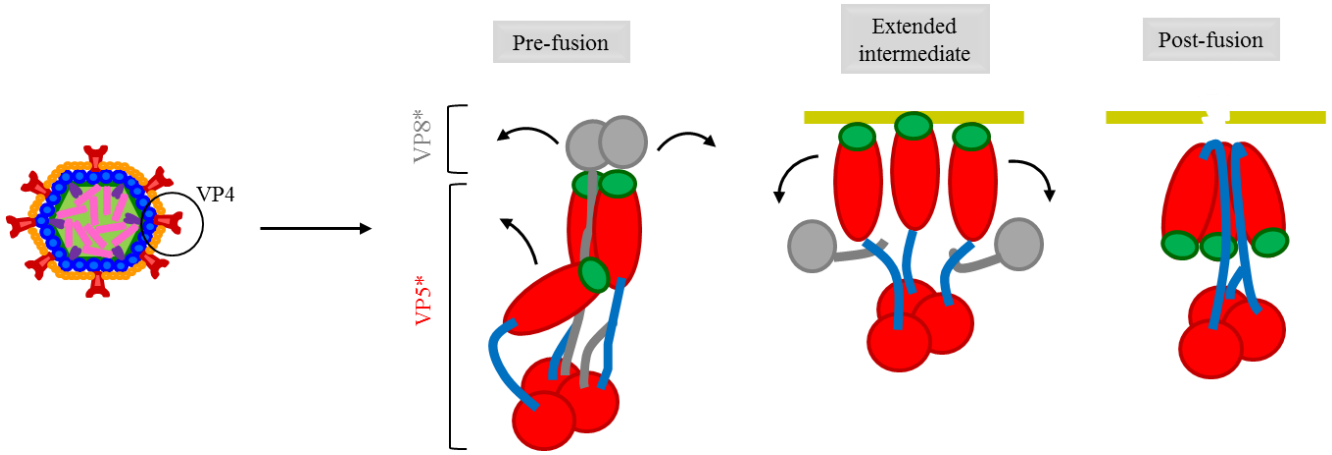

1.2.6 Rotavirus hosts

Rotavirus group A severe disease is mostly limited to children <5 years of age but may affect adults and the elderly (section 1.8). Group B affects mainly adults and it has been linked with water-borne outbreaks in East and South Asia (Hung *et al.*, 1984; Nakata *et al.*, 1987; Chitambar *et al.*, 2011; Lahon *et al.*, 2013). Group C affects all age groups as outbreaks or sporadic cases, with around half of the 60-year-old population seropositive and a very low incidence in the infant population (<5% of AGE-associated hospitalisations) (Nilsson *et al.*, 2002; Rahman, Banik, *et al.*, 2005; Joshi, Jare and Gopalkrishna, 2017).

In animals, group A rotaviruses have been identified in horses (first three months of life) (Collins *et al.*, 2008), cattle (first four week of life) and pigs (first eight weeks of life) causing significant morbidity; and also in dogs and cats (Marshall *et al.*, 1984, 1987). Group B has been identified in pigs, cattle, sheep, lamb and rats (Theil *et al.*, 1985; Chasey and Banks, 1986; Parwani, Lucchelli and Saif, 1987; Eiden *et al.*, 1991; Tsunemitsu *et al.*, 1991; Barman *et al.*, 2004). Group C has been identified in pigs, ferrets, dogs and cattle (Saif *et al.*, 1980; Torres-Medina, 1987; Tsunemitsu *et al.*, 1991; Chang *et al.*, 1999; Otto, Schulze and Herbst, 1999; Collins, Martella and O'Shea, 2008; Tuanthap *et al.*, 2018). Groups A, D, F, G have been identified in birds (Falcone *et al.*, 2015; McCowan *et al.*, 2018). Group E has been identified in pigs (Chasey, Bridger and McCrae, 1986; Martella *et al.*, 2010). Group H has been identified in piglets (Wakuda *et al.*, 2011; Marthaler *et al.*, 2014; Molinari *et al.*, 2014). Candidate group I infect dogs and candidate group J infect bats (Mihalov-Kovács *et al.*, 2015; Bányai *et al.*, 2017). Other animals susceptible to infection by rotavirus are monkeys, goats, cats, mice and rabbits (Martella *et al.*, 2010). Weaning and post-weaning piglets and young calves are those most affected by rotavirus diarrhoea (Rosen *et al.*, 1994; Lanz Uhde *et al.*, 2008).

There is evidence for zoonotic transmission in rotavirus group A, and suspicion of zoonotic transmission in groups B and C (Cook *et al.*, 2004; Luchs and Sampaio Tavares Timenetsky, 2016). Although exceptional zoonoses have occurred originating from rotaviruses in pigs and cattle jumping species into humans, rotaviruses in humans are usually transmitted human strains transmitted from person to person (Martella *et al.*, 2010).

1.3 Systems to study rotavirus infection

1.3.1 Animal models

Although the neonatal mouse model can be used to study infection and disease, the short duration of diarrhoea in neonatal mice infected with RV (susceptible during the first two weeks of life) impairs the study of immunity (Franco and Greenberg, 1999). However, the adult mouse is susceptible to infection by certain RV murine strains, rendering it a useful model to study RV infection (Franco and Greenberg, 1999). In this model, it was found that B cells expressing the α4β7 gut homing receptor are key for resolution of infection via non-neutralising anti-VP6 IgA, which are protective *in vivo*. It was also found that J-chain deficient mice were not able to produce sIgA, suggesting transcytosis of IgA as a mechanism to produce protective antibodies (Desselberger and Huppertz, 2011). Moreover, it has been found that passive transfer of neutralising anti-VP4 and anti-VP7 antibodies contribute to infection resolution in a dose-dependent manner and that the neutralizing IgA was anti-VP4 IgA (Desselberger and Huppertz, 2011). Shedding patterns have been studied in this mouse model showing protection against shedding after reinfection (Eydelloth *et al.*, 1984; Ward, McNeal and Sheridan, 1990; Burns *et al.*, 1995). In vaccinated mice, local IgA has been shown to correlate with protection although not as the only effector (Ward, 2003).

Rotaviruses have also been studied in the gnotobiotic piglet, susceptible to human and porcine RV strains and which present diarrhoea within the first six weeks of life (Saif *et al.*, 1996; Yuan and Saif, 2002). The gnotobiotic piglet lacks microbiome, affecting mechanisms of mucosal immunity. In this model, it was found that specific anti-VP4 and anti-VP7 antibodies provided heterotypic protection against challenge and that anti-VP6 IgA was not protective (Desselberger and Huppertz, 2011). Serum and intestine RV-specific IgA were the main correlates of protection against human RV challenge and vaccination (Azevedo *et al.*, 2004; Desselberger and Huppertz, 2011).

Although there have been attempts at developing monkey models of human RVA infection (Chege *et al.*, 2005), only very young monkeys are susceptible to diarrhoea (Leong and Awang, 1990) and the proportion of monkeys developing diarrhoea is low even in those infected with homologous simian RVA despite

shedding of virus in stool (McNeal *et al.*, 2005; Bentes *et al.*, 2018) or viremia (Yin *et al.*, 2018).

Although they have been useful models to understand RV biology, biological and experimental differences with respect to humans contribute to limited transferability as predictors of protection (Desselberger and Huppertz, 2011).

1.3.2 Reverse genetics systems

The functions of rotavirus proteins have been studied in spontaneous mutants and in several reverse genetics systems which depended on the use of a helper virus and strong selection conditions (Komoto and Taniguchi, 2013; Desselberger, 2014). Now, there is a plasmid-only based system that can yield rotavirus with specific changes, heterologous inserts in the genome, to study functionality of rotavirus proteins (Kanai *et al.*, 2017). It is possible to study packaging signals of RV ss(+)RNAs (replication), to identify sequences of segments involved in genome reassortment (safety), to study compatibility of proteins from different species (e.g. RdRp, evolution), to study host restriction, pathogenicity, virulence and attenuation (therapy), to generate direct rotavirus mutants with GFP for imaging (pathogenesis) and to generate RV with highly cross-reactive epitopes (wide immunity, universal vaccine candidate) (Crawford *et al.*, 2017; Kanai *et al.*, 2017). For example, it was found that NSP6 is not essential for viral replication in cell culture (Komoto *et al.*, 2017) and that basal interferon limits RV replication and interferon treatment could inhibit RV replication (Hakim *et al.*, 2018). This system will be useful in further studying the phenotype elicited by engineered mutations and in developing candidate vaccines and antivirals against RV.

1.3.3 Human Intestinal Enteroids

Previously, there had been a lack of models for the human small intestine. However, in the last few years, human stem cells from the crypts of small intestine have been differentiated into intestinal cell-like cultures as monolayers or in 3D a few years ago (Spence *et al.*, 2011). It was observed that these cultures can be infected with lab strains and clinical isolates (Finkbeiner *et al.*, 2012). These human intestinal organoids/enteroids (HIEs) are multicellular, containing cell types from the intestinal epithelium, such as enterocytes, goblet cells, enteroendocrine cells and

Paneth cells (Sato and Clevers, 2013; Saxena *et al.*, 2016). These HIEs are used to study rotavirus replication (Kovbasnjuk *et al.*, 2013), pathophysiology and epithelial cell restriction (Saxena *et al.*, 2016), as well as the innate immune response to RV (Saxena *et al.*, 2017). Human intestinal enteroids appear to be a robust and reproducible model to study human rotaviruses and may overcome the limitations of cell-based and animal models.

1.4 Molecular pathogenesis

1.4.1 Intestinal infection

RV mainly infects mature enterocytes in the middle and upper part of the villi in the small intestine (Fig. 1.7; Lundgren and Svensson, 2001). When RV uncoats from the endocytic vesicles into the cytoplasm, it increases intracellular Ca^{2+} levels which in turn increase paracellular permeability, thereby disrupting tight junctions (Dickman *et al.*, 2000; Lundgren and Svensson, 2001; Obert, Peiffer and Servin, 2002). There is a resulting increase in epitelial turnover, loss of microvilli and atrophy of the villi (Davidson and Barnes, 1979; Tafazoli *et al.*, 2002) and a decrease in absorptive function (Barnes and Townley, 1973; Holmes *et al.*, 1975), leading to non-inflammatory osmotic diarrhoea. Viral progeny are released, spreading the infection and contributing to the non-inflammatory diarrhoea.

NSP4, a viral enterotoxin (Horie *et al.*, 1999) and viroporin, is responsible for interfering with Ca^{2+} balance and resulting in loss of plasma membrane integrity and altered epithelial homeostasis (Ball *et al.*, 1996; Newton *et al.*, 1997). This RER membrane protein acts on phospholipase C, activating Ca^{2+}-dependent chloride channels and causing the exit of water into the lumen in parallel to chloride and resulting in secretory diarrhoea (Hyser *et al.*, 2010). It also impairs the sodium-glucose cotransporter 1 and prevents water reabsorption (Halaihel *et al.*, 2002; Svensson *et al.*, 2016). Moreover, NSP4 induces the release of peptides and amines that stimulate the enteric nervous system (ENS), such as 5-hydroxytryptamine (5-HT or serotonin) from enteroendocrine cells, increasing intestinal motility and contributing to secretory diarrhoea (Bialowas *et al.*, 2016). NSP4 can activate the ENS directly (Weclewicz *et al.*, 1993; Lundgren *et al.*, 2000; Lundgren and Svensson, 2001). Another hallmark of RV disease is signalling for early vomiting via

the vagus nerve, after Ca^{2+}-dependent secretion of 5-HT (Hagbom *et al.*, 2011). Individuals with rotavirus disease also present with fever (Uhnoo, Olding-Stenkvist and Kreuger, 1986): higher levels of TNF and IL-6 have been detected in serum of infected infants (Jiang *et al.*, 2003), although the mechanisms driving fever in rotavirus infection are currently unknown. NSP4 also binds to extracellular matrix proteins laminin-β3 and fibronectin (Boshuizen *et al.*, 2004), which may allow further systemic infection.

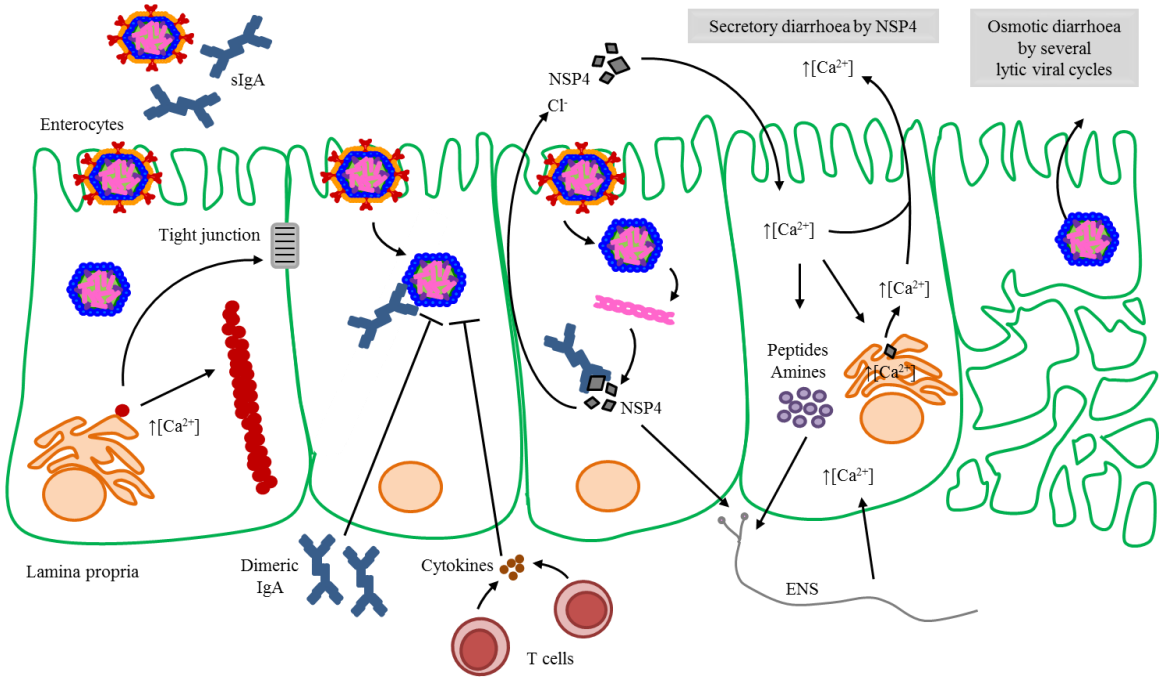

Fig. 1.7. Pathogenesis of diarrhoea and immunity to rotavirus. Neutralizing antibodies against VP4 and VP7 in the lumen can prevent attachment and internalization, also by viral exclusion mechanisms. Rotavirus replication increases intracellular calcium levels, disrupting tight junctions and increasing paracellular permeability. Secretory anti-VP6 antibodies transcytosed across enterocytes may inhibit viral replication. Rotavirus-specific T cells (suspected Th1 type, $CD4^+$) may inhibit viral replication by secreting cytokines into enterocytes (IFNγ). Rotavirus NSP4 acts as a toxin inducing the non-cystic fibrosis transmembrane conductance regulator (CFTR) and causing secretory diarrhoea. Moreover, NSP4 can also stimulate the (ENS), causing secretory diarrhoea and increased motility in the intestine. Rotavirus kills the host cell, causing further malabsorptive or osmotic diarrhoea. sIgA, Secretory IgA. Adapted and reproduced from Bomsel & Alfsen, 2003; Angel, Franco and Greenberg, 2007, with permission from Nature Reviews Microbiology Copyright Clearance Center's RightsLink® order no. 4620280499363 (01/07/19).

1.4.2 Systemic and extraintestinal infection

It has been reported that children with RV infection have infectious RV and viral antigens in blood (viraemia and antigenemia, respectively) and other sites up to 5 days after onset of sypmtoms; those with antigenaemia present with more severe symptoms (Blutt *et al.*, 2007). Further studies found that antigenaemia was more common among children with extraintestinal symptoms (Ramani, Paul, *et al.*, 2010; Hemming *et al.*, 2014). Individuals with systemic infection have been found to present more severe symptoms than those with only intestinal infection (Hemming *et al.*, 2014).

Rotavirus-elicited extraintestinal symptoms have been previously observed in children with neurological illness, seizures being the most frequent (Lloyd *et al.*, 2010; Rivero-Calle, Gómez-Rial and Martinón-Torres, 2016). Apart from the central nervous system, rotavirus has been found in liver, heart, bladder, lung, kidney and testes of children and animals (Blutt *et al.*, 2007; Candy, 2007; Alfajaro and Cho, 2014). Systemic infection may be due to direct spread of RV to the blood or the lymphatic system after reaching the lamina propria or by infecting cells of the immune system (Boshuizen *et al.*, 2004; Alfajaro and Cho, 2014; Mossel and Ramig, 2016). Rotavirus may reach the central nervous system by attaching to specific receptors or using axon transport (Weclewicz, Svensson and Kristensson, 1998). Other extraintestinal manifestations are usually isolated cases (Rivero-Calle, Gómez-Rial and Martinón-Torres, 2016). RV infection has also been associated with autoimmune diseases, such as diabetes mellitus type I or celiac disease (Honeyman *et al.*, 2000, 2014; Stene *et al.*, 2006; Ballotti and De Martino, 2007; Dolcino *et al.*, 2013; Pane, Webster and Coulson, 2014; Sarkar *et al.*, 2014). Although there is no direct evidence of extraintestinal infection generated from systemic infection derived from intestinal infection (as opposed to direct extraintestinal infection by other mechanisms), the frequency of neurological illness and seizures indicate that RV is a systemic pathogen (Rivero-Calle, Gómez-Rial and Martinón-Torres, 2016; Gómez-Rial *et al.*, 2019a, 2019b; Salas *et al.*, 2019).

1.5 Symptoms, diagnosis and treatment

Rotavirus infection can be asymptomatic or manifest as mild non-bloody diarrhoea of short duration, or it can manifest as severe diarrhoea accompanied by vomiting and fever and resulting in severe dehydration (Parashar, Nelson and Kang, 2013). Rotavirus disease typically presents with cold-like symptoms, moderate fever and early vomiting, followed by secretory diarrhoea with frequent stools (Parashar, Nelson and Kang, 2013). The majority of infants with asymptomatic RV infection are under 2 years of age (Phillips *et al.*, 2010). Nowadays, rotavirus is being considered a systemic disease by clinicians, with links to autoimmune disease and seizures appearing to be the most frequent and severe extraintestinal symptoms (section 1.4.2).

Rotavirus diagnosis was originally performed by electron microscopy or latex agglutination tests (Pai, Shahrabadi and Ince, 1985). Then, polyacrylamide gel electrophoresis was used to identify the electrophoretic migration patterns of the rotavirus segments (Herring *et al.*, 1982). Antigen detection assays are available, as well as reverse-transcription polymerase chain reaction (RT-PCR), which has greater sensitivity (Pang *et al.*, 2004). Testing of stool and antigenemia are not routine diagnostic tools as treatment remains the same regardless of molecular diagnosis (Parashar, Nelson and Kang, 2013; Gómez-Rial *et al.*, 2019b).

The main treatment for rotavirus gastroenteritis (RVGE) in children with repeated vomiting and mild dehydration is oral rehydration therapy using a hyposmolar oral rehydration solution (ORS), composed of 75 mM sodium plus glucose, potassium, chloride and citrate (WHO, 2005), which aims to restore glucose-coupled sodium and water adsorption, based on rapid turnover of enterocytes. In severe dehydration cases or milder cases where vomiting impairs adequate ORS administration, intravenous rehydration therapy is used (Chow, Leung and Hon, 2010). In such cases, food intake is stopped until the patient has improved, whereupon breastfeeding or regular milk formulas are introduced, followed by solid food (WHO, 2005; Gregorio, Dans and Silvestre, 2011). Zinc supplementation is recommended by the WHO and United Nations International Children's Emergency Fund (UNICEF) for cases of diarrhoea in developing countries and has been found to reduce the duration of diarrhoea in children >6 months of age (Lazzerini and Ronfani, 2012). Although probiotics are not part of the standard treatment, they have

been shown to accelerate recovery from gastroenteritis symptoms and to reduce stool frequency (Allen *et al.*, 2011). Bacteria that produce lactic acid, such as *Lactobacillus* and *Bifidobacterium* species, in combination with prebiotics have shown an antiviral effect against rotavirus, as well as reduced duration and severity of disease (Gonzalez-Ochoa *et al.*, 2017).

Drugs that affect the nervous system, such as antiemetics and antisecretory drugs, are generally not recommended in children. However, in cases of vomiting impaired ORS or intravenous therapy, ENS inhibitors used in gastroenteritis treatment are serotonin or 5-HT_3 receptor antagonists, which help reduce vomiting and water and electrolyte secretion, reduce intestinal motility, ultimately reducing dehydration. One such type of inhibitor, ondansetron, has proven effective at reducing vomiting and the need for intravenous therapy (Fedorowicz, Va and Carter, 2011; Hagbom *et al.*, 2017). Anti-viral drugs that selectively affect rotavirus receptors, polymerase, replication, viroplasm assembly, RNA assortment, packaging and maturation could be of great use. Nitazoxanide is an example of an anti-viral drug inhibiting RV replication, potentially by targeting cellular pathways of protein synthesis, that has been shown to reduce duration of rotavirus disease in hospitalised patients (Rossignol and El-Gohary, 2006; Rossignol *et al.*, 2006). The use of antibodies has resulted in reduction of stool output and disease severity (Sarker *et al.*, 2013; Thu *et al.*, 2017).

1.5.1 Rotavirus faecal shedding

Rotavirus shedding in stool has been observed in infected infants before the onset of diarrhoeal symptoms for up to 10 days (Nagavoshi *et al.*, 1980; Vesikari, Sarkkinen and Mäki, 1981), and in hospitalised children from 4 to 57 days after the onset of symptoms (Richardson *et al.*, 1998), with 70% of children ceasing shedding within 20 days of diarrhoea onset. Children who shed RV over an extended period of time appear to be less protected against rotavirus disease than those who do not shed continously (Richardson *et al.*, 1998). Shedding may be longer in duration and to higher levels where symptoms are evident, as compared to asymptomatic children (onset of infection unknown), with intermittent shedding observed in symptomatic and asymptomatic children (Mukhopadhya *et al.*, 2013). Rotavirus gastroenteritis severity correlated with RV viral loads (VLs) in infants in Southern India (Kang *et*

al., 2004). However, this correlation was not observed in neonates (Ramani, Sankaran, *et al.*, 2010).

1.6 Immune response

1.6.1 Innate immune response

In a primary infection, innate immune response mechanisms are triggered rapidly (Angel, Franco and Greenberg, 2012). Because RV dsRNA is not fully uncoated when entering enterocytes, macrophages, dendritic cells (DCs) or naïve B and T cells, recognition by pattern recognition receptors (PRRs) is prevented (Estrozi *et al.*, 2013). However, sub-populations of uncapped and partially capped viral transcripts can activate the host innate immune response through (RIG-I)-like receptors (RLRs) and Toll-like receptors (TLRs) (Uzri and Greenberg, 2013), subsequently activating transcription factors of the IFN pathway involved in antiviral response (Fig. 1.8). These migrate to the nucleus and stimulate IFN and IFN stimulatory genes (ISG), to trigger types I, II and III responses. Secreted IFN binds to IFN receptors on cells in an autocrine and paracrine manner, stimulating the JAK-STAT signalling cascade and activating a second wave of transcription. An 'antiviral state' is then established when a multitude of genes encoding antiviral proteins are expressed and a positive feedback for IFN expression ensures its amplification (Angel, Franco and Greenberg, 2012).

However, the RV protein NPS1 interacts with cellular proteins involved in IFN production such as β-TrCP, degrades them –via the proteasome by NSP1´s suspected E3 ubiquiting-ligase activity (Barro and Patton, 2007; Graff, Ettayebi and Hardy, 2009; Morelli, Dennis and Patton, 2015; Davis and Patton, 2017)– and interacts with other proteins such as p53 to avoid early apoptosis, while VP3 inhibits the mitochondrial antiviral state and prevents dsRNA degradation (reviewed by Desselberger, 2014; reviewed by Arnold, 2016; Ding *et al.*, 2018), resulting in low levels of IFN transcription or secretion. NSP1 has also been reported to antagonise the JACK-STAT pathway (Sen *et al.*, 2014), further preventing the establishment of an antiviral state. Although the NSP1 modulatory activity on the IFN response is conserved between strains, the molecular targets differ in a strain-dependent manner (Barro and Patton, 2007; Graff *et al.*, 2007; Sen *et al.*, 2009; Arnold and Patton,

2011). Recently, it was found in suckling mice that rotavirus re-programmes INF receptor signalling to reduce antiviral and anti-inflammatory functions (Sen et al., 2019).

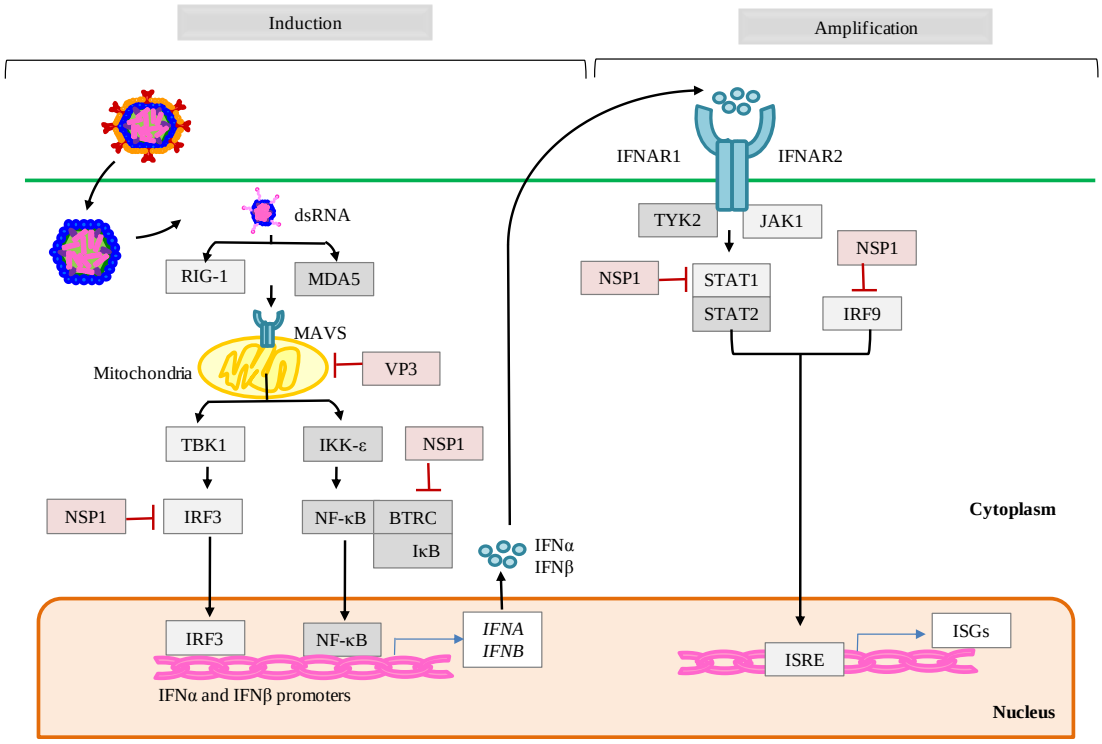

Fig. 1.8. Rotavirus interference with the host immune system. Rotavirus enters the cells and the actively transcribing virus is recognised by the pattern recognition receptors ATP-dependent RNA helicase DDX58 (RIG-1) and interferon (IFN)-induced helicase C domain-containing protein 1 (MDA5), which activate transcription factors IFN regulatory factor 3 (IRF3) and nuclear factor κB (NF-κB) through mitochondrial antiviral-state signalling protein (MAVS); inducing IFN type I, II and III responses. The viral protein NSP1 interacts with IRF3 and NF-κB-related proteins to inhibit IFN production, in some cases by degrading IRFs via the proteasome. When IFN is secreted in an autocrine manner, it interacts with IFN receptors and activates the signal transducer and activator of transcription 1 (STAT1), 2 (STAT2) and IRF9 transcription factors, which stimulate IFN stimulated response element (ISRE), activating IFN stimulatory genes (ISG) and leading to amplification of IFN production and the so called 'antiviral state'. NSP1 also interacts with STAT1 and IRF9 to prevent this state. BTRC, beta-transducin repeat containing E3 ubiquitin protein ligase; IFNAR1, IFN-α/β receptor; IκB, inhibitor of nuclear factor-κB; IKK-ε, inhibitor of NF-κB kinase subunit ε; ISRE, IFN-stimulated response element; JAK1, Janus kinase 1; TBK1, TANK(TRAF(TNF(tumour necrosis factor) receptor-associated factor)) family member-associated NF-κB activator)-binding kinase 1; TYK2, non-receptor tyrosine kinase 2; VP3, Viral protein 3. Adapted and reproduced from Angel, Franco and Greenberg, 2012; Desselberger, 2014; Crawford *et al.*, 2017, with permission from Nature Reviews Disease Primers Copyright Clearance Center's RightsLink® order no. 4620891497970 (02/07/19); and with added information from Ding *et al.*, 2018.

1.6.2 Adaptive immune response

The adaptive immune response is elicited after the innate immune response or is rapidly triggered in a secondary infection: it is mainly a mucosal response in the case of rotavirus (Uhnoo *et al.*, 1988; Franco, Angel and Greenberg, 2006). Rotavirus-specific $CD4^+$, $CD8^+$ T cells and B cells express the gut homing receptor α4β7 (Gonzalez *et al.*, 2003; Rojas *et al.*, 2003), showing they are recruited to the gut-associated lymphoid tissue (GALT) in the event of an infection. In an immunocompetent host, rotaviral antigens are transported to mesenteric lymph nodes in the GALT, such as Peyer's patches (pre-natal; the major induction sites of adaptive IgA responses) (Gonzalez *et al.*, 2003) and mesenteric lymph nodes (Blutt *et al.*, 2002). There, they undergo processing by antigen-presenting cells (APCs; B cells, plasmacytoid DCs or macrophages) and RV antigens are presented to T helper (Th) cells. Next, rotavirus-specific B cells are stimulated to produce antibody as plasma cells. The polymeric secretory IgA (sIgA), which binds the J chain covalently to stabilise the dimers, is generated by plasma cells in the lamina propria (LP) of the small intestine. Polymeric sIgA is transcytosed across epithelial cells towards the gut lumen by the polymeric Ig receptor (pIgR) through the secretory component (SC).

Neutralising antibodies (NAbs) directed against VP4 and VP7 can prevent viral binding and penetration, inducing aggregation and viral immune exclusion and preventing damage to epithelium. Anti-VP4 and anti-VP7 sIgA secreted into the lumen have been shown to be neutralizing *in vitro* (Ball *et al.*, 1996; Feng *et al.*, 2002; Franco, Angel and Greenberg, 2006). In a secondary infection, VP4 and VP7 antibodies mediate heterotypic immunity (Nair *et al.*, 2017). Anti-NSP4 antibodies may prevent disease but not infection (Ball *et al.*, 1996; Angel *et al.*, 1998). Moreover, both humoral and cellular immune responses to NSP4 have been reported, as well as increases in IL-2 and INFγ (Johansen *et al.*, 1999). Viral replication in the cytosol can be inhibited by anti-VP6 sIgA during transcytosis across enterocytes. Anti-VP6 non-neutralizing sIgA binds intracellularly to VP6 in the viroplasm and prevents uncoating of the inner capsid as well as viral assembly (Burns *et al.*, 1996), resulting in protection *in vivo* (Herrmann *et al.*, 1996; Chen *et al.*, 1997; O'Neal *et al.*, 1997; Feng *et al.*, 2002). The sIgA is believed to bind to a transcriptional pore to block viral transcription (Aiyegbo *et al.*, 2013).

B cells, together with $CD8^+$ T cells are believed to mediate rotavirus clearance (Blutt *et al.*, 2002). Rotavirus-specific cytotoxic $CD8^+$ T lymphocytes are believed to be the main cellular effectors in rotavirus clearance in mice (Franco, Tin and Greenberg, 1997). In infants with rotavirus infection, low levels of these have been detected (Rojas *et al.*, 2003; Mesa *et al.*, 2010). Another study detected significantly higher levels of $CD8^+$ and $CD4^+$ IFNγ-secreting cells in blood of symptomatic adults and faeces-exposed workers with respect to asymptomatic adults and children with severe RVGE (Jaimes *et al.*, 2002).

The main cytokines found in children with RVGE were IL-6, IL-10 and IFNγ, with patients with fever presenting higher IL-6 levels, and patients with fever and more diarrhoea episodes presenting higher levels of TNFα (Jiang *et al.*, 2003). IL-2 was found at lower levels in children with a high number of stools passed and IFNγ was lower in those patients presenting vomiting. The Th1 response has been shown to be predominant in acute RVGE (Azim *et al.*, 1999; Jiang *et al.*, 2003) despite neonates being skewed to Th2 response (Wegmann *et al.*, 1993; Sykes *et al.*, 2012). Cytokines in rotavirus infection appear to be linked to symptoms, such as in the case of fever (Jiang *et al.*, 2003).

Natural infection reduces the risk of subsequent severe disease and severity decreases with time. The first infection is usually more severe than the second or third infections (Velázquez *et al.*, 1996), as acquired antibodies contribute to decreasing the acuteness of the disease. The G/P genotypes present in a second infection are likely to be different from those present in the primary infection (Hungerford *et al.*, 2014) and protection against infection or disease is usually type-specific. Subsequent infections with the same strain are less severe, although high protection against severe disease has been observed when infected by heterotypic strains. Most older children and adults (except when encountering a more virulent strain, when immune-supressed or depending on the type of gut microbiota and secretor status) are not susceptible to RV disease, as they present acquired immunity from childhood (Griffin *et al.*, 2002; Mikami *et al.*, 2004; Rodríguez-Díaz *et al.*, 2017).

Immunocompromised individuals like children with severe-combined immunodeficiency (SCID) present prolonged viral shedding and systemic disease, thus highlighting the importance of the B and T cell response in clearing RV

infection (N. C. Patel *et al.*, 2012; Kaplon *et al.*, 2015; Rosenfeld *et al.*, 2017). Moreover, it has been observed that children with IgA-D deficiency overcompensate with specific anti-RV IgG (Istrate *et al.*, 2008), suggesting that IgA is not crucial for resolution of RVGE in humans, in contrast to later studies in mice suggesting a key role for IgA in immunity against RV (Blutt *et al.*, 2012).

1.6.3 Correlates of protection

Mechanisms underlying protection against rotavirus are not well understood, and antibody effector functions have been the most used predictors of protection so far.

Maternal transplacental antibodies (IgG) may provide mild protection against rotavirus infection and diminish the need for the infant to mount a neutralizing immune response (Ramachandran *et al.*, 1998; Ward *et al.*, 2006; Appaiahgari *et al.*, 2014; Moon *et al.*, 2016; Mwila *et al.*, 2017). Breastfeeding may also provide maternal antibodies with neutralising capacity and other protective factors (Asensi, Martınez-Costa and Buesa, 2006; Chattha *et al.*, 2013; Moon, Tate, *et al.*, 2013). Some studies have found breastmilk maternal antibodies to be correlated with protection (Espinoza *et al.*, 1997) and other studies have described mild protection (Glass *et al.*, 1991) due to lactadherin (Newburg *et al.*, 1998). The highest levels of antibodies in breastmilk are present in colostrum, with lower levels as breastfeeding continues (Chan *et al.*, 2011; Tino De Franco *et al.*, 2013).

Correlates of protection against natural infection have been identified as neutralising and cross-reactive antibodies against various RV types in Japan and the United States of America (USA) (Chiba *et al.*, 1986; Ward and Bernstein, 1994). They have also been identified as RV-specific IgA and IgG in serum, with IgA titre increases of >1:200 and IgG titre increases of >1:800 correlating with protection against infection and disease; with IgA titre increases of >1:800 presenting low risk of disease and protection against moderate/severe disease; and with IgG titre increases of >1:6400 presenting protection against infection and not illness (O'Ryan *et al.*, 1994; Velázquez *et al.*, 1996, 2000). RV-specific intestinal mucosal secretory IgA has also been identified as a natural correlate of protection, with a four-fold titre increase in infected with respect to uninfected children and higher copro-IgA associated with protection against infection and RV disease (Matson *et al.*, 1993). In

an earlier study, it was found that there was a mild correlation between serotype-specific neutralising IgA levels in serum and protection against severe disease and vomiting, as well as between older age (>1.5 years) and milder symptoms (Hjelt and Grauballe, 1990). These serum antibodies where thought to be polymeric IgA and originated from the intestine and spilled over into serum (Hjelt *et al.*, 1987). Later, serum anti-RV IgA was observed to be related to clinical protection against infection (Ward, Knowlton, *et al.*, 1997) and seropositivity for RV-specific IgA was defined as an increase in titre of >20 U/mL (Bernstein *et al.*, 1999) In another study, individuals who did not generate serum NAbs were at higher risk of rotavirus disease than those who did (De Vos *et al.*, 2004). The best correlate of protection in RV natural infection appeared to be NAbs in serum since they reflected intestinal anti-VP6, anti-VP4 and anti-VP7 (Svensson, Sheshberadaran, Vene, *et al.*, 1987; Franco, Angel and Greenberg, 2006).

Regarding antibodies in stool, patterns of faecal IgA are not well understood either. Copro-IgA has been described as a good surrogate marker of duodenal secretory IgA (sIgA) (Grimwood *et al.*, 1988; Coulson *et al.*, 1992; Matson *et al.*, 1993). Anti-RV copro-IgA was associated with protection against infection and disease, and asymptomatic children presented higher levels at baseline (Matson *et al.*, 1993). Frequent infection was seen to produce sustained copro-IgA, protecting against infection and disease, with copro-IgA persisting for a few weeks (Coulson *et al.*, 1992). Low or no copro-IgA has been associated with risk of reinfection and copro-conversion was found to be more sensitive than seroconversion in secondary infection (Coulson *et al.*, 1990). Continuous RV faecal shedding has been associated with copro-IgA boosts and with likelihood of mild diarrhoea during convalescence (Richardson *et al.*, 1998). Copro-IgA is usually detected at <150 units/g of stool (or <50 total IgA index) (Coulson and Masendycz, 1990), ranging from 520 to 2040 µg/mL (Martin, 2000). It was noted that rotavirus-specific copro-IgA (cIgA) concentrations peaked from 14 to 17 days after infection and persisted for longer than a year and up to two years, although at declining concentrations (from 2-4 months after secondary infection (Coulson *et al.*, 1992)) (Bernstein, McNeal, *et al.*, 1989). However, cIgA has sometimes not been detected or inconsistently detected (Offit, 1996). Children usually present copro-IgA for less time than serum IgA, maybe due to mounting of primary responses and a lack of boosting necessary to

generate long-life antibodies in stool (Franco, Angel and Greenberg, 2006). At high levels, copro-IgA has been observed to be correlated with protection (Coulson *et al.*, 1992; Matson *et al.*, 1993). Copro-IgA is considered a marker of protection at a population level but it is not clearly indicative of protection at an individual level (Clarke and Desselberger, 2015).

The correlates observed in challenge studies have been type-specific NAbs in serum (Kapikian *et al.*, 1983), serum RV-specific IgG (Ward *et al.*, 1986; Ward, Bernstein, *et al.*, 1990), RV-VP7-epitope-specific antibodies in serum (Green and Kapikian, 1992) and intestinal NAbs (Ward *et al.*, 1989). In animal studies in mice, adult mice have appeared to be protected by intestinal secretory IgA (Feng *et al.*, 1994; Burns *et al.*, 1995). In non-human primates, serum IgG appeared to be responsible for mucosal immunity against RV (Westerman *et al.*, 2005).

1.7 Molecular epidemiology

Despite rotavirus diversity and strain prevalence changing yearly (Patton, 2012), a few rotavirus serotypes have been identified as the more common ones infecting humans globally in the recent decades: G1, G2, G3, G4 and G9 and G12 strains in combination with P[4], P[6] or P[8] (Matthijnssens et al. 2009; Santos & Hoshino 2005). G1P[8], G2P[4], G3P[8], G4P[8] and G9P[8] strains have been the cause of >90% of human RVA infections worldwide, with G1P[8] being the most common circulating strain in Europe, North America and Australia and globally (Santos and Hoshino, 2005). Although G1P[8], G2P[4], G3P[8], G4P[8] were common in Europe (91.6%), North America (92%) and Australia (99.4%) from 1989 to 2004, they were less common in South America and Asia (68%), and in Africa (50%). G9P[8] and G12P[8] have emerged since the 1990's and 2000's respectively, and have become major strains worldwide (Pongsuwanna *et al.*, 2002; Rahman, Matthijnssens, *et al.*, 2005; Ghosh *et al.*, 2006; Rahman *et al.*, 2007, 2008; Matthijnssens *et al.*, 2009, 2010; Arana *et al.*, 2019).

These same strains were circulating in the UK prior to vaccine introduction in 2013 (section 1.12), with G1P[8] being the most common circulating strain (Iturriza-Gómara *et al.*, 2000, 2008, 2011; Hungerford *et al.*, 2016). Since rotavirus vaccination has been offered to all infants, the strain distribution has changed, with a vaccine-derived G1P[8] being the most common strain in <6 month-olds, likely

representing vaccine shedding post-vaccination; and G2P[4] followed by G9P[8] being the most frequently detected strains in >6 month-olds (Hungerford *et al.*, 2019), showing that there are strain differences in age distribution.

1.8 Population epidemiology

In temperate climates, rotavirus infection peaks annually in winter and spring (Kapikian *et al.*, 1976; Cook *et al.*, 1990). In contrast, in tropical climates, it is spread during the year and there is no defined peak, probably due to higher strain diversity and a lower transmission rate, maintaining infection levels in humans as reservoir (Cook *et al.*, 1990). In the USA, around 10 years after vaccine introduction (section 1.10.3), biannual peaks in rotavirus cases have been observed due to accumulation of susceptible children (Payne, 2019).

Most of the fatal disease caused by RV (>80%) affects children in developing countries due to their hygiene and sanitation, nutritional status, potential co-infections and reduced access to rapid treatment (Parashar *et al.*, 2003, 2006). Rotavirus infects almost every child by the age of 5, causing more severe disease in those younger than 2 years, except neonates (infants younger than one month), whose infections are less frequent and severe likely due to protection by maternal antibodies (Parashar *et al.*, 2003). Children undergo sequential rotavirus infections in early infancy, with less severe symptoms after each infection (Velázquez *et al.*, 1996; White *et al.*, 2008; Gladstone *et al.*, 2011). Although less of a public health burden, RVAs have also been associated with diarrhoea in adults and the elderly, which may go unreported or appear as sporadic cases or outbreaks (Anderson and Weber, 2004; Centers for Disease and Control (CDC), 2011; Anderson *et al.*, 2012). Wild-type and vaccine derived RV chronic infections have been described in immunodeficient infants (Saulsbury, Winkelstein and Yolken, 1980; N. C. Patel *et al.*, 2012; Kaplon *et al.*, 2015; Rosenfeld *et al.*, 2017), as well as adults (Mori *et al.*, 2002); and RV diarrhoea has been observed in travelers to the Caribbean and surroundings (Bolivar *et al.*, 1978; Steffen *et al.*, 1999), as well as in healthcare settings (Cubitt and Holzel, 1980; Abbas and Denton, 1987; Ryan *et al.*, 1997).

Horizontal transmission of WT and vaccine-derived RV from infected children to older siblings, adults or the elderly in the household has been reported, showing that WT transmission leads to RV infection with a protective effect in the

newly infected individuals (Rodriguez *et al.*, 1979; Grimwood *et al.*, 1983; Rivera *et al.*, 2011; Miura *et al.*, 2017; Bennett *et al.*, 2019). In other cases, the outcome for the household contacts of infected infants was unclear (Kaneko *et al.*, 2017) or resulted in gastroenteritis (Payne *et al.*, 2010; Wikswo *et al.*, 2019). Vaccination of infants (sections 1.10 & 1.12) has also resulted in protection of other unvaccinated children and adults (Lopman *et al.*, 2011; Paulke-Korinek *et al.*, 2011; Gastañaduy *et al.*, 2013; Pollard *et al.*, 2015; Prelog *et al.*, 2016). In developing countries, the indirect effects of vaccination are less clear (Bennett, Bar-Zeev and Cunliffe, 2016; Bennett *et al.*, 2018). Herd protection may be due to a decrease in WT RV transmission among vaccinated infants, reducing the overall transmission in the population (Parashar, Nelson and Kang, 2013), including adults. In the UK, the herd effect in older children the year after vaccine introduction was large, likely due to vaccination starting in July (2013), well in advance of the rotavirus season in the country, and rapid high vaccine coverage (PHE, 2014; Marlow *et al.*, 2015).

1.9 Disease burden

According to the World Health Organization (WHO) estimate for 2008, rotavirus was responsible for 453,000 deaths per year worldwide (Tate *et al.*, 2012), most of them in developing countries (Figs. 1.9 & 1.10). Using data from 2013, after vaccine introduction in many countries, the WHO estimated that the annual RV-associated mortality had dropped to 215,000 deaths/year (Angel, Steele and Franco, 2014; Tate *et al.*, 2016; WHO, 2016). Rotavirus hospitalization worldwide ranged from 30% to 50% of those infected, and 38% of diarrhoea cases in the under 5-year-olds are due to rotavirus (Parashar *et al.*, 2006; Lanata *et al.*, 2013). After vaccine introduction, hospitalisation cases reduced by 16-99% in developed countries (Curns *et al.*, 2010; Braeckman *et al.*, 2012; David and Kirk, 2014; Shah *et al.*, 2018) and by 11-81% in developing countries (Molto *et al.*, 2011; Quintanar-Solares *et al.*, 2011; Yen, Armero Guardado, *et al.*, 2011; Abeid *et al.*, 2016; Bennett *et al.*, 2018).

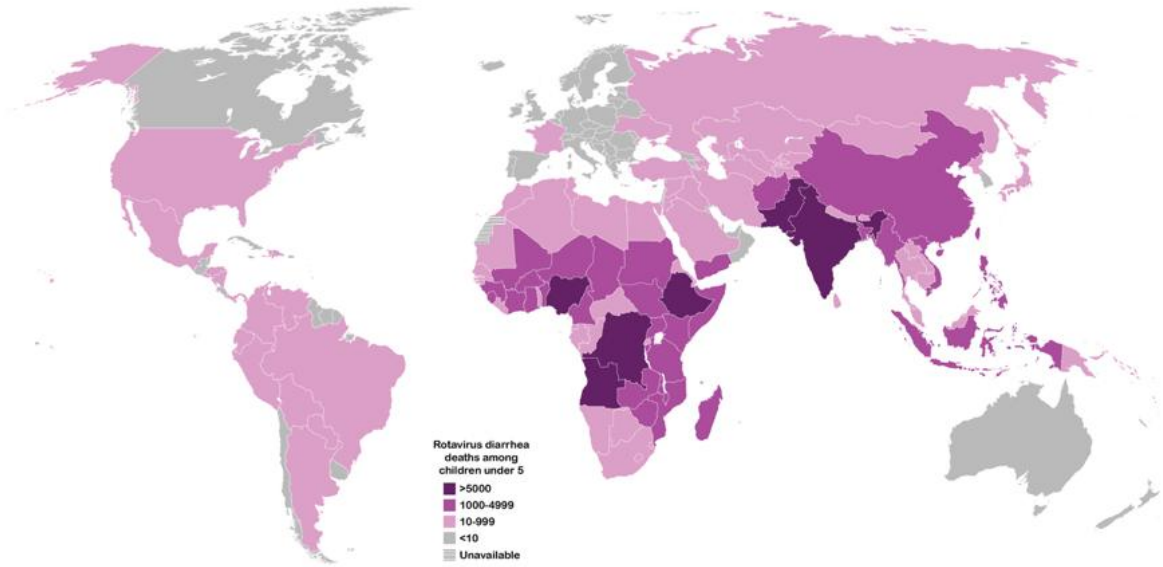

Fig. 1.9. Rotavirus diarrhoea deaths among children under 5 years of age worldwide, 2013. From www.rotacouncil.org, originally from Tate *et al.*, 2016. With permission from Clinical Infectious Diseases Copyright Clearance Center's RightsLink® order no. 4625820118538 (11/07/19).

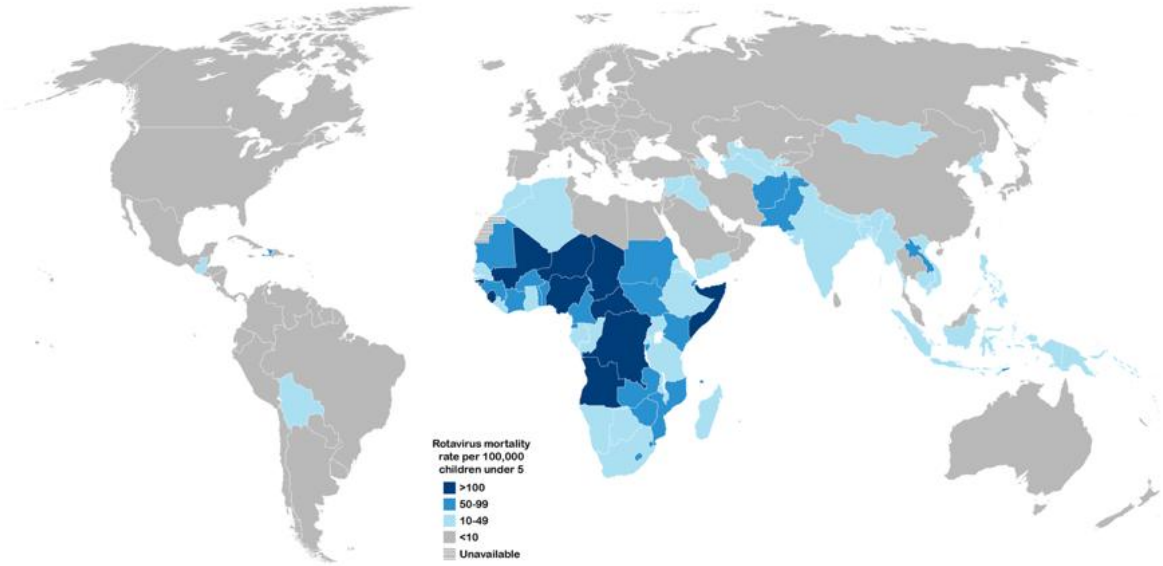

Fig. 1.10. Rotavirus mortality rate per 100,000 among children under 5 years of age worldwide, 2013. From www.rotacouncil.org, originally from Tate *et al.*, 2016. With permission from Clinical Infectious Diseases Copyright Clearance Center's RightsLink® order no. 4625820118538 (11/07/19).

In the UK, the Department of Health estimated that RV infection prior to vaccination introduction accounted for 140,000 cases of diarrhoea each year in under-5s, of which around 10% result in hospitalizations due to dehydration Before vaccine introduction, it was estimated by modelling that RV was responsible for 45%

of hospitalisations, 25% of GP consultations, 27% of national health service (NHS) calls and 20% of emergency attendances related to severe GE (Harris *et al.*, 2007). Other reports estimated that there were 750,000 diarrhoea episodes and 80,000 general practice consultations per year in the UK (Hungerford *et al.*, 2014). Later, it was estimated that the economic cost of rotavirus disease in the UK in the period of 2008 to 2009 was about £25 million (Tam and O'Brien, 2016).

1.10 Rotavirus vaccines

Rotavirus disease burden has led to extensive vaccine development, in order to protect against the high morbidity and mortality caused by severe RVGE. Animal rotavirus vaccines are available for cows (Rotavec®Corona, MSD), pigs (Prosystem®Rota, Merck, 2012) and horses (Equip Rotavirus Emulsion, Zoetis). Vaccines against RV for humans have been available as prophylaxes for >10 years and are the focus of this section.

Since rotavirus replicates in the gut, oral, live-attenuated vaccines that mimicked the natural rotavirus infection and elicited a similar mucosal response to that against WT RV infection were the first to be designed. The two or three dose administration schedule is based on second and following infections being more effective at protecting against severe disease and different RV strains.

1.10.1 History of rotavirus vaccines

Based on the Jennerian approach that strains from animals are naturally attenuated in humans and generate an immune response, the first rotavirus vaccines were based on animal RV strains.

1.10.1.1 RIT 4237

RIT 4237 was an oral, live-attenuated, monovalent, bovine neonatal calf diarrhoea virus (NCDV) strain (G6P6[1]), manufactured by Smith Kline Beecham (Belgium), safe (Vesikari *et al.*, 1983) and shown to be highly efficacious (>80%) against severe diarrhoea in Finland (Vesikari *et al.*, 1985, 1986). However, it was discontinued later due to lack of efficacy and lack of cross-protection when tested in

developing countries (De Mol *et al.*, 1986; Hanlon *et al.*, 1987; Lanata *et al.*, 1989; Santosham *et al.*, 1991).

1.10.1.2 Bovine WC3 (G6P7[5])

WC3 was an oral live-attenuated, monovalent bovine G6P[5] strain manufactured by Merck Research Laboratories (Merck & Co. Inc.; West Point, PA, USA) in Pennsylvania in 1981 at the Wistar Institute of Anatomy and Biology (Clark *et al.*, 1986). It was generated from a bovine isolate from a calf at the veterinary school of the University of Pennsylvania, passaged 12 times in a *Cercopithecus* CV1 cell line and tested in clinical trials (Clark *et al.*, 1986, 1988; Bernstein, Kacica, *et al.*, 1989). Although it presented good safety and immunogenicity, protection was inconsistent. There were no adverse effects, but it failed due to lack of protection against RVGE (Bernstein *et al.*, 1990). Vaccination was protective against human RV in a small proportion of vaccinees, but did not modify the WT infection rate in vaccinees and did not prevent reinfection (Ward, Sander, *et al.*, 1990). In a trial in central Africa, there was lower severity of RVGE in the vaccinated group, although the appearance of RV-specific antibodies did not guarantee protection (Georges-Courbot *et al.*, 1991).

1.10.1.3 Rhesus rotavirus vaccine (RRV)

RRV was an oral, live-attenuated, monovalent, simian strain MMU 18006 (G3P5B[3]). It was generated by passaging a monkey isolate six times in primary megakaryoblastic cells (CMK) (Stuker, Oshiro and Schmidt, 1980). It was immunogenic and it protected vaccinated children against RVGE in North America, South America and Europe (Anderson *et al.*, 1986; Losonsky *et al.*, 1986; Vesikari *et al.*, 1986; Wright *et al.*, 1987; Flores, Daoud, *et al.*, 1988; Flores *et al.*, 1989; Gothefors *et al.*, 1989; Madore *et al.*, 1992), but was not as efficacious in certain populations in North America (Santosham *et al.*, 1991, 1997). It failed due to secondary effects, such as fever and GE (Losonsky *et al.*, 1986; Vesikari *et al.*, 1986).

1.10.1.4 RotaShield®

RotaShield® was an oral, live-attenuated, human-rhesus rotavirus tetravalent (RR-TV) reassortant manufactured by Wyeth Lederle Vaccines S.A. (Philadelphia, USA) and licensed in 1998 in the USA. It expressed RRV G3 and three human G serotypes RRV-based G1, G2 and G4 (Ward, 2008) and was administered in three doses. Its efficacy was higher for severe disease (>70%) than for all rotavirus disease (>49%) (Rennels *et al.*, 1996; Joensuu *et al.*, 1997; Santosham *et al.*, 1997; Ward, Knowlton, *et al.*, 1997).

In 1999, RotaShield® was found to correlate with intussusception in 1/10,000 cases of vaccinated infants and was therefore withdrawn from the market a year later (Centres for Disease Control (CDC), 1999; Murphy *et al.*, 2001, 2003; Peter *et al.*, 2002). Intussusception is a condition that causes part of the intestine to invaginate or fold into another section of the intestine and can lead to obstruction, necrosis, ischemia and sepsis (Poole and Penny, 2018). It is the commonest cause of acute bowel obstruction in children younger than two years old (Bines *et al.*, 2004; Waseem and Rosenberg, 2008), idiopathic in most of the cases, with a potential origin in viral infections by rotavirus, adenovirus and others. Ruling out such a risk has become critical for the licensure and universal use of any new rotavirus vaccine. There was a gap in availability of a global rotavirus vaccine when RotaShield® was withdrawn from the market, as well as a need for large clinical trials (Phase III) designed to guarantee safety and reduce the risk of intussusception in future vaccines (Yung, Chong and Thoon, 2016).

1.10.2 Current licensed vaccines used globally

There are two live attenuated rotavirus vaccines available globally for public use since 2010: RotaTeq® and Rotarix®. Such vaccines are highly effective at protecting individuals against infection. However, as they contain live virus, they may cause mild disease and the virus may acquire mutations that alter genetic stability. As G1P[8] was the most common strain of RVA circulating globally at the time, these VP7/VP4 serotypes have been included in both vaccines in order to provide wide protection.

1.10.2.1 RotaTeq®

RotaTeq® is an oral, live-attenuated, pentavalent human-bovine (strain WC3) reassortant manufactured by Merck Sharp & Dohme Corp. (MSD, White Station, NJ, USA) and licensed in 2006. Rotaviruses were reassorted in cell culture, with an animal rotavirus genetic background plus human rotavirus VP4 and VP7 genes representing common P and G types circulating globally. RotaTeq® contains four human G types G1-G4 and one human P type P1A[8], plus bovine serotypes G6 and P[5] from strain WC3 (Midthun *et al.*, 1985; Hoshino *et al.*, 1997; Clark *et al.*, 2006). It was well tolerated and highly efficacious at protecting against severe RVGE, with neutralizing IgA generated in a proportion of vaccinees (Clark, Borian and Plotkin, 1990; Treanor *et al.*, 1995; Clark *et al.*, 2004; Vesikari, Matson, *et al.*, 2006; Ciarlet and Schödel, 2009; Vesikari *et al.*, 2009; Staat *et al.*, 2011; El Khoury *et al.*, 2014). There was some correlation between protection and serotype-specific NAb levels, but none between efficacy and IgA levels in serum or stool (Ward *et al.*, 2004; Vesikari, Clark, *et al.*, 2006).

RotaTeq® is recommended to be administered in three doses: Dose 1 at 6-12 weeks of age followed by booster doses in a 4- to 10-week interval before 32 weeks of age (MerckVaccines.com, 2018). In the USA, it has been included since 2006 in the vaccination programme and administered at 2, 4 and 6 months of age (CDC, 2018).

1.10.2.2 Rotarix®

Rotarix® is an oral, live attenuated, monovalent human G1P[8] strain manufactured by Glaxo SmithKline Biologicals SA (GSK, Rixensart, Belgium) and licensed in 2008. It is administered in two doses at between 6 and 14 weeks of age for dose 1 with an interval between doses of at least 4 weeks (EMA, 2008). The second dose should be given preferably before 16 weeks of age and the last dose must be administered before 24 weeks of age (EMA, 2008) to prevent any association with age of incidence of intussusception, given the history of RotaShield® withdrawal from the market in 1998.

Rotarix® is derived from a single strain of human rotavirus RIX4414, 89-12 strain from a child suffering from RV infection and diarrhoea in the 1988-89 season

(Bernstein *et al.*, 1999). To attenuate the virus, it was passaged 26 times in primary African green monkey kidney (AGMK) cells and a further seven times in an AGMK cell line (Bernstein, 1998). This candidate RV vaccine virus was passaged 43 times in Vero cells, plaque-purified and lyophilised at GSK. Rotarix® contains no less than $10^{6.0}$ cell culture infectious dose 50 ($CCID_{50}$) per dose (1.5 mL).

The manufacturing process of Rotarix® consists of an initial master viral seed G1P[8] RV strain, which is used to infect Vero cells, passaged multiple times (working seed) to attenuate the virus and an intermediate virus culture (inoculum) is used as to produce the single harvest called vaccine bulk (Ruiz-Palacios *et al.*, 2006; EMA, 2008). Harvests are pooled (bulk virus pool), clarified to discard Vero cell debris, DNAse-treated with benzonase and ultrafiltered (final bulk). Following sterile filtration, the final bulks are filled into sterile containers (final fill) (EMA, 2008) which are the biological medicine that is delivered to the vaccinee.

Rotarix® was tested in a randomised, double-blind, Phase III clinical trial in South America and Finland (Ruiz-Palacios *et al.*, 2006). It was shown to be 85% effective at protecting against rotavirus AGE and rotavirus-associated hospitalisation, and 100% against most severe RVGE. During the trial, hospitalisations for diarrhoea decreased by 42%. Rotarix® provided protection from the first dose and resulted cross-protective against other RV, such as G2P[4] (Vesikari *et al.*, 2007; Yen, Tate, *et al.*, 2011). Infection with monovalent G1P[8] vaccine virus has been shown to cross-protect against non-G1 rotaviruses (Ward *et al.*, 2006), which supported the idea of heterotypic protection of this vaccine. Rotarix® has been reported to be over 85% effective at protecting against severe rotavirus infection in the first two years of life in countries with low mortality rates (Soares-Weiser *et al.*, 2012). In a study comparing the safety and immunogenicity of Rotarix® in 2005, vaccine 'take' for Rotarix® was defined as serum RV-specific IgA seroconversion or vaccine RV shedding between the date of the first dose and two months after the second dose, as a measure to consider the vaccine had elicited a response in the vaccine recipient (Dennehy *et al.*, 2005).

1.10.3 Vaccines licensed for restricted markets

Other RV vaccines are or have been available for use in more restricted capacities or geographical areas.

1.10.3.1 Lanzhou lamb rotavirus (LLR)

LLR is an oral, live-attenuated, monovalent, lamb G10P[12] strain isolated in 1984 in primary calf kidney cells, manufactured by the Lanzhou Institute of Biological Products (Lanzhou, China) and licensed for use in China since 2000 (Fu, Tate and Jiang, 2010). It was developed from the lamb strain LLR-85 (Chang *et al.*, 2010). Before its use, G10 was the main G type circulating, while currently G3, G1 and G9 are filling the niche (Zhen *et al.*, 2015). It is administered every year for three years between 2 and 35 months of age. LLR presented an efficacy of 44.3% in preventing hospitalisation (Fu *et al.*, 2007) and a recent publication has confirmed vaccine efficacy of >30% against GE (Li *et al.*, 2019).

1.10.3.2 Rotavin-M1®

Rotavin-M1® is an oral, live-attenuated, monovalent, human G1P[8] strain (KH0118-2003) isolated in 2003 from a child in Vietnam (Le *et al.*, 2009). It was developed by the Vietnamese Center for Research and Production of Vaccines (POLYVAC) and licensed in 2007. It is attenuated by serial passage in Vero cells. Rotavin-M1® is administered in two doses at $10^{6.3}$ focus forming units (FFU)/dose, the first dose from 6 weeks of age and the second dose after 1-2 months (before 6 months of age), with seroconversion of 73% and good safety and immunogenicity in Vietnamese infants (Clinicaltrials.gov, 2012, 2016c, 2016a; Dang *et al.*, 2012). Another study to test the safety and immunogenicity of its liquid formulation is on-going (Clinicaltrials.gov, 2018). A later trial will assess efficacy of Rotavin-M1® (Carey, 2017).

1.10.3.3 ROTAVAC® or 116E

ROTAVAC® is an oral, live-attenuated, monovalent, human G9P[11] strain 116E isolated from asymptomatic neonates born during 1986-88 (Bhan *et al.*, 1993; Das *et al.*, 1994). It is manufactured at the All India Institute of Medical Sciences, New Delhi, in collaboration with Bharat Biotech International Ltd (Hyderabad, India) (Glass *et al.*, 2005; Bhan *et al.*, 2014) and was licensed in India in 2014. It was attenuated by serial passage in Vero cells and administered in three doses separated by a month each, starting at 6 weeks of age, containing 0.5 mL with not less than

$10^{5.0}$ FFU of live rotavirus (BharatBiotech, 2018). It protects against subsequent disease and presents an efficacy of 53.6% against severe diarrhoea during the first year and 48.9% during the second year (Bhandari *et al.*, 2014a; Bhandari *et al.*, 2014b). It was modelled to have a substantial impact on RV-related mortality and morbidity in India directly due to vaccination and not herd immunity, with introduction being cost-effectiveness (Rose *et al.*, 2017). This vaccine has now received WHO prequalification status making it available for procurement by agencies such as UNICEF or GAVI for use in low and middle-income countries (LMIC) (PATH, 2018).

1.10.3.4 RotaSIIL®

This vaccine was co-developed by the Serum Institute of India and the USA National Institute of Allergy and Infectious Diseases and the Programme for Appropriate Technology in Health (PATH) as a pentavalent human-bovine reassortant. Several studies have shown an efficacy >60% at protecting against severe RVGE in infants in Niger and have deemed the vaccine safe (Isanaka *et al.*, 2017; Coldiron *et al.*, 2018). Recently, it has shown safety and immunogenicity similar to Rotarix® (Rathi *et al.*, 2018). It has been licensed in India since 2016 and was granted WHO prequalification status in September 2018 (PATH, 2018b).

1.10.4 Live-attenuated vaccines in development

1.10.4.1 RV3-BB rotavirus vaccine

RV3-BB is an oral, live-attenuated, monovalent human G3P2[6] strain isolated from an asymptomatic child in Australia, developed by PT Biofarma (Indonesia), Murdoch Children's Research Institute (Australia) and DynCorp (USA). The vaccine is designed with a view of administration to neonates (Bishop *et al.*, 1983). It is a naturally-attenuated RV strain that replicates despite maternal sIgA present and provides heterotypic protection against severe disease by other human strains (Chen *et al.*, 2017). It has been shown to be well tolerated and immunogenic (Danchin *et al.*, 2013; Bines *et al.*, 2015). RV3-BB has been shown to have an efficacy of up to 75% in neonates in Indonesia.

1.10.4.2 UK-based reassortants (UK-BRV) (NIH)

UK-Compton bovine rotavirus vaccine (UK-BRV) is an oral, live-attenuated, quadrivalent, human-bovine reassortant developed by several manufacturers, such as Butantan, Brazil; Wuhan & Chengdu, China; SSI, India; Shanta, Biologicals E, Bharat, India. It originally contained the G6P[5] bovine backbone plus the human G types G1, G2, G3, G4, and later G types G8 and G9 were also added. The first UK-BRV reassortants are well tolerated, safe, immunogenic and efficacious (Clements-Mann *et al.*, 1999, 2001; Kapikian *et al.*, 2005; Vesikari, Karvonen, *et al.*, 2006). The resassortant manufactured by the Serum Institute of India was safe, immunogenic and efficacious (Zade *et al.*, 2014). The development of several candidate UK-BRV reassortants was stopped due to market competition from the oral rotavirus vaccines currently licensed.

1.10.5 Non-replicating vaccines

Non-replicating vaccines are developed to improve safety (e.g. intussusception related to early live attenuated rotavirus vaccines, reversion to virulence in the immunocompromised recipient or following transmission to immunocompromised or susceptible contacts or contamination with adventitious viruses), as well as efficacy and effectiveness (which are low in LIMCs). They may also be used in combination vaccines, be administered following a different dosing schedule and may be more cost-effective in LIMCs (cost of live-attenuated vaccines still high).

1.10.5.1 P2-VP8 protein subunit vaccine*

P2-VP8* is a non-replicating RV vaccine (NRRV) that contains a recombinant VP8* subunit RV from G1P[8] (Wa) strain or human P types P[4] or P[6] fused to the tetanus toxin P2 CD4 epitope (Wen *et al.*, 2012). It was developed by PATH and the USA National Institutes of Health (NIH). It was designed for parenteral administration. P2-VP8* was safe, highly immunogenic (homotypic and heterotypic immunity in guinea pigs) and highly efficacious against severe RVGE (Wen *et al.*, 2012, 2015; Clinicaltrials.gov, 2013; Fix *et al.*, 2015). In humans, it was well tolerated and immunogenic in healthy toddlers and infants (Clinicaltrials.gov,

2014, 2016b; Groome *et al.*, 2017). A Phase III superiority trial against the comparator (Rotarix®) will commence soon in three African countries (Malawi, Ghana, Zambia) and India (Clinicaltrials.gov, 2019).

1.10.5.2 Inactivated rotavirus vaccine (IRV)

CDC-9 is a heat-inactivated monovalent strain G1P[8], generated by the USA Centers for Disease Control and Prevention. It was grown in Vero cells, heat-inactivated and formulated with aluminium phosphate (Jiang, Gentsch and Glass, 2008; Esona *et al.*, 2010). Studies in mice, guinea pigs and gnotobiotic piglets indicated it was immunogenic when administered intramuscularly (Wang *et al.*, 2010; Jiang, Wang and Glass, 2013) and it can be administered intradermally (Moon, Wang, *et al.*, 2013; Wang *et al.*, 2016). This candidate vaccine induced mucosal immunity in mice (Resch *et al.*, 2018) and it is still in pre-clinical stages with a Phase I trial set up yet to be established (Steele, Kirkwood and Ma, 2018).

1.10.5.3 RV subunits and virus-like particles (VLPs)

Mice immunised with chimeric VP6 and an adjuvant were protected against shedding and did not require intestinal IgA (Choi *et al.*, 1999; McNeal *et al.*, 2006). MBP:VP6 candidate was immunogenic and protective in mice (Ward and McNeal, 2010). A combination of RV recombinant VP6 and norovirus VLPs have been shown to elicit immune responses able to inhibit viral replication both *in vitro* and *in vivo* in mice (Lappalainen *et al.*, 2014) and RV nanostructures have been shown to act as local adjuvants in combination with norovirus VLPs (Malm *et al.*, 2017). They have also been shown to induce heterogeneous $CD4^+$ T cell subsets (Heinimäki *et al.*, 2018).

VLPs have been designed as candidate vaccines as triple-layered or double-layered and tested in mice for immunogenicity (Bertolotti-Ciarlet *et al.*, 2003; Lappalainen *et al.*, 2015). Human VLPs have been tested in the gnotobiotic pig model of human RV disease, generating immunogenicity and protection in combination with an oral attenuated human RV (Azevedo *et al.*, 2013). Although in discovery phase, rotavirus VLPs may provide an advantage as next generation vaccine in terms of covering the genotypes by region and triggering both cellular and humoral immune responses (Changotra and Vij, 2017).

Rotavirus vaccines summary

The rotavirus vaccines previously described are summarised in Table 1. 2.

Table 1.2. Summary of rotavirus vaccines and their stage of development. Vaccine name, vaccine type and stage of development.

Vaccine name	Type	Development stage
RIT4237	Live-att., monovalent, neonatal calf strain	Discontinued (lack of efficacy)
Bovine WC3	Live-att., monovalent, bovine strain	Discontinued (inconsistent protection)
RRV	Live-att., monovalent simian strain	Discontinued (2^{ary} effects: fever, GE)
RotaShield®	Live-att., tetravalent human-rhesus reassortant	Discontinued (intussusception)
RotaTeq®	Live-att., pentavalent human-bovine reassortant	In use worldwide
Rotarix®	Live-attenuated, monovalent human strain	In use worldwide
LLR	Live-att., monovalent lamb strain	In use in China
Rotavin-M1®	Live-att., monovalent human strain	In use in Vietman
ROTAVAC®	Live-att., monovalent human strain	In use in India (& WHO prequalification)
RotaSIIL®	Live-att., pentavalent human-bovine reassortant	In use in India (& WHO prequalification)
RV3-BB	Live-att., monovalent neonate human strain	Phase Iia trial
UK-BRV	Live-att., teatravalent human-bovine reassortant	Discontinued (market competition)
P2-VP8*	Non-replicating, recombinant protein subunit	Phase III superiority trial
CDC-9	Heat-inactivated, monovalent human strain	Phase I trial
RV subunits	VP6 or MBP:VP6	Preclinical
RV VLPs	TLPs or DLPs	Preclinical

1.11 Vaccine efficacy and effectiveness

Rotavirus vaccines have had reduced impact in low-income countries (LICs) compared to developed countries with respect to vaccine efficacy (Ruiz-Palacios *et al.*, 2006, 2007; Vesikari *et al.*, 2007; Linhares *et al.*, 2008; Madhi *et al.*, 2010; Vesikari, 2012; Bhandari, Rongsen-Chandola, Bavdekar, John, Antony, Taneja, Goyal, Kawade, Kang, Rathore, Juvekar, Muliyil, Arya, Shaikh, Abraham, Vrati, Proschan, Kohberger, Thiry, Glass, Harry B Greenberg, *et al.*, 2014; Liu *et al.*, 2014; Jonesteller *et al.*, 2017; Velázquez *et al.*, 2017; Bar-Zeev *et al.*, 2018) and rotavirus infection remains the main cause of severe infantile gastroenteritis, with the greatest impact on infant mortality and morbidity in LICs. Several factors related to the specific immune response to the vaccine, their induced global immune response and epidemiology of RV influence the reduction and prevention of disease in vaccinated individuals.

1.11.1 Vaccine-specific host immune response

The main factors related to rotavirus vaccine virus reaching the gut epithelium and being able to infect mature enterocytes are described below. It is believed that early vaccination may improve vaccine immunogenicity (Bhan *et al.*, 1993; Bines *et al.*, 2015, 2018; Vesikari, 2015; Cowley *et al.*, 2017).

1.11.1.1 Maternal antibodies and breast milk

Babies acquire antibodies from their mothers transplacentally, mainly IgG, that remain at similar titres to those in the mother's serum for one to six months and may interfere with oral rotavirus vaccination (Becker-Dreps *et al.*, 2015; Moon *et al.*, 2016; Parker, Ramani, *et al.*, 2018). Although the placenta does not allow for IgA transfer, newborns can acquire IgA when breastfed (Patel *et al.*, 2009; Parker, Ramani, *et al.*, 2018). If maternally-acquired antibodies are neutralizing for rotavirus, they would likely target RV vaccine virus together with receptor analogues present in breast milk (lactadherin), inhibiting the vaccine virus replication (Morrow *et al.*, 2005; Patel *et al.*, 2009; Moon *et al.*, 2010; Parker, Ramani, *et al.*, 2018). The effect of breastfeeding on vaccine efficacy and effectiveness is not well elucidated. While some studies had observed lower immunogenicity in breastfed infants (Pichichero,

1990; Glass *et al.*, 1991; Rennels, 1996; Dennehy *et al.*, 2005), others testing the effect of withdrawal of breastfeeding around vaccination observed no improvement on vaccine effectiveness (Groome *et al.*, 2014; Rongsen-Chandola *et al.*, 2014; Ali *et al.*, 2015). The theory that breastfeeding inhibits vaccine virus is currently not supported because a reduction in immunogenicity has been observed at a group/population level but not at the individual level (Patel *et al.*, 2009). Moreover, breastfeeding is important for regulatory T cell activation in infants (M'Rabet *et al.*, 2008), since breast milk contains factors that may buffer the virus from stomach acid and allow it to travel to the small intestine (Rennels, 1996) and it contains binding oligosaccharides and other immunoglobulins that are protective against different enteric pathogens (Bilenko *et al.*, 2008; Cacho and Lawrence, 2017).

1.11.1.2 Stomach acid

Because low pH can inactivate rotavirus (Weiss and Clark, 1985), Rotarix® contains a buffer (calcium carbonate) to neutralise stomach acid (EMA, 2008; Lal and Jarrahian, 2017). However, stomach acid levels may vary in different populations (Patel *et al.*, 2009) and so vaccination may be less effective in those populations with higher stomach pH levels, important for protection against salmonellosis, cholera and other bacterial infections.

1.11.1.3 Microbiome

At birth, the gastrointestinal tract is colonised by commensal bacteria that are different depending on mode of child delivery, subsequent feeding (breast milk, formula-fed; solid food diet) and any use of antibiotics (Dominguez-Bello *et al.*, 2010; Dzidic *et al.*, 2018). The composition of the human microbiota changes with age; it stabilises and becomes differentiated around the age of 3-5 years, and this composition is strongly influenced by geographical location and diet (Dzidic *et al.*, 2018). In the case of rotavirus, susceptibility to infection may be partly influenced by certain gut bacteria (and viruses). For instance, in a small adult cohort in Spain, a negative correlation of *Faecalibacterium* and *Ruminococcaceae* with susceptibility to RV infection and a positive correlation of *Akkermansia* with susceptibility to RV infection were inferred from IgA titres in saliva (Rodríguez-Díaz *et al.*, 2017). In a study in vaccinated adults, antibiotics did not alter absolute RV-specific IgA titres

but they were associated with an increase in RV-specific IgA boosting and RV faecal shedding at day 7 (Harris, Haak, *et al.*, 2018). In a small study in Ghana, it was found by the same group that the infant Bacteroidetes phylum correlated positively and bacteria such as *Streptococcus bovis* correlated negatively with RV vaccine immunogenicity (Harris *et al.*, 2017). In another small cohort study by that group, in Pakistan, it was found that infant Proteobacteria correlated with RV vaccine immunogenicity, although the control group were assumed to be high vaccine responders but had not been given the vaccine (Harris, Ali, *et al.*, 2018). In another study in infants in India, however, a modest correlation was found between microbiota richness and Rotarix® shedding (Parker, Praharaj, *et al.*, 2018).

1.11.1.4 Oral poliovirus immunisation

Co-administration of live-attenuated oral poliovirus vaccine (OPV) with Rotarix® has been observed to lower seroconversion of rotavirus vaccination in developing settings such as South Africa and Bangladesh, where OPV was mainly used (Patel, Steele and Parashar, 2012). OPV is thought to outcompete rotavirus vaccine replication after the first dose, while after subsequent RV doses the interference is overcome. In other settings in Latin America, OPV presented no interference with Rotarix® efficacy (Patel, Steele and Parashar, 2012). In Malawi, no interference with Rotarix® shedding was observed and shedding of OPV showed common patterns with the response to Rotarix® (Pollock, 2018). In 2012, the WHO recommended the inactivated poliovirus vaccine (IPV) to gradually substitute OPV due to the risk of vaccine-derived polio higher than the benefits of OPV vaccination (WHO, 2012), therefore potentially reducing the risk of OPV interference with rotavirus vaccination in those settings where IPV vaccination has been implemented.

1.11.1.5 Host genetic polymorphism

Common genetic polymorphisms determining RV susceptibility could contribute to population differences in vaccine efficacy as well as RV epidemiology. Genetic polymorphisms in HBGAs are encoded by fucosyltransferase genes such as *FUT2* and *FUT3*, which define secretor status and Lewis antigen status respectively. Interactions of rotavirus with HBGA depend on the VP4 genotype, with binding depending on strain. Recently, it was found that the presence of fucosylated ligands

was related to susceptibility to RV-genotype-specific infection and that lack of fucosylated ligands on HBGAs was associated with resistance to GE caused by P[8] RVAs (Imbert-Marcille *et al.*, 2014; Nordgren *et al.*, 2014; Barbé *et al.*, 2018). However, in LMICs such as Malawi, secretory and Lewis status did not predict vaccine (Rotarix®) uptake, although non-secretor phenotype was associated with a lower risk of vaccine failure (Pollock *et al.*, 2018). This counterintuitive finding can be explained by G1P[8] strains being the most prevalent in Malawi, and non-secretors having a degree of natural resistance to severe disease associated with this RV genotype. Non-secretors in Malawi were susceptible to infection by G1P[8] RV, shedding virus at lower levels than secretors and they were significantly resistant to severe GE (Pollock *et al.*, 2018). In Nicaragua, it was found that a small proportion of Rotarix® vaccinees of secretor phenotype remained susceptible to RVGE, while non-secretors completely resisted RVGE (Bucardo *et al.*, 2018). Moreover, they recently found that non-secretors did not shed vaccine virus following Rotarix® vaccination (Bucardo *et al.*, 2019).

1.11.1.6 Gastrointestinal tract infection/inflammation

Infants in developing countries may present a high proportion of enteroviruses at time of vaccination, which has been shown to influence OPV vaccine take and RV vaccine take slightly, potentially by binding to neighbouring receptors to the poliovirus receptor and prevent attachment and entry into target cells (Parker *et al.*, 2014; Naylor *et al.*, 2015; Taniuchi *et al.*, 2016). Moreover, in these settings, environmental enteric dysfunction (EED) or 'environmental enteropathy' is a common subclinical condition that causes flattening of the villi, malabsorption and intestinal inflammation in infants, who then present with altered GI immunity (Parker, Ramani, *et al.*, 2018). The immune response to rotavirus vaccination was found to be decreased under EED caused by enterovirus infection, likely due to the difficulty to replicate in a gut with an active antiviral state (Taniuchi *et al.*, 2016).

1.11.2 Global host immune response

The factors related to the infant's immune system state are described below.

1.11.2.1 Malnutrition

The nutritional state affects susceptibility to RV (Colgate *et al.*, 2016) and other enteric infections, having a large effect in morbidity in the under-5s in developing countries (Caulfield *et al.*, 2004). Vitamin A and zinc supplementation have helped prognosis of diarrhoeal disease and prevented mortality (Ching *et al.*, 2000; Aggarwal, Sentz and Miller, 2007). In Bangladesh, a negative correlation was found between levels of malnutrition and rotavirus infection, although authors mention other factors may have influenced rotavirus transmission (Das *et al.*, 2017). However, others have not found a correlation between malnutrition and rotavirus vaccine uptake (Parker, Ramani, *et al.*, 2018).

1.11.2.3 Co-infections (HIV, malaria, TBC)

Susceptibility to RV infection may increase in the case of certain co-infections. Mostly in developing countries, there may be concurrent enteric pathogens, viral (poliovirus, non-polio enteroviruses) or non-viral (*Escherichia coli*, *Salmonella*, *Campylobacter*, *Helicobacter pylori*, helminths), and other systemic pathogens, such as HIV, malaria or tuberculosis, affecting RV susceptibility and vaccine uptake (Patel *et al.*, 2009; Parker, Ramani, *et al.*, 2018).

1.11.3 Viral epidemiology

Vaccines that provide stronger homotypic than heterotypic protection will likely result in an increase of heterotypic strains and those which provide as strong heterotypic immunity will likely result in maintenance of the homotypic strain (Pitzer *et al.*, 2011). In the first instance, vaccination may result in a greater reduction in vaccine efficacy against heterotypic strains over time, affecting LMICs where uncommon RV types circulate (Santos and Hoshino, 2005).

Moreover, exposure to the vaccine target by undergoing a WT infection before vaccination may affect vaccine immunogenicity and prevent seroconversion (Groome *et al.*, 2014; Becker-Dreps *et al.*, 2015; Chilengi *et al.*, 2016; Moon *et al.*, 2016). This would appear to be especially relevant in developing countries, where neonates are usually exposed to WT rotavirus prior to vaccination due to a RV strong force of infection (rate at which susceptible individuals acquire an infectious disease)

(Chilengi *et al.*, 2016; Parker, Ramani, *et al.*, 2018). The levels of its force of infection, as well as the viral loads, may affect vaccine efficacy if the threshold of immunity generated by the vaccine is overcome by the intensity of transmission or amounts of infectious virus (Parker, Ramani, *et al.*, 2018).

1.12 Rotavirus vaccine implementation worldwide

In 2006, the WHO recommended the implementation of rotavirus vaccination in North and South America and in Europe (WHO, 2006). It was first introduced in Mexico (Rotarix®) and the USA (RotaTeq®) in 2006 (the USA introduced Rotarix® in 2008), followed by other countries in Latin America and Europe. Between 2006 and 2010, 27 countries implemented rotavirus vaccination in their NIPs (Patel *et al.*, 2011). In 2009, the WHO extended recommendation to worldwide vaccination (WHO, 2009, 2013). While some of the countries that bear the highest disease burden have introduced vaccination, such as Afghanistan, Angola, Ethiopia, India, Kenya and Pakistan (Tate *et al.*, 2012; RotaCouncil, 2018), others have yet to introduce the vaccine, including Chad, the Democratic Republic of Congo, Niger and Nigeria (Tate *et al.*, 2016; RotaCouncil, 2018). These countries face difficulties in rolling out rotavirus vaccination due to large birth cohorts, financial challenges to commit to GAVI-funding if eligible, costs of purchasing the vaccine if GAVI-funding-ineligible and suboptimal logistics of cold-chain storage and transport (Deen *et al.*, 2017).

To date, rotavirus vaccines have been introduced in 98 countries worldwide: 92 NIPs, and 6 sub-national introductions (Figs. 1.11 & 1.12; RotaCouncil, 2018; ViewHubRV, 2018b). Worldwide coverage is <80% in 30 countries and >80% in 60 countries (ViewHubRV, 2018c), with 70 million children lacking access to rotavirus vaccines (RotaCouncil, 2018; ViewHubRV, 2018a) due to vaccine costs and logistics (Abou-Nader *et al.*, 2018).

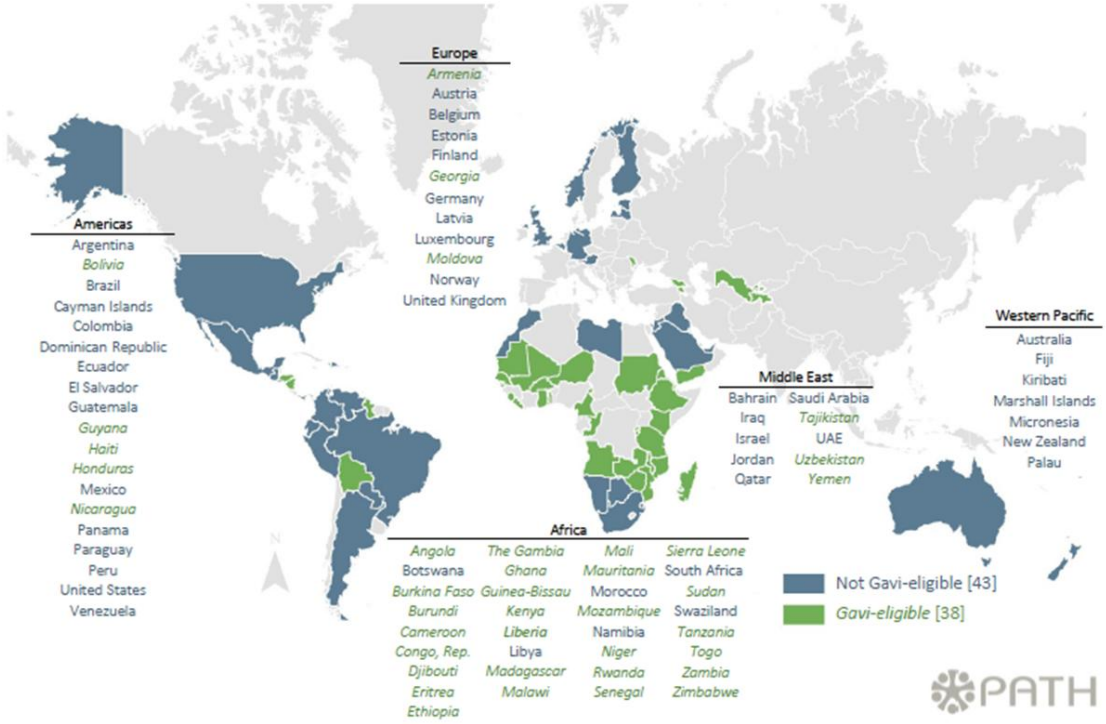

Fig. 1.11. Rotavirus national vaccine introduction worldwide, by geographic region, May 2016. A total of 81 countries had introduced rotavirus vaccination, either GAVI-eligible (in indigo) or non-GAVI eligible (in green). GAVI, global alliance for vaccines and immunization; PATH, Programme for appropriate technology in health. From Vaccineresources.org, 2016.

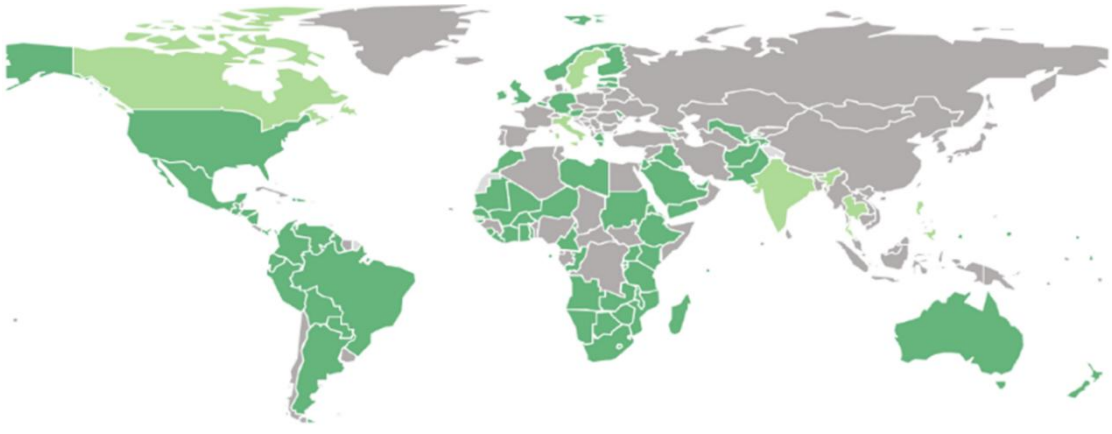

Fig. 1.12. Rotavirus vaccine introduction worldwide, August 2018. A total of 96 countries have introduced rotavirus vaccination: 89 national introductions, three ongoing phased introductions and four pilot or sub-national introductions. From RotaCouncil&ViewHubRV, 2018.

Following vaccine introduction, there was a large reduction in disease burden in many countries worldwide, with deaths from all causes of diarrhoea reduced by 17-55% and rotavirus-related hospitalizations reduced by 49-92% (M. M. Patel *et al.*,

2012; Tate and Parashar, 2014) and a decrease in nosocomial cases (Zlamy *et al.*, 2013). There has also been observed indirect protection of neonates, ineligible unvaccinated young infants, older children (two to five-year-old) and the elderly (Lopman *et al.*, 2011; Prelog *et al.*, 2016), as well as shortening of the rotavirus season and lower seasonal peaks (Tate *et al.*, 2013).

1.12.1 UK national vaccination programme

The United Kingdom (UK) implemented a national vaccination programme in July 2013 for infants of 8 and 12 weeks of age using Rotarix® (Iturriza-Gómara and Cunliffe, 2013; Gov.uk, 2014). Now, at 2 months old, as well as Rotarix®, all children concomitantly receive a licensed diphtheria, tetanus, pertussis, inactivated polio, Haemophilus influenzae type b conjugate vaccine (DTaP/IPV(polio)/Hib) (Pediacel® or Infanrix IPV Hib®), a pneumococcal conjugate vaccine (PCV) (Prevenar 13®) and a meningitis B vaccine (Bexsero®), and depending on year, some also receive the meningococcal group B vaccine (Fig. 1.13). In the UK, IPV has been administered instead of OPV since 2004. At 3 months old, infants receive the second dose of Rotarix® and the second dose of DTaP/IPV/Hib and, depending on year, some also received the meningococcal group C vaccine and the hepatitis B vaccine. Rotarix® is the only oral vaccine in the current UK childhood NIP.

Between 600,000 and 700,000 children were born every year between 2013 and 2017 in the UK (ONS, 2018). Vaccination coverage was 87.5% for both doses in the first year after vaccination introduction (PHE, 2014), 88.1% in the second year after vaccine introduction (PHE, 2015) and 88.9-89.7% in the third year (PHE, 2016a, 2016b), with more than half a million infants vaccinated per year in the UK.

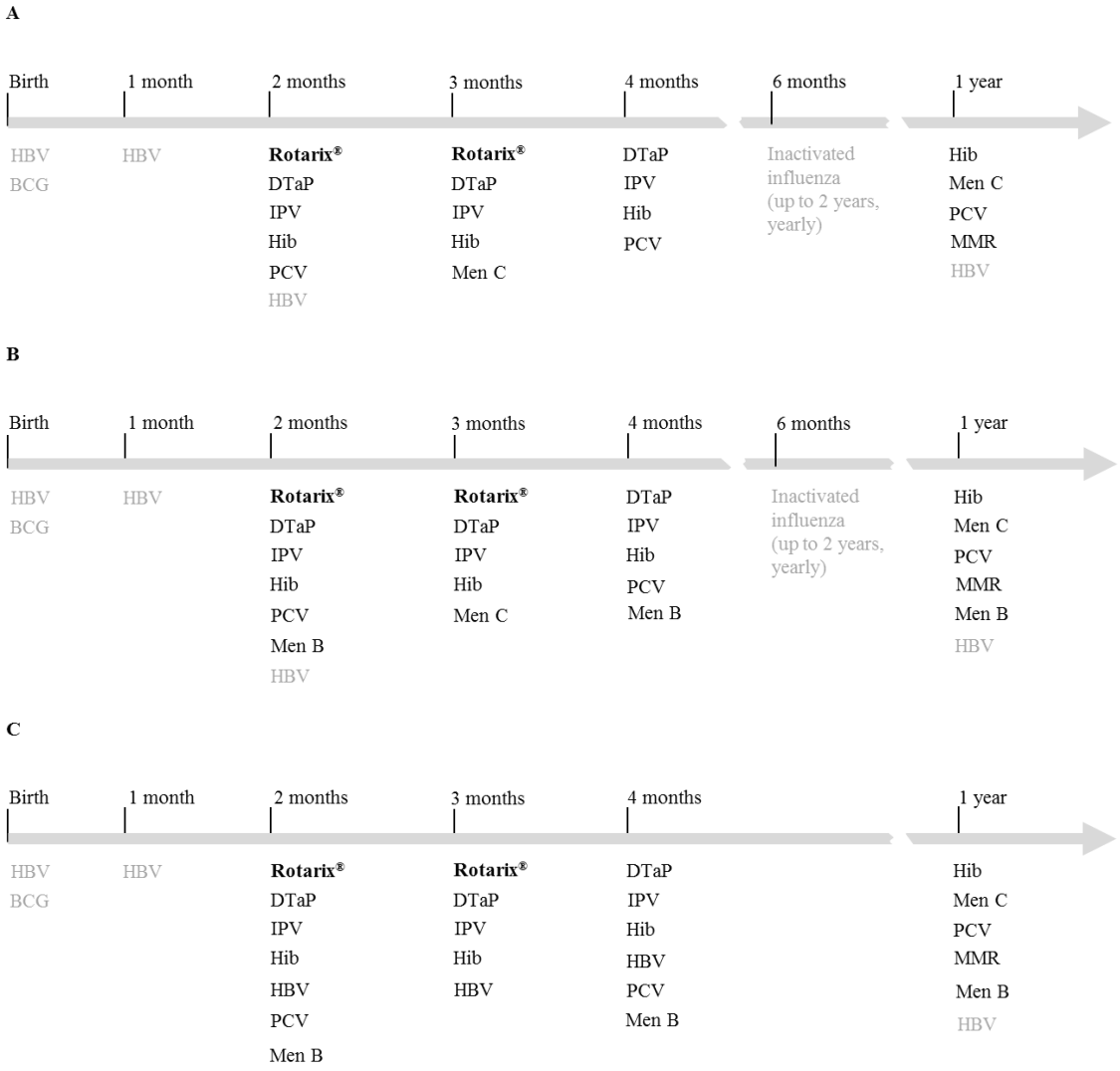

Fig. 1.13. Routine childhood immunisation programme in the UK 2013-2018. (A) 2013-2014, (B) 2015-2016 and (C) 2017-2018. Vaccinations in grey if infants at risk. BCG, Bacille Calmette Guerin vaccine; DTaP, diphtheria, tetanus and pertussis vaccine; HBV, Hepatitis B vaccine; Hib, *Haemophilus influenzae* type b vaccine; IPV, inactivated poliovirus vaccine; Men B, meningococcal group B vaccine; Men C, meningococcal group C vaccine; MMR, measles, mumps and rubella vaccine; PCV, pneumococcal conjugate vaccine. Constructed with data from Gov.uk, 2018a, 2018b.

A 77% reduction in cases of RV infection in the UK was recorded in the first year after vaccine implementation (Atchison *et al.*, 2016). Concomitantly, there was also a reduction in cases in older children (63%), adults and elderly people (42% of all averted all-cause severe GE-associated hospital admissions) (Atchison *et al.*, 2016), probably due to herd immunity and/or reduced carriage and hence lower exposure to the virus. The implementation of the vaccination programme has been estimated to save the UK National Health Service around £12.5 million in the first

year after vaccination introduction through prevented primary care, emergency department visits and hospitalisations (Thomas *et al.*, 2017).

1.13 Adventitious agent in Rotarix®

Rotarix® and RotaTeq® are live-attenuated vaccines grown in cell lines utilising trypsin derived from pig intestines (EMA, 2006, 2008) used to activavte rotavirus by generating a conformational change in the spike protein that allows cell penetration (section 1.2.5, Figs. 1.5 & 1.6). Victoria and colleagues identified DNA and viral particles of porcine circovirus 1 (PCV1) in Rotarix® using next generation sequencing (NGS) (Victoria *et al.*, 2010) and viral particles were confirmed soon after (Howe *et al.*, 2010). Following these findings, DNA -but not infectious virus- from PCV1 and PCV2 was identified in the other globally licensed rotavirus vaccine RotaTeq® (Ranucci, Tagmyer and Duncan, 2011). The use of trypsin points to the source of this contamination (Baylis *et al.*, 2011; Ma *et al.*, 2011; Dubin *et al.*, 2013).

PCV1 is an icosahedral, non-enveloped, single-stranded, circular DNA virus from the family of *Circoviridae* and genera *Circovirus* (Tischer, Rasch and Tochtermann, 1974; Mankertz *et al.*, 1997) (Fig 1.14). Circoviruses are the smallest viruses that replicate in mammalian cells: the PCV1 virion is just 17 nm in diameter. PCV1 presents a circular genome that is 1,768 bp long and very compact: there is an intergenic region flanked by two open reading frames (Fig 1.15). The *cap* gene encodes the structural protein forming the capsid and the *rep* gene encodes two replicases, both required for DNA replication and able to initiate replication at the origin of replication of PCV2 (Mankertz and Hillenbrand, 2001; Mankertz *et al.*, 2004). Although circoviruses have been found in stool of adults and pork products in the USA (Li *et al.*, 2010), PCV1 has not been found to be infectious in humans to date. PCV1 infects pigs, although no disease has been associated with infection.

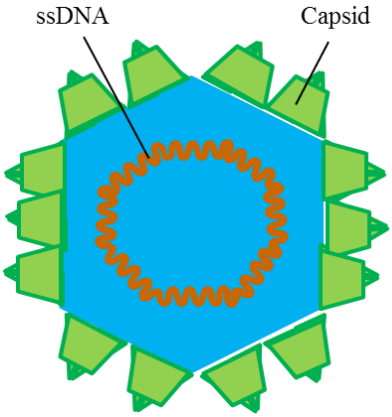

Fig. 1.14. PCV1 virion. Capsid protein in green, core in blue and single-stranded DNA (ssDNA) in orange. Adapted from ViralZone, 2008.

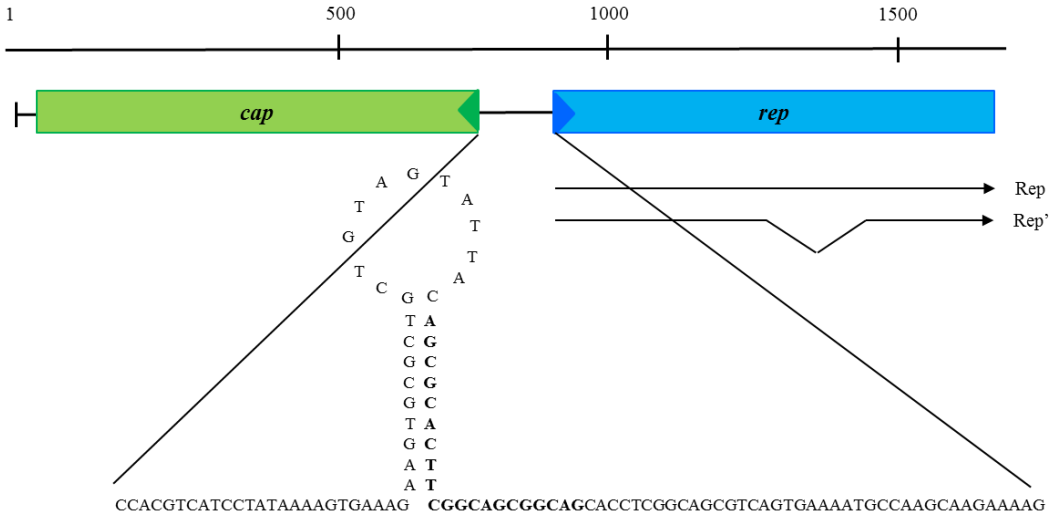

Fig. 1.15. PCV1 genome linear map. Open reading frames for capsid protein (*cap*) and replicase (*rep*) indicated in green and blue respectively, with transcription direction indicated by triangles. The intergenic region contains the origin of replication, with a stem loop and hexamer repeats. Bold letters indicate the binding site for replication initiator proteins Rep and Rep'. Reproduced from Mankertz *et al.*, 2004, with permission from first author.

PCV2 is a closely related porcine circovirus, with 75% sequence identity (Meehan *et al.*, 1998), but belonging to a different phylogenetic cluster from PCV1 (Allan *et al.*, 2012). PCV2 was identified in the 1990's for the first time as the agent causing post weaning multi-systemic wasting syndrome (PMWS) in pigs (Meehan *et al.*, 1997, 1998; Mankertz and Hillenbrand, 2002). The mechanism of PCV2 pathogenicity is unknown to date (Mankertz, 2012). The genome of a new circovirus named PCV3 was recently identified in pigs with cardiac and systemic inflammation

(Phan *et al.*, 2016). The replicase of PCV3 and capsid proteins is distantly to those of PCV1 and PCV2.

Contamination of Rotarix® with PCV1 is believed to have originated from the porcine-derived trypsin used to subculture cells and/or activate RV in order to infect the Vero cells in an early stage of vaccine production (Ma *et al.*, 2011). PCV1 may have established chronic infection in Vero cells since the trypsin used in the master bank in 1983 was not irradiated (Dubin *et al.*, 2013). When this unintended contaminant was identified, GSK tested the vaccine derived from all stages of the manufacturing process. Presence of PCV1 DNA and low levels of PCV1 viral particles were found up to the stage of vaccine final fill (Table 1.2, Howe *et al.*, 2010). Sequencing of the contaminant PCV1 viral genome revealed two mutations in the *cap* (viral capsid) gene region: mutation A222G results in a non-conserved amino acid substitution (I172T), while the T706G mutation is 'silent' (R11R) (McClenahan, Krause and Uhlenhaut, 2011; Gilliland *et al.*, 2012; Dubin *et al.*, 2013). These mutations may have occurred as a result of virus adaptation to the Vero cell line where the vaccine virus was generated, and their significance is currently unknown. To that point, PCV1 infection assays in human cell lines had not shown any infectious capability (Mankertz *et al.*, 2003; Hattermann *et al.*, 2004; Baylis *et al.*, 2011; Kumar *et al.*, 2012; Mankertz, 2012). At the time, there was no immunological evidence of PCV1 infection in vaccinated infants. Therefore, GSK stated that PCV1 was non-infectious in humans, a position which was supported by the USA Food and Drug Administration (FDA) (Kuehn, 2010), the WHO (WHO, 2010) and the European Medicines Agency (EMA) (EMA, 2010). Nevertheless, GSK initiated the development and manufacture of a PCV1-free Rotarix® vaccine (Dubin *et al.*, 2013; GSK personal communications to the NIBSC, 2018; GSK personal communications at the 8th European Rotavirus Biology Meeting, 2019).

Table 1.3. PCV1 DNA in Rotarix® vaccine during manufacturing by GSK. Copies/mL were measured by qPCR in viral harvests, purified bulks and final containers (Howe, B., *et al.*, 2010. Rotarix® GSK's PCV1 Investigation).

Rotarix® vaccine	PCV1 DNA (copies/mL)
Viral harvest	10^{10}
Purified bulk	10^{9}
Final container	10^{7}

Since then, PCV1 viral loads in infants vaccinated with Rotarix® have been measured by quantitative PCR (qPCR) in stool, with no increase in viral loads found for the period of shedding, suggesting there was no replication of PCV1 and only transient passage through the gastrointestinal tract (Mijatovic-Rustempasic *et al.*, 2017). PCV1 serologic response in infants vaccinated with Rotarix® has been measured by ELISA in their serum with an antibody seropositivity rate very similar in vaccinees and placebo (Han *et al.*, 2017). However, the current vaccine is administered to several hundred thousand infants every year in many countries and there is inconclusive evidence (Baylis *et al.*, 2011; Beach *et al.*, 2011) on whether PCV1 can replicate in humans. PCV1 might become infectious in humans if the changes it undergoes in cell culture adaptation alter its pathogenicity, with health issues potentially similar to those caused by PCV2. Therefore, further studies about PCV1 shedding in vaccinees and confirming the lack of replication in humans were required to respond to concerns regarding vaccination of children with weaker immune systems (undiagnosed at the time of vaccination).

1.14 Rotarix® vaccine faecal shedding

Rotarix® contains $\geq 10^6$ $CCID_{50}$/mL of RV (EMC, 2018) and approximately 10^7 genome copies/mL of vaccine dose (Mijatovic-Rustempasic *et al.*, 2017). In clinical trials, several patterns of viral shedding after vaccination with Rotarix® have been found (Table 1.3) and Rotarix® shedding reported through clinical trials has been related to younger age (infants), lack of pre-existing rotavirus antibodies and a higher vaccine dose (Anderson, 2008). As indicated in Table 1.3, vaccine virus shedding is more common after dose 1 than after dose 2, perhaps owing to a level of immunity developing after the dose 1 and shedding after dose 2 appearing as a catch-up effect in the absence of increased titres. While numbers vary between cohort studies, typically around 40-80% of vaccinated infants shed virus at day 7 after dose 1 and up to approximately 25% shed at day 7 after dose 2. In some of the trials, horizontal transmission of Rotarix® shed in stool has been reported, with a potential for herd immunity (vaccine virus transmitted) as well as for infection of immunocompromised individuals (vaccine-derived variant transmitted) (Anderson, 2008).

Table 1.4. Summary of studies reporting vaccine virus shedding data following vaccination with Rotarix®. Country of study, percentage (%) of infants shedding after dose 1 (D1), % of infants shedding after dose 2 (D2), comments, citation.

		Percentage of infants shedding			
Year	**Country**	**After D1**	**After D2**	**Comments**	**Citation**
2004	Finland	38-60% (days 7-9)	13% (days 7-9)	Response dose 2 mostly in non-responders to dose 1; No transmission to placebo	Vesikari *et al*., 2004
2005	Canada, USA	47.5-54.6% (days 1-7)	0.8% (day 30)	One infant shed 2 months after dose 1; Transmisison to placebo	Dennehy *et al*., 2005
2005	Singapore	80% (day 7), 24% (day 30)	29% (day 7), 16% (day 15)	Transmission to placebo	Phua *et al*., 2005
2005	Brazil, Mexico, Venezuela	44% (day 7)	21% (day 7)	One infant shed 2 months after dose 1; WT infection in placebo	Salinas *et al*., 2005
2007	Mexico	61% (day 7)	14% (day 7)	One infant shed 2 months after dose 1; Transmisison to placebo? WT?	Ruiz-Palacios *et al*., 2007
2014	China	87.9% (days 6-7)	17.9% (days 6-7)	10^4 - 10^9 copies/g of stool	Hsieh *et al*., 2014
2016	USA	63-75% (days 7 and 9)	17% (day 15)	10^2 - 10^{10} copies/g of stool	Mijatovic-Rustempasic *et al*., 2017
2018	Malawi	30% (day 6)	35% (day 6)	10^2 - 10^{10} copies/g of stool	Bennett *et al*., 2019

1.15 Genetic stability of a live-attenuated RV vaccine

Live-attenuated vaccines are inexpensive and generally safe, as well as highly effective against disease in individuals with a functional immune system (Minor, 2015). However, they can acquire mutations during manufacture or during replication in vaccinated individuals (Hanley, 2011), with a potential to alter its phenotype, as well as the immune responses elicited in vaccinees. Examples of vaccines that became virulent causing disease after replicating in vaccine recipients are OPV reverting to wild type (Cann *et al.*, 1984; Minor, 1993; Chumakov, 1999; Kew *et al.*, 2005; Burns *et al.*, 2014; Famulare *et al.*, 2016) and genetically unstable live-attenuated HIV-1 strain deletants (Berkhout *et al.*, 1999). Other examples are a study on a mumps vaccine that resulted in chronic encephalitis in an immunocompromised child (SCID-diagnosed after vaccination) after allogeneic transplantation (Morfopoulou *et al.*, 2017) or a varicella zoster virus that became virulent in immunocompromised vaccine recipients (Willis *et al.*, 2017).

In the case of Rotarix®, despite clinical trials addressing vaccine safety and immunogenicity, the genetic changes that confer attenuation to the vaccine virus are not well characterised. It was suspected that amino acid substitutions in the VP4 fusion domain (amino acid 385) and another amino acid substitution in NSP4 (T45M) are probably correlated with a loss of virulence in humans (Tsugawa and Tsutsumi, 2016). Other studies have pointed at sites undergoing positive selection and sites differing from circulating G1P[8] RV in Belgium by Sanger sequencing, theoretical models and NGS (Zeller *et al.*, 2012, 2015, 2017). However, it is unknown whether attenuation of Rotarix® is due to a few mutations or an epistatic effect of several mutations. Rotavirus vaccination with a live-attenuated strain may allow for genetic variation of the vaccine through replication in vaccine recipients, potentially affecting immunogenicity, efficacy and virulence. On the other hand, the introduction of a live-attenuated vaccine may also impact on circulating WT RV dynamics, by exerting selective pressure on vaccine types and potentially leading to the emergence or re-emergence of novel or rare strains which could affect vaccination efficacy and/or lead to disease. Hence, it is of importance to monitor the stability and consistency of vaccine batches during manufacture as well as to monitor the vaccine shed by vaccine recipients in order to evaluate whether vaccine virus

may accumulate changes that would impact on infectivity, virulence or immunogenicity.

Identification of single nucleotide polymorphisms (SNPs) at high and low frequencies has allowed the study of genetic diversity and minority variants in live-attenuated vaccine populations (Peters *et al.*, 2012; Bidzhieva *et al.*, 2014; Depledge *et al.*, 2014; Zapata *et al.*, 2014; Majid *et al.*, 2015; Jeon *et al.*, 2016; Beck *et al.*, 2018; Riemersma *et al.*, 2018). Because quasispecies appear usually at low frequency levels, they are difficult to detect by Sanger sequencing accurately if they are below 10-25% in an heterogeneous viral population (Leitner *et al.*, 1993). However, high-throughput sequencing technologies allow the study of minority variants avoiding the time-consuming cloning followed by Sanger sequencing. Next generation sequencing is used to study intra-strain virus diversity and temporal evolution of variants, as well as the dynamics and emergence of escape mutants under different types of pressure. NGS has been used to identify minority variants and potential adventitious agents within live attenuated vaccines (Victoria *et al.*, 2010; Watson *et al.*, 2013; Isakov *et al.*, 2015).

1.16 Rotarix® vaccine correlates of protection

Correlates of protection for current rotavirus vaccines are also not well defined. Differences in vaccine efficacy have been observed in developed (high) versus developing (low) countries and many factors may contribute to the difficulty in defining robust correlates (section 1.11). Currently, it is impractical to predict individual protection as a follow-up of 12 to 18 months is needed to determine protection (Coulson *et al.*, 1990).

Serum IgA as a correlate of protection has been investigated: heterotypic antibodies may be protective against common RV types (Green *et al.*, 1990) and vaccine-induced serum Abs have appeared to be protective against WT infection (Jiang, Gentsch and Glass, 2002). Moreover, Rotarix® seroconversion has been related to protection against RVGE (Vesikari, Karvonen, Puustinen, *et al.*, 2004) and seroconversion rates have been observed to be >60% at two months after dose 2 (Salinas *et al.*, 2005). Serum IgA has been observed to correlate with vaccine efficacy at population level (Patel *et al.*, 2013). Later, seropositivity of anti-RV IgA

after Rotarix® vaccination was associated with a reduction in severe RVGE, although a proportion of the seronegative subjects were also protected (Cheuvart *et al.*, 2014). In a recent study in Bangladesh, serum RV-specific IgA responses have appeared to correlate in a suboptimal manner with protection (Lee *et al.*, 2018). In contrast, serum IgA was correlated with protection against disease in studies in Finland and Latin America (Ward, 1996; Velázquez *et al.*, 2000; De Vos *et al.*, 2004) and anti-VP4 and anti-VP7 serum NAbs have been observed to generate heterotypic immunity (Johansen and Svensson, 1997). Specific anti-RV IgA seroconversion has shown no correlation with protection against severe RVGE in the first year after vaccination (Angel, Franco and Greenberg, 2012). Of note, Rotarix® generates heterotypic immunity, protecting against other RV types (Angel, Franco and Greenberg, 2012). Apart from NAbs anti-VP7 and anti-VP4 homotypic protection, heterotypic protection is also induced by vaccination, similarly for Rotarix® and RotaTeq® and beyond strain variation worldwide (Clarke and Desselberger, 2015). Specific anti-RV IgA bound to secretory component has recently been correlated with protection against RVGE (Herrera *et al.*, 2013). Specific, non-NAbs anti-VP6 have been detected after vaccination in humans (Svensson, Sheshberadaran, Vesikari, *et al.*, 1987; Lappalainen *et al.*, 2017) and demonstrated protective effects in mice (Burns *et al.*, 1996; Corthésy *et al.*, 2006; Lappalainen *et al.*, 2015). VP6 might be transcytosed via the polymeric Ig receptor and may "expulse" RV into the gut lumen or it may inhibit transcription intracellularly (Thouvenin *et al.*, 2001; Feng *et al.*, 2002; Aiyegbo *et al.*, 2013, 2014). Mucosal specific anti-VP6 IgA has been found to inhibit viral replication *in vitro* and *in vivo* (Lappalainen *et al.*, 2014). Moreover, anti-VP6 antibody fragments have been found to be protective against infection and severe disease in the neonatal mouse model (Maffey *et al.*, 2016). Specific anti-VP6 IgA are the most common antibodies produced by B cells (Weitkamp *et al.*, 2003, 2014). Since most copro-IgA is composed of anti-VP6 non-NAbs, anti-VP6 intracellular antibodies may be the most appropriate correlate of protection in infants.

Research so far has shown that serum specific anti-RV IgA is the preferred marker of rotavirus vaccine immunogenicity, since it correlates with vaccine efficacy at a population level in developed countries (Patel *et al.*, 2013). However, in studies of vaccine immunogenicity, specific anti-RV copro-IgA is a good correlate at high

levels and the most widely accepted for severe RVGE protection (Desselberger and Huppertz, 2011).

1.17 Summary

Rotavirus vaccination has been successful in reducing RV-associated mortality worldwide, however, questions remain around the extent of replication in vaccine recipients, the consequences (if any) of the presence of PCV1, the correlates of protection and the impact of genetic variation on vaccine kinetics and efficacy. Samples tested in clinical trials and clinical settings usually represent cross-sections, making investigation of the above issues challenging. However, access to a longitudinal set of samples would allow a much more focussed analysis.

1.18 Hypothesis and aims

The hypothesis for this study is that childhood rotavirus immunisation would result in high-frequency vaccine, revertant and/or novel variants while replicating within vaccine recipients. Mutations may appear because of biological immune pressure and assessment of the IgA response will contribute to understanding viral replication patterns and may indicate whether such changes alter the immune profile. The concomitant dispersal of the porcine circovirus found in the vaccine as an unintended contaminant could occur in parallel with rotavirus vaccine. We recruited a cohort of 12 vaccine recipients and obtained samples immediately before dose 1, after dose 1 at varying periods thereafter up until two to three months after dose 2 and, for some vaccinees, at one year after dose 1.

To test the hypothesis the work presented hereafter addresses the following aims:

1. Define longitudinal Rotarix® faecal shedding patterns as a surrogate of Rotarix® replication in vaccinees.
2. Evaluate whether PCV1 is amplified in infants through rotavirus vaccination.
3. Assess the genetic stability of faecal Rotarix® by identifying and/or quantifying minority variants/quasispecies in the population of vaccinees.

4. Assess the host immune response through faecal IgA as a correlate measure of protection.

While cell lines, animal models and HIEs, are excellent systems for the dissection of specific mechanisms, the data from this unique cohort of vaccinated infants will provide novel insight in the most biologically relevant model: infants. Moreover, the analysis of longitudinal samples collected very frequently will provide a detailed picture of the kinetics and genetic polymorphisms of rotavirus vaccine in vaccinated infants and into their mucosal immune response to the vaccine virus.

Chapter 2: Materials and methods

2.1 Materials

2.1.1 Manufacturers

Unless otherwise stated, reagents were of analytical grade and purchased as described in Table 2.1.

Table 2.1. Manufacturers and location.

Manufacturer	City, country
Abcam	Cambridge, UK
Agilent Technologies	Waldbronn, Germany
BDH Chemicals Ltd.	Poole, UK
Beckman Coulter, Inc.	High Wycombe, UK
Bio-Rad Laboratories, Inc. (formerly AbD Serotec)	Kidlington, UK
Bio-Rad Laboratories Ltd.	Watford, UK
BMG LABTECH	Offenburg, Germany
Corning Inc.	Amsterdam, The Netherlands
Delta Lab	Barcelona, Spain
Eurofins Genomics	Ebersberg, Germany
Fisher Chemical	Loughborough, UK
Fisher Scientific	Loughborough, UK
GraphPad Software, Inc.	La Jolla, USA
Henleys Medical Supplies	Welwyn Garden City, UK
Invivogen	Toulouse, France
Illumina UK	Cambridge, UK
Invitrogen	Paisley, UK
Life Technologies	Paislay, UK
Merck KGaA	Darmstadt, Germany
New England Biolabs Ltd.	Hitchin, UK
Premier International Foods Ltd. (Marvel)	Spalding, UK
Promega UK	Southampton, UK
Qiagen	Craley, UK
ReAgent Chemicals Ltd.	Cheshire, UK
Roche Products Ltd.	Welwyn Garden City, UK
Sigma-Aldrich	Gillingham, UK
STARLAB Ltd.	Milton Keynes, UK
Stratech Scientific Ltd. (for Jackson Immuno Research or Salimetrics)	St Thomas's Place, UK
Thermo Fisher Scientific (for Applied Biosystems)	Lutterworth, UK
VWR	Lutterworth, UK

2.1.2 Chemicals and reagents

Table 2.2. Chemicals and reagents, and corresponding manufacturer.

Product	Manufacturer
Amphotericin B solution 250 µg/mL in deionized water, sterile-filtered (A2942)	Sigma-Aldrich
Bovine Serum Albumin (BSA) lyophilized powder, essentially globulin free, low endotoxin, ≥98% (agarose gel electrophoresis) (A2934)	Sigma-Aldrich
β-mercaptoethanol (M6250)	Sigma-Aldrich
Carbonate bicarbonate buffer capsules (C3041)	Sigma-Aldrich
Chloroform anhydrous, contains amylenes as stabilizer, ≥99% (372978)	Sigma-Aldrich
Distilled H_2O (dH_2O) Purelab® Ultra	ELGA VEOLIA
DNAse I (AMPD1)	Sigma-Aldrich
Dried Skimmed Milk Powder 198g Marvel Original	Premier International Foods Ltd
Ethanol 99%+, Absolute, Extra Pure, SLR (10048291)	Fisher Chemical
Foetal bovine serum (FBS) (10270, lot 41A073K)	Gibco (Thermo Fisher Scientific)
Glycogen from mussles 20 mg/mL (10901393001)	Sigma-Aldrich (Roche)
HEPES solution 1M pH 7-7.6 sterile-filtered (H0887)	Sigma-Aldrich
1Kb Plus DNA ladder (10787-018)	Invitrogen by Life Technologies
Lambda DNA/HindIII marker (SM0101)	Thermo Fisher Scientific
L-glutamine 200nM (G7513)	Sigma-Aldrich
Lithium chloride (213233)	Sigma-Aldrich
Minimum Essential Medium (MEM) (M5650)	Sigma-Aldrich
Penicillin-Streptomycin with 10,000 units penicillin and 10 mg/mL streptomycin in 0.9% NaCl sterile-filtered (P0781)	Sigma-Aldrich
ϕX174 DNA/BsuRI (HaeIII) marker (SM0251)	Thermo Fisher Scientific
Potassium chloride 99.5-101.0%, AnalaR NORMAPUR® Reag. Ph. Eur. analytical reagent (26764.260)	BDH Chemicals (VWR)
Potassium dihydrogen phosphate 99.5-100.5%, AnalaR NORMAPUR® Reag. Ph. Eur. analytical reagent (26936.260E)	BDH Chemicals (VWR)
2-Propanol, BioReagent, for molecular biology, ≥99.5% (I9516)	Sigma-Aldrich
RNAse-free DNAse Set (79254)	Qiagen
RNAse-free H_2O (445847D/129112)	VWR/Qiagen
Sodium chloride 99.5+%, for analysis, AR, meets the specification of Ph. Eur. (S/3160/53)	Fisher Chemical
Disodium hydrogen phosphate, anhydrous ≥99.0%, AnalaR NORMAPUR® ACS, Reag. Ph. Eur. analytical reagent (10249)	BDH Chemicals (VWR)
Sulfuric acid Titripur® Reag. Ph Eur, Reag. USP 0.5 mol/L (1N) (109072)	Merck KGaA
3, 3', 5, 5'-Tetramethylbenzidine (TMB) liquid substrate for ELISA peroxidase susbstrate (T-0440)	Sigma-Aldrich
TRI Reagent® (T9424)	Sigma-Aldrich
Trizma® hydrochloride solution (Tris-HCl) pH 8.0, 1 M, BioReagent, for molecular biology (T-3038)	Sigma-Aldrich
Trypsin 2.5 mg/mL (T4049)	Sigma-Aldrich
Tween® 20 viscous liquid, cell culture tested (P2287)	Sigma-Aldrich
UltraPure™ Agarose (16500500)	Thermo Fisher Scientific (Invitrogen)
UltraPure™ Ethidium Bromide 10 mg/mL (15585011)	Thermo Fisher Scientific (Invitrogen)
UltraPure™ Herring Sperm DNA Solution 10 mg/mL (15634017)	Thermo Fisher Scientific (Invitrogen)
"Ultrapure" sterilised H_2O	Reverse osmosis H_2O: 18.2 MΩ, type 3 RNAse/DNAse-free water, Triple Red® (Bucks, UK).

2.1.3 Buffers and cell culture media

Phosphate buffered saline (PBS) was prepared by the Scientific Support Services (SSS) Division at the National Institute for Biological Standards and

Control (NIBSC) at a final concentration of 137 mM NaCl, 2.7 mM KCl, 10 mM Na_2HPO_4 and 1.8 mM KH_2PO_4 in ultrapure distilled water and adjusted to pH 7.4 with HCl.

Table 2.3. Buffers used in enzyme-linked immunosorbent assays (ELISAs) and corresponding recipes. Reagents in grey tested during optimisation, reagents in black used in final testing.

Buffer	Recipe
Blocking buffer	5% (w/v) dried skimmed milk in PBS or 3% BSA in PBS
Carbonate bicarbonate buffer	1 capsule in 100 mL of sterilized dH_2O (0.05M, pH 9.6)
Dilution buffer	1% (w/v) dried skimmed milk in PBS or 3% BSA in PBS
Washing buffer	0.05% or 0.1% Tween 20 in PBS

Table 2.4. Cell culture media and corresponding recipes.

Media	Recipe
Growth media	MEM supplemented with 10% FBS, 15mM HEPES, 100 µg/mL penicillin/streptomycin, 2 mM L-glutamine and 2.5 µg/mL amphotericin B
Replacement media	MEM supplemented with 15mM HEPES, 100 µg/mL penicillin/streptomycin, 2 mM L-glutamine and 2.5 µg/mL amphotericin B
Maintenance media	MEM supplemented with 1 µg/mL trypsin, 15mM HEPES, 100 µg/mL penicillin/streptomycin, 2 mM L-glutamine and 2.5 µg/mL amphotericin B

2.1.4 Kits

Table 2.5. Kits and corresponding manufacturer.

Kit	Manufacturer
Agencourt® AMPure XP system (A63881)	Beckman Coulter
Agencourt® RNA Clean XP system (A63987)	Beckman Coulter
QIAamp® DNA Mini Kit (51304)	Qiagen
QIAamp® Viral RNA Mini Kit (52904)	Qiagen
High Pure RNA Isolation kit (11828665001)	Roche
High Pure Viral Nucleic Acid kit (11858874001)	Roche
MinElute® Gel Extraction kit (28604)	Qiagen
Nextera® XT Index Kit v2 Set A (FC-131-2001)	Illumina, Inc.
Nextera® XT DNA Library Preparation kit v2 (FC-131-1024)	Illumina, Inc.
MiSeq Reagent Kit v2 (MS-102-2001)	Illumina, Inc.
Phusion Hot Start II DNA Polymerase 2 U/µL (F549L)	Thermo Fisher Scientific
Platinum™ Quantitative PCR SuperMix-UDG (11730025)	Thermo Fisher Scientific (Invitrogen)
Qubit® dsDNA HS Assay Kit (Q32851)	Thermo Fisher Scientific (Invitrogen)
Qubit® RNA HS Assay Kit (Q32852)	Thermo Fisher Scientific (Invitrogen)
RNA ScriptSeq™ v2 library preparation kit (SSV21124)	Illumina, Inc (Epicentre)
Salivary Secretory IgA enzyme immunosay (1-1602)	Salimetrics®
SuperScript™ III First Strand Synthesis system for RT-PCR (18080051)	Thermo Fisher Scientific (Invitrogen)
SuperScript™ III One-step RT-PCR System with Platimum™ Taq High Fidelity DNA Polymerase (12574035)	Thermo Fisher Scientific (Invitroegen)
TaqMan™ Universal Master Mix II, no UNG (4440040)	Thermo Fisher Scientific (Applied Biosystems)

2.1.5 Primers and probes

Table 2.6. Rotavirus segment-specific cDNA synthesis and standard PCR full-length primers. [A] Adapted from Cho *et al.* 2013 and [B] adapted from Matthijnssens *et al.* 2008 by J. Mitchell (NIBSC). Degenerate primers; R = A/G, W = A/T, Y = C/T. Full-length primers generated by J. Mitchell to be used for lamb, porcine and human rotavirus, extending before and after Rotarix® coding region (Mitchell, Lui, *et al.*, unpublished). *VP3: 38-17 bp before A of start codon; VP4: 64-43 bp before A of start codon; VP6: 23-3 bp before A of start codon; VP7: 48-27 bp before A of start codon; GENNSP2: 46-27 bp before A of start codon; NSP4: 41-20 bp before A of start codon.

Primer name	Degenerate sequence (5' → 3')	Amplicon size (bp)	Nucleotides	Tm (°C)
VP3F[A]	CAG TAY TAG TAG TGC GTT TTA (21)	2569	1-21*	53.0
VP3R[A]	GAC TAG TGT GTT AAG TTT TTA (21)		2549-2569	50.1
VP4F[A]	GGC TAT AAA ATG GCT TCR CYM (21)	2359	1-21*	56.9
VP4R[A]	GGT CAC ATC CTC DAT DVC MKT (21)		2339-2359	58.5
VP6F[A]	GGC TTT WAA ACG AAG TCT TC (20)	1356	1-20*	53.2
VP6R[A]	GGT CAC ATC CTC TCA CT (17)		1340-1356	52.8
VP7F[A]	GGC TTT AAA AGM GAG AAT TTC (21)	1063	1-21*	53.0
VP7End9R[A]	GGT CAR ATC RTA CAA TTC TAA TCT AAG (27)		1037-1063	58.9
GENNSP2F[B]	GGC TTT TAA AGC GTC TCA G (19)	1062	1-19*	54.5
GENNSP2R[B]	GGT CAC ATA AGC GCT TTC (18)		1045-1062	53.7
NSP4F[B]	GGC TTT TAA AAG TTC TGT TCC (21)	750	1-21*	54.0
NSP4R[B]	GGW YAC RYT AAG ACC RTT CC (20)		731-750	57.3

Table 2.7. Rotarix® NSP2 standard PCR primers for TOPO TA cloning. Designed by C. Bronowski and M. Iturriza Gómara, the University of Liverpool.

Primer name	Degenerate* sequence (5' → 3')	Amplicon size (bp)	Nucleotides	Tm (°C)
RV_NSP2_STD3-F	ACT GCT ACT GCT GAA GGA (18)	503	445-462	50.1
RV_NSP2_STD1-R	CCG ACA TGT GAA ACT TCA TCC A (22)		926-947	52.8

Table 2.8. Rotarix® NSP2-specific quantitative PCR assay primers and probe. Aligned to Rotarix® NSP2 reference number JX943605 (Gautam *et al.*, 2014).

Primer/probe name	Sequence (5' → 3')	Amplicon size (bp)	Nucleotides	Tm (°C)
Rotarix® NSP2-F	GAACTTCCTTGAATATAAGATCACACTGA (29)	281	546→574	61.0
Rotarix® NSP2-R	TTGAAGACGTAAATGCATACCAATTC (26)		826→801	58.5
Rotarix® NSP2- P	FAM-TCCAATAGATTGAAGTCAGTAACGTTTCCA-BHQ1 (30)		782→753	69.3

Table 2.9. Pan-rotavirus VP6-specific quantitative PCR assay primers and probe. From Mukhopadhya *et al.*, 2013.

Primer/probe name	Sequence (5' → 3')	Amplicon size (bp)	Nucleotides	Tm (°C)
Rotavirus VP6-F	GACGGVGCRACTACATGGT (19)	380	747→766	58.7
Rotavirus VP6-R	GTCCAATTCATNCCTGGTG (19)		1126→1108	50.0
Rotavirus VP6-P	FAM-CCACCRAAYATGACRCCAGCNGTA-MGB (24)		912→935	65.3

Table 2.10. PCV1-specific quantitative PCR assay primers and probe. Called *PCV1fw and **PCV1rev in original paper (Gilliland *et al.*, 2012).

Primer/probe name	Sequence (5' → 3')	Amplicon size (bp)	Nucleotides	Tm (°C)
PCV1repfw*	CAGCGTGATTGGAAGACAG (19)	104	475→493	52.6
PCV1reprev**	TTCCAGTAGGTGTCGCTAGG (20)		578→559	55.0
PCV1probe	FAM-AGCCAGTGGGCCCGTAATTT-BHQ1 (20)		532→551	68.5

2.1.6 Antibodies

Table 2.11. Antibodies used in ELISAs.

Antibody	Manufacturer
Rabbit anti-human IgA (309-005-011; batches: 120971, 130024)	Stratech Scientific Ltd (for Jackson Immuno Research)
Mouse anti-human rotavirus VP6 (ab156660; batch GR216263-1) [clone0541]	Abcam
Mouse anti-human rotavirus VP6 (MCA2635) [clone0541]	Bio-Rad Laboratories, Inc
Purified human secretory IgA (PHP133; batches: 020615, 290415, 170516, 171215)	Bio-Rad Laboratories, Inc
Purified human secretory IgA (ctrl-iga; batch GAC-36-01)	Invivogen
Purified human secretory IgA (I1010; batch SLBP7516V)	Sigma-Aldrich
Goat anti-human IgA:HRP (STAR141P; batches: 151207, 170818)	Bio-Rad Laboratories, Inc (formerly AbD Serotec)

2.1.7 Miscellaneous

Table 2.12. Miscellaneous products and corresponding manufacturer.

Product	Manufacturer
Agilent High Sensitivity DNA chip	Agilent Technologies
Corning® 1 x 8 Stripwell™ 96 well plates, high Binding surface, clear (CLS2592)	Sigma-Aldrich
Falcon® 25cm², 75cm², 175cm² Rectangular Straight Neck Cell Culture Flask with Plug Seal Cap (353014, 355024, 353028)	Corning, Inc.
Qubit® Assay Tubes (Q32856)	Thermo Fisher Scientific (Invitrogen)

2.1.8 Vaccine material

Archived Rotarix® vaccine material was available at the NIBSC for control testing purposes and permission from the manufacturer was obtained to perform research related to Rotarix® vaccine materials. Rotarix® final fills were stored at 4ºC. Viral RNA (vRNA) and viral DNA (vDNA) extracted from the vaccine final fills were used as positive controls in RT-PCR or qPCR reactions.

2.1.9 Faecal sample collection

Faecal samples were collected from a cohort of 12 infants born and vaccinated in around Hertfordshire, South East England, UK. The NIBSC Human Materials Advisory Committee (HuMAC) reviewed and approved the project (reference 13/009). The activities fall beyond the scope of the Human Tissue Authority. The scope of the project is to undertake research on faecal samples from infants pre- and post-Rotarix® administration, including isolation of rotavirus genetic material to confirm viral shedding patterns, virus identity and stability (including post-one-year samples); isolation of PCV1 genetic material to determine viral shedding (excluding post-one-year samples); and measurement of faecal IgA levels (including post-one-year samples). Parents or guardians who agreed to participate in the study signed an informed consent form and completed a study questionnaire enquiring about age at time of vaccinations and type of feeding (breast milk, formula or mixed feeding). Infant sample collections were assigned a unique identifier number which was further anonymously randomised for data display. Sample collection and storage complied with the Human Tissue Act (HTA), 2004 (*Human Tissue Act 2004*, 2004) (license 12321-holder the NIBSC) and information was handled in line with the Caldicott Principles ('The Caldicott Report.', 1999) and the Data Protection Act 1998 (*Data Protection Act 1998.*, 1998).

Recruitment started in June 2014 and finalised in February 2017, with the last after-a-year sample collected in January 2018. Age at dose 1 was eight or nine weeks and at dose 2 it was 12 or 13 weeks. Six infants were breastfed, one infant was exclusively formula-fed and five infants were mixed-fed breastmilk; and faecal samples were collected throughout the two-month vaccination period or beyond (Table 2.13). Parents provided samples collected from 17 to 45 days along the vaccination period. Pre-vaccination samples were provided for eleven infants. After the first dose, samples were collected in most cases every other day up to one month or beyond after the second dose. Samples for individual M were provided for a week only after dose 2 (samples were provided for all other individuals for a month after dose 2). Post-one-year samples were provided for eight infants. The total number of samples collected, and the periodicity of collection varied across the cohort (Appendix I, Tables 8.1.1-8.1.12). Samples were collected non-invasively from nappies, placed in a 30 mL vial with a unique participant number and stored at -20°C

in home freezers until delivery to the NIBSC, frozen, by parents/guardians. Subsequently, samples were stored at -80°C until aliquoted and/or tested. Samples were prioritised for viral load quantification in technical triplicates (section 2.2.5), then for measuring total and rotavirus-specific copro-IgA in duplicate (2.2.7) and for NGS measuring in triplicate from the faecal suspension stage (2.2.6).

Table 2.13. Faecal sample collection. Individuals B-M. Number of days with at least one available sample pre-vaccination, after dose 1 and after dose 2. Total number of samples indicated in parentheses. See Appendix I for more detailed information about the cohort and faecal sample collection. (): Total samples, considering some recruits provided several samples from the same day. *Samples not provided for a period when collection not possible.

Individuals	Feeding	No. of day samples pre-vaccination	No. of day samples after dose 1	No. of day samples after dose 2	No. of day samples post-a-year	Total no. of day samples
B	Mix-fed	2	8 (10)	15	1(2)	26
C	Formula-fed	10	27	7	1 (3)	45
D	Breastfed	2 (5)	13 (14)	19	Not provided	34
E	Breastfed	4	10	21	1 (1)	36
F	Breastfed	0	17 (19)	16 (23)	1 (3)	34
G	Breastfed	4	8	10	2 (2)	24
H	Breastfed	1	13	17	1 (2)	32
I	Mix-fed	4	16 (23)	25 (31)	1 (2)	46
J	Mix-fed	1	16 (18)	22	Not provided	39
K	Mix-fed	1	17	24	Not provided	42
L	Breastfed*	4	12	11 (13)	1 (1)	28
M	Mix-fed*	1	13	3	Not provided	17

2.2 Methods

2.2.1 Faecal sample aliquoting

Each sample was thawed, weighed and aliquoted into 200 mg to 1 g of faecal matter (Appendix I, Tables 8.1.1 to 8.1.12) before being snap-frozen in an ethanol and dry ice bath and then stored at -80°C until used. Inevitably, owing to the nature of collection and amount of material, several timepoints yielded low weight aliquots, which preclude the use of biological replicates for some sections of the study (Appendix I). Although homogeneity between aliquots was similar by eye, the heterogeneous nature of faecal matter composition represents a caveat of this study.

2.2.2 Nucleic acid extraction from vaccine material

RNA from Rotarix® vaccine material was used as a positive control in cDNA synthesis and qPCR assays. RNA from vaccine material was extracted using the Trizol/chloroform method further adapted or a published method (Potgieter *et al.*, 2009) further adapted as follows. Total RNA was extracted from a volume of 200 µL of vaccine, mixed with an equal volume of PBS and 1200 µL of TriReagent® (Chomczynski and Sacchi, 1987, 2006). The mixture was vortexed briefly and incubated for 15 min at ambient temperature (AT). A 240 µL volume of chloroform ($CHCl_3$) was added, the mix vortexed briefly and incubated at AT for 15 min. Following centrifugation at 13,200 × *g*' and 4ºC for 15 min, the upper phase was removed to new sterile microcentrifuge tubes. Glycogen was added to a final concentration of 0.05 µg/mL. A 1200 µL volume of ice-cold 2-propanol was added, mixed by inversion ten times and incubated for 10 min at AT. Samples were centrifuged at 13,200 × *g*' for 10 min at 4ºC. The upper phase was discarded, the pellet washed with 1.2 mL of 75% ethanol and centrifugation followed at 13,200 × *g*' and 4ºC for 5 min. The upper phase was discarded and the pellet inverted and allowed to air dry for 10 min. The pellet was resuspended in 40 µL of RNAse-free water and stored at -80ºC until required. Some additional RNA from vaccine material was also extracted as described in section 2.2.3.2.

PCV1 DNA from vaccine material was extracted using the QIAamp® DNA Mini Kit (run in plates testing samples from all infants except individuals C and E after dose 1) or the QIAamp® Viral RNA Mini Kit (run in plates testing samples from infants C and E after dose 1 and in plates testing samples from all infants after dose 2) or and following the manufacturer's instructions.

2.2.3 Nucleic acid extraction from stool

2.2.3.1 Sample preparation for viral load quantification and sequencing

In order to obtain a homogenous working sample, faecal suspensions were prepared from faecal aliquots and used on the same day, to minimise the effects of degradation. Surplus from the faecal suspensions was stored at -80°C for potential future use (only fresh suspensions were used for experiments in this thesis).

A 10% faecal suspension was prepared using 200 mg of faecal sample, 1.5 mL PBS, 0.5 mL $CHCl_3$ (or proportional amounts) and 1 g of glass beads. The samples were homogenised by thorough vortexing and centrifuged at 3,500 × *g*' for 10 min. The upper phase was transferred to new sterile tubes and used to perform viral nucleic acid extractions. Chloroform was used in the faecal suspensions for nucleic acid extraction in order to inactivate bacteria in faecal matter as adapted by Dr Dimitra Klapsa in the poliovirus group at the NIBSC from the WHO Polio laboratory manual 4th Ed. (WHO, 2004) section 6.2.1 on 'Preparation of faecal samples for virus isolation'.

2.2.3.2 Extraction for viral load quantification

Viral nucleic acids (vNAs) were extracted using the High Pure Viral Nucleic Acid column-based kit (Roche) following the method adapted by Dr Dimitra Klapsa (NIBSC) as described below. The kit contains polyA RNA as a carrier to increase the yield of extracted vNAs and a buffer with 'inhibitor removal technology' (proprietary) to eliminate contaminants that might inhibit downstream PCR. A volume of 200 µL of faecal suspension was mixed thoroughly with 400 µL of working solution (1 µL of polyA RNA per 100 µL of binding buffer) and incubated for 10 min at AT. The mix was transferred to the columns and centrifuged for 1 min at 8,000 × *g*'. Filter tubes were replaced and 500 µL of inhibitor removal buffer added, followed by a centrifugation for 1 min at 8,000 × *g*'. Filter tubes were replaced and 450 µL of wash buffer added, followed by a centrifugation 1 min at 8,000 × *g*'. The wash was repeated, followed by an extra centrifugation step for 1 min at full speed 13,000 × *g*'. Samples were eluted using 50 µL of elution buffer, followed by a centrifugation for 1 min at 8,000 × *g*', transferring samples to clean tubes and stored at -80ºC. Viral RNA concentration was measured by fluorescence using the Qubit® RNA HS Assay Kit according to manufacturer´s instructions.

2.2.3.3 Extraction for NGS by Nextera®

A number of methods were evaluated:

TriReagent® and chloroform method. Viral nucleic acids were extracted from 250 µL of 10% faecal suspension (see 2.2.3.1) by mixing with 750 µL of Tri-Reagent® (Chomczynski and Sacchi, 1987, 2006), vortexing for 5 s and incubating

for 15 min at AT. A volume of 200 µL of $CHCl_3$ (1.492 g/mL at 25ºC) was added and the samples were vortexed and incubated for 15 min at AT before being centrifuged at 13,200 × *g*' for 15 min at 4ºC. The upper phase was transferred to a new sterile tube and glycogen was added to a final concentration of 0.05 µg/µL and mixed by inverting ten times. A volume of 750 µL of ice-cold 2-propanol (0.785 g/mL at 25ºC) was added and mixed by inverting ten times. Samples were incubated overnight at -20ºC. The following day, samples were centrifuged at 13,200 × *g*' for 10 min at 4ºC. The upper phase was discarded, and the pellet was washed with 1 mL of 75% ethanol, by inverting and flicking. Samples were centrifuged at 13,200 × *g*' for 10 min at 4ºC. The upper phase was removed, and the pellet was allowed to air-dry for 1 h, at AT and resuspended in 40 µL of RNAse/DNAse-free water. Samples were stored at -80ºC.

Roche nucleic acid kit method. Viral nucleic acids (vNAs) were extracted using the High Pure Viral Nucleic Acid adapted as described in section 2.2.3.2.

Of the methods tested, the latter was the one chosen due to higher RNA yields. Following method testing, RNA was freshly extracted again using the Roche column-based adapted method. Single faecal matter aliquots generating single faecal suspensions, used in triplicate to extract from were used in this work.

2.2.4 cDNA synthesis and PCR amplification

The six rotavirus gene segments were amplified by RT-PCR with six sets of previously reported primers (Matthijnssens, Ciarlet, Rahman, *et al.*, 2008; Cho *et al.*, 2013), which were modified as required so that they would span a number of G1P[8] serotypes species (Table 2.6).

Either the SuperScript™ III One-step RT-PCR System with Platimum™ *Taq* High Fidelity (HF) DNA Polymerase kit (one cycle at 60°C for 30 min and 94°C for 2 min, then 40 cycles at 94°C for 15 s, 45°C for 30 s and 68°C for 4 min, then one cycle at 68°C for 5 min, followed by 4°C on hold) for viral segments encoding VP6, VP7 and NSP2; or the SuperScript™ III First Strand Synthesis system for RT-PCR kit (dNTPs, molecular-grade water and RNA one cycle at 85°C for 2 min, followed by 4°C on hold; plus 50°C for 50 min, 85°C for 5 min, followed by 4°C on hold) followed by the Phusion Hot Start II HF DNA Polymerase kit (one cycle at 98°C for 1 min, then 35 cycles at 98°C for 10 s, 61°C [63°C for VP2] for 20 s and 72°C for 90

s, then one cycle at 72°C for 5 min, followed by 4°C on hold) for viral segments encoding VP3 (Appendix II), VP4 and NSP4 were used to amplify the extracted RNA. Three technical replicates were performed from the same vNA extraction.

The SuperScript™ III First Strand Synthesis system for RT-PCR kit was used with random hexamers (provided in the kit) to synthesise cDNA following the manufacturer's instructions prior to pan-rotavirus VP6 qPCR, following the manufacturer's instructions.

2.2.5 Quantitative PCR

In order to quantify rotavirus RNA levels in stool, two robust, published (Mukhopadhya *et al.*, 2013; Gautam *et al.*, 2014, 2016) and validated standard operating procedures used in the Rotavirus Response to Immunisation & Transmission Epidemiology (RotaRITE) programme to quantify Rotarix® and all-rotavirus viral loads in stool were kindly provided by M. Iturriza Gómara's lab.

2.2.5.1 Rotarix®-specific NPS2

cDNA synthesis of NPS2 was performed using the modified primers mentioned in section 2.1.5 and the SuperScript™ III First Strand Synthesis system for RT-PCR kit. cDNA was synthesised in triplicate (technical replicates) from any one faecal suspension extract.

The Rotarix® NSP2 qPCR assay was designed for detection of Rotarix® vaccine strain due to the difference in sequence of NSP2 gene in vaccine and other G1P[8] strains (Gautam *et al.*, 2014, 2016). In the original paper, the assay demonstrated 100% sensitivity, 99% specificity and 94% efficiency with a limit of detection (LoD) of two copies per reaction (Gautam *et al.*, 2014). Absolute quantification of RV cDNA from faecal samples using the Platinum® qPCR SuperMix-UDG was performed in triplicate, adapting the Rotarix® NSP2-PCR standard operating procedure, kindly provided by M. Iturriza Gómara. A pCR4™-TOPO®-TA plasmid (3956 bp) containing a Rotarix® specific half-length NSP2 amplicon of 281 bp was a kind gift from C. Bronowski and M. Iturriza Gómara, University of Liverpool, and was used to generate the standard curve for quantification. The plasmid copy number was calculated as follows:

$$\frac{\text{molecules}}{\mu\text{L}} = \frac{\left[\text{concentration } \left(\frac{\text{ng}}{\mu\text{L}}\right) \times 6.022 \times 10^{23} \left(\frac{\text{molecules}}{\text{mol}}\right)\right]}{\left[\text{length of amplicon (bp)} \times 650 \left(\frac{\text{g}}{\text{mol}}\right) \times 10^{9} \left(\frac{\text{ng}}{\text{g}}\right)\right]}$$

Rotarix® NSP2 qPCR specific primers and probe (Table 2.8) were optimised (considering the highest Ct value and lower probe concentration) for use at final 300 nM and 100 nM respectively; adding ROX at 50 nM as recommended by the manufacturer. The LoD was determined after ten replicates of two-fold serial dilutions of the plasmid in herring sperm DNA (60 µg/mL), ranging from 5×10^{-1} to 7.8125×10^{-3} copies/µL. The last dilution at which signal was detected was 0.125 copies of DNA/µL (equating to 1.25×10^{3} copies of DNA/g of stool), indicating the LoD.

Vaccine material concentration was calculated using $copies/mL\ of\ vaccine = copies\ of\ DNA/\mu L \times 5 \times 8 \times 5 \times 10$, where 5 is the times mg used to make 1 mL, 8 relates to the 1/8 extraction volume run in the reverse-transcription reaction, 5 relates to a 1/5 dilution of the eluate and 10 relates to the 1/10 reverse-transcription volume run in the qPCR. Amplification of vaccine virus in stool was calculated as *i.e.* $copies/g\ of\ stool = copies\ of\ DNA/\mu L \times 10 \times 10 \times 10 \times 5$, where 10 relates to the 1/10 reverse-transcription volume run in the qPCR, the next 10 relates to 1/10 eluate volume run in the reverse-transcription reaction, the last 10 relates to the 10% faecal suspension and the 5 relates to the times mg used were to make 1 g. As an example: 1.2×10^{3} copies in 2 µL [copies in reaction volume] × 10 [2 µL out of 20 µL of the RT final product volume are used in the qPCR, so 1/10] × 10 [5 µL out of 50 µL of eluate are used for the RT reaction, so 1/10] × 10 [faecal suspension are prepared with approximately 200 mg of stool in a 2 mL volume, so 10%] × 1000 mg/225 mg [to calculate amount in one 1 g of stool with respect to amount of stool used, hence the "5" as a general approximation in the equation above]= 5.35×10^{6} copies/g of stool. Neat and 1/10 eluates were previously tested for RT and PCR inhibition and neat samples were amplified better than 1/10 dilutions when visualised by agarose-gel electrophoresis.

The samples were incubated in an Agilent Mx3005P QPCR System with a programme comprising incubation at 50°C for 2 min; followed by one cycle at 95°C for 2 min; then, 40 cycles at 95°C for 15 s and 60°C for 1 min; and held at 4°C. For

data analysis, triplicates were treated collectively as described in the manual for MxPro QPCR Mx3000P and Mx3005P QPCR Systems software version 4.10, meaning "fluorescence values for all wells that are identified with the same replicate symbol are averaged, so that the results for all wells with the same replicate number will be identical". The threshold fluorescence level (ΔRn), used to derive cycle threshold (Ct) values, was manually assigned at 0.1 in logarithmic scale, around the middle of the linear phase of exponential amplification, for consistency. Only assays with standard curves an R^2 ≥0.99 and efficiency between 90% and 110% were considered valid. A sample was considered positive if at least two of three replicates had a Ct <38 (based on Ct value of false positive non-template controls) and a standard deviation ≤0.3. Samples with Ct values >38 or standard deviations ≥0.3 were repeated to assess veracity of results. Values for viral loads in the qPCR reaction were defined as copies/2 µL of reaction. Estimate values followed by copies/g of stool in the original sample. Any value that appeared to deviate from the general profile trend (unexpected dips in viral loads) was repeated to confirm viral load levels.

2.2.5.2 Pan-rotavirus VP6

cDNA synthesis from VP6 RNA was carried out using the modified primers mentioned in section 2.1.5, table 2.9, and the SuperScript™ III First Strand Synthesis system for RT-PCR kit in section 2.2.5, in triplicate from any one faecal suspension yielding three technical replicates.

The Rotarix® VP6 qPCR assay (Mukhopadhya *et al.*, 2013) was designed for the detection of any rotavirus strain in stool samples due to the conserved nature of the VP6 gene sequence (Tang *et al.*, 1997). Absolute quantification of cDNA from faecal samples was performed as described for the NSP2 assay. A pCR4™-TOPO®-TA plasmid containing a pan-rotavirus VP6 amplicon of 380 bp was a kind gift from C. Bronowski and M. Iturriza Gómara, University of Liverpool, and was used to generate the standard curve for quantification. The copy number was calculated as described for the NSP2 assay.

Pan-rotavirus VP6 qPCR specific primers and probe (Table 2.9) were optimised for use at 400 nM and 100 nM respectively; ROX and reaction conditions and analysis were performed as described for the NSP2 assay. The LoD determined

after ten replicates of two-fold serial dilutions of the plasmid (from 5×10^{-1} to 7.8125×10^{-3} copies/µL) in herring sperm DNA at 60 µg/mL was 0.25 copies of DNA/µL, resulting in 2.5×10^{2} copies of DNA/g of stool, *i.e.* $copies/g\ of\ stool = copies\ of\ DNA/\mu L \times 5 \times 10 \times 10 \times 10$, where 5 is the times mg used to make 1 g, 10 relates to the 10% faecal suspension, another 10 relates to the 1/10 eluate volume run in the reverse-transcription reaction and the last 10 relates to the 1/10 reverse-transcription volume run in the qPCR.

Vaccine material (Rotarix® final fills) amplification was calculated using $copies/mL\ of\ vaccine = copies\ of\ DNA/\mu L \times 5 \times 8 \times 5 \times 10$, where 5 is the times mg used to make 1 mL, 8 relates to the 1/8 extraction volume run in the reverse-transcription reaction, 8 relates to the 1/8 eluate volume run in the reverse-transcription reaction, 5 relates to a 1/5 dilution of the eluate and 10 relates to the 1/10 reverse-transcription volume run in the qPCR.

Reaction conditions and data analysis were performed as described in 2.2.5.1.

2.2.5.3 PCV1-specific qPCR

Absolute quantification of PCV1 DNA from faecal samples was performed as previously described (Gilliland *et al.*, 2012), using the Taqman Universal Master Mix II, no UNG, in triplicate (technical triplicates from extract from one faecal suspension). A pCR4™-TOPO® plasmid containing 1757 bp full-length PCV1 DNA was kindly provided by S. Connaughton and used for generation of the standard curve for quantification. The copy number was calculated as previously described for the NSP2 assay.

Specific primers and probe (Table 2.10) were used at 400 nM and 200 nM, respectively. Reaction conditions followed manufacturer's recommendations: 95°C for 10 min; then, 40 cycles at 95°C for 15 s and 60°C for 1 min; and held at 4°C. Analysis was performed as described for the NSP2 assay The LoD determined after ten replicates of two-fold serial dilutions of the plasmid (from 5×10^{-1} to 7.8125×10^{-3} copies/µL) in herring sperm DNA at 60 µg/mL was 0.125 copies of DNA/µL, resulting in 1.25×10^{3} copies of DNA/g of stool, *i.e.* $copies/g\ of\ stool = copies\ of\ DNA/\mu L \times 5 \times 10 \times 25$, where 5 is the times mg used to make 1 g, 10 relates to the 10% faecal suspension and 25 relates to the 1/25 extraction volume run in the qPCR.

DNA from vaccine material (Rotarix® final fills) amplification was calculated using $\frac{copies}{mL} of\ vaccine = copies\ of \frac{DNA}{\mu L} \times 7.14 \times 30$ or $copies/mL\ of\ vaccine = copies\ of\ DNA/uL \times 5 \times 25$ where 7.14 or 5 is the times mg used to make 1 mL and 30 or 25 relates to the 1/25 eluate volume run in the qPCR, respective to the extraction methods (QIAamp® Viral RNA Mini Kit or QIAamp® DNA Mini Kit). This material was detected at 10^5-10^6 copies/mL.

Reaction conditions and data analysis were performed as described in 2.2.5.1.

2.2.6 Next generation sequencing of faecal rotavirus RNA

Amplicons for sequencing were first visualised by agarose gel electrophoresis and ethidium bromide staining (0.5 µg/mL final concentration), pooled in equimolar amount based on relative intensity on gel (amplicons encoding VP6 and VP7, Chapter 4) (Appendix II, section 8.2.1) or not pooled (amplicons encoding VP4 and NSP4, Chapter 4), purified using the Agencourt® AMPure XP system of magnetic beads, eluted in 20 µL of RNAse-free water and quantified by Qubit® DNA HS Assay (Invitrogen) following the manufacturer's instructions. Samples were run on an Agilent High Sensitivity DNA chip using the Agilent 2100 Bioanalyser and Agilent 2100 Expert Software B.02.08 to assess the segments of interest. The mixture was then diluted to 0.2 ng/µL in 10 mM Tris-HCl pH 8.0.

The Nextera® XT DNA Library Preparation kit v2 was used to prepare the sequencing libraries as indicated in the manufacturer's protocol, using at least 1 ng of input DNA per sample. Libraries were sequenced on the MiSeq platform using the 2 × 251 paired end v2 flow cells.

2.2.7 Bioinformatic analysis

The sequencing data generated was analysed by the bioinformatics team at the NIBSC. Data was trimmed and adapter sequences removed using Trimmomatic (Trimmomatic 0.32) to search for average Phred score below 30 (Phred score cutoff ≤Q30; accepting an error probability no bigger than 1 in a thousand or 0.001) (Andrews, 2010), within 5 bp windows, and trimmed off 3′ sequence from reads following the first window failing to pass, and discarding reads trimmed to under 50 bp (Bolger, Lohse and Usadel, 2014). Data was indexed ready for alignment to

vaccine reference standards JX943604-JX943614 by Burrows Wheeler Algorithm (BWA) and prepared for processing with SamTools and Picard (BWA mem v0.7.12-r1039; Samtools v1.2) (Li and Durbin, 2009; Li, 2011; BroadInstitute & GitHub, 2018). Read pairs and singleton trimming survivors were aligned to the reference using BWA, merged, marked for duplicates and indexed using Picard. SamTools was used to obtain coverage and pileup information, next converted to a table showing bases aligned at positions using a custom script. Coverage was plotted and results summarised using an R script. Mutation loci were identified, and a mutation was called if there were ≥100 aligned reads covering that position supporting the alternative allele, present at a frequency ≥1% and in at least 2 of 3 or more replicates (VcfUtils, BcfTools, Picard). Integrative Genomics Viewer was used for alignment visualisation (Robinson, 2012). Custom scripting tools were used for data processing and bioinformatic analysis (Perl, R, Bash).

2.2.8 Sequencing data analysis

The longitudinal analysis was focused on describing the type of mutation, whether it was synonymous, non-synonymous, a reversion to WT or a stop codon. It was highlighted whether it had been identified in vaccine material or in stool from other infants, if it had been observed alongside the timepoints tested and how the frequency fluctuated. Isolated timepoints at low frequencies were not considered. A Python script was used to sort sequencing data by project, sample, recruit, viral segment, timepoint and repeat; written by Edward T. Mee (Appendix III).

Relevant SNP loci were annotated in Geneious 10.2.3 and compared to RVA WT G1P[8] reference standards JN887809-10, JN887818-19 to highlight the SNP and amino acid changes. A search was run using the Basic Local Alignment Search Tool (BLAST) in to compare the modified sequences with RVA WT sequences.

Molecular modelling of amino acid changes common to several infants was performed with LigPlot^{+} (Laskowski and Swindells, 2011) and RasMol (Sayle and Milner-White, 1995) using the Protein Databank resolved rotavirus structures available (detailed in Chapter 4).

2.2.9 ELISAs

To quantify specific anti-RV copro-IgA initially, total copro-IgA was measured using a direct sandwich ELISA with a standard for total IgA followed by another direct sandwich ELISA measuring specific anti-RV IgA and using the same total IgA standard (section 2.2.9.3). This would yield a relative quantification of specific anti-RV copro-IgA with respect to total copro-IgA. However, due to shortage of the working standard and failure to reproduce its dynamic range with other commercial standards (Chapter 5), an indirect competitive commercial ELISA was used to quantify total copro-IgA (section 2.2.9.1), followed by specific anti-RV copro-IgA quantification using the remainder of the total IgA standard and the direct sandwich ELISA for specific anti-RV IgA (section 2.2.9.3), yielding a trend of specific anti-RV IgA with respect to total. Samples, standards and controls were assayed in duplicate. A strongly positive stool sample was used as a positive control along tested plates and a negative sample from pre-vaccination (previously tested as negative) was used as a negative control along the tested plates. Total IgA was measured in µg/mL using the Salimetrics® Salivary Secretory IgA standard and specific IgA was measured in µg/mL (equivalent to µg/g relating to stool, assuming a density of 1 g/mL) using the total purified human secretory IgA standard by Bio-Rad (PHP133, batch 290415). Specific IgA was expressed initially as units (ng) of RV-specific IgA with respect to 100 µg of total IgA. However, due final testing of total IgA with an indirect competitive kit, specific IgA was expressed as the readout with the total IgA standard and therefore a trend with respect to total IgA measured by the commercial kit.

2.2.9.1 Sample preparation

A 10% faecal suspension (in 1 × PBS) from faecal samples of infants vaccinated with Rotarix® was centrifuged at 1,500 × *g*' for 15 min at 4°C on the day of the ELISA. The upper phase was used to quantify total and rotavirus-specific copro-IgA and the remainder was snap-frozen and stored at -80°C between and after assays. Samples were assayed within two days to minimise IgA degradation interfering with results.

2.2.9.2 Total copro-IgA quantification

Total IgA in stool was measured using the Salimetrics® Salivary Secretory IgA indirect enzyme immunoassay kit, following the manufacturer's instructions. The kit, designed to measure salivary IgA (range 93.2-974.03 µg/mL), has a dynamic range from 2.5-600 µg/mL (for samples diluted five-fold, hence from 12.5-3000 µg/mL; determined by subtracting two standard deviations to the mean of 18 sets of duplicates and interpolating at 0 µg/mL, with minimal distinguished concentration from 0 being 2.5 µg/mL). Precision was determined from the mean of 10 replicates each control (high, medium and low) and from the mean of average duplicates for eight separate runs (high and low controls). Although originally designed for salivary IgA, this kit also detects secretory IgA from faecal samples in the range 520-2040 µg/mL.

Serial 1:3 dilutions of standard material were prepared from a stock of 600 µg/mL in 1× SIgA Diluent, obtaining 200 µg/mL, 66.7 µg/mL, 22.2 µg/mL, 7.4 µg/mL and 2.5 µg/mL. 10% faecal suspensions (see 2.2.3.2) were diluted 1:5 in 1× SIgA Diluent. A volume of 10 µL of each standard, control (high and low), 1:5 diluted sample and 1X SIgA Diluent was added to 4 mL of 1× SIgA Diluent, making a further 1:400 dilution (a total 1:2000 dilution for faecal suspension samples). A 1:120 dilution of Antibody Enzyme Conjugate in 1× Diluent was prepared and 50 µL were added to each of the previous tubes, making for a further 1:80 dilution of the Antibody Enzyme Conjugate. Tubes were incubated at for 90 min. A volume of 50 µL from each tube was transferred into the SIgA pre-coated microtitre plate, as well as 50 µL of 1× Diluent as a non-specific binding control (in duplicate). The plate was covered and incubated at AT and 400 rpm and 2 mm motion radius for 90 min. Next, it was washed six times with 300 µL of 1× wash buffer and blotted on a paper towel. A 50 µL volume of TMB Substrate Solution were added to each well and the plate was incubated at AT and 500 rpm and 2 mm motion radius for 5 min. Following incubation at AT for 40 min in the dark, a volume of 50 µL of Stop Solution were added and the plate was incubated at AT and 500 rpm and 2 mm motion radius for 3 min. The absorbance was read at 450 nm and a secondary filter correction at 492 nm, within 10 min of adding Stop Solution in a FLUOstar® Omega microplate reader using Mars software (BMG LABTECH). Data was analysed using the four-parameter logistic (4PL) curve as described for the direct ELISA for total IgA in

MyAssays® Desktop Basic software, including an initial step to calculate percent bound with respect to the 'zero' (tube containing only goat anti-human IgA:HRP conjugate, hence all free antibody binding to the SIgA-coated plate). Graphs were plotted using GraphPad Prism 5.

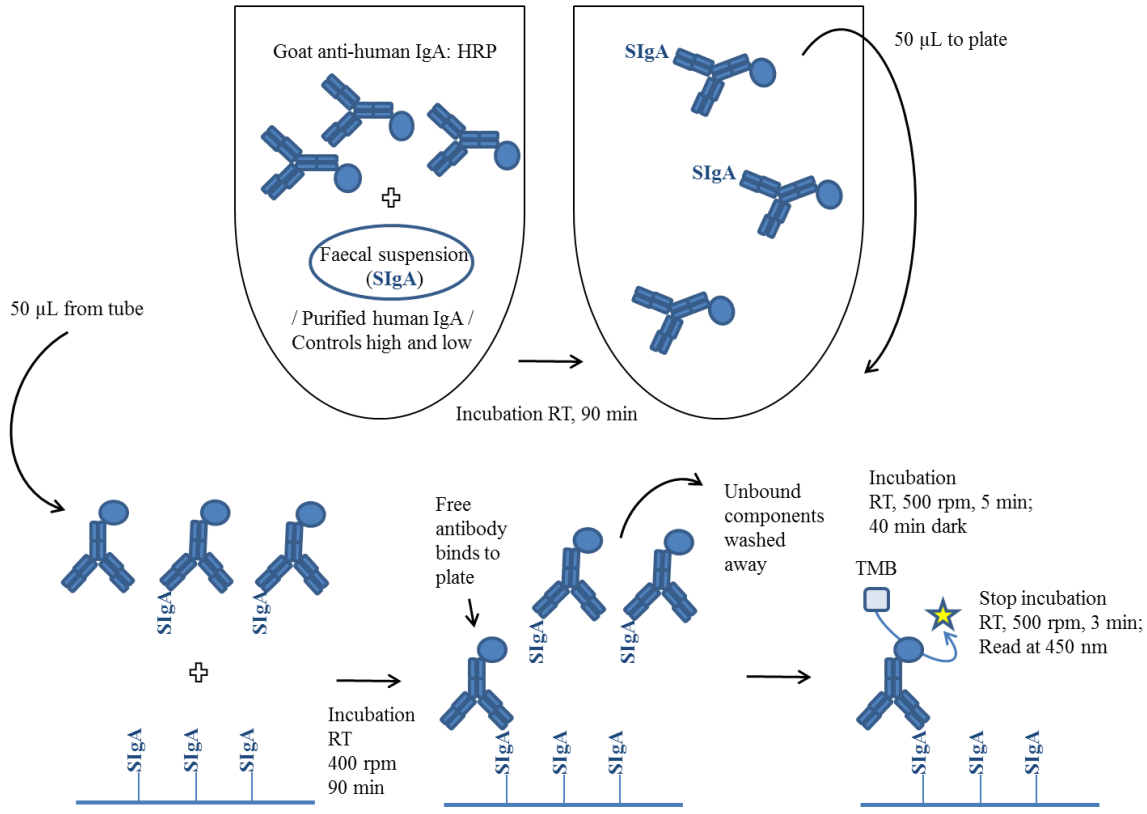

Fig. 2.1. Total IgA in stool of infants vaccinated with Rotarix® by indirect competitive ELISA. A constant amount of goat anti-human SIgA conjugated to HRP was added to tubes containing specific dilutions of standards or faecal suspensions. The antibody enzyme conjugate bound to the SIgA in the standard or saliva samples. The amount of free antibody enzyme conjugate remaining was inversely proportional to the amount of SIgA present in the sample. After incubation and mixing, an equal volume of solution from each tube was added in duplicate to the microtitre plate coated with human SIgA. The free or unbound antibody enzyme conjugate bound to the SIgA on the plate. After incubation, unbound components were washed away. Bound SIgA antibody enzyme conjugate was measured by the reaction of the HRP enzyme to the substrate TMB. This reaction produced a blue colour. A yellow colour was formed after stopping the reaction with an acidic solution. The absorbance was read on a standard plate reader at 450 nm. The amount of SIgA antibody enzyme conjugate detected was inversely proportional to the amount of SIgA present in the sample. Adapted from Salimetrics® Salivary Secretory IgA enzyme immunoassay kit manual.

2.2.9.3 Specific anti-RV copro-IgA detection

Total copro-IgA ELISA for standard relative quantification

A direct sandwich ELISA for total IgA was performed to assay the total IgA standard in parallel to the rotavirus-specific IgA ELISA, generating a relative trend quantification for specific IgA in stool. Adapted from an ELISA method developed by Anna Pulawska-Czub for total IgA in saliva at the University of Liverpool (personal communication) and a published method (Bernstein, Ziegler and Ward, 1986). The LoD of this in-house assays was established by determining the average plus 3 standard deviations (SD) of the optical density (OD) of duplicates from negative pre-vaccination samples for all recruits (OD=0.503). Corning® 1 × 8 Stripwell™ 96 well microtitre plates were coated with rabbit anti-human IgA 1:4000 overnight at 4°C. The coating solution was removed and the plates washed five times with 300 µL of washing buffer. The wells were blocked with 300 µL of blocking buffer and incubated for 2 h at 37°C in a moist chamber. The 10% faecal suspensions were diluted 1:6000 (after optimization at different dilutions ranging from 1:1500 to 1:6000) in PBS 1X. Positive control purified human secretory IgA was prepared in duplicate in PBS 1× at dilutions 1:500, 1:1000, 1:2000, 1:4000, 1:8000, 1:10000. PBS 1× was used as negative control. A volume of 100 µL of sample, positive or negative control were added to each well and the plates were incubated for 2 h at 37°C in a moist chamber. The plates were washed three times with 300 µL of washing buffer. Enzyme-conjugated detection antibody goat anti-human IgA:HRP (horseradish peroxidase) was diluted 1:6000 in dilution buffer, 100 µL were added per well and the plates were incubated for 1 h at 37°C in a moist chamber. The plates were washed five times with 300 µL of washing buffer. A volume of 100 µL of 3, 3', 5, 5'-Tetramethylbenzidine (TMB) liquid substrate were added to each well and the plates were kept in darkness for 10 min. The reaction was stopped by adding 50 µL of 1M H_2SO_4. Absorbance was read at 450 nm in a FLUOstar® Omega microplate reader and Mars software (BMG LABTECH). Data was analysed using the four-parameter logistic (4PL) curve in MyAssays® Desktop Basic software (MyAssays® Analysis Software Solutions). This model is used to calculate concentrations from symmetrical sigmoidal calibrators and widely used for ELISAs. Graphs were plotted using GraphPad Prism 5 (GraphPad Software, Inc., San Diego, USA).

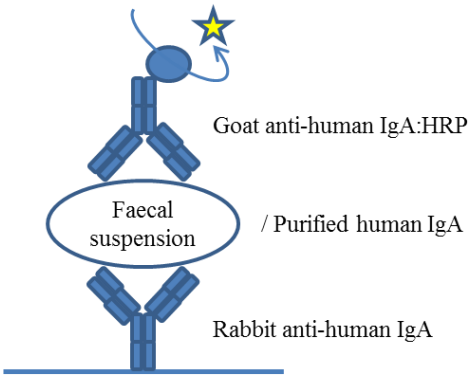

Fig. 2.2. Total IgA in stool of infants vaccinated with Rotarix® by direct sandwich ELISA. Coating with rabbit anti-human IgA, adding the 10% faecal suspension in PBS or purified human IgA as a standard, followed by a primary antibody goat anti-human IgA conjugated with HRP. Next, adding the substrate TMB and stopping the reaction with H_2SO_4 to read the signal.

Production of Rotarix® antigen for specific anti-RV copro-IgA detection

MA104 African green monkey kidney cells (Cell Supply and internal Cell Bank, NIBSC; originally from the European Collection of Authenticated Cell Cultures (ECACC) in May 1999, catalogue number 85102918) at passage 23 were incubated for 3 days at 37ºC and 5% CO_2 in T25, T75 and T175 cell culture flasks. They were then washed with PBS 1×, trypsinised with 2 mL, 5 mL and 7 mL of 2.5 mg/mL trypsin respectively for 5 min at 37ºC and trypsin was neutralised by adding 5mL, 10 mL and 15 mL of growth media containing heat-inactivated foetal bovine serum (FBS). Cells were centrifuged at 360 × *g*' for 5 min, the supernatant was discarded, and the pellet was resuspended in growth media so as to be split in a 1 to 6 ratio from initial density. This cell culture was repeated until MA104s were used for infection at passage 29. Cells were used at 100% confluency.

For cell culture adaptation of rotavirus, growth media was removed from the T25 MA104 flask. After washing with PBS 1×, replacement serum-free media was added, and cells were incubated at 37ºC and 5% CO_2 for 5 h. Maintenance media (replacement media containing 1 µg/mL trypsin) was prepared and Rotarix® cell suspension was thawed from -80ºC to AT. Rotarix® was activated by incubating 500 µL of virus suspension at 37ºC for 20 min with 20 µg/mL trypsin. After activation, 9.5 mL of replacement media were added to dilute the virus to a final trypsin concentration of 1 µg/mL. Replacement media was removed from the T25 flask and cells were washed with PBS 1×. The virus suspension in replacement media was added to the cells and these were incubated at 37ºC for 1 h. Meanwhile, the T75 and

T175 MA104 flasks were split in a 1 to 6 ratio. After infection with Rotarix®, the T25 MA104 flask was washed with PBS 1× and 12.5 mL of maintenance media were added. The flask was incubated at 37ºC and 5% CO_2, observing daily for cytopathic effect (CPE; rounded up and clumped, detached cells that appear 'floating').

Once CPE was observed (around 3-6 days later), the flask was freeze-thawed three times from -80ºC to 37ºC (in water bath) and then centrifuged at 360 × *g*' for 15 min. The supernatant was stored at -80ºC. Once the T75 MA104 flask was 100% confluent, it was infected with Rotarix® supernatant from the T25 in the same fashion. The infection was repeated with Rotarix® supernatant from the T75 into the T175 flask. They were passages 32 and 33 respectively.

The Rotarix® cell suspension material was used in enzyme-linked immunosorbent assays (ELISAs) to detect rotavirus-specific IgA.

Specific anti-RV copro-IgA ELISA

A direct sandwich ELISA was used for rotavirus-specific IgA detection. A 10% faecal suspension (see 2.2.3.2) was used to quantify specific IgA in faecal samples from infants vaccinated with Rotarix®. Adapted from an ELISA method developed by Anna Pulawska-Czub for norovirus specific IgA in saliva at the University of Liverpool (personal communication) a published method (Bernstein, Ziegler and Ward, 1986). Corning® 1 × 8 Stripwell™ 96 well microtitre plates were coated with mouse anti-human rotavirus VP6 1:3000 overnight at 4°C. The coating solution was removed, and the plates washed three times with 300 µL of washing buffer. The wells were blocked with 300 µL of blocking buffer and incubated for 1 h at 37°C in a moist chamber. Rotarix® suspension (section 2.2.8.1) was diluted 1:4 in PBS 1× and 100 µL were added to each well (in duplicate). Plates were incubated for 1.5 h at 37°C in a moist chamber. The coating solution was removed, and the plates were washed three times with 300 µL of washing buffer. The 10% faecal suspensions were diluted 1:10 (after optimization at different dilutions ranging from 1:2 to 1:400) in duplicate in PBS 1×. PBS 1× was used as negative control. A 100 µL volume of sample or negative control were added to each well and the plates were incubated for 1.5 h at 37°C in a moist chamber. The plates were washed three times with 300 µL of washing buffer. Enzyme-conjugated detection antibody goat anti-human IgA:HRP was diluted 1:6000 in dilution buffer, 100 µL were added per well and the plates

were incubated for 1 h at 37°C in a moist chamber. The plates were washed five times with 300 µL of washing buffer. A volume of 100 µL of 3, 3', 5, 5'-Tetramethylbenzidine (TMB) liquid substrate were added to each well and the plates were kept in darkness for 10 min. The reaction was stopped by adding 50 µL of 1M H_2SO_4. Absorbance was read at 450 nm in a FLUOstar® Omega microplate reader and Mars software (BMG LABTECH). Data was analysed using the 4PL as described for the direct ELISA for total IgA. The readout from the ELISA is expressed as µg/mL (in the range of 0.1 to 2 or 2.5 to 600), and specific IgA is normalised relative to total IgA concentration in 1g (1mL) of stool. Example: Child M, sample 13 (day 21 after dose 1), total IgA 3481 µg/ml, specific IgA 15 µg/ml. Therefore, 15/3481= 0.0043 µg of RV IgA per 1 µg of total IgA, equivalent to 4.3 ng of RV IgA per 1 µg of total IgA, plus ×10 because of the faecal suspension.

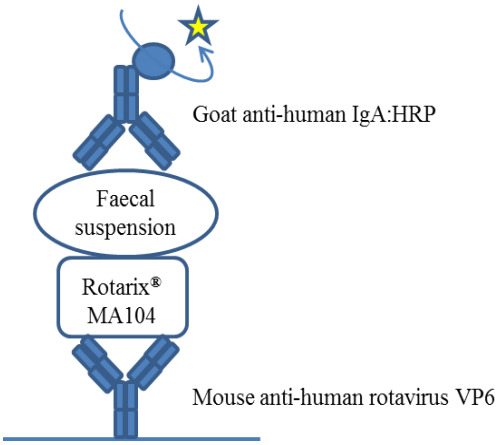

Fig. 2.3. Specific rotavirus IgA in stool of infants vaccinated with Rotarix® by direct sandwich ELISA. Coating with mouse anti-human rotavirus VP6, adding vaccine virus grown in MA104s, then adding the faecal suspension in PBS (containing the IgA), followed by a primary antibody goat anti-human IgA conjugated with HRP. Next, adding the substrate TMB and stopping the reaction with H_2SO_4 to read the signal.

2.2.10 Limitations

This project was designed as an exploratory and descriptive study, with a low number of recruits (n=12) but a large number of sequential samples provided by each recruit every other day (n=17-45), sometimes with >1 sample from the same day, and each sample yielding from one to >30 aliquots of 200 mg to 1g of stool. Despite the small cohort, longitudinal samples provided granularity to the study. Logistics varied as parents stored samples in their -20°C freezer at home and brought different

numbers of sample vials at different times to the NIBSC to be stored at -80°C. The samples from the first infants recruited were stored for longer than those from the latest recruits before being aliquoted. Aliquoting was performed comparably but at different points in time, with samples from one infant being aliquoted before or after samples from other infants.

Regarding storage, stool samples were kept as aliquoted stool matter at -80°C to prevent nucleic acid and/or protein degradation, since faeces contain less liquid and lower pH than faecal suspensions. Faecal suspensions, more homogeneous than faecal matter, were the working samples prepared on the day of extractions to minimise degradation from freeze-thaw impact and used once to extract nucleic acid or to test copro-IgA. They were then stored to be used shortly only if any repeats were required. Although stool samples were not filtered or treated with UV light, chloroform in the faecal suspension for NA extraction was used to inactivate bacteria. Both at the stage of aliquoting and at the stage of faecal suspension preparation there may have been sampling bias due to the heterogeneous nature of the starting material. Results may have originated from a small set of cells or from many cells across the gut and differently representative of the whole vaccine infection.

Due to inconsistent stooling patterns in infants, low volume of sample at certain timepoints and feasibility of parental collection, it was not possible to collect a fully comparable set of samples across infants. The low amounts of stool sample available for collection during the vaccination period for most of the infants represents a caveat for the study as biological replicates for some timepoints were not possible. Therefore, testing of samples was prioritised for Rotarix® viral load quantification (three technical replicates from one faecal suspension), NGS of virus shed in stool (three biological replicates from three faecal suspensions) and RV-specific copro-IgA quantification (two technical duplicates from one faecal suspension). Although biological replicates were not possible for all the tests, faecal suspensions were a more homogeneous working sample than stool and reduced the chance of sample bias at that stage. Regarding variability of collection timepoints across infants, relevant timepoints (e.g. peak shedding, last day of shedding and highest and median viral loads) were selected to implement comparisons.

2.2.11 Statistical analysis

Biological significance was the main analytical focus whenever statistical analysis did not add value to the results. The number of replicates is reported in the section above and in the Experimental Methodology section in each chapter. Data representation and statistical analyses were performed using GraphPad Prism 8. Due to a small cohort (n=12), data was considered non-parametric. Tests included Wilcoxon matched-pairs signed ranks and Kolmogorov-Smirnov unpaired test for comparison of distribution. Statistical tests and reported significance are denoted in the figure legends.

Chapter 3: Human monovalent G1P[8] rotavirus vaccine shedding patterns in a cohort of vaccinated infants in the UK

3.1 Introduction

In a naturally acquired rotavirus infection, the mature enterocytes of the villi are infected and the virus replicates to high levels in the gut, causing mild to severe osmotic diarrhoea (Chapter 1, section 1.4). Rotavirus is shed in faeces of infected children, with lower amounts of virus shed by asymptomatic children and intermittent shedding by both symptomatic and asymptomatic children (Mukhopadhya *et al.*, 2013). Moreover, continuous shedders appear to be less protected than those who control shedding rapidly (Chapter 1, section 1.5.1) (Richardson *et al.*, 1998).

The design of live-attenuated vaccines is based on mimicking natural infection; their attenuation minimises the risk of initiating full symptomatic infection, while the active viral replication induces an immune response as close as possible to that achieved by the WT pathogen. Vaccine virus is shed in stool and several trials have studied the faecal shedding of Rotarix®, with a higher proportion of infants shedding after dose 1 than after dose 2 likely due to a catch-up effect of the second dose (Chapter 1, section 1.14). Moreover, horizontal transmission of the vaccine to placebo recipients was reported in some of the trials, which could contribute to herd immunity or to RVGE depending on immunocompetency of individuals.

Replication of Rotarix® in the gut and viral shedding of rotavirus vaccine in stool were anticipated (Hsieh *et al.*, 2014) and the measurement of vaccine viral load in faecal samples is a useful, non-invasive approach to assess vaccine take (Chapter 1, section 1.10.2) in an individual. Typically, clinical trials report faecal vaccine virus load over short periods following the dosing regimen. Further shedding data come from studies in hospital settings and therefore will frequently be a single point in time linked to the clinical evaluation.

A clear understanding of vaccine virus take would come from a more granular investigation of shedding dynamics, studying multiple timepoints throughout the vaccination period (from dose 1 to dose 2) and beyond. This would help to elucidate the variation in vaccine take between individuals. It would also provide an opportunity to study the shed vaccine virus to determine its sequence as a surrogate for the genetic stability of vaccine virus in the gut and to determine if vaccine virus variability may impact on overall immunity. Coupled with faecal IgA, viral load data would provide a non-invasive basis for better understanding immunity to rotavirus through vaccination.

Of note, Rotarix® contains an unintended contaminant DNA virus, PCV1 (Victoria *et al.*, 2010), which, despite being a porcine virus, is non-pathogenic in pigs and has not been reported to cause disease in humans (Chapter 1, section 1.13) (Mankertz *et al.*, 2003; Hattermann *et al.*, 2004; Baylis *et al.*, 2011; Kumar *et al.*, 2012; Mankertz, 2012). However, porcine circoviruses have been detected in human faecal matter from adults, possibly as a result of ingesting pork products (Li *et al.*, 2010). It is unknown whether PCV1 can replicate in the human GI tract or simply pass through without amplification. The investigation by GSK and previous studies have detected Rotarix® PCV1 DNA in vaccine stocks at 10^7 copies/mL of dose (Howe *et al.*, 2010; McClenahan, Krause and Uhlenhaut, 2011; Hsieh *et al.*, 2014; Mijatovic-Rustempasic *et al.*, 2017). The availability of longitudinal samples from a cohort vaccinated with Rotarix® enables additional investigation of whether shedding of PCV1 DNA can be detected following vaccination. Transient shedding may indicate simple pass-through of viral genome whereas prolonged shedding may be indicative of replication within the human gut.

3.2 Aims

The first aim of the work presented in this chapter was to perform a detailed longitudinal analysis of Rotarix® faecal shedding in infants vaccinated with Rotarix® in the UK to understand the rotavirus vaccine replication kinetics in this population. The second aim was to evaluate the quantity of PCV1 DNA shed -and persistence of shedding- alongside the vaccine rotavirus.

3.3 Experimental methodology

To address the vaccine virus shedding, a cohort of infants was recruited, and a series of samples acquired from each individual typically spanning the pre-vaccination period through to four weeks after the second dose, and for some infants one year after dose 1. Detailed materials and methods are provided in Chapter 2 and Appendix I. Faecal samples were processed and stored appropriately until needed for analysis (Chapter 2, sections 2.1.9 & 2.2.1). Inevitably, due to the nature of the material and the age of the donors, some samples were of low quantity and thus experimental design and analysis reflected this. To maximise the information obtained from this limited resource, the reproducibility of data was addressed by quantifying viral loads across three technical replicates from material extracted from a single faecal suspension. Viral load was quantified by RT-qPCR as it has been shown to be a sensitive assay for rotavirus detection (Pang *et al.*, 2004; Hsieh *et al.*, 2014). It was important to distinguish vaccine virus from naturally-circulating rotaviruses, thus for the samples collected prior to vaccination, on day of vaccination (before or after vaccine administration), and after one year, a VP6 pan-rotavirus RT-qPCR assay was employed (Chapter 2, section 2.2.5.2), with a view to identifying any pre-existing infection with naturally-circulating rotavirus. Samples collected from all timepoints pre-, during and post- vaccination regimen were subjected to a Rotarix®-NSP2-specific RT-qPCR (Chapter 2, section 2.2.5.1) to determine the amount of shed vaccine virus. Viral loads for PCV1 DNA (Chapter 2, section 2.2.5.3) were evaluated by qPCR on a subset of timepoints. Nucleic acid extracted from vials of Rotarix® vaccine served as positive controls and were used as spiking material to establish limits of detection of virus from stool (Chapter 2, section 2.1.8).

3.4 Results

3.4.1 Sample set

It was not possible to obtain samples from equivalent timepoints from all infants due to stooling patterns and feasibility of collection. Where low volumes of material were available, priority was assigned to testing Rotarix® faecal shedding throughout the two to three-month vaccination period. Similarly, PCV1 was

quantified in pre-vaccination sample and from three to ten timepoints after dose 1 and dose 2, where samples were available.

3.4.2 Rotavirus vaccine RNA faecal shedding after Rotarix® vaccination

Shedding was considered if infants presented detectable and sustained viral loads after either dose of vaccine.

Rotarix® vaccine material

Rotarix® in the vaccine vial was detected in the range of 2.46×10^8 to 2.21×10^9 copies/mL due to variability in extraction methodology (Chapter 2, section 2.2.2), which is one $\log_{10}$ higher than a previous report (Mijatovic-Rustempasic *et al.*, 2017). The vaccine potency reported by the manufacturer is 10^6 $CCID_{50}$/mL of dose. Viral loads from vaccine material are expressed in molecules/mL, equivalent to molecules/g in VLs from stool, assuming a density of 1 g per mL.

Rotarix® RNA detection in faecal suspensions

The sensitivity of vaccine virus detection on a background of nucleic acid extracted from faecal matter was determined using pre-vaccination samples spiked with 10-fold dilutions of Rotarix® vaccine material (from expected 10^8 to 10^1 copies/mL) and amplified using the vaccine-specific NPS2 RT-qPCR (Fig. 3.1). The LoD was determined as 10^3 copies/mL.

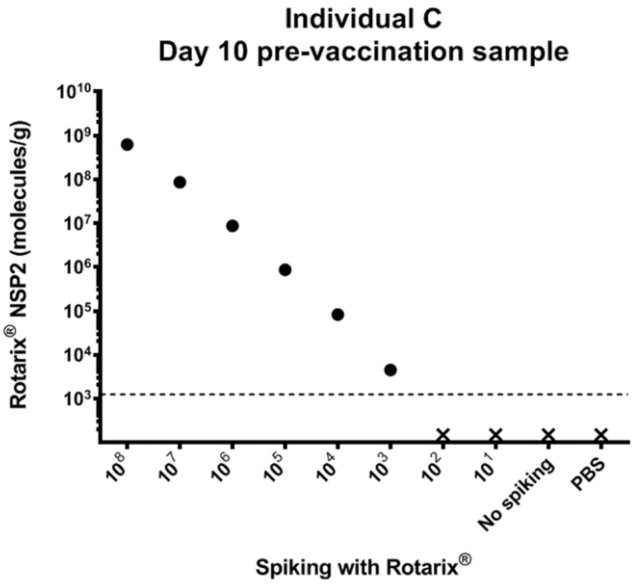

Fig. 3.1. Determination of the limit of detection of Rotarix® RNA from faecal-derived samples. Quantitation of rotavirus vaccine genome copy numbers by RT-qPCR: The X axis shows a serial 10-fold dilution of stool suspension spiked with Rotarix® vaccine material as well as negative controls (stool suspension and PBS). NSP2 gene copy numbers are shown in the Y axis.

Rotarix® faecal shedding in infants

None of the infants' pre-vaccination samples (n=12) revealed shed Rotarix® or WT RV. Similarly, none of the infants from whom a sample was available one year after vaccination (n=8) shed Rotarix® or WT RV. The pattern of shedding varied across the cohort. Following dose 1, shed vaccine virus was detected in all infants and following dose 2, viral shedding was identified in 11 of the 12 infants. Out of 12 infants, four (33%) controlled Rotarix® VLs to below the LoD after dose 1 and before dose 2, nine (75%) controlled VLs after dose 2 and before the end of the observation period and five (42%) controlled VLs during both periods. Rotarix® viral loads ranged between 10^3-10^9 copies/g of faeces with sustained shedding (Tables 3.1. A & B).

The day of peak of shedding after dose 1 ranged from day 2 to day 15, with a median of day 8 (Fig. 3.2 A). Out of 12 infants, six (50%) presented highest shedding between days 2-5 after dose 1 and six (50%) between days 6-15 after dose 1. After dose 2, the day of peak shedding was between days 1-3 after dose 2 for 10 infants (91%), and for one infant (9%) it was at day 7 after dose 2. The day of peak shedding occurred significantly later after dose 1 than after dose 2. Regarding the last day of

shedding, after dose 1 it varied from day 12 to day 34, with the median at day 27 (Fig. 3.2 B). After dose 2, the last day of shedding varied from day 1 to day 25, with an outlier at day 41, the median at day 8 and the majority of infants ceasing to shed virus by day 20. The duration of shedding was significantly longer after dose 1 than after dose 2.

The highest viral load after dose 1 ranged from 10^6 to 10^9 copies/g of stool across the cohort, with a median peak VL of 1.58×10^8 copies/g of stool (Fig. 3.3. A), comparable to the copy number range quantified within vaccine material. After dose 2, the highest VL ranged from 10^5 to 10^7 copies/g of stool, with a median highest VL of 1.35×10^6 copies/g of stool. The highest VL after dose 1 was significantly higher than after dose 2. The median viral load after dose 1 ranged from 10^4 to 10^7, with a median at 10^6 copies/g of stool (Fig. 3.3. B). After dose 2, the median VL ranged from 10^4 to 10^6 copies/g of stool, with a median of 10^5 copies/g of stool. The median viral load was significantly higher after dose 1 than after dose 2.

Table 3.1. Rotavirus RNA viral loads of individuals B-M after A) dose 1 and B) dose 2. Individuals, detectable range of shedding after dose 1 and dose 2 or day of dose 2 (D2), shedding period, day of peak shedding, last day of shedding, highest viral load and median viral load. Days with respect to dose 1 in (). NA, not applicable.

A)

		After dose 1 (D1)				
Individual	**Range (copies/g)**	**Shedding**	**Day of highest VL**	**Day of longest detectable VL**	**Highest VL**	**Median VL**
B	E+07 to E+04	All period	9	27	8.79E+07	5.36E+06
C	E+09 to E+05	All period	8	30	3.50E+09	1.73E+07
D	E+07 to E+03	All period	8	34	2.78E+07	7.75E+04
E	E+08 to E+03	All period except day 13	3	29	1.58E+08	1.61E+06
F	E+07 to E+03	All period	8	27	1.57E+08	2.25E+06
G	E+06 to E+03	All period	4	28	6.06E+06	3.09E+05
H	E+06 to E+03	Up to day 12	3	12	5.35E+06	5.61E+05
I	E+08 to E+03	Up to day 11, then 13, 14, 16	2	16	1.23E+08	5.21E+06
J	E+08 to E+04	All period	13	27	5.48E+08	1.28E+07
K	E+08 to E+03	Up to day 10, then 33 alone	7	33	6.13E+08	2.89E+06
L	E+08 to E+03	Up to day 23	15	23	2.33E+08	4.16E+06
M	E+08 to E+05	All period	5	27	3.24E+08	4.57E+06

B)

		After dose 2 (D2)				
Individual	**Day of D2**	**Shedding**	**Day of highest VL**	**Day of longest detectable VL**	**Highest VL**	**Median VL**
B	29	Up to day 21 (50)	3 (32)	21 (50)	2.79E+06	1.18E+06
C	31	All period up to day 7 (38)	1 (32)	7 (38)	1.16E+07	2.09E+06
D	35	Up to day 9 (44)	1 (36)	9 (44)	3.57E+06	6.31E+05
E	31	Up to day 10 (41)	3 (34)	10 (41)	4.99E+06	1.33E+06
F	28	Up to day 25 (53)	1 (29)	25 (53)	2.16E+05	5.35E+04
G	29	Up to day 11 (40)	7 (36)	11 (40)	4.09E+05	9.27E+04
H	30	Up to day 2 (32)	1 (31)	2 (32)	3.64E+05	1.87E+05
I	27	No	NA	NA	NA	NA
J	29	Up to day 41 (70)	3 (32)	41 (70)	4.35E+06	2.30E+05
K	34	Up to day 3 (37)	1 (35)	3 (37)	1.35E+06	8.33E+04
L	33	Up to day 7 (40)	2 (35)	7 (40)	6.50E+05	1.09E+05
M	28	Up to day 1 (29)	1 (29)	1 (29)	1.33E+06	1.33E+06

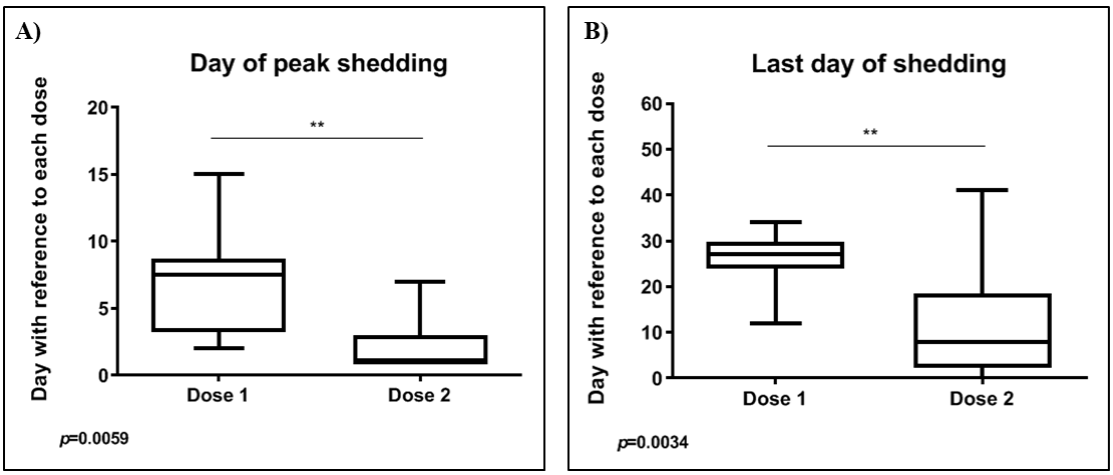

Fig. 3.2. A) Day of peak faecal Rotarix® shedding and B) last day of faecal Rotarix® shedding after dose 1 (D1) and dose 2 (D2). Statistical differences were assessed using a Wilcoxon matched pairs signed rank test (*$p < 0.05$; **$p < 0.01$; ***$p < 0.001$).

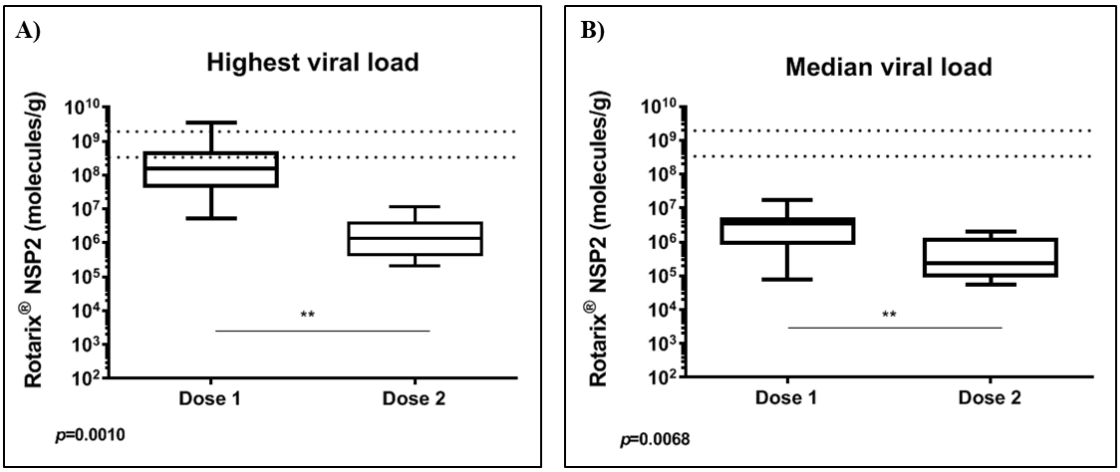

Fig. 3.3. A) Highest and B) median faecal Rotarix® shedding after dose 1 (D1) and dose 2 (D2). Quantitation of rotavirus vaccine genome copy numbers by RT-qPCR. Rotarix® copy number range in vaccine material delimited by dotted lines. Statistical differences were assessed using a Wilcoxon matched pairs signed rank test (*$p < 0.05$; **$p < 0.01$; ***$p < 0.001$).

Patterns of Rotarix® faecal shedding in infants

Amongst the 12 infants there were four clear patterns of shedding.

Profile 1 was defined by a single infant (I) who yielded a profile reflecting efficient control of viral shedding after dose 1 (Fig. 3.4 A). Initial high levels of virus reduced gradually to non-detectable levels by day 20. Although sample was not

available on day 28 (one day after dose 2), there was no detectable vaccine virus after dose 2 in the following days.

Profile 2 was defined by three infants (H, K, L) who yielded profiles whereby vaccine virus was shed following dose 1 and dropped to undetectable levels prior to dose 2 (Fig 3.4 B). Fewer samples were available from individual L immediately around the period of first vaccination. On receipt of the second dose, each individual shed vaccine virus but to levels approximating (H) or several logs lower (K, L) than those detected following dose 1. The duration of shedding in all three infants was no longer than 10-23 days after dose 1 and 2-7 days after dose 2. Longer shedding after dose 1 by individual L may be due to illness around the time of first vaccination. Interestingly, in individual K, the day before dose 2 was positive for vaccine virus, one log lower than VLs one day after dose 2. No vaccine or vaccine-derived variants were detected at frequency ≥1% at that timepoint (Chapter 4).

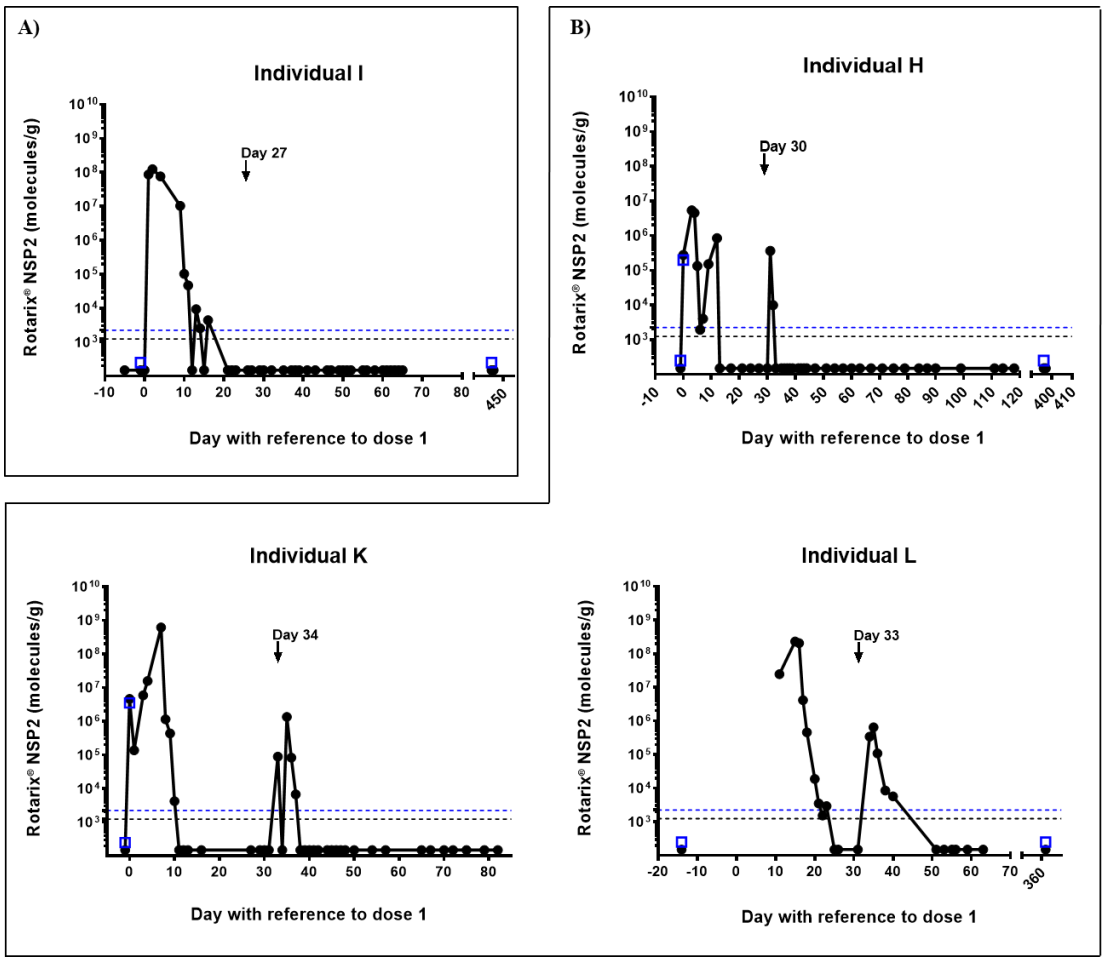

Fig. 3.4. Faecal shedding of Rotarix® and WT RV in A) individual I; B) individuals H, K and L; C) individuals B, E, D, G and M; and D) individuals C, F and J. Quantitation of RV vaccine genome copy number by NSP2-specific RT-qPCR and of pan-RV genome copy number by VP6-specific RT-qPCR: the X axis shows days with respect to dose 1 and the Y axis shows Rotarix® copy number. Black dots, vaccine VLs (molecules/g) throughout the two to three-month vaccination period; blue empty squares, WT VLs (molecules/g) at specific timepoints (pre-vaccination, on day of dose 1, six days after dose 1 or after-a-year). Black dashed line, LoD for vaccine virus assay (1.25×10^3 copies/g; negative values below this line and of unknown value); blue dashed line, LoD for WT virus assay (2.25×10^3 copies/g; negative values below this line and of unknown value). Day 0: Day of dose 1. Arrow: Day of dose 2.

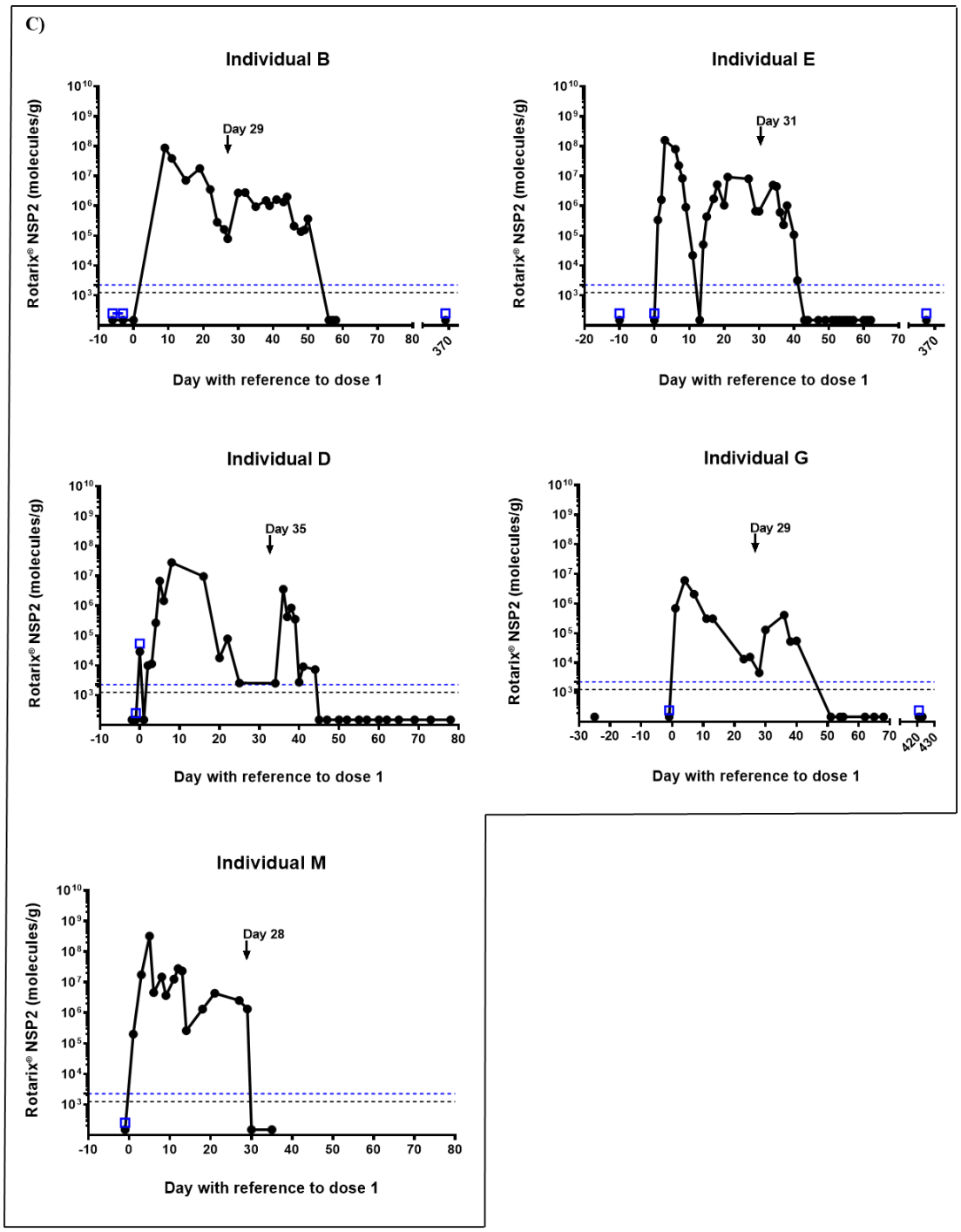
C)
Individual B
Day 29
Rotarix® NSP2 (molecules/g)
Day with reference to dose 1
Individual E
Day 31
Rotarix® NSP2 (molecules/g)
Day with reference to dose 1
Individual D
Day 35
Rotarix® NSP2 (molecules/g)
Day with reference to dose 1
Individual G
Day 29
Rotarix® NSP2 (molecules/g)
Day with reference to dose 1
Individual M
Day 28
Rotarix® NSP2 (molecules/g)
Day with reference to dose 1

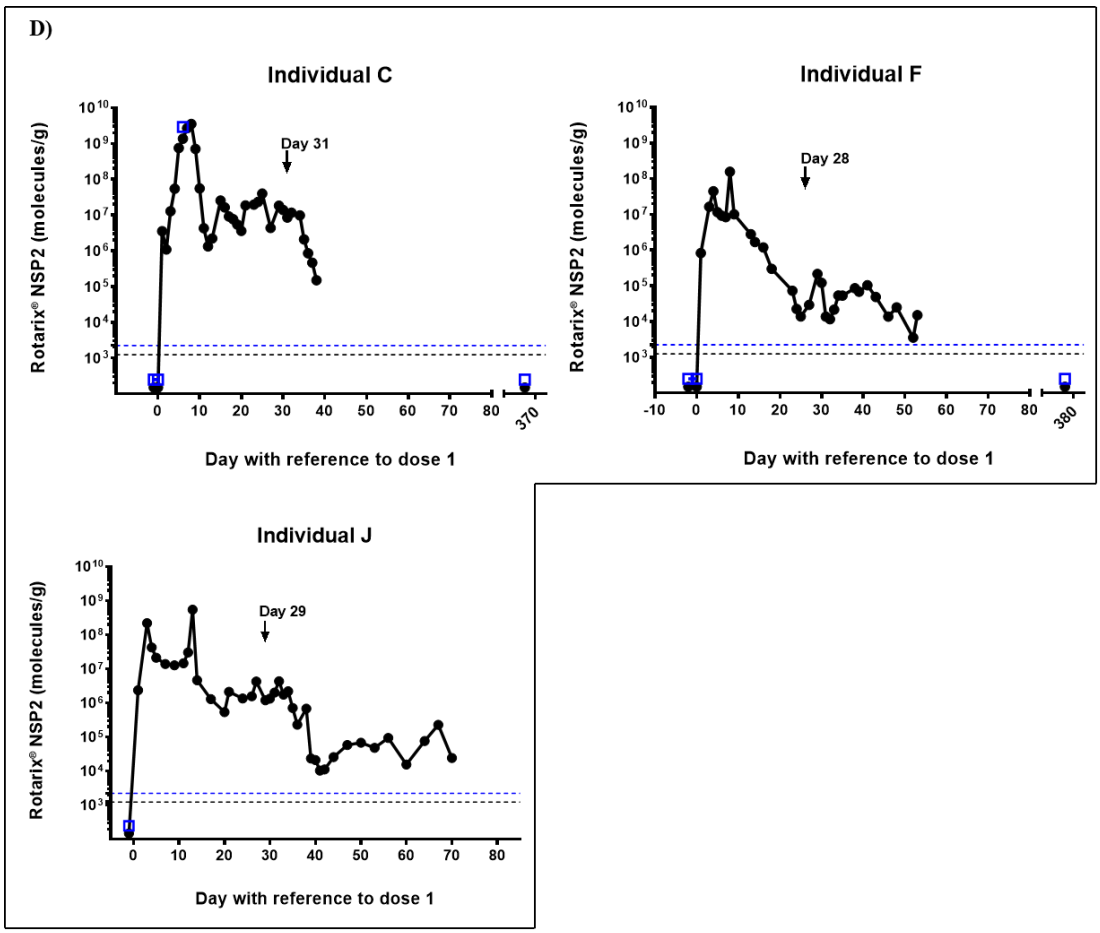

Profile 3 was defined by five infants (B, D, E, G, M) who yielded profiles whereby vaccine virus was shed after dose 1 and while typically waning, remained detectable at the point when dose 2 was administered (Fig. 3.4 C). Upon receiving dose 2, each infant shed virus for varying time ranging from day 1 to day 21 after dose 2, at lower amounts than after dose 1. However, shed virus was not detectable thereafter and the infants appeared to have ceased viral shedding. For individual E, a sample point at day 13 contained no detectable virus. The sample was retested to confirm this profile as accurate.

Profile 4 was defined by three infants (C, F, J) who presented continuous shedding after dose 1 until and following dose 2 (Fig 3.4 D). Initial shedding was amongst the highest in the cohort from days 1-13, followed by a three to four-log decrease in VLs that decreased again after dose 2.

Rotarix® RNA detection in faecal suspensions from particular infants

On occasion, samples appeared to yield data that were contrary to the general trend of the shedding profile. In these instances, the samples were re-extracted where material remained, and re-examined by RT-qPCR. Another series of spiking experiments were performed with Rotarix® final fills at a specific dilution for each of the infants' pre-vaccination samples tested (Table. 3.2). In most cases, the original viral load was confirmed (although pre-vaccination samples may yield different results, they are the closest samples to a stool negative control). On the sample from individual C spiked with vaccine material at 10^5 copies/mL, more copies at 10^6 were detected, probably due to assay variability or a dilution error in vaccine material. On the profile of individual H, there was a sharp dip on day six after dose 1, followed by an increase in shedding up to day 12, almost as high as the initial peak at day four after dose 1. This dip may be due to mild diarrhoea followed by increased replication until immune response controlled the infection. Individual L at timepoint 22 was on the limit of viral detection. Viral load quantification of stool suspensions spiked with vaccine material proved detection of low Rotarix® vaccine material viral loads spiked into stool and suggested the dips observed in profiles may be genuine based on pre-vaccination samples as the closest sample to a negative control (Fig. 3.5).

Table 3.2. Testing of specific timepoints with unexpected viral loads from several infants. Individuals and timepoints with dip or limit in VL from stool and vaccine material spiked into faecal suspensions to test detection.

Individual	Timepoint(s)	Vaccine spiked (copies/mL)
C	General; VLs ≥E+05 copies/mL	E+05
G	VL dips on days 23 & 25 after D1	E+04
H	VL dips on days 6 & 7 after D1	E+03
J	General; VLs >E+04 copies/mL	E+04
L	VL dip on day 22 after D1	E+03
M	VL dip on day 14 after D1	E+05

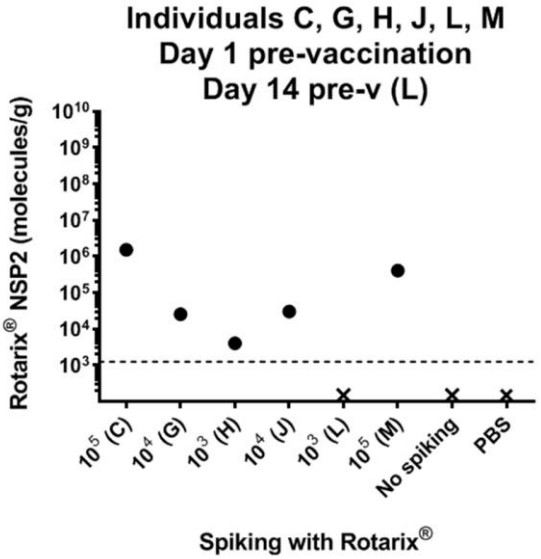

Fig. 3.5. Determination of the positivity of Rotarix® RNA from faecal-derived samples in different infants. Quantitation of rotavirus vaccine genome copy numbers by RT-qPCR. The X axis shows stool suspensions from several infants (C, G, H, J, L, M) spiked with Rotarix® vaccine material at different dilutions as well as negative controls (stool suspension and PBS). NSP2 gene copy numbers are shown in the Y axis.

3.4.3 Rotavirus WT RNA faecal shedding after Rotarix® vaccination

It was important to determine whether the infants had had a prior exposure to naturally circulating rotavirus before vaccination, as this could have implications for determining the effect of the vaccine. Similarly, detection of such 'wild-type' rotavirus at timepoints after vaccination would be suggestive of ineffective or failed immunisation.

The pre-vaccination status was determined by applying a VP6-pan-rotavirus RT-qPCR to samples where available. The sample set comprised 12 samples collected before day of first vaccination and six samples which were obtained on the day of vaccination (one before vaccine administration, infant C; and five after vaccine administration, infants D, E, F, H, K; time of vaccination provided retrospectively). None of the 12 pre-vaccination day samples yielded detectable rotavirus sequence (Fig. 3.4.).

All three positive samples from day of dose 1 (D, H, K) presented VL levels detected using the pan-RV assay that were not different from those achieved by the Rotarix®-specific assays. One of the infants tested on day of dose 1 with negative

results for WT RV (C) was also tested at day 6 after dose 1 and presented pan-RV VLs at non-significant levels with respect to those of vaccine. From the cohort, samples were available from eight infants at a year post-dose 1 and none yielded detectable rotavirus sequence (Fig. 3.4).

3.4.4 Breastfeeding and rotavirus vaccine RNA faecal shedding

The amounts of highest shedding after dose 1 and after dose 2 did not appear to be significantly lower in breastfed infants (n=6 - D, E, F, G, H, L after both doses) versus mixed-fed (n=5 - B, I, J, K, M after dose 1; n=4 – B, J, K, M after dose 2) infants (Fig. 3.6). The only infant fed with formula (C) presented high amounts of shedding after both doses.

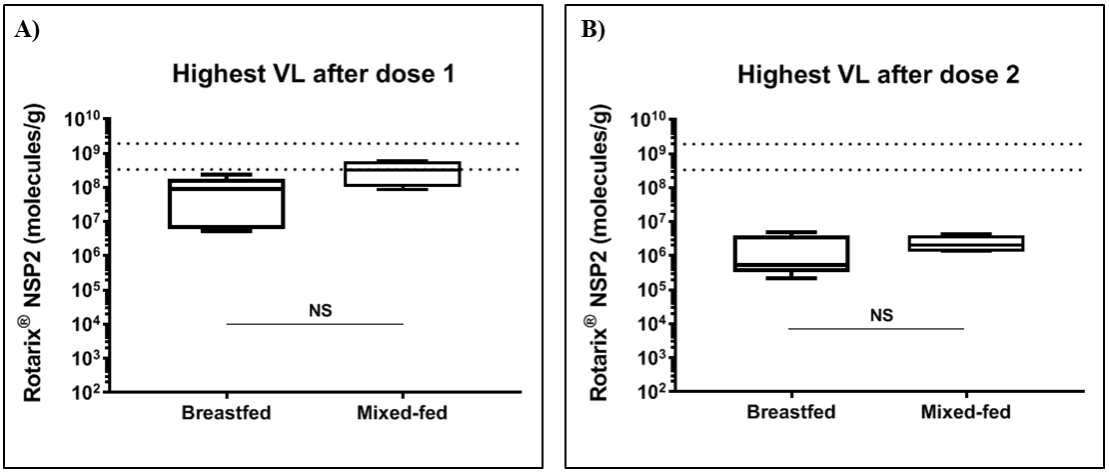

Fig. 3.6. Highest viral load in breastfed versus mixed-fed infants A) after dose 1 and B) after dose 2. Quantitation of rotavirus vaccine genome copy numbers by RT-qPCR. Rotarix® copy number range in vaccine material delimited by dotted lines. Statistical differences were assessed using the Kolmogorov-Smirnov test (*$p < 0.05$; **$p < 0.01$; ***$p < 0.001$). VL, viral load.

3.4.5 PCV1 DNA faecal shedding in infants after Rotarix® vaccination

Detection of PCV1 in the infant cohort was assessed by DNA qPCR and shedding defined as being detectable at similar or higher levels than in vaccine material and in a sustained manner after either dose of vaccine.

Rotarix® vaccine material

The viral load of PCV1 in Rotarix® vaccine was determined to be between 1.03×10^5 to 1.41×10^5 copies/mL of vaccine for DNA extracted using the QIAamp® DNA Mini Kit and between 1.83×10^6 to 5.47×10^6 copies/mL of vaccine for DNA extracted using the Viral RNA Mini Kit (Chapter 2, section 2.2.2), similar amounts to those measured in a recent study in the USA (Mijatovic-Rustempasic *et al.*, 2017). Viral loads from vaccine material are expressed in molecules/mL, equivalent to molecules/g in VLs from stool, assuming a density of 1 g per mL. This material was used as a control in the assessment of the faecal sample collection.

PCV1 faecal viral loads in infants

PCV1 in stool of vaccinees was detected in the range of 10^3-10^4 copies/g (Tables 3.3 A & B), similarly to a recent report (Mijatovic-Rustempasic *et al.*, 2017). None of the infants had detectable PCV1 prior to vaccination (n=12). One infant (G) had no evidence of PCV1 shed in faeces at any of the 14 timepoints tested which spanned the administration of doses 1 and 2. Viral DNA was detected in nine of the 12 infants after dose 1 although to levels not exceeding the PCV1 content of the vaccine dose (Fig. 3.7 A & C). While eight of the 12 infants shed PCV1 after dose 2, levels did not exceed the VLs quantified in vaccine material and were eliminated within three days (Fig. 3.7 B & C). The virus was not detected in stool after the third day after dose 1 or the second day after dose 2. The median highest VL was 1.16×10^4 copies/g of stool for dose 1 and 8.88×10^3 copies/g for dose 2. None of the infants were tested for PCV1 viral loads post one year.

Table 3.3. PCV1 DNA viral loads of individuals B-M after A) dose 1 and B) dose 2. Individuals, nothing or day of dose 2 (D2), detectable range of shedding, shedding period, day of peak shedding, last day of shedding, highest viral load and median viral load. Days with respect to dose 1 in (). NA, not applicable.

A)

	After dose 1 (D1)					
Individual	**Range (copies/g)**	**Shedding**	**Day of highest VL**	**Longest detectable VL**	**Highest VL**	**Median VL**
B	NA	No	NA	NA	NA	NA
C	E+04	Yes, days 1-2	1	Day 2	5.02E+04	3.26E+04
D	E+03	Yes, day 0	0	Day 0	6.78E+03	6.78E+03
E	E+03	Yes, day 1	1	Day 1	8.32E+03	8.32E+03
F	E+04	Yes, days 0-1	0	Day 1	7.65E+04	4.63E+04
G	NA	No	NA	NA	NA	NA
H	E+03	Yes, day 3	3	Day 3	8.88E+03	8.88E+03
I	E+03	Yes, day 1	1	Day 1	9.86E+03	9.86E+03
J	E+04	Yes, day 1	1	Day 1	4.08E+04	4.08E+04
K	E+04	Yes, day 0	0	Day 0	2.54E+04	2.54E+04
L	NA	No	NA	NA	NA	NA
M	E+04	Yes, day 3	3	Day 3	1.12E+04	1.12E+04

B)

		After dose 2 (D2)					
Individual	**Day of D2**	**Range (copies/g)**	**Shedding**	**Day of highest VL**	**Longest detectable VL**	**Highest VL**	**Median VL**
B	29	E+03 (nearly E+04)	Yes, day 1	1 (30)	Day 1	9.99E+03	9.99E+03
C	31	E+03	Yes, day 1	1 (32)	Day 1	3.75E+03	3.75E+03
D	35	E+03 to E+04	Yes, days 1-3	1 (36)	Day 3	1.11E+04	2.36E+03
E	31	NA	No	NA	NA	NA	NA
F	28	E+03	Yes, days 1-2	1 (29)	Day 2	7.97E+03	6.38E+03
G	29	NA	No	NA	NA	NA	NA
H	30	E+03 to E+04	Yes, days 1-2	1 (31)	Day 2	4.07E+04	2.20E+04
I	27	NA	No	NA	NA	NA	NA
J	29	E+04	Yes, day 0	0 (29)	Day 0	2.36E+04	2.36E+04
K	34	E+03	Yes, day 1	1 (35)	Day 1	3.53E+03	3.53E+03
L	33	E+03	Yes, days 1-2	2 (35)	Day 2	3.87E+03	3.44E+03
M	28	NA	No	NA	NA	NA	NA

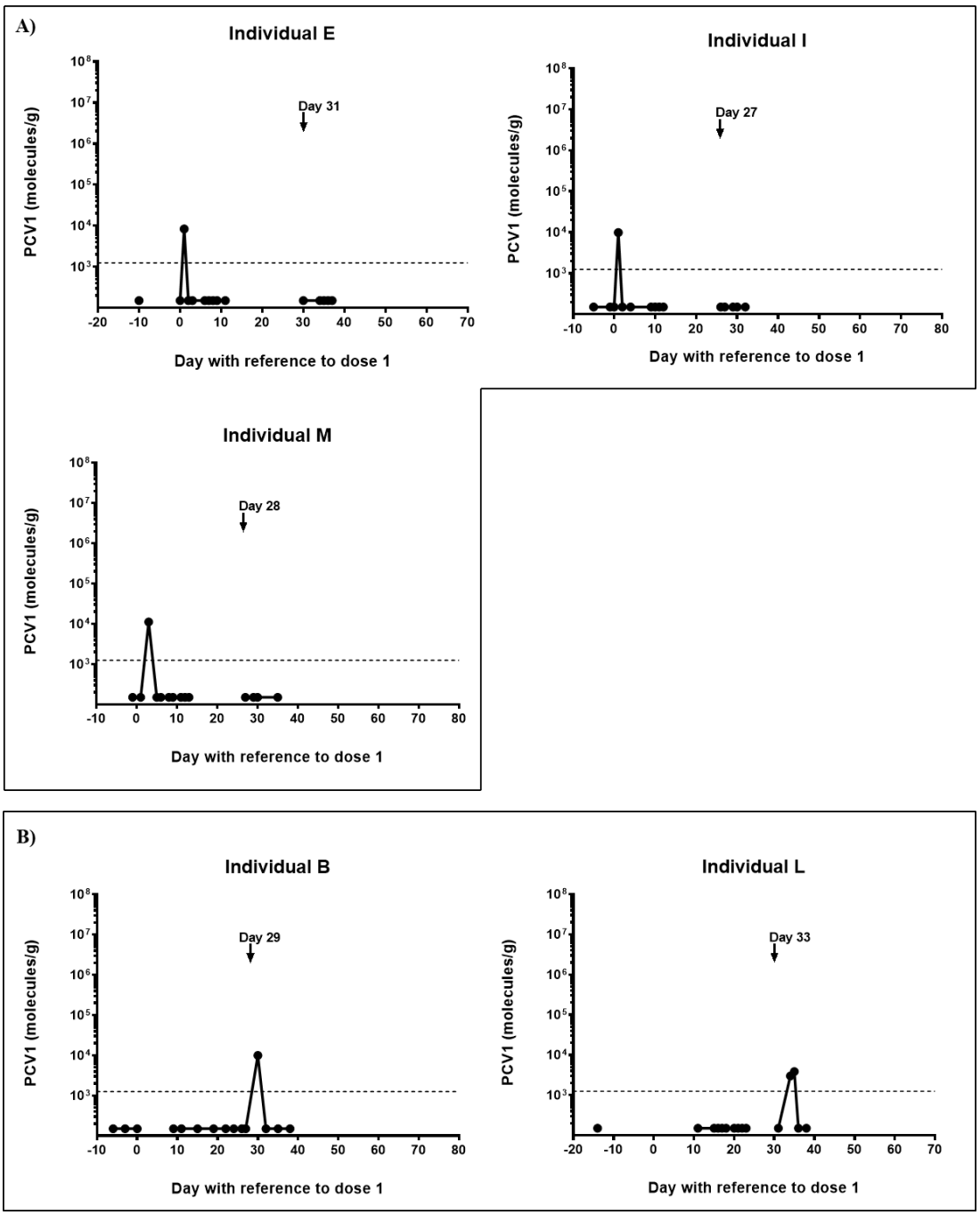

Fig. 3.7. Faecal shedding of PCV1 in A) individuals E, I and M; B) individuals B and L; and C) individuals C, D, F, H, J and K. Quantitation of PCV1 genome copy number by PCV1-specific qPCR: The X axis shows days with respect to dose 1 and the Y axis shows PCV1 copy number. Black dots, PCV1 VLs (molecules/g) at pre-vaccination and throughout the first three to ten timepoints after dose 1 and dose 2 (depending on sample availability). Black dashed line, LoD for PCV1 virus assay (6.25×10^2 copies/g; negative values below this line and of unknown value). Day 0: Day of dose 1. Arrow: Day of dose 2.

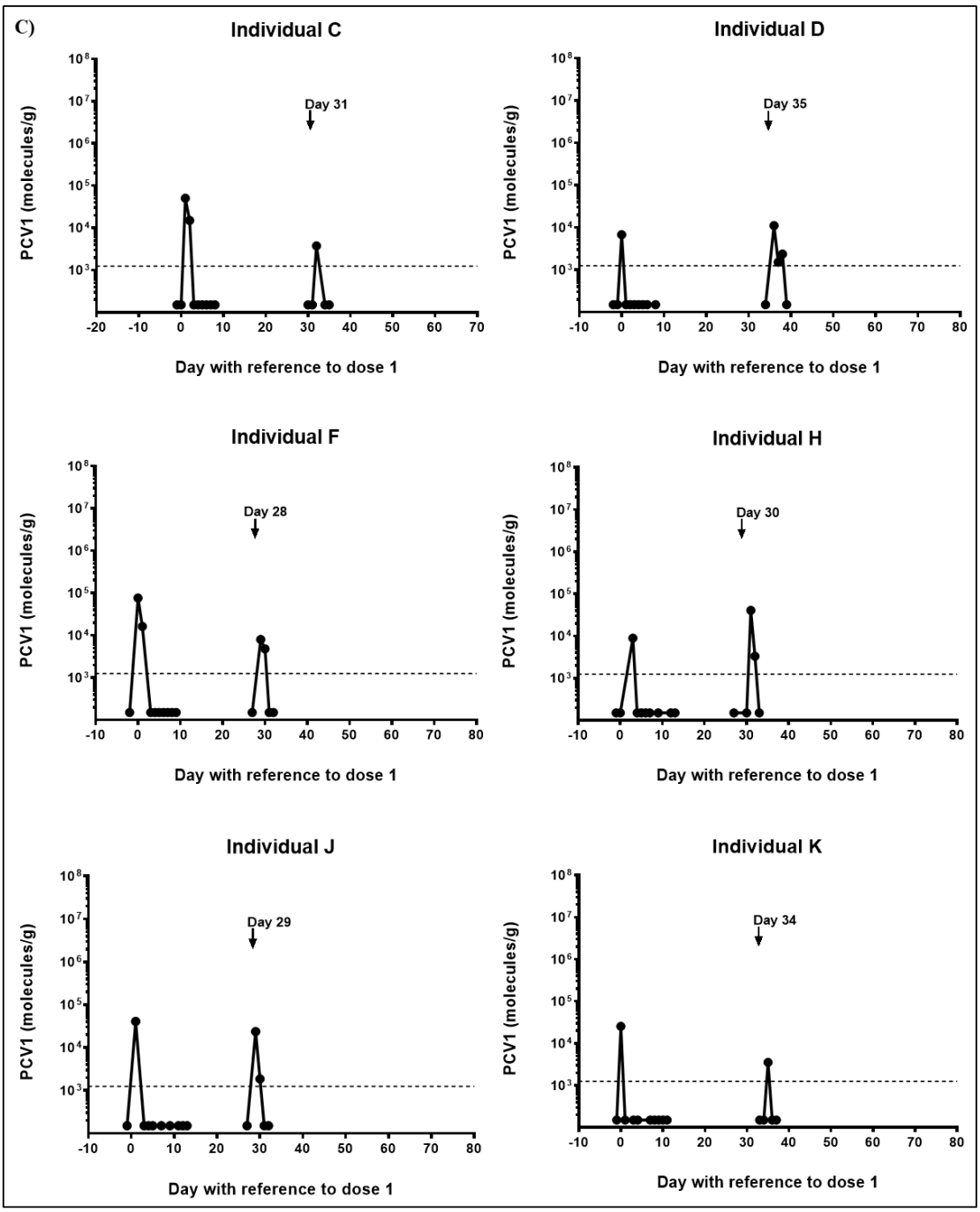

3.4.6 Rotavirus vaccine RNA and PCV1 DNA faecal shedding

On equivalent timepoints, Rotarix® viral loads were detected at two to three logs higher than PCV1 viral loads, as expected from the difference in viral loads in vaccine material. Of the three infants who had detectable PCV1 VLs only after dose 1, one shed Rotarix® only after dose 1 (I), another one mostly after dose 1 and after dose 2 for a day (M), and another one after both doses, and of the two infants who

shed PCV1 only after dose 2, both shed Rotarix® after the two doses (B, L), suggesting PCV1 detection is independent of Rotarix® detection.

In individual L, the pattern of PCV1 detection coincides with the pattern of Rotarix® detection in that viral loads at day 35 are slightly higher than those detected at day 34 for quantification of both viruses. Of the six infants who presented detectable PCV1 viral loads after both doses, four presented a similar decrease in viral load after dose 1 (C) and dose 2 (D, H, F) to that of Rotarix® VLs. Individual F also presented detectable PCV1 viral loads on day of dose 1 while no Rotarix® viral loads were detected on that day, suggesting again that detection of both viruses is unrelated. Individual J maintained Rotarix® VLs at days 29 and 30 after dose 2 while PCV1 viral loads decreased one log between those days.

3.5 Discussion

Pre-licensure and later studies have quantified Rotarix® shedding after vaccination using ELISAs (Bernstein, 1998; Vesikari, Karvonen, Korhonen, *et al.*, 2004; Dennehy *et al.*, 2005; Phua *et al.*, 2005; Salinas *et al.*, 2005; Ruiz-Palacios *et al.*, 2007; Hsieh *et al.*, 2014). They have also assessed a limited number of timepoints at vaccination, one week after dose 1, one week after dose 2 and extra timepoints in cases who developed any GE symptoms during the two-month period following vaccination (Bernstein, 1998; Vesikari, Karvonen, Korhonen, *et al.*, 2004; Dennehy *et al.*, 2005; Phua *et al.*, 2005; Salinas *et al.*, 2005; Ruiz-Palacios *et al.*, 2007). Sequential timepoints have been assessed during the month after vaccination until two consecutive negative samples were detected or during the first week after each dose (Hsieh *et al.*, 2014; Mijatovic-Rustempasic *et al.*, 2017), as well as at pre-vaccination, post dose 1 days 2-10 plus post dose 2 day of vaccination and days 2-10 plus post dose 2 week 2 (Pollock, 2018). Timepoints from within the first and second week after vaccination from vaccine recipients have been tested for horizontal transmission within the household (Bennett *et al.*, 2019). Regarding quantification methodology, molecular methods have proven to be more sensitive than ELISAs in rotavirus detection (Pang *et al.*, 2004; Hsieh *et al.*, 2014) and have been used in recent studies (Hsieh *et al.*, 2014; Mijatovic-Rustempasic *et al.*, 2017; Bennett *et al.*, 2019; Parker, 2019; Pollock, 2019). This study aimed at counteracting the previous

sampling limitations by using a small cohort to test multiple sequential samples following Rotarix® vaccination for one month after each dose using RT-qPCR to better define the kinetics of replication in vaccine recipients.

Infants usually encounter rotavirus at a young age thus vaccination is scheduled early in life to minimise the risk of infection with a WT strain and to generate better protection against severe disease (Bhan *et al.*, 1993; Bines *et al.*, 2015, 2018; Vesikari, 2015; Cowley *et al.*, 2017). In this cohort, no vaccine or pan-rotavirus viral loads were detected at pre-vaccination, suggesting infants had not encountered rotavirus before vaccination. The absence of either vaccine or pan-rotavirus viral loads in the after-a-year samples indicated infants had not encountered rotavirus following vaccination (unlikely) or they had (likely) and were protected against it. Previous studies have observed Rotarix® shedding in a greater proportion of infants after dose 1 (30-80%) than after dose 2 (11-35%) (Bernstein, 1998; Vesikari, Karvonen, Korhonen, *et al.*, 2004; Dennehy *et al.*, 2005; Phua *et al.*, 2005; Salinas *et al.*, 2005; Ruiz-Palacios *et al.*, 2007; Hsieh *et al.*, 2014; Mijatovic-Rustempasic *et al.*, 2017) (Chapter 1, section 1.14, Table 1.3) or similarly (30%) after both doses in Malawi (Pollock, 2018; Bennett *et al.*, 2019). A recent multicentre study that measured Rotarix® vaccine shedding in the UK observed 90% of vaccinated infants shedding vaccine virus after dose 1 and 60% after dose 2 (Parker, 2019). In this cohort vaccine virus was also detected in more infants after dose 1 (100%) than after dose 2 (91.7%), although not in the same proportion, which may be due to a small cohort.

While Rotarix® is reported to contain 10^6 $CCID_{50}$/mL, we quantified stocks as 2-3 $\log_{10}$ higher, suggesting the vaccine contains more RNA copies than infectious particles. Rotarix® viral loads in this UK cohort ranged between 10^3-10^9 copies/g of faeces with sustained shedding for >3 days after vaccination, suggesting detected viral loads were not attributable to inoculum. Since the transit time through the gut in Western infants is around 24 hours (Jayanthi *et al.*, 1989; Mihatsch, Hoegel and Pohlandt, 2006), a long period of shedding is less likely to be caused by slow clearance of inoculum, and more likely to be caused by prolonged viral replication. These levels were comparable to copy numbers quantified within vaccine material (10^8 to 10^9 copies/mL) and to those reported previously in USA-based (1.2×10^2 to 1.3×10^{10} copies/mL of stool) (Mijatovic-Rustempasic *et al.*, 2017) and China-based

studies (10^4 to 10^7 copies/g of stool) (Hsieh *et al.*, 2014). Rotarix® faecal viral loads were two logs lower than those reported in WT infection by others (10^5 to 10^{11} copies/g of stool) (Kang *et al.*, 2004; Kaplon *et al.*, 2015), as expected for a live-attenuated virus. Although live virus was not assayed, high and persistent viral loads for days after vaccination as well as the actual amount of virus in the gut being much higher, were strongly suggestive of active replication.

In previous studies, peak shedding occurred within the first week after dose 1 around day 7 (Bernstein, 1998; Vesikari, Karvonen, Korhonen, *et al.*, 2004; Dennehy *et al.*, 2005; Phua *et al.*, 2005; Salinas *et al.*, 2005; Ruiz-Palacios *et al.*, 2007; Hsieh *et al.*, 2014; Mijatovic-Rustempasic *et al.*, 2017) for all or >40% of infants. In this cohort shedding also occurred early after dose 1, although within the first week for half of the infants or within the second week for the other half, an observation facilitated by the comprehensive and longitudinal nature of the sampling. Most of the infants with early peak shedding ceased shedding early although not all (individuals G, M) and most of the infants with protracted shedding presented late peak shedding, with exceptions (individual L).

In early studies, shedding occurred as early as one or three days after vaccination and as late as 28 or 45 days after dose 1 (Bernstein, 1998; De Vos *et al.*, 2004; Dennehy *et al.*, 2005; Phua *et al.*, 2005; Salinas *et al.*, 2005; Ruiz-Palacios *et al.*, 2007; Hsieh *et al.*, 2014; Mijatovic-Rustempasic *et al.*, 2017; Pollock, 2018). Similarly, in this cohort, median longest shedding duration after dose 1 was day 27, which suggested that Rotarix® persists in the gut for approximately a month before it becomes undetectable in stool. By contrast, shedding was detected beyond 45 days after dose 1 in several infants, with the longest shedding detected at more than 70 days after dose 1 in one of them. These results highlight the possibility that shorter shedding detected in previous studies may have been due to a shorter follow up period, the lack of continuous sampling or insufficient sampling or recruits; and that shedding duration may depend on the recipient's susceptibility to infection and immune response.

In this cohort, significantly higher viral loads were detected after dose 1 compared to after dose 2 at both highest and median viral loads, indicating vaccine take after dose 1 and a catch-up effect after dose 2. Previous studies in developed countries have also quantified higher viral loads after dose 1 with respect to dose 2

(Hsieh *et al.*, 2014; Mijatovic-Rustempasic *et al.*, 2017), as opposed to those in a LIMC such as Malawi, with similar peak viral loads after both doses (Pollock, 2018; Bennett *et al.*, 2019). Moreover, the highest viral loads of breastfed infants were lower than those of mixed-fed infants after dose 1 and dose 2 (although non-significantly), as previously observed in a larger cohort where reduced Rotarix® shedding was detected in breastfed infants (Bautista-Marquez *et al.*, 2016).

Regarding shedding patterns, in this cohort of 12 infants, it was clear that vaccine virus shedding occurred in all. Profile 1 showed apparent effective control of virus shedding after one dose from the 2-dose regimen: high initial viral loads decreasing within two weeks and suggesting replication followed by rapid control of virus shedding after the first dose, with an absence of shedding after the second dose. The other early responders (Profile 2) who controlled vaccine virus after the first dose with low shedding after the second dose also appeared to present a robust immune response through a prime-boost effect following the two doses. In each infant there was a window during which vaccine virus was not detected, suggesting effective control of viral shedding. A positive sample on the day before dose 2 for one individual (K) may be due to a sample labelling mistake or to sample bias with virus still replicating at that stage. Of relevance to these profiles, it has been previously found that individuals with a non-secretor or $FUT2^{-/-}$ phenotype are resistant to severe RVGE by G1P[8] strains (Imbert-Marcille *et al.*, 2014). Given that the proportion of individuals with that phenotype in the Caucasian population is approximately 20% (Marionneau *et al.*, 2001), these early responders who ceased shedding after dose 1 within 15 days (I, H, K; 25%) may be non-secretors. Similarly, results in recent studies in Nicaragua (Bucardo *et al.*, 2018) and Malawi (Pollock *et al.*, 2018) have highlighted that "non-secretors" presented reduced Rotarix® shedding. Vaccinated infants in Malawi presented Rotarix® shedding patterns identified in this cohort (early and late responders and continuous shedders) and a large proportion of "low-shedders" who appear to present poor vaccine take (Pollock, 2018, 2019). Likewise in another system, Rotarix® replication was found to be attenuated in a human intestinal enteroid developed from a non-secretor patient (Saxena *et al.*, 2016). However, in the case of this cohort, this is a conjecture since no genetic data was available and ethical approval to obtain genetic information on these infants is unlikely to be obtained in the future due to the design of the study.

Therefore, future studies in a similar cohort would have to be performed to confirm this.

Other infants (Profile 3) did not clear vaccine virus between the doses, suggesting they were not able to mount an immune response capable of controlling the initial vaccine virus in the one-month period, but they were capable of eliminating the virus effectively on receipt of the booster dose. The second dose might have had little effect in some of them who were decreasing shedding (D, G) and some catch-up effect on those who presented higher viral loads before dose 2 (B, E, M). For individual E, the increase in VL from day 14 may be due to a minority variant replicating at higher frequency than previously (Chapter 4). A correlation between viral loads and Vesikari's GE severity score was previously observed in WT infection (Kang *et al.*, 2004). Hence, the dip in viral loads at day 13 may also be due to mild diarrhoea at a previous timepoint of high shedding ($>10^6$ copies/g of stool) and insufficient replication of the virus around day 13. For individual G, shedding after dose 1 might have been fully controlled if there had not been a second dose. It was previously observed that children who do not continuously shed rotavirus vaccine appear to be protected against severe disease better than extended shedders, and to a level similar to that afforded by natural immunity following infection with WT rotavirus (Richardson *et al.*, 1998). Protection for infants in this profile may be lower than in those who control infection rapidly, although the slow immunity built in these infants may be stronger and more mature.

A fourth profile (Profile 4) was similar to Profile 3 in that vaccine virus was shed between doses. However, owing to the reduced timespan of the samples available from individual C and to the lack of further samples from individuals F and J, it was not possible to obtain a sufficient number of data points to conclusively prove clearance of vaccine virus following dose 2. Nevertheless, the absence of vaccine/WT virus at the one-year-after-vaccination timepoint suggested elimination of vaccine virus in that period. Higher levels of Rotarix® shedding than those observed in this cohort have only been reported in infants with severe-combined immunodeficiency, with Rotarix® detected at $>10^{11}$ copies/mL at nine days before haematopoietic stem cell transplantation and up to 10^6 copies/mL at six months after transplantation (Rosenfeld *et al.*, 2017) or with Rotarix® detected at $>10^{12}$ copies/mL before gene therapy dropping to undetectable 270 days after first infusion

(N. C. Patel *et al.*, 2012). Infants in this cohort may have developed a less rapid vaccine response in Profile 4, possibly as a result of a low mucosal immune response. This variability in vaccine uptake and shedding duration points towards a difference in susceptibility to infection by G1P[8] RV strain as well as to differences in immune response among the cohort in this study.

All infants and especially the continuous shedders described above may act as virus reservoirs if selection of variants in the presence of NAbs takes place as the vaccine virus replicates (Richardson *et al.*, 1998). Examples of horizontal transmission have been described for RotaTeq® in Australia, the USA and Finland, where transmission of vaccine and vaccine-derived strains was observed within two weeks of vaccination in healthy and immunodeficient contacts, in some cases causing RVGE (Payne *et al.*, 2010; Yen, Jakob, *et al.*, 2011; Bowen and Payne, 2012; Donato *et al.*, 2012; Hemming and Vesikari, 2012; Wikswo *et al.*, 2019). In the case of Rotarix®, there are a number of reports on potential, occasional and asymptomatic horizontal transmission of vaccine derived virus from vaccinated to unvaccinated twins (Dennehy *et al.*, 2005) and from vaccinated infants to unvaccinated infants -vaccine strain confirmed in this study- in the clinical setting or community (Phua *et al.*, 2005). Another study reported detection of vaccine strains in unvaccinated infants who presented GE symptoms and needed treatment (Boom *et al.*, 2012). A study in the Dominican Republic assessed horizontal transmission of Rotarix® where contacts acquired the vaccine strain without developing RVGE symptoms, indicating Rotarix® may provide indirect protection to unvaccinated individuals (Rivera *et al.*, 2011). In another study in Taiwan, Rotarix® shedding was found to be significantly higher than that of RotaTeq® probably due to Rotarix® containing a RVA G1P[8] human strain which may replicate better in the intestine, and suggesting horizontal transmission may be more likely in infants vaccinated with Rotarix® (Hsieh *et al.*, 2014). A study in Japan reported suspected horizontal transmission of Rotarix® in infants with AGE and other enteric pathogens detected apart from vaccine-derived and WT rotavirus strains (Kaneko *et al.*, 2017). Another study in Japan detected low transmission of Rotarix® within a foster home without detection of the vaccine strain in symptomatic unvaccinated individuals (Miura *et al.*, 2017) and another study in Malawi also detected low transmission of Rotarix® within the household with probably very little effect to contacts (Bennett *et al.*, 2019).

Another group in Japan studied the possibility of rotavirus vaccine virus dissemination among neonates in the intensive care unit under contact precautions: Rotarix® vaccinees presented different shedding patterns with longer shedding after first dose and no unvaccinated infants shedding detectable vaccine virus (Hiramatsu *et al.*, 2018). In the UK, rotavirus vaccination is recommended in the neonatal intensive care unit despite a risk of horizontal transmission since the benefits of protection against RVGE and other derived conditions such as necrotizing enterocolitis are larger than the risk of vaccination in stable neonates (Jaques *et al.*, 2014, 2015; Ladhani and Ramsay, 2014). In contrast, although the risk of transmission of a vaccine or vaccine-derived variant is lower than that of WT RV due to lower levels and shorter periods of replication, the immunocompromised are advised to avoid vaccination and contact with vaccinees especially after the first dose (Anderson, 2008). Cases of acute RVGE and/or continuous shedding have been described in immunocompromised individuals after rotavirus vaccination (N. C. Patel *et al.*, 2012; Kaplon *et al.*, 2015; Rosenfeld *et al.*, 2017). Therefore, any potential horizontal transmission from the cohort of infants studied in this work may result in herd immunity or may pose a health risk to susceptible or immunocompromised individuals. Moreover, if vaccine-derived variants with pathogenic potential arise either in early responders or in continuous shedders they may also pose a health risk to healthy individuals. The use of NGS will help elucidate minority variants that increase throughout the shedding period following vaccination.

Finally, the study of PCV1 in stool of vaccine recipients highlighted that it only transiently passes through the gut of vaccinated infants. It was detected in the range of 10^3-10^4 copies/g, similarly to a previous report detecting PCV1 DNA in stool of Rotarix®-vaccinated infants in the USA (Mijatovic-Rustempasic *et al.*, 2017). Mijatovic-Rustempasic and colleagues detected very little PCV1 and there was no overt evidence of virus replication: lower VLs of PCV1 in stool with respect to the vaccine stock and a short-lived pulse of VL followed by a rapid drop to levels below the limit of detection suggested that PCV1 did not replicate in the gut of vaccine recipients following vaccination. Similarly in this cohort, although the possibility of low-level replication below the detection limit of the assay or in another organ could not be ruled out and live virus was not assayed, the lack of

persistent virus detection in stool also suggested that PCV1 did not replicate, transiently passed through the gastrointestinal tract of infants and was cleared after both doses. Although we have not studied whether PCV1 may enhance Rotarix® replication (which would require cell culture co-infectivity studies), it appeared that PCV1 infection or replication were not enhanced by rotavirus vaccine.

Studies on genetic diversity of PCV1 from pigs in Hungary and in the UK have found very low diversity in strains sequenced two decades apart. This suggests that genetic stability of porcine circoviruses may mean PCV1 is at an advanced state of evolution (Tombácz *et al.*, 2014) and it may explain the differential non-pathogenic adaptation of PCV1 in pigs (Cortey and Segalés, 2012). Moreover, since Rotarix® is not the only source of PCV1, which can also be found in pork products and in human faeces (Li *et al.*, 2010), infants may be exposed to it regardless of rotavirus vaccination as suggested by a study in 2017 in which 0.3% infants who received placebo were seropositive for PCV1 compared to 1% seropositive Rotarix® vaccine recipients (Han *et al.*, 2017). Further studies would be needed to elucidate whether PCV1 enhances Rotarix® replication (cell culture co-infectivity studies), as well as being needed to elucidate whether transient PCV1 may be horizontally transmitted to contacts.

A few caveats considered in the design of this study may have impacted on results. Stool samples were divided into small working aliquots of 200 mg to 1 g, therefore potentially having an effect on quantified copy numbers due to sampling bias and stool being heterogeneous. The faecal suspensions used to extract nucleic acid were prepared on the day of extraction from faecal material to prevent any extra degradation occurring during storage of faecal suspensions. Due to low sample availability and to ensure enough sufficient samples were available for subsequent analyses, VLs were tested as technical replicates from single faecal suspensions, a more homogeneous sample than faecal matter. The timepoints available from each infant were not identical, so comparisons were made between the most relevant events during the vaccination period: Days of peak shedding (early from days 2-6 and late from days 7-15), last day of shedding, highest and median viral loads. Despite the small cohort, given the large number of samples available from each infant, the granularity of data allowed for effective viral shedding profiling and

comparison between infants. Regarding low PCV1 VLs, at specific days for which samples were not provided, we may have missed highest VLs.

This is the first study to undertake a comprehensive assessment of longitudinal faecal shedding of Rotarix® in a cohort of vaccinated infants. The viral shedding data profiling point to variation in the immune response and control of vaccine virus shedding. Furthermore, having confirmed the veracity of apparent outlier data points of VL profiles, the immune pressure on the vaccine virus can be considered through genetic variation. The opportunity for the vaccine virus to mutate or adapt in the context of a developing immune response is addressed through next generation sequence analysis of virus at selected timepoints from the cohort infants vaccinated with Rotarix® (Chapter 4).

Chapter 4: Genetic stability of faecal rotavirus RNA in a cohort of infants vaccinated with Rotarix® in the UK

4.1 Introduction

The fact that some live-attenuated vaccines have been found to present mutations that pose a risk to vaccine efficacy and/or safety (*e.g.* Cann *et al.*, 1984; Victoria *et al.*, 2010) has highlighted the importance of monitoring genetic consistency of vaccines in use. Although some studies had assessed the genetic stability of WT RV strains in cell culture and others have pointed at certain sequence or amino acid changes that could be associated with attenuation (Flores, Sears, *et al.*, 1988; Tsugawa and Tsutsumi, 2016), the genetic changes conferring attenuation to Rotarix® have not been well characterised (Chapter 1, section 1.15). Recently, a viral RNA in-house sequence of Rotarix® vaccine stocks was established at the NIBSC (Mitchell, Lui, *et al.*, unpublished): In Rotarix® vaccine material, 25 SNP loci were identified at consistent frequencies across independent bulks and fills. Eighteen of these were present in both virus harvest bulks and final fills and spanned six genes (VP1, VP3, VP4, VP6, VP7 and NSP1). Thirteen SNP loci were identified in VP4 and one of them was the same as WT with a mean frequency greater than 50% (nucleotide position 1103). Genes encoding for VP1, VP3, VP6 and VP7 and NSP1 contained one mutation each. For most SNP loci (except two positions in the VP4 gene) the variant frequency was <17%. There were 23 non-synonymous amino acid substitutions identified in the 25 SNPs detected, 20 of them resulting in a residue different to that seen in WT strains and vaccine virus, two of them resulting in the residue observed in WT and one of them coding for a residue seen in both WT and vaccine virus. Most of the changes were identified in VP4, suggesting that mutation of the outer capsid protease-sensitive protein was key for cell culture adaptation of the vaccine virus during manufacture, as well as mutation of the glycoprotein (VP7) and inner capsid protein (VP6), viral polymerase complex and interferon antagonist (VP1+VP3 and NSP1). Changes in these proteins are likely to be crucial for cell

culture adaptation, although they may have occurred earlier in the generation of a candidate vaccine virus and be maintained during manufacture. These data showed a very high nucleotide identity between virus harvest bulks and final fills, suggesting a consistent vaccine manufacturing process (Mitchell, Lui, *et al.*, unpublished).

As described earlier (Chapter 3) and in previous studies (Hsieh *et al.,* 2014; Mijatovic-Rustempasic *et al.,* 2017), Rotarix® is shed throughout after both doses at viral loads similar to or lower than vaccine inoculum and shedding patterns can vary from a few days to weeks. Sustained replication of vaccine inoculum in vaccine recipients is likely to lead to the establishment of minority variants that may persist and confer an advantage on the virus as vaccine-derived variants, as observed previously (Chapter 1, section 1.8).

4.2 Aims

The aim of the work presented in this chapter was to assess the genetic stability of Rotarix® during replication in vaccinees by identifying and quantifying SNPs differing from the published Rotarix® reference sequence (GenBank ref. nos. JX943604- JX943614) (Gautam *et al.*, 2014) and from the NIBSC-generated Rotarix® sequence (Mitchell, Lui, *et al.*, unpublished) at relevant timepoints for each viral load profile (section 4.4.1). A second aim was to determine the relationship between Rotarix® faecal shedding and vaccine and vaccine-derived variants in this population.

4.3 Experimental methodology

To address the vaccine genetic stability, faecal material was available as described (Chapter 3). Detailed materials and methods are described in Chapter 2 and Appendix I. Faecal samples were processed and stored until used (Chapter 2, sections 2.1.9 and 2.2.1). Some samples were of low quantity owing to stooling patterns and the analysis reflected this. To maximise the information obtained from this limited resource, the reproducibility of data in this chapter was addressed by sequencing relevant timepoints along the viral load profile of each infant in triplicate from independent faecal suspensions. Rotarix® and/or rotavirus from stool of vaccinees was extracted following the methods in Chapter 2, section 2.2.3.3. Next,

cDNA synthesis and PCR amplification were performed on extracted RNA (Chapter 2, section 2.2.4) and purified and sequenced using the Nextera® XT DNA Library Preparation kit v2 following the methods in Chapter 2, section 2.2.6. Bioinformatic analysis (Chapter 2, section 2.2.7) and further data analysis (Chapter 2, section 2.2.8) were performed in collaboration with the NIBSC NGS core facility. Criteria were set to validate data for SNP calling as having a quality score of at least Q30, coverage of ≥100 mean reads for each studied position and a mean frequency of ≥1% observed in ≥2 of 3 replicates. The longitudinal analysis of SNPs focused on describing the type of mutation, whether it had been identified in vaccine or stool material, whether it had been detected in several timepoints and the fluctuation of its frequency over the timepoints tested. Molecular modelling of selected amino acid changes was performed with LigPlot^{+} (Laskowski and Swindells, 2011) and RasMol (Sayle and Milner-White, 1995) using the Protein Databank resolved rotavirus structures available.

4.4 Results

4.4.1 Sample set

Timepoints provided were not equivalent between infants due to stooling patterns and parental collection. Where low amounts of stool were available, priority was assigned to Rotarix® faecal shedding quantification throughout the sample collection, followed by NGS of relevant timepoints from each infant, based on their shedding profiles: Timepoints of peak shedding, timepoints just before a large decrease in shedding and timepoints during sustained shedding. All the timepoints chosen presented viral loads of $\geq 10^4$ viral copies/mL (Chapter 3). From one to five timepoints from each infant were sampled and assayed throughout the two-month vaccination period.

Due to the complexity of amplifying all 11 RV segments from limited faecal material (Appendix II, section 8.2.1.3, subsection ‘sample set’), genetic characterization was performed on genes encoding VP4, VP7, VP6 and NSP4. These segments were chosen on the basis of reported selection pressure in cell culture (VP4, VP7, NSP4) (Tsugawa and Tsutsumi, 2016) and number of mutations during manufacture (VP4, VP6, VP7) (Mitchell, Lui, *et al.*, unpublished). Moreover, VP4

and VP7 were identified as targets of neutralizing heterotypic protection in humans (Nair *et al.*, 2017) and VP6 as the target of neutralizing protection *in vivo* (Burns *et al.*, 1996; Feng *et al.*, 2002; Corthésy *et al.*, 2006). NSP4 was also chosen on the basis that it may induce immunogenicity as a viral enterotoxin (Ball *et al.*, 1996). The data presented below were generated using Nextera® kit libraries as previously described.

4.4.2 Genetic stability of rotavirus faecal RNA in infants after Rotarix® vaccination

In this cohort of 12 infants, SNP profiles were generated for each of the vaccine recipients in gene segments encoding VP4, VP7, VP6 and NSP4 and from one to five timepoints during the vaccination period (Table 4.1). These SNPs were compared to the vaccine reference sequence and in-house sequence, assessed against WT RVA human G1P[8] (GenBank reference numbers JN887809, JN887818, JN887819, JN887814) and compared to human WT consensus by BLAST in Geneious (>92% identity) in order to identify potential WT reversion mutations. The SNP frequency was quantified as the percentage of sequencing reads in which a SNP was detected along the genome. It indicated differences between SNP profiles and vaccine material and, therefore, between viral quasispecies as Rotarix® replicated in each infant. Each mutation was identified at a different frequency at each timepoint, viral segment and infant. For some of the genes at some timepoints for some infants, there were no SNPs identified due to the sequence not differing from the reference sequence or due to low amounts of DNA following extraction and RT-PCR (tested on Bioanalyzer chip after RT-PCR and agarose-gel electrophoresis). The SNPs identified were described based on the nucleotide position from A in first codon encoding the first methionine for each gene segment: a 12 nucleotide shift (from original ref. no. JX943612) when aligned to WT GenBank reference JN887809 for gene segment 4 (encoding VP4); the original nucleotide position (in ref. no. JX943614) when aligned to WT GenBank reference JN887818 for gene segment 9 (encoding VP7); the original nucleotide position (in ref. no. JX943613) when aligned to WT GenBank reference JN887819 for gene segment 6 (encoding VP6); and a 41 nucleotide shift (from original ref. no. JX943607) when aligned to WT GenBank reference JN887814 for gene segment 10 (encoding NSP4).

The SNP genetic profile of Rotarix® vaccine material was validated at the NIBSC (Mitchell, Lui, *et al.*, unpublished). The sequence was similar to the previously published Rotarix® sequence (GenBank ref. nos. JX943604- JX943614) (Gautam *et al.*, 2014), but it presented low level SNPs (Mitchell, Lui, *et al.*, unpublished). Within the four gene segments 4, 9, 6 and 10 across infants, timepoints and at a varying number of repeats (one to three repeats), 270 SNP loci were identified (Table 4.2). Following the criteria described in section 4.3, a total of 81 SNP loci were identified within the four genes encoding VP4, VP7, VP6 and NSP4 (Figs. 4.1, 4.5, 4.9 & 4.13), an increase with respect to the 25 SNPs identified in vaccine material (Mitchell, Lui, *et al.*, unpublished). In vaccine material, 23 of the 25 SNPs appear at frequency ≤17%, while in stool mutations were detected at similar or higher frequencies than in vaccine. No SNPs were identified under the criteria described in section 4.3 in stool from one of the 12 infants in this cohort (individual G) for any of the four gene segments studied (Table 4.1). Single nucleotide polymorphism loci were identified in eight infants for gene segment 4, in four infants for gene segment 9, in two infants for gene segment 6 and in 10 infants for gene segment 10. One infant (individual G) yielded low amounts of RNA that resulted in low coverage and mapping to RVA for all repeats for gene segment 4, and all but one repeat for gene segments 9 and 6. Low level SNPs (<15%) were identified in single replicates for gene segment 10 in stool from this infant.

Table 4. 1. Timepoints tested by next generation sequencing in individuals B-M for viral segments encoding VP4, VP7, VP6 and NSP4. Individual, timepoints tested after dose 1 and after dose 2 (with respect to dose 1) and timepoints where enough material was available for sequencing and which were positive for reads mapping to rotavirus following the criteria in section 5.3.

	Timepoints tested		Timepoints positive for gene segments encoding			
Individuals	**Days after dose 1**	**Days after dose 2 (with respect to dose 1)**	**VP4**	**VP7**	**VP6**	**NSP4**
B	19	32, 44	19, 32, 44			19, 32, 44
C	9	34	9, 34	9		9, 34
D	8	39, 44	8, 39			8
E	6	35	6, 35			6, 35
F	7	30, 41	7, 30			7, 30, 41
G	4, 13	40				
H	3, 9	31	3			
I	9		9			9
J	3, 13, 27	38, 67	3, 13, 27, 38, 67	13	13	13, 27, 38, 67
K	4	36	4			4
L	15	35	15, 35	15		15
M	5, 13		5, 13	5, 13	5	13

Table 4. 2. Summary of SNPs identified in genes encoding VP4, VP7, VP6 and NSP4. Individuals, number of SNPs, classification of mutation, number identified previously in vaccine material, SNP frequencies and SNPs identified in several children. Individ., individual; SNP, single nucleotide polymorphism; S, synonymous; NS, non-synonymous; WTrev, reversion to WT human RVA G1P[8] (GenBank reference numbers JN887809, JN887818, JN887819, JN887814,); V, previously identified in vaccine material (Mitchell, Lui, *et al.*, unpublished); common SNPs, SNPs common to several infants; comments, days when SNPs identified. White, full 3 repeats or 2 repeats for most; darkest grey, some 3 repeats some 2 repeats some 1 repeat; middle dark grey, some 2 repeats some 1 repeat; lightest grey, only 1 repeat for most.

Encoded protein	Individ.	SNP No.	S	NS	WTrev	Stop codon	V	SNP frequency (%)	Common SNPs	
VP4	**B**	14	5	8	1		3	2.2-100.0; 10 SNPs <14% (4 S, 6 NS), 1 SNP at 70-73% (1 NS), 2 SNPs at >50-100% (1 S, 1 NS), 1 SNP at 92-100% (1 WTrev)	5	1 S; 3 NS; 1 WTrev
	C	9	2	5	2		3	2.4-100.0; 4 SNPs <4% (2 S, 2 NS), 1 SNP 53-55% (1 NS), 1 SNP 65-66% (1 NS), 1 SNP 35-95% (1NS), 1 SNP 97-99% (1 WTrev), 1 SNP 97-100% (1 WTrev)	6	4 NS; 2 WTrev
	D	27	5	20	2		10	1.3-100.0; 25 SNPs <34%, 1 SNP >50% (1 NS), 1 SNP >50-100% (1 WTrev)	14	1 S; 11 NS; 2 WTrev
	E	9	1	6	2		6	1.2-100.0; 5 SNPs <16% (5 NS), 1 SNP 4-95% (1 NS), 1 SNP 98-100% (1 WTrev), 2 SNPs 100% (1 S, 1 WTrev)	9	1 S; 6 NS; 2 WTrev
	F	17	2	13	2		9	1.2-100.0; 14 SNPs <22%, 2 SNPs >50% (1 NS, 1 WTrev), 1 SNP >50-100% (1 WTrev)	12	10 NS; 2 WTrev
	G									
	H	13		12	1		11	1.3-65.0; 12 SNPs at <19% (12 NS), 1 SNP at 57-65% (1 WTrev)	12	11 NS; 1 WTrev
	I	15	4	9	2		8	1.3.99.5; 14 SNPs at <35%, 1 SNP at 97-99% (WTrev)	11	2 S; 8 NS; 2 WTrev
	J	41	12	28	1		8	1.0-100.0; 35 SNPs at <50%, 4 SNPs >50% (4 NS), 1 SNP >50-96% (1 NS), 1 SNP 90-100% (1 WTrev)	13	2 S; 10 NS; 1 WTrev
	K	11	2	8	1		8	1.2-91.7; 10 SNPs <19% (2 S, 8 NS), 1 SNP 89-92% (1 WTrev)	9	1 S; 7 NS; 1 WTrev

	L	12	2	8	2		7	1.7-100.0; 9 SNPs <20% (2 S, 7 NS), 1 SNP 57-100% (1 WTrev), 2 SNPs >95% (1 NS, 1 WTrev)	8	6 NS; 2 WTrev
	M	13		11	2		8	1.2-98.7; 11 SNPs <50%, 1 SNP 68-72% (1 NS), 1 SNP 94-99% (1 WTrev)	11	9 NS; 2 WTrev

Encoded protein	**Individ.**	**SNP No.**	**S**	**NS**	**Rev. to WT**	**Stop codon**	**V**	**SNP frequency (%)**	**Common SNPs**	
VP7	**B**	4	2	1		1		4.2-99.9; 1 SNP <5% (1 S), 2 SNPs < 27% (1 S, 1 STOP), 1 SNP at 99.9% (1 NS)	1	1NS
	C	6	1	4	1		1	2.0-17.3	1	1 WTrev
	D									
	E	2		2				8-30.6		
	F	3	2	1				9.9-89.8; 2 SNPs <12% (1 S, 1 NS), 1 SNP at 89.9%		
	G	1	1					7.3		1 S
	H	2	2					3.6-6.0		
	I									
	J	8	4	3	1		1	3.4-32.5; 6 SNPs <32% (3 S, 3 NS), 1 SNP 6-34% (1 S), 1 SNP 6-33% (1 WTrev)	1	1 WTrev
	K									
	L	3		3				5.5-47.8		
	M	9	4	3	1	1	1	4.7-99.9; 8 SNPs <50%, 1 SNP up to 99.9% (1 WTrev)	1	1 WTrev

Encoded protein	Individ.	SNP No.	S	NS	Rev. to WT	Stop codon	V	SNP frequency (%)	Common SNPs	
VP6	**B**	9	3	6				1.2-31.9; 5 SNPs <4.7% (2 S, 3 NS), 4 SNPs 16-32% (1 S, 3 NS)	1	1 NS
	C	5	2	3				1.4-6.2	1	1S
	D	1		1				4.1		
	E	9	4	5				1.1-99.9; 8 SNPs <10.7% (4 S, 4 NS), 1 SNP at 99.9% (1 NS)	2	2 NS
	F	4	2	2				1.7-34.0		
	G	2	1	1			1	4.1-51.9	1	1 S
	H	4	1	3				1.3-17.3; 3 SNPs <3.6% (1 S, 2 NS), 1 SNP at 17.3% (1 NS)	1	1 NS
	I	2		2				1.7-8.7; 1 SNP at 8.7% (1 NS), 1 SNP at 1.7% (1 NS)		
	J	13	6	7			1	1.0-16.6; 12 SNPs <8.7%, 1 SNP 12-16% (1 S)	6	2 S; 4 NS
	K	9	4	5				1.1-18.47; SNPs <3.9% (3 S, 4 NS), 2 SNPs 15.-19% (1 S, 1 NS)	3	1 S; 2 NS
	L	6	4	2				1.0-17.7		
	M	10	3	7			1	1.0-5.7	1	1 S

Encoded protein	Individ.	SNP No.	S	NS	Rev. to WT	Stop codon	V	SNP frequency (%)	Common SNPs	
NSP4	B	10	1	9				1.0-100.0; 8 SNPs <4.4% (1 S, 7 NS), 1 SNP up to 63% (1 NS), 1 SNP 18-92-100% (1 NS)	5	5 NS
	C	8	1	6	1			1.5-85.4; 7 SNPs <15% (1 S, 5 NS, 1 WTrev), 1 SNP 83-86% (1 NS)	6	1 S; 6 NS; 1 Wtrev
	D	9	2	5	1	1		1.1-37.5; 8 SNPs <4.1%, 1 SNP 35-37% (1 NS)	3	2 NS; 1 WTrev
	E	4		3	1			1.1-100.0; 3 SNPs <5.3% (2 NS, 1 WTrev), 1 SNP at 100% (1 NS)	3	2 NS; 1 WTrev
	F	6	2	3	1			1.6-71.9; 4 SNPs <50%, 1 SNP >50% (1 NS), 1 SNP >50-72% (1 NS)	3	2 NS, 1 WTrev
	G	5	3	1		1		1.1-13.9		
	H	7	1	6				1.0-7.8	1	1 NS
	I	5	1	4				1.2-12.9; 3 SNPs <3.7% (3 SN), 1 SNP at 10.8% (1 S), 1 SNP 7.9-12.9% (1 NS)	2	2 NS
	J	25	6	17	2			1.1-80.7; 23 SNPs at <50%, 1 SNP 50-61% (1 NS), 1 SNP 50-81% (1 NS)	8	7 NS; 2 WTrev
	K	5	3	2				1.1-2.6		
	L	12	1	10	1			D1 2.4-36.4; D2 1.3-2.9; 11 SNPs <23% (1 S, 9 NS, 1 WTrev), 1 SNP 35-36% (1 NS)	7	6 NS; 1 Wtrev
	M	7		6	1			1.2-41.5; 7 SNPs <15%, 1 SNP 39-42% (1 NS)	6	5 NS; 1 WTrev

Gene segment 4, encoding VP4

In total, 39 SNP loci were found in gene segment 4, encoding VP4: 13 synonymous and 26 non-synonymous, with two reversions to WT identified (Table 4.3, Fig. 4.1). The number of non-synonymous SNPs more than doubled with respect to vaccine material: 13 SNPs (Mitchell, Lui, *et al.*, unpublished). Three pairs of contiguous SNP loci affecting an amino acid each were identified in one and nine infants: nucleotide positions 1087 and 1088, leading to amino acid change N363G in infant I; and nucleotide positions 1090 and 1092, leading to amino acid change M364V in infants J, I, D, F, M, H, K, L, and E, respectively. Of all the SNP loci identified in VP4, 11 were detected previously in vaccine material (Mitchell, Lui, *et al.*, unpublished) appearing at similar or higher frequencies in stool of vaccine recipients. Twenty-seven SNP loci were novel in stool, appearing at varying frequencies from 1-100%.

All the SNP loci previously identified in vaccine material were non-synonymous. Ten of them diverged from virus in vaccine material, human WT G1P[8] sequence (GenBank reference JN887809) and human WT consensus. Mutation case A1090G plus G1092A leading to amino acid substitution M364V also diverged from virus in vaccine material, human WT G1P[8] sequence (GenBank reference JN887809) and human WT consensus. Mutation A1103G leading to amino acid substitution K368R diverged from virus in vaccine material, converging towards human WT G1P[8] sequence (GenBank reference JN887809) and human WT consensus. Mutation, T1153C leading to amino acid substitution Y385H, diverged from virus in vaccine material and did not converge towards human WT G1P[8] sequence (GenBank reference JN887809) or human WT consensus.

From the novel SNP loci, 17 were non-synonymous. Of those, 14 diverged from virus in vaccine material, human WT G1P[8] sequence (GenBank reference JN887809) and human WT consensus. Mutation cases T796A plus A797G leading to amino acid substitution Y2666S and A1087G plus A1088G leading to amino acid substitution N363G also diverged from virus in vaccine material, human WT G1P[8] sequence (GenBank reference JN887809) and human WT consensus. Mutation T761C leading to amino acid substitution I254T diverged from virus in vaccine material and human WT consensus and converged towards human WT G1P[8] sequence (GenBank reference JN887809). Mutation G1338T leading to amino acid

substitution L446F diverged from virus in vaccine material and human WT consensus.

A triallelic SNP locus at nucleotide position 797, mutation A>C, leading to a non-conservative amino acid substitution Y266S was previously detected in vaccine material at 0.8-3.5% frequency (Mitchell, Lui, *et al.*, unpublished). This SNP locus was not detected in stool of the cohort studied, although the other allele (nucleotide substitution A>G, amino acid substitution Y>C) was detected in stool of individual H, at day 3 after dose 1 and frequency of 5%.

Out of the 39 SNP loci found in VP4, 24 were present in faecal matter from one infant. Most of these SNP loci appear transiently at low frequency (<30%). Other SNP loci present frequencies that are initially low and increase by the latest timepoint. To focus the data analysis, SNP loci identified in ≥3 infants were further investigated. Out of these 12 SNP loci, nine had been detected in vaccine material previously (Mitchell, Lui, *et al.*, unpublished) and three were novel with respect to vaccine in-house sequence (Table 4.3), and some had also been previously identified in stool within this project (segments encoding VP4, VP7 and VP6; Appendix II, Preliminary data).

Of those nine SNP loci previously identified in Rotarix®, the locus at nucleotide position 754, mutation G>A, led to non-conservative amino acid substitution D252N in the VP8* subunit (Fig. 4.3). In Rotarix®, D252N was found at frequencies from 13.8-16.6% (Mitchell, Lui, *et al.*, unpublished) while in stool it was found at either early or late single timepoints in four infants (individuals D, H, K, L) at similar frequencies <20% (Table 4.3, Fig. 4.2). Molecular modelling of VP4 at this position was performed using LigPlot^{+} and RasMol (Fig. 4.4 C) and the Protein Databank Rhesus rotavirus VP4 structure (PDB entry 4V7Q). This analysis predicted that phenylalanine (F) 252 formed hydrogen bonds with aspartic acid (D) 249 and with asparagine (N) 253. A negatively charged amino acid like aspartic acid (D) (in vaccine material) and a polar uncharged amino acid with a similar structure such as asparagine (N) (in stool) would likely present different interactions than hydrophobic phenylalanine (F).

A cluster of SNP loci in the VP5* subunit between nucleotides 1088 and 1162, corresponding to amino acids 363 to 388, was detected at high frequency variation (>50% to >90%). These are near and within the putative fusion domain of

the virus: amino acids 384 to 401 (Mackow *et al.*, 1988; Dormitzer *et al.*, 2004; Trask *et al.*, 2010). The changes observed in the proposed hotspot were already present in vaccine material at a range of frequencies from 1.1-59.3% (Mitchell, Lui, *et al.*, unpublished). In stool, the frequencies were either similar or higher than those in vaccine material (Table 4.3).

Within the variation hotspot in VP5*, there were SNP loci affecting amino acids N363S and M364V/I (Fig. 4.3). In Rotarix®, N363S was found at 1.1-1.8% frequency, M364V at 6.2-9.6% frequency and M364I at 4.1-5.9% frequency (Mitchell, Lui, *et al.*, unpublished). In stool, they were identified in seven, nine and ten individuals respectively, at similar frequencies as in vaccine material and high (>50%) and very high (>90%) for some infants by the latest timepoints (Table 4.3, Fig. 4.2). Their increase or decrease in frequency goes parallel to the increase or decrease in viral loads in stool. They were molecularly modelled (Fig. 4.4 D), showing that glutamic acid (E) 363 was predicted to form hydrophobic contacts with isoleucine (I) 360 and threonine (T) 399, and T364 with aspartic acid (D) 400. The polar or hydrophobic changes are likely to maintain similar interactions.

Of interest, the locus at nucleotide position 1103, mutation A>G, leading to a conservative amino acid substitution K368R (Fig. 4.3) was found in vaccine material at approximately 50-60% (Mitchell, Lui, *et al.*, unpublished), while in stool of vaccine recipients it appeared at >50% up to 99-100% in several infants after both doses (individuals B, C, D, F, J, L) and in several other infants after dose 1 (individuals E, H, I, K, M) (Table 4.3, Fig. 4.2). Those infants where this mutation was identified after both doses are continuous shedders or shed between doses and those where the mutation was identified only after dose 1 control shedding after dose 1 (except individual L, who presented this mutation after dose 2 after viral load control after dose 1). Depending on timepoints of measurement, SNP frequency increased or decreased in parallel with viral loads. Individual J stands out as a continuous shedder in whose stool this mutation was maintained along the vaccination period at very high frequencies. This amino acid substitution K368R was molecularly modelled (Fig. 4.4 D), showing that threonine (T) 368 was predicted to form hydrophobic interactions with other atoms within the polypeptide chain and with T582. A positively charged amino acid such as tyrosine (Y) or arginine (R) will

likely establish other molecular interactions different to a hydrophobic amino acid such as T.

Within the variation hotspot region in VP5*, two more variant SNP loci at nucleotide positions and mutations T1153C and A1162C, corresponding to amino acid substitutions Y385H and I388L fall within the limits of the virus fusion domain (amino acids 384 to 404) (Fig. 4.3). In Rotarix®, Y385H was identified at 12.1-19.2% frequency (Mitchell, Lui, *et al.*, unpublished). In stool, it was identified in eight vaccinees (individuals, J, D, F, M, B, H, K, L) at similar frequencies as in vaccine material (Table 4.3, Fig. 4.2), except for individual J, whose detected SNP frequency increased from after dose 1 until before dose 2 up to 80% and then decreased down to 50% by the latest timepoint tested. Molecular modelling of VP4 (Fig 4.10 E) showed that alanine (A) 385 was predicted to form a hydrogen bond with threonine (T) 381 and some hydrophobic contact with methionine (M) 392. This hydrogen bond is likely to be similar in Rotarix® presenting a tyrosine (Y) at amino acid 385 and in stool of vaccine recipients presenting a histidine (H) since it is formed through the amine group. However, the hydrophobic nature of the alanine (A) would be disrupted with the aromatic ring of the tyrosine (Y) and the aromatic and positive charge of the histidine (H), which may disrupt the protein structure.

The conservative substitution at amino acid I388L is located in epitope region 5-1 (Zeller *et al.*, 2012) (Fig. 4.3). In Rotarix®, it was found at 2.7-4.8% frequency (Mitchell, Lui, *et al.*, unpublished). In stool, it was identified in nine infants (individuals J, I, D, F, M, H, K, E, C) at similar frequencies as in vaccine material and high frequencies (>50%) in individual C after dose 1, although it decreased to low frequencies similar to vaccine after dose 2 (Table 4.3, Fig. 4.2). Molecular modelling of VP4 (Fig 4.10 E) showed that the side chain hydroxyl group in serine (S) 388 was predicted to form some hydrophobic contact with threonine (T) 322, likely a hydrogen bond since side chains of serine and threonine are hydrophilic. In the case of I388L, one hydrophobic amino acid would be substituted by another hydrophobic one, potentially with a less significant effect than if the change was non-conservative.

After the variation hotspot, another locus was identified at nucleotide position 1409 in VP5*, mutation T>C, leading to non-conservative amino acid substitution I470T, at the base of the β-barrel (Fig. 4.3). In Rotarix®, I470T was detected at

frequencies 6.3-10.4% (Mitchell, Lui, *et al.*, unpublished). In stool, it was detected in seven vaccine recipients (individuals J, I, F, M, H, K, E) at similar frequencies to vaccine material (<11%) or <20%, except for individual F after dose 1 whose frequency was identified at just over 50% and then decreased to levels similar to vaccine material after dose 2 (Table 4.3, Fig. 4.2). Molecular modelling of VP4 (Fig. 4.4 F) showed that asparagine (N) 470 was predicted to form hydrogen bonds with phenylalanine (F) 466 and glutamine (Q) 467, as well as some hydrophobic contacts with further amino acids such as alanine (A) 509. These contacts are likely to differ in Rotarix®, which presented a hydrophobic amino acid as isoleucine (I) 470. However, threonine (T) 470 in stool of vaccine recipients is likely to present similar interactions as a polar uncharged amino acid.

Another locus identified at nucleotide position 1435 in VP5*, mutation T>C, led to non-conservative amino acid substitution Y479H at the base of the β-barrel (Fig. 4.3). In Rotarix®, Y479H was identified at 2.4-5.2% (Mitchell, Lui, *et al.*, unpublished). In stool, it was detected in four infants (individuals J, D, M, H) at similar frequencies to vaccine material (<7%) at early timepoints for all individuals except for individual D (day 39) (Table 4.3, Fig. 4.2). Molecular modelling of VP4 showed that glutamine (Q) 479 presented some atoms affected by hydrophobic contacts with neighbouring amino acids (Fig. 4.4 F). A hydrophobic amino acid such as tyrosine (Y) at that residue position in Rotarix® would likely form different interactions, and so would a histidine (H) as a positively charged amino acid detected in stool of vaccinees.

Two novel SNP loci were in the VP8* subunit and another one in the VP5* subunit. A locus at nucleotide position 340, mutation C>A, led to non-conservative amino acid substitution P114T located in epitope region 8-3 (Zeller *et al.*, 2012) (Fig. 4.3). In stool, P114T was detected in two infants (individuals C and M) at three and 13 days after dose 1 and frequencies of <55% and <71% and in one infant (individual J) after both doses at frequencies from 40% to 19% after dose 1 and from 30% to 48% after dose 2 (Table 4.3, Fig. 4.2). Molecular modelling of VP4 (Fig. 4.4 A) showed that glutamic acid (E) 114 was predicted to form no amino acid contacts outside the amino acid primary sequence and no hydrophobic contacts (Fig. 4.4 A). Contacts are likely to differ with the proline (P) present in Rotarix® due to its cyclical inflexible nature and more similar with the threonine (T) detected in stool of vaccine

recipients, due to its polar nature. The absence of that proline (P) in virus from stool may result in a less tight conformation.

Another novel locus at nucleotide position 499, mutation T>C, led to conservative amino acid substitution F167L located in the VP8* subunit (Zeller *et al.*, 2012) (Fig. 4.3). In stool of this cohort, F167L was detected in five infants (individuals C, F, M, L, E) at varying frequencies (Table 4.3, Fig. 4.2). After dose 1, it was detected at low (individual M), 50% frequency (individual F) and high frequency (individual L), after dose 2 at high frequency (individual E) and at high frequency after both doses (individual C). Molecular modelling of VP4 (Fig 4.4 B) showed that leucine (L) 167, within a hydrophobic region, was predicted to form a hydrogen bond with arginine (R) 163, two hydrogen bonds with glutamic acid (E) 164, one hydrogen bond with asparagine (N) 168 and two hydrogen bonds with leucine (L) 169. Contacts are likely to be similar in Rotarix® presenting phenylalanine (F) 167 since the hydrogen bonds are formed with the leucine (L) backbone and the hydrophobic head of phenylalanine (F) would be buried in the adjacent hydrophobic pocket (threonine 154, leucine 155, methionine 686), and more similar in stool from the five vaccine recipients who also presented a leucine (L) at amino acid position 167.

Of the three novel SNP loci, the locus in the VP5* subunit presented a mutation A>G at nucleotide position 1430, leading to a non-conservative amino acid substitution D477G located at the base of the β-barrel (Fig. 4.3). In stool, D477G was detected in three infants (individuals J, M, E) at early timepoints and frequencies <16% (Table 4.3, Fig. 4.2). Molecular modelling of VP4 (Fig. 4.4 F) showed that asparagine (N) 477 was involved in hydrophobic contact with threonine (T) 68. This contact is likely to differ in Rotarix® presenting a negatively charged aspartic acid (D), and in stool of three vaccine recipients who presented a glycine (G) at that position.

Table 4. 3. Single nucleotide polymorphism loci identified in stool of individuals B-M for viral segment encoding VP4. Nucleotide (nt) original, nucleotide position in GenBank reference JX943612. Nucleotide+12, nucleotide position from A in first codon encoding the first methionine (12 nucleotide shift when aligned to WT GenBank reference JN887809). Nucleotide change. Amino acid (aa) change. Vaccine frequency (%), frequency of SNP in Rotarix® previously (Mitchell, Lui, *et al.*, unpublished). Vaccine recently, if SNP loci identified in Rotarix® control within these sequencing runs. Individuals, individuals in whose stool the SNP has been identified. Timepoints, timepoints where SNP has been identified. Faecal frequency (%), frequency range in which the SNP has been identified. Underlined nucleotides, consensus identity. Nucleotides or amino acids in red, found in WT G1P[8] (GenBank reference JN887809). Amino acids in black bold, amino acid change. Amino acids in red bold, possible reversion to WT strain. [1] Identified in vaccine material at the NIBSC (Mitchell, Lui, *et al.*, unpublished). Shaded in blue, loci present in ≥2 infants. Marked in purple, loci present in ≥3 infants.

nt original	nt+12	nt change	aa change	Individuals	Timepoints	Faecal frequency (%)
74	86	A>G	K29**R**	J	1(day38)	10
162	174	G>A	S58S	D	1(day8)	8.2-12
241	253	A>G	N85**D**	B	1(day19)	9.9-13.2
328	340	C>A	P114**T**	J, M, C	4(day13, 27, 38, 67) //1(day13)//1(day34)	18.6-57.1//68.4-72.2//53.2-55.6
431	443	A>G	Q148**R**	B	1(day19)	2.9-3.2
487	499	T>C	F167**L**	F, M, L, E, C	1(day7)//2(day5, day13)//1(day15) //1(day35)//2(day9, 34)	53.8-58.1//3.5-17.8//98.7-99.2 //100.0//97.0-99.9
513	525	A>G	T175T	I, E	1(day9)//1(day35)	1.8-2.8//100.0
535	547	G>A	A183**T**	J	2(day38, day67)	3.4-64.7
555	567	T>C	S189S	J	1(day67)	30.0-34.4
742	754	G>A	D252**N**[1]	D, H, K, L	1(day39)//1(day3)//1(day4)//1(day35)	16.2-17.4//10.9-18.6//14.5-16.5 //15.3-19.6
749	761	T>C	I254**T**	D	1(day8)	15.3-21.0
785	797	A>G	Y266**C**[1]	H	1(day3)	4.9-6.6
834	846	G>A	K282K	J	1(day67)	27.5-33.0

	895	907	A>G	N303**D**	J	1(day670	9.8-16.1
	987	999	C>T	P333P	J	1(day67)	23.2-55.4
	1007	1019	G>A	R340**K**	I	1(day9)	7.3-10.0
	1075	1087	A>G	N363**D**	I, B	1(day9)//2 (day19, 32)	8.7-10.6//3.4-73.4
	1076	1088	A>G	N363**S**[1]	J, I, D, F, M, C	1(day3)//1(day9)//2(day8, 39)//1(day7)// 1(day5)//2(day9, 34)	2.2-3.2//2.0-3.7//5.1-50.7//3.8-4.9//5.0-5.1//35.1-95.2
	1075&1076	1087&1088	A>G & A>G	N363**G**	I		
	1078	1090	A>G	M364**V**[1]	J, I, D, M, H, K, L, E	5(days3, 14, 27, 38, 67)//1(day9)//2(day8, 39)//1(day5)//1(day3)//1(day4)//1(day35)// 1(day6)	13.5-58.1//3.4-6.8//1.4-17.1//8.5-9.2//8.0-15.2//10.1-13.1//9.5-20.8//4.8-5.0
	1080	1092	G>A	M364**I**[1]	J, I, D, F, M, B, H, K, E	2(day3, 13)//1(day9)//2(day8, 39) //1(day7)//2(day5, 13)//3(days19, 32, 44)//1(day3)//1(day4)// 1(day6)	12.8-18.6//26.3-34.9//3.5-14.3//11.8-13.5//18.1-26.7//19.1-99.9//3.0-5.4//13.1-14.7//12.7-15.2
	1078 & 1080	1090 & 1092	A>G & G>A	M364**V**[1]	J, I, D, F, M, H, K, L, E		
	1091	1103	A>G	K368**R**[1]	J, I, D, F, M, B, H, K, L, E, C	5(days3, 14, 27, 38, 67)//1(day9)//2(days8, 39)//2(day7, 30)//2(day5, 13)//3(day19, 32, 44)//1(day3)//1(day4)//2(day15, 35) //2(day6, 35)//2(day9, 34)	90.5-100.0//97.9-99.5//52.1-100.0//31.5-100.0//94.8-98.7//92.6-100.0//57.2-65.0//89.3-91.7//57.8-100.0//98.7-100.00//97.1-.100.0
	1141	1153	T>C (consensus G)	Y385**H**[1]	J, D, F, M, B, H, K, L	5(days3, 14, 27, 38, 67)//1(day39)//1(day7) //2(day5, 13)//1(day32)//1(day3)//1(day4) //1(day35)	4.3-96.4//7.1-33.2//3.9-4.6//1.8-4.5 //2.2-2.3//10.1-15.4//4.8-5.9//6.9-17.6
	1150	1162	A>C	I388**L**[1]	J, I, D, F, M, H, K, E, C	2 (days3, 13)//1(day9)//1(day39)//1(day7) //2(day5, 13)//1(day3)//1(day4)//1(day6) //2(day9, 34)	4.5-12.7//5.9-8.4//1.6-4.2//6.2-6.9 //13.4-45.4//2.9-3.1//6.2-7.4//9.5-11.2 //2.8-66.7
	1150	1162	A>T	I388**L**	J	1(day 3)	1.2-3.6
	1171	1183	G>A	V395**I**	L	1(day15)	1.7-2.1
	1269	1281	T>C	F427F	B	3(days19, 32, 44)	16.5-100.0
	1311	1323	A>G	T441T	K	1(day4)	1.7-3.2
	1326	1338	G>T	L446**F**	D	1(day8)	1.2-2.7
	1350	1362	A>C	P454P	J	1(day38)	6.0-13.6

1397	1409	T>C	I470**T**[1]	J, I, D, F, M, H, K, L, E	1(day3)//1(day9)//1(day39)//2(day7, day30)//1(day5)//1(day3)//1(day4) //1(day15) //1(day6)	6.1-13.0//2.6-5.6//1.3-14.3//13.9-51.6 //6.4-7.1//3.5-7.9//9.1-12.4//1.7-2.1 //1.7-2.3
1413	1425	T>C	T475T	K	1(day4)	1.5-3.7
1415	1427	A>C	N476**T**[1]	H	1(day3)	1.3-6.7
1418	1430	A>G	D477**G**	J, M, E	1(day3)//2(days5, 13)//1(day6)	1.0-1.8//8.5-15.3//1.4-2.5
1423	1435	T>C	Y479**H**[1]	J, D, M, H, K	1(day3)//1(day39)///1(day5)//1(day3) //1(day4)	1.4-1.8//1.3-6.4//1.4-1.9//2.7-3.2 //1.2-1.8
1470	1482	G>A	E494E	J	1(day67)	16.9-32.4
1682	1694	A>G	N565**S**	M	1(day5)	2.7-3.1
1830	1842	T>C	I614I	J	1(day67)	8.5-13.1
1881	1893	C>T	S631S	J	1(day13)	33.7-5.3
2040	2052	T>C	N684N	I	1(day9)	3.2-4.0

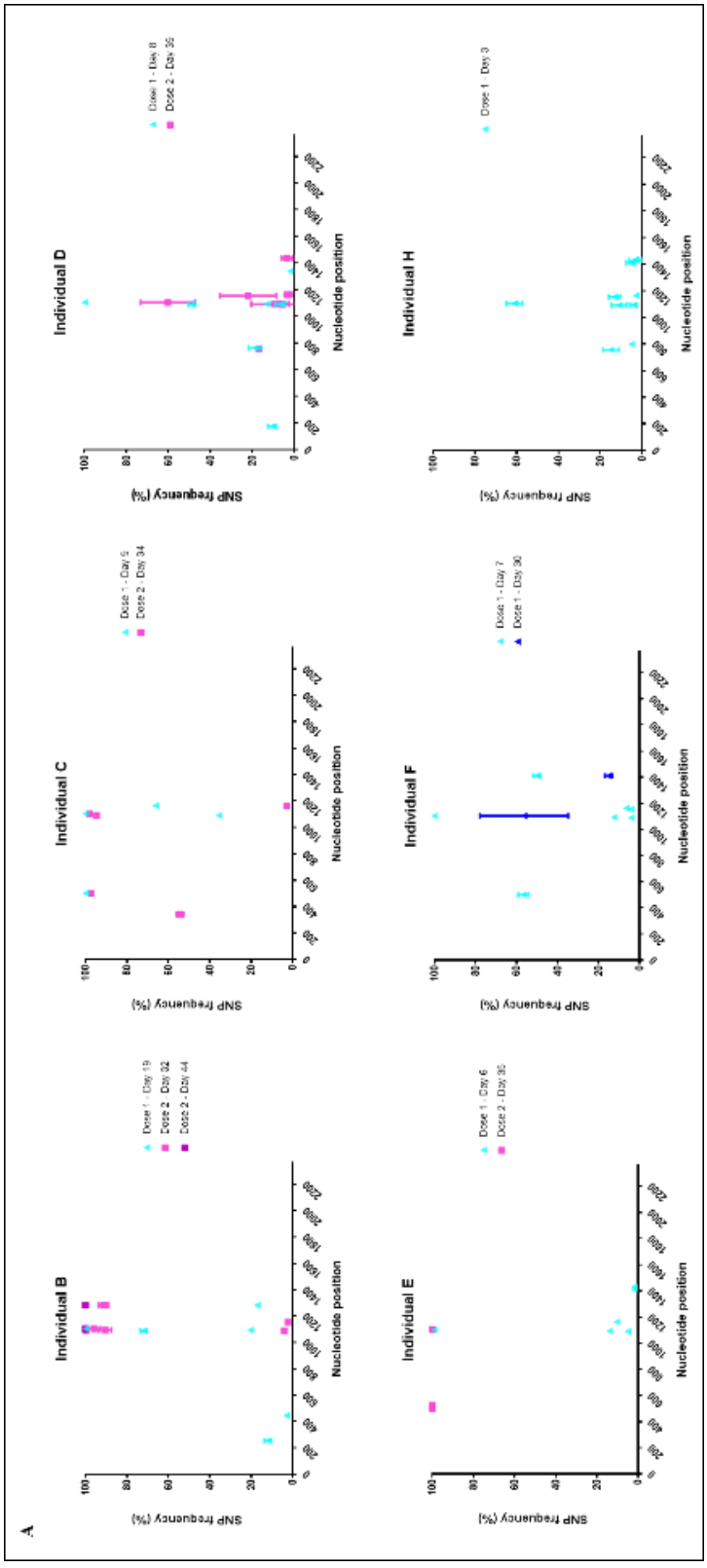

Fig. 4.1. Frequency of SNP loci over rotavirus genome segment 4 (VP4) in stool from A) infants B-F, H; and B) infants I-M. Percentage of reads containing each SNP for each nucleotide position at several timepoints after dose 1 (blue triangles) and dose 2 (pink squares); error bars for triplicates shown. All days in reference to dose 1. Nucleotide position refers to full length coding sequence (JN887809).

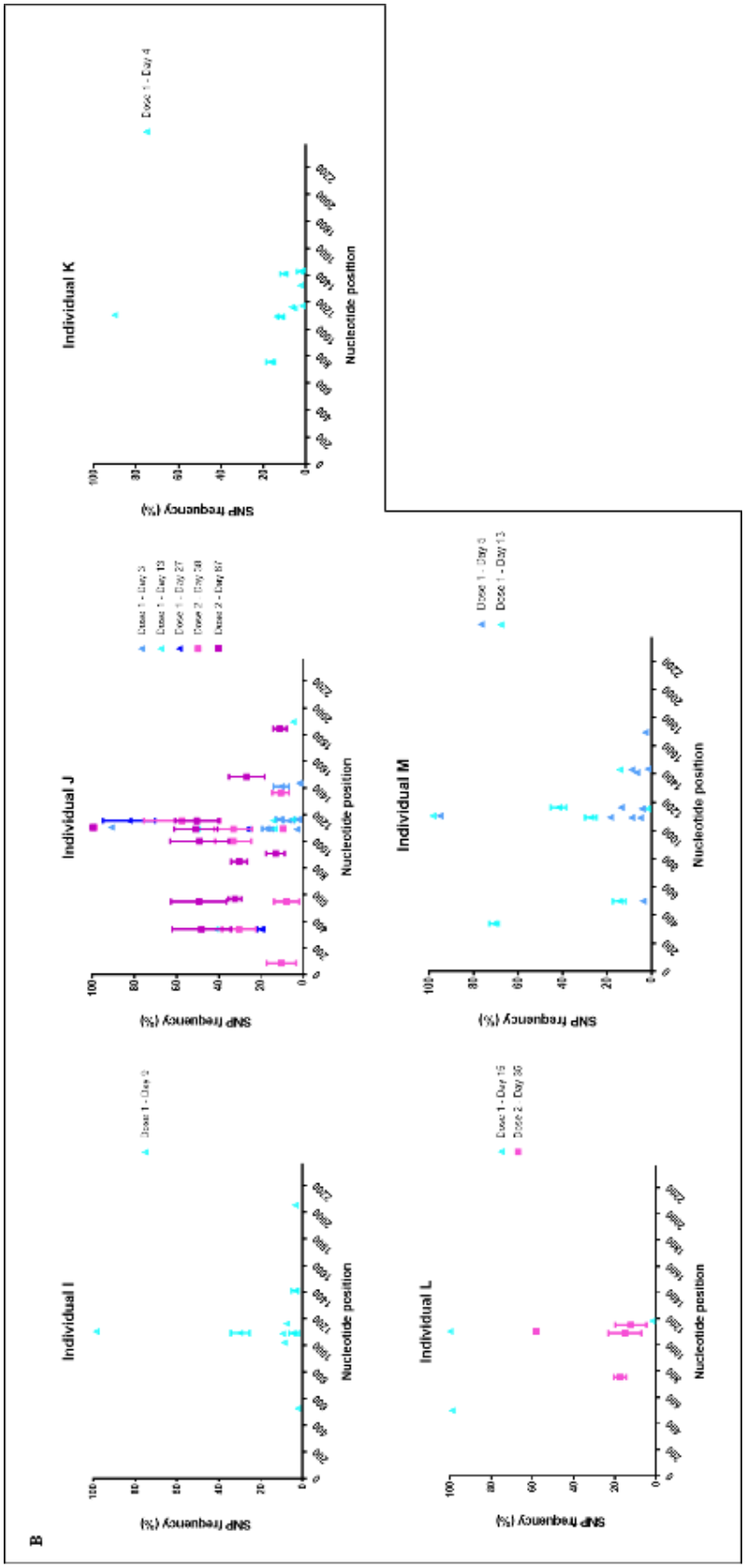
B
Individual K
Individual J
Individual M
Individual I
Individual L
SNP frequency (%)
Nucleotide position

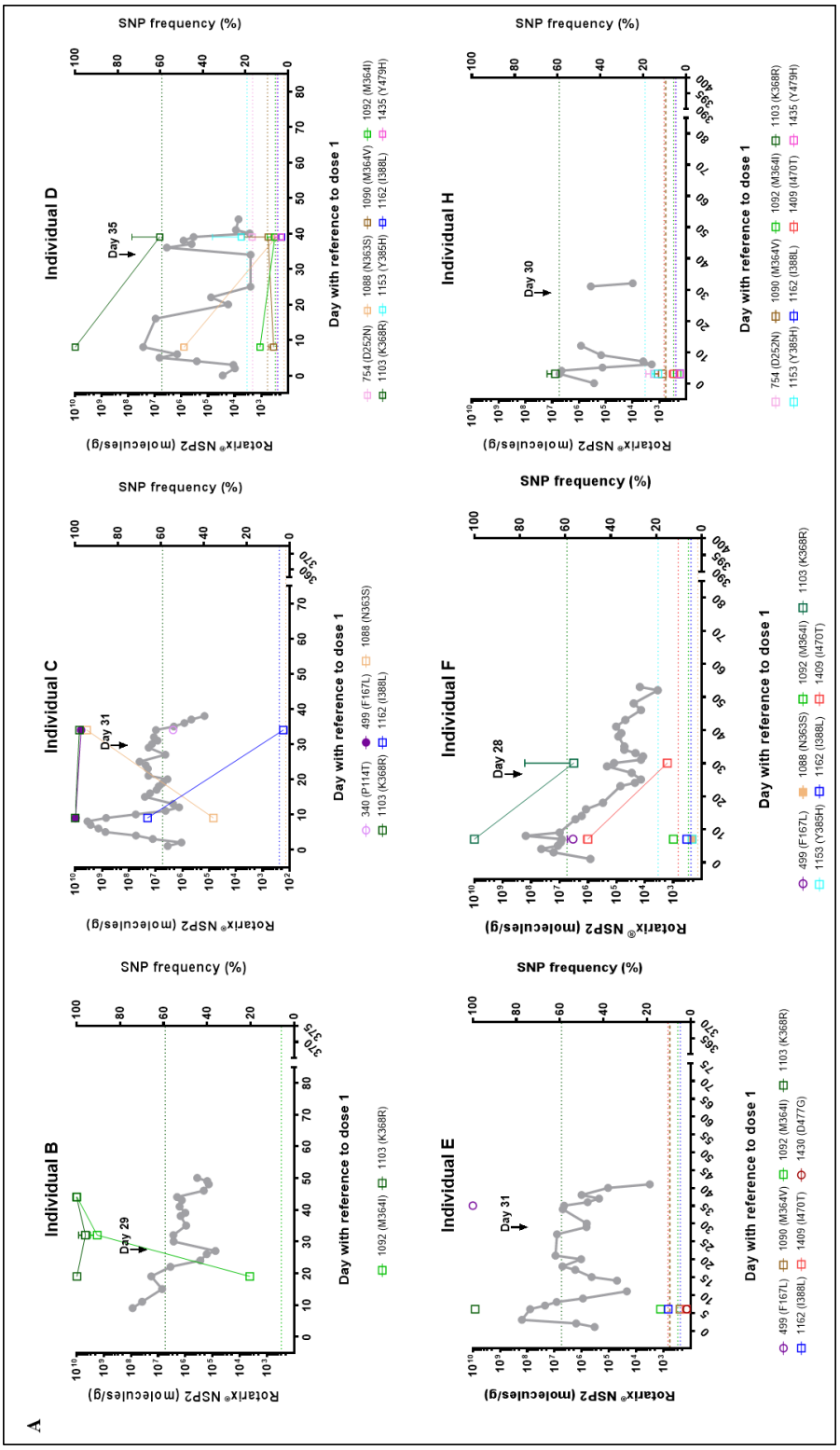

Fig. 4.2. Frequency of SNP loci identified in rotavirus genome segment 4 (VP4) over timepoints tested in stool from A) infants B-F, H; and B) infants I-M. Vaccine genome copy number indicated on the left Y axis for reference and in grey on the graphs. Frequency of SNP loci indicated in right Y axis. SNP loci identified in stool from each infant described in key; error bars for triplicates shown. Dotted lines: Upper limit of SNP frequency in vaccine material for a particular SNP (key). Day: Day of dose 1. Day by black arrow: Day of dose 2. All days in reference to dose 1.

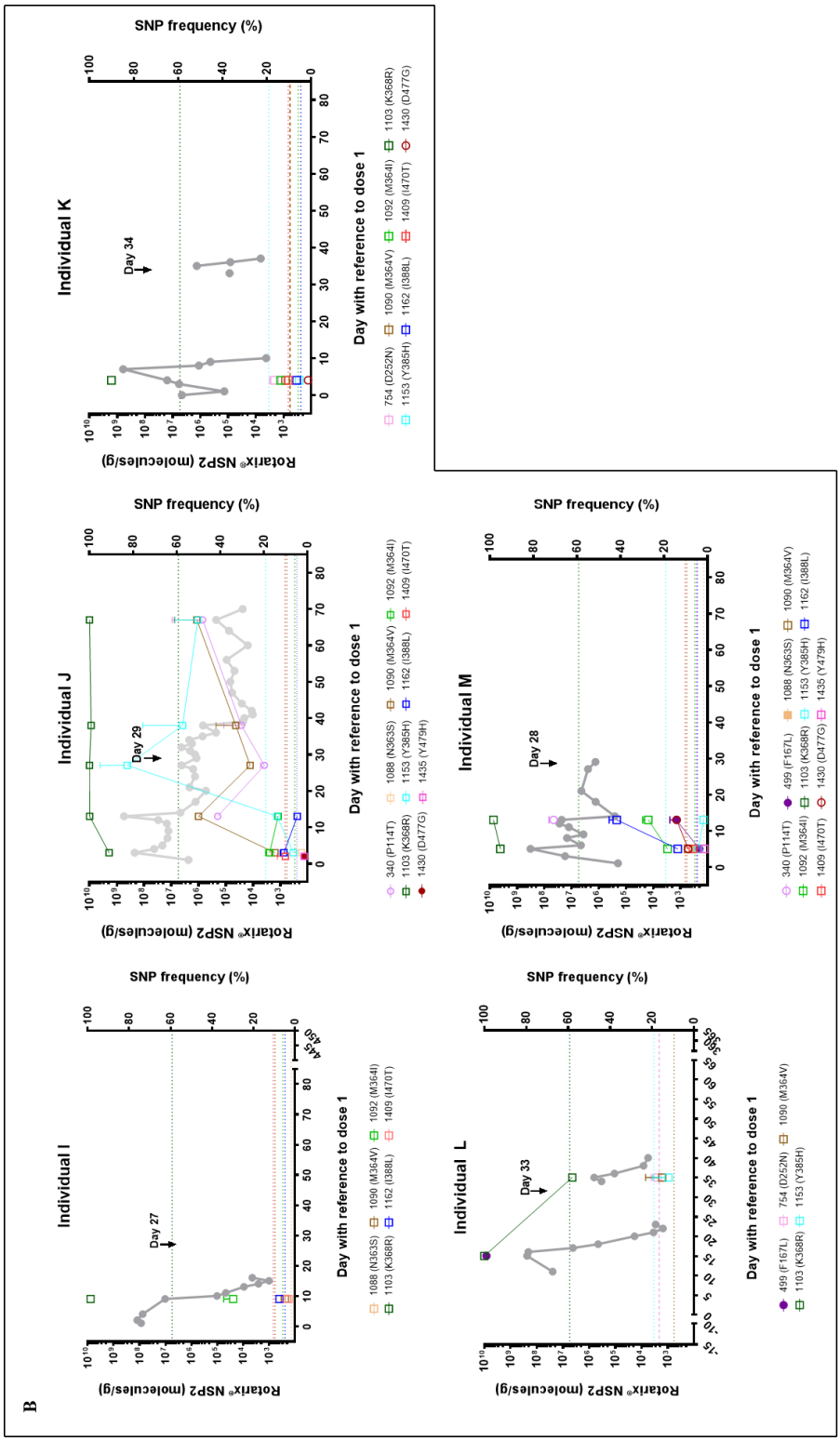
B
Individual K
Day 34
Individual J
Day 29
Individual M
Day 28
Individual I
Day 27
Individual L
Day 33
SNP frequency (%)
Day with reference to dose 1
Rotarix® NSP2 (molecules/g)

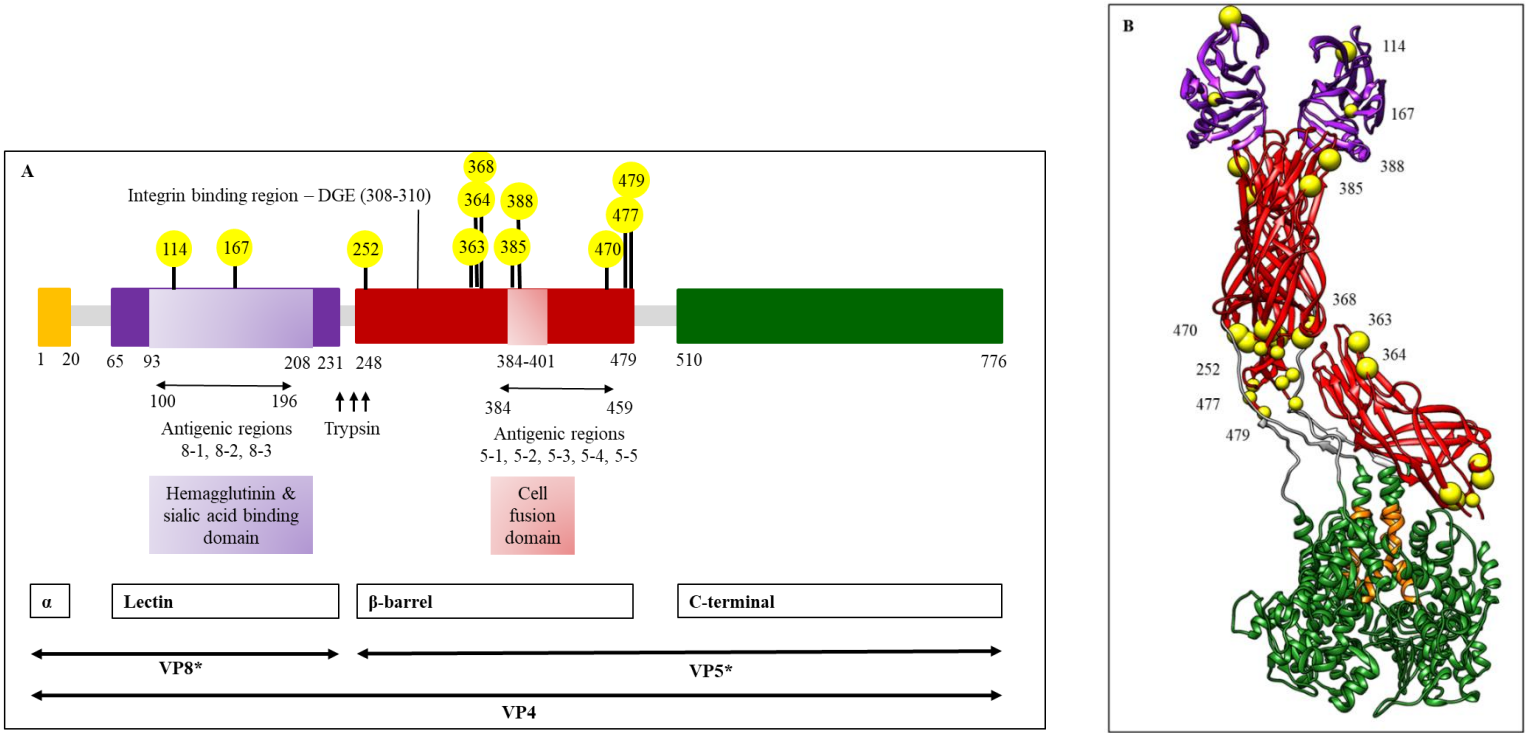

Fig. 4.3. A) Schematic of VP4 primary amino acid sequence and B) Atomic model of the VP4 spike, highlighting the non-synonymous amino acid substitutions originating from SNP loci identified in stool of ≥3 infants (B-M). A) Numbers indicate amino acid position. The VP8* subunit is indicated in purple (lectin) and the VP5* subunit is indicated in red (the β-barrel, body and stalk, antigen domains) and green (the C-terminal, foot domain) (Settembre *et al.*, 2011). Trypsin cleavage sites are indicated by small black upward-pointing arrows (Arias *et al.*, 1996; Crawford *et al.*, 2001). The hemagglutinin binding domain is indicated in light purple (Weiner *et al.*, 1978; Yeung *et al.*, 1987; López and Arias, 2004) and the cell fusion domain in light red (Mackow *et al.*, 1988; Dormitzer *et al.*, 2004; Trask *et al.*, 2010). Antigenic regions in VP8* and VP5* are indicated by horizontal double-direction arrows (Dormitzer *et al.*, 2004; Monnier *et al.*, 2006; Zeller *et al.*, 2012). Affected residues are indicated in yellow spheres. **B)** Ribbon representation of the VP8* subunit in purple (the lectin, head) and orange (the α), VP5* subunit in red (the β-barrel, body and stalk, antigen domains) and green and (the C-terminal, foot domain), and residues affected as yellow spheres. From Protein Data Bank (PDB) entry 4V7Q (Settembre *et al.*, 2011).

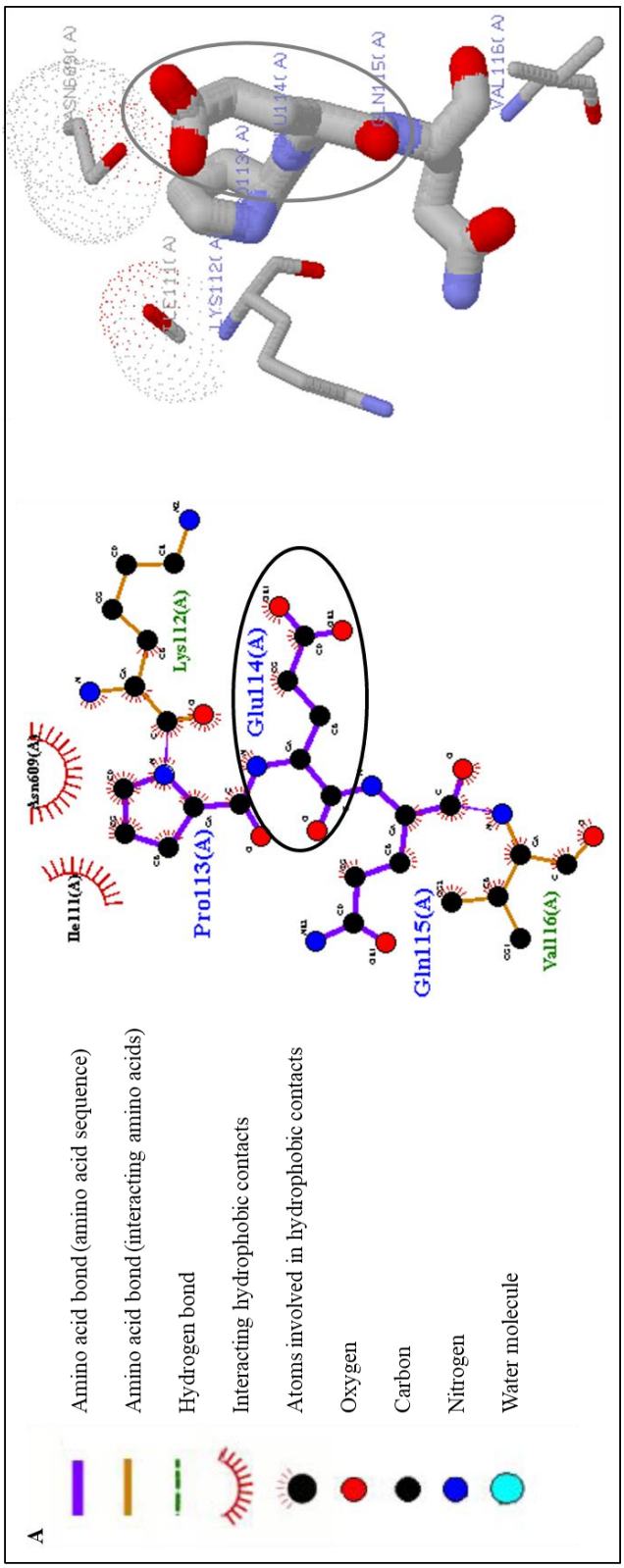

Fig. 4.4. Molecular schematic of residues in VP4 that interact with A) amino acid 114; B) amino acid 167; C) amino acid 252; D) amino acids 363, 364 and 368; E) amino acids 385 and 388; and F) amino acids 470, 477 and 479. Chain structure and 3D structure shown: Amino acid (s) circled in black and grey respectively.

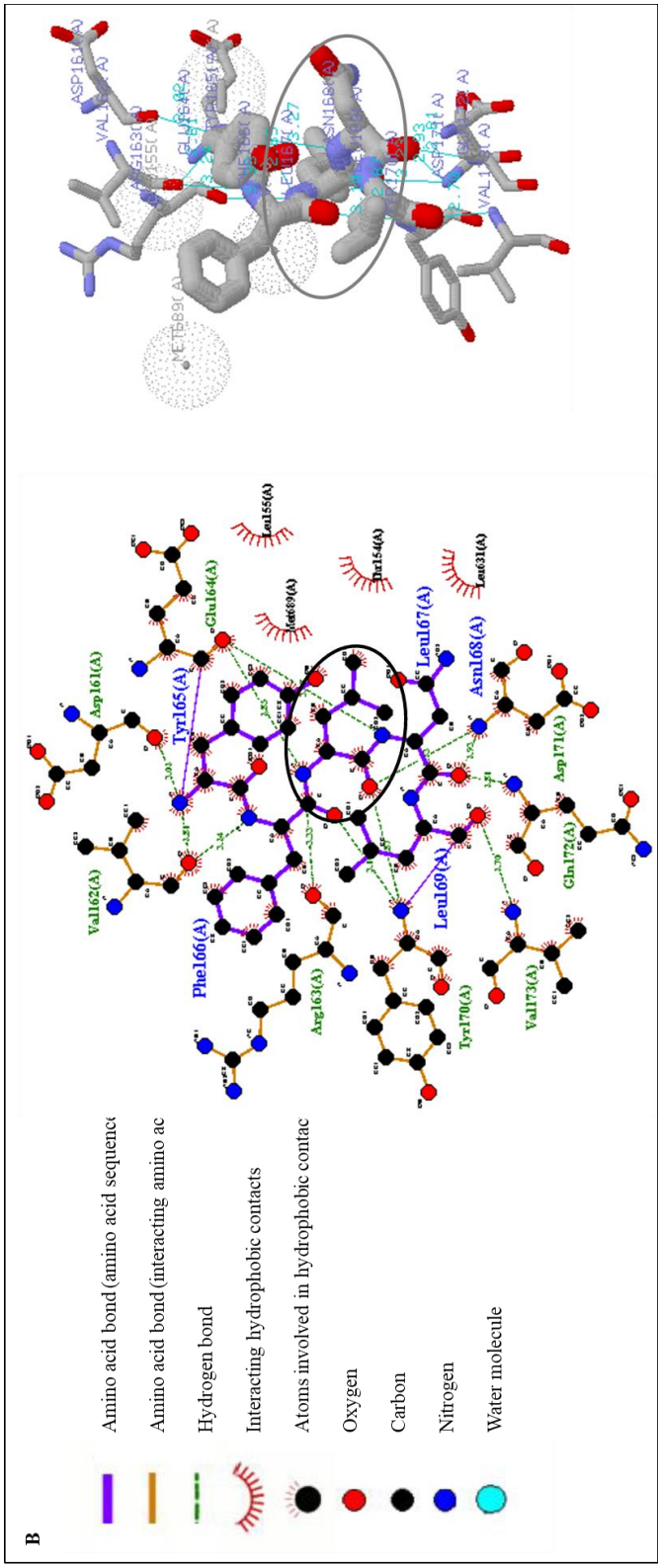
B
Amino acid bond (amino acid sequenc
Amino acid bond (interacting amino ac
Hydrogen bond
Interacting hydrophobic contacts
Atoms involved in hydrophobic contac
Oxygen
Carbon
Nitrogen
Water molecule
Val162(A)
Asp161(A)
Glu164(A)
Tyr165(A)
Phe166(A)
Arg163(A)
Leu167(A)
Asn168(A)
Leu69(A)
Tyr170(A)
Asp171(A)
Gln172(A)
Val173(A)
Leu156(A)
Thr154(A)
Leu631(A)

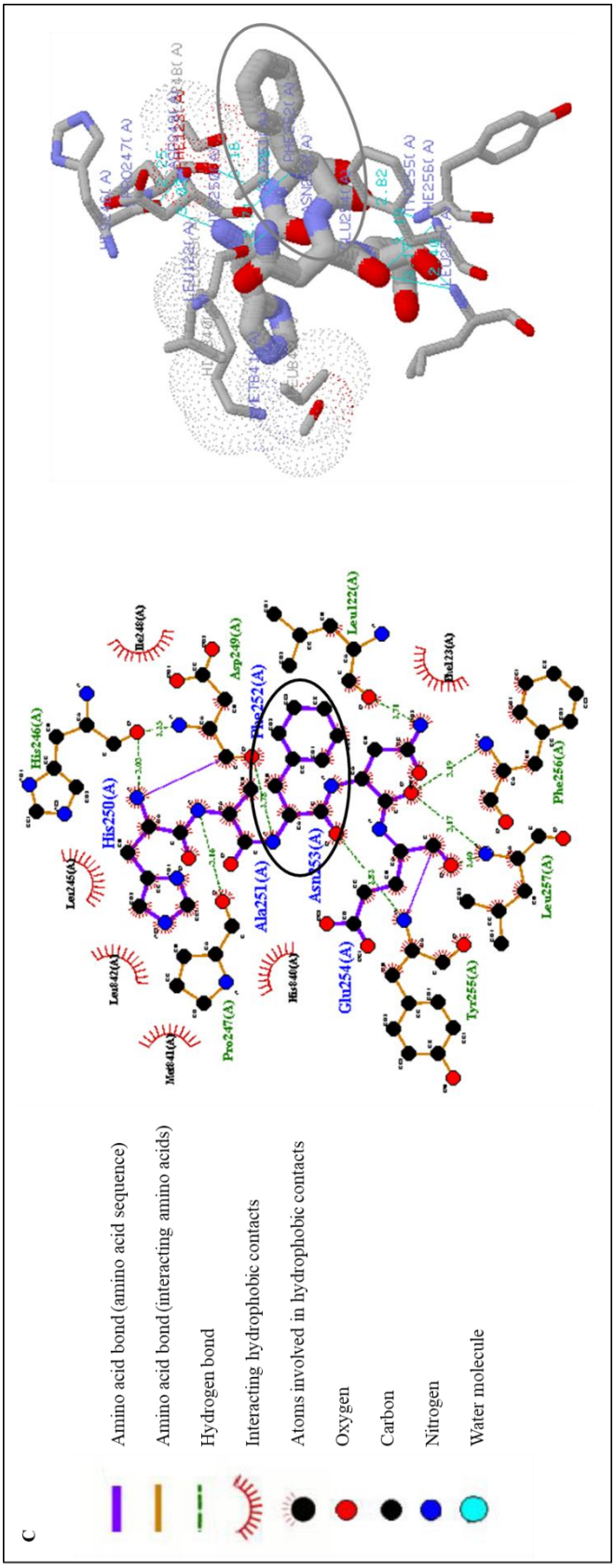
C
Amino acid bond (amino acid sequence)
Amino acid bond (interacting amino acids)
Hydrogen bond
Interacting hydrophobic contacts
Atoms involved in hydrophobic contacts
Oxygen
Carbon
Nitrogen
Water molecule
His246(A)
His250(A)
Leu245(A)
Leu442(A)
Met441(A)
Pro247(A)
Ala251(A)
His440(A)
Asp249(A)
Phe252(A)
Asn253(A)
Glu254(A)
Leu122(A)
Phe123(A)
Tyr255(A)
Phe256(A)
Leu257(A)

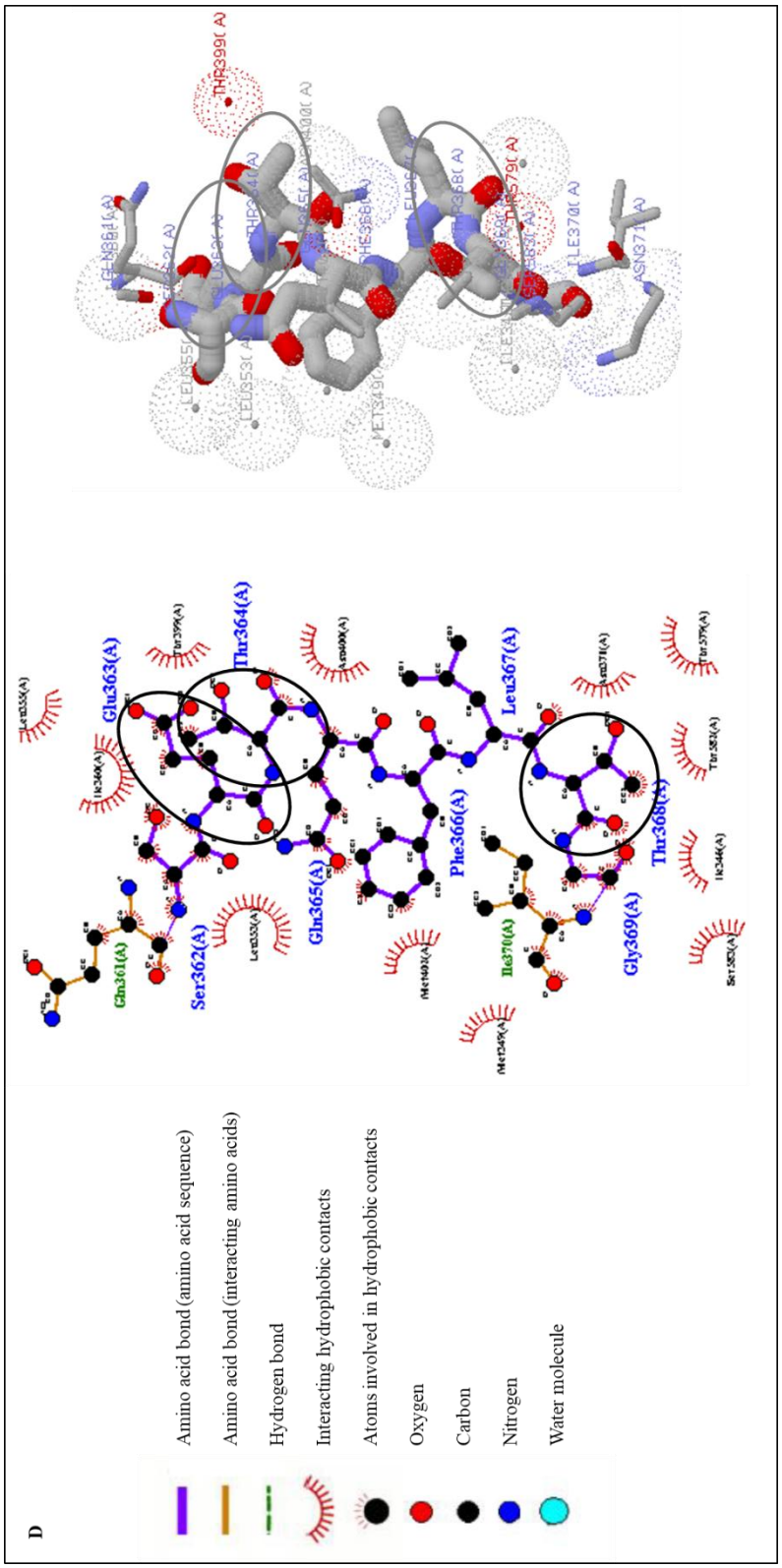
D
Amino acid bond (amino acid sequence)
Amino acid bond (interacting amino acids)
Hydrogen bond
Interacting hydrophobic contacts
Atoms involved in hydrophobic contacts
Oxygen
Carbon
Nitrogen
Water molecule
Gln361(A)
Ser362(A)
Glu363(A)
Thr364(A)
Gln365(A)
Phe366(A)
Leu367(A)
Thr368(A)
Gly369(A)
Ile370(A)

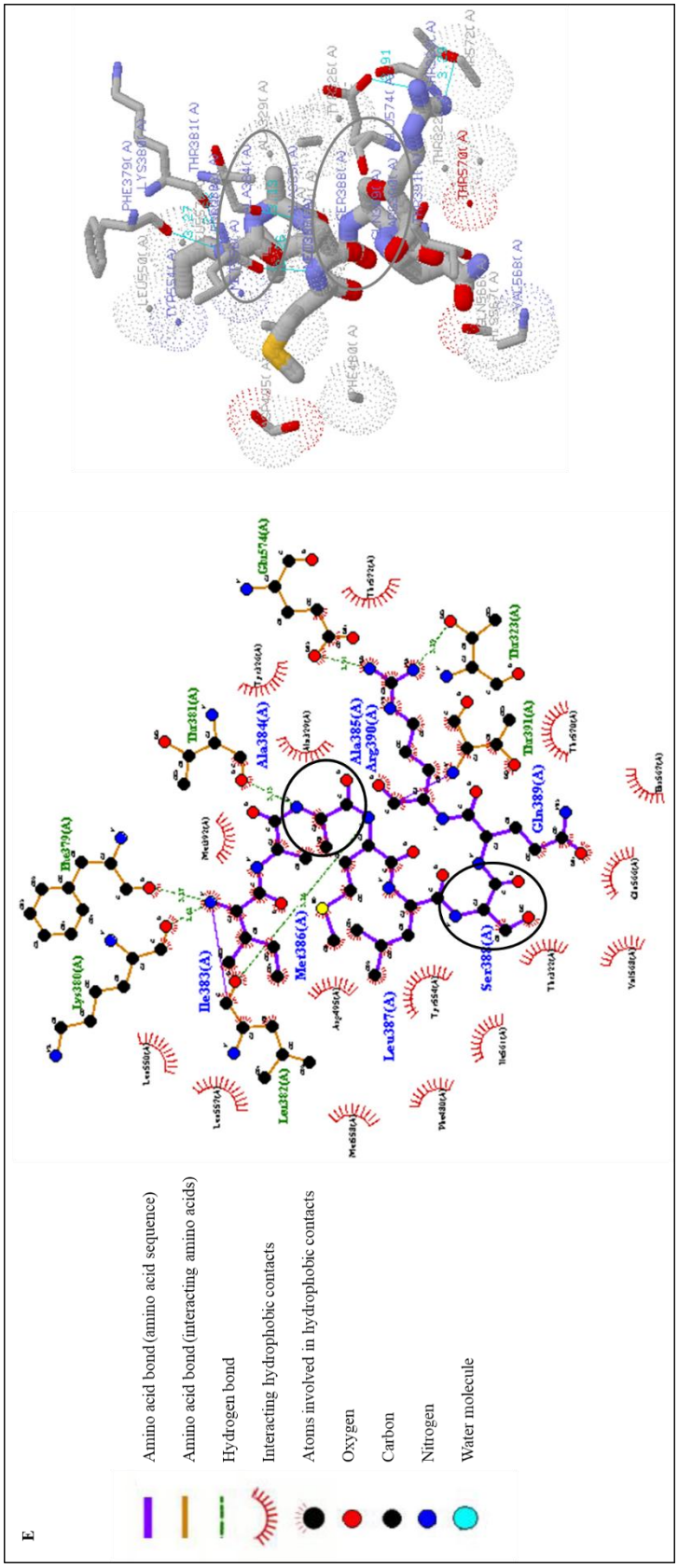
Amino acid bond (amino acid sequence)
Amino acid bond (interacting amino acids)
Hydrogen bond
Interacting hydrophobic contacts
Atoms involved in hydrophobic contacts
Oxygen
Carbon
Nitrogen
Water molecule
E

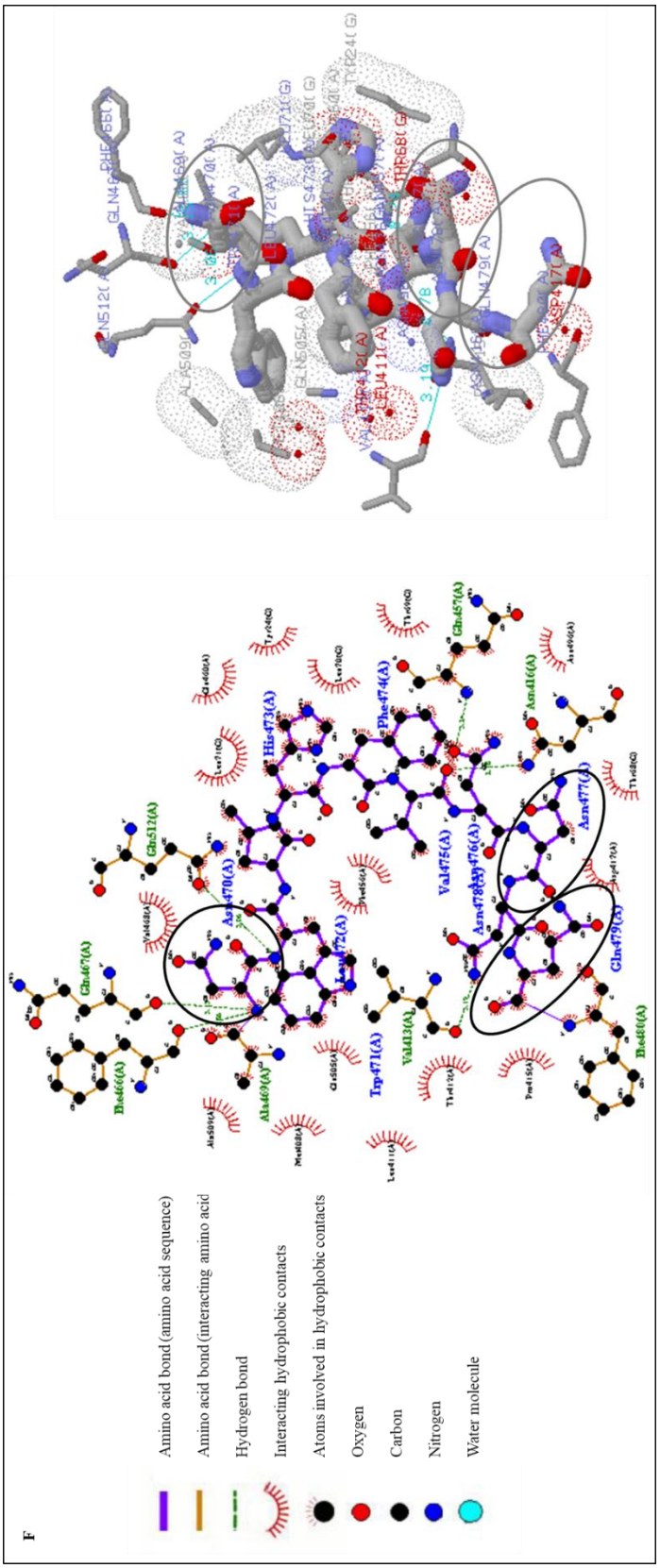
F
Amino acid bond (amino acid sequence)
Amino acid bond (interacting amino acid
Hydrogen bond
Interacting hydrophobic contacts
Atoms involved in hydrophobic contacts
Oxygen
Carbon
Nitrogen
Water molecule

Gene segment 9, encoding VP7

In the gene encoding VP7, six SNP loci were identified: two synonymous and four non-synonymous, with one reversion to WT (Table 4.4, Fig. 4.5). The number of non-synonymous SNPs increased from one in vaccine material (Mitchell, Lui, *et al.*, unpublished) to four in stool. One of the SNP loci identified in vaccine material in gene segment 9 was not identified in stool of this cohort: SNP locus at nucleotide position and mutation T771C, leading to silent amino acid substitution N257N, at 0.1-3.4% frequency in Rotarix® (Mitchell, Lui, *et al.*, unpublished). One SNP locus was previously identified in vaccine material and five were novel, particular to one infant each and detected at one timepoint from one week to two weeks after dose 1 at frequencies <50% (Table 4.4).

The SNP locus previously identified in vaccine material was non-synonymous and diverged from virus in vaccine material and consensus, converging towards virus in human WT G1P[8] sequence (GenBank reference JN887818). From the novel SNP loci, three were non-synonymous and diverged from virus in vaccine material, human WT G1P[8] sequence (GenBank reference JN887818) and human WT consensus.

No SNP loci were observed in ≥3 infants. Therefore, to focus data analysis, SNP loci common to ≥2 infants were further investigated. Of the SNP loci in VP7, nucleotide position 368, mutation G>A, led to conservative amino acid substitution S123N located in known epitope region 7-1a (Zeller *et al.*, 2012) (Fig. 4.7). Amino acid substitution S123N was previously detected in vaccine material at the NIBSC at frequencies 3-17% (Mitchell, Lui, *et al.*, unpublished). In stool of two infants it was detected at similar frequency at day 13 for individual J, and at similar frequency at day 5 and frequency of >50% at day 13 for individual M (Table 4.4, Fig. 4.6). Modelling of VP7 (Fig. 4.8) was performed following the Protein Data Bank Rhesus VP7 structure (PDB entry 3FMG). This analysis showed that asparagine (N) 123 was predicted to form hydrogen bonds with alanine (A) 125, serine (S) 126 and phenylalanine (F) 127, A125 part of epitope region 7-1a. There are likely to be similar interactions in Rotarix® presenting serine (S) 123 due a similar polar amino acid with an uncharged side chain and in stool of two infants presenting asparagine (N) 123.

Table 4. 4. Single nucleotide polymorphism loci identified in stool of individuals B-M for viral segment encoding VP7. Nucleotide (nt) original, nucleotide position in GenBank reference JX943614. Nucleotide change. Amino acid (aa) change. Vaccine frequency (%), frequency of SNP in Rotarix® previously (Mitchell, Lui, *et al.*, unpublished). Vaccine recently, if SNP loci identified in Rotarix® control within these sequencing runs. Individuals, individuals in whose stool the SNP has been identified. Timepoints, timepoints where SNP has been identified. Faecal frequency (%), frequency range in which the SNP has been identified. Underlined nucleotides, consensus identity. Nucleotides or amino acids in red, found in WT G1P[8] (GenBank reference JN887818). Amino acids in black bold, amino acid change. Amino acids in red bold, possible reversion to WT strain. [1] Identified in vaccine material at the NIBSC (Mitchell, Lui, *et al.*, unpublished). Shaded in blue, loci present in ≥2 infants. Marked in purple, loci present in ≥2 infants.

nt original	nt change	aa change	Individuals	Timepoints	Faecal frequency (%)
118	A>G	I40**V**	L	1(day15)	13.7-31.1
133	T>C	F45**L**	L	1(day15)	5.5-47.8
162	G>A	G54G	J	1(day13)	5.8-34.0
368	G>A	S123**N**[1]	J, M	1(day13)//2(day5, 13)	6.3-32.5//9.1-99.9
585	G>A	V195V	C	1(day9)	5.1-10.7
689	T>C	V230**A**	C	1(day9)	1.6-2.0

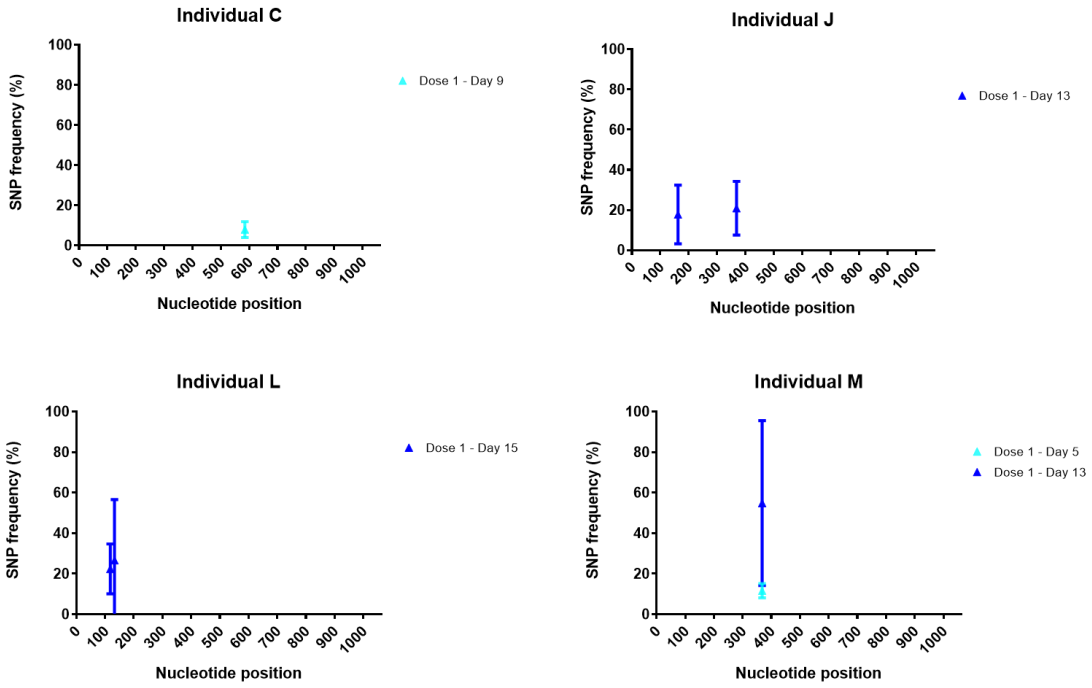

Fig. 4.5. Frequency of SNP loci over rotavirus genome segment 9 (VP7) in stool from infants C, J, L, M. Percentage of reads containing each SNP for each nucleotide position at several timepoints after dose 1 (blue triangles); error bars for triplicates shown. All days in reference to dose 1. Nucleotide position refers to full length coding sequence (JN887818).

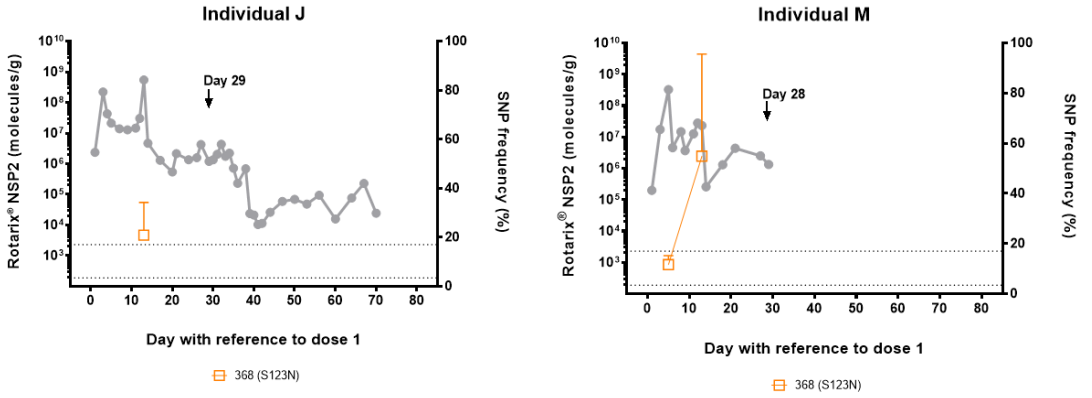

Fig. 4.6. Frequency of SNP loci identified in rotavirus genome segment 9 (VP7) over timepoints tested in stool from infants J, M. Vaccine genome copy number indicated on the left Y axis for reference and in grey on the graphs. Frequency of SNP loci indicated in right Y axis. SNP loci identified in stool from each infant described in key; error bars for triplicates shown. Dotted lines: Upper limit of SNP frequency in vaccine material for a particular SNP (key). Day: Day of dose 1. Day by black arrow: Day of dose 2. All days in reference to dose 1.

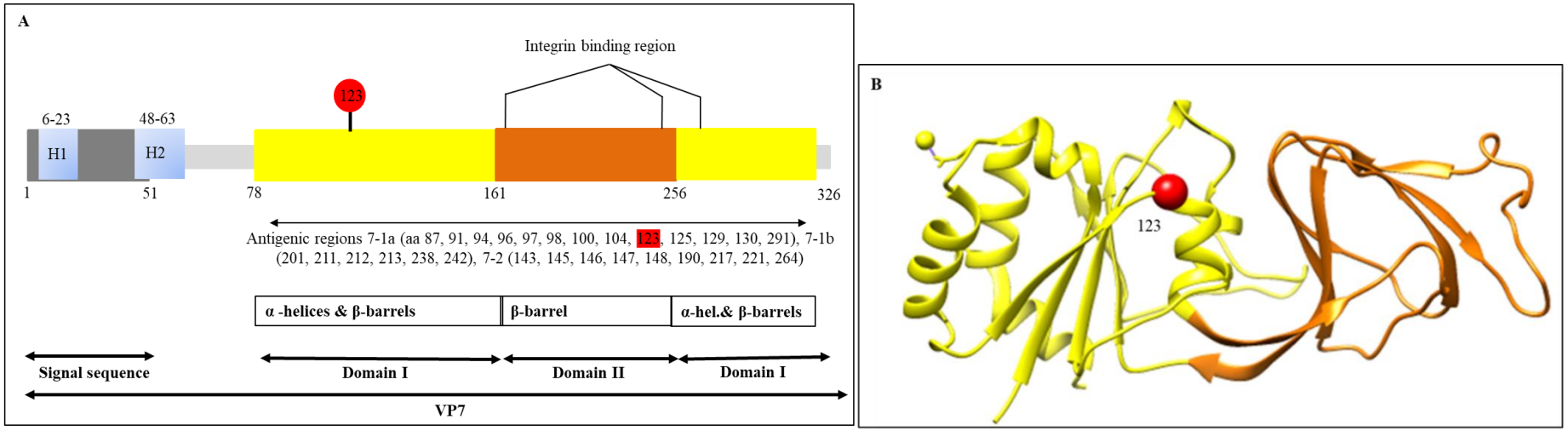

Fig. 4.7. A) Schematic of VP7 primary amino acid sequence and B) Atomic model of the VP7 glycoprotein, highlighting the non-synonymous amino acid substitution originating from SNP loci identified in stool of ≥2 infants (J, M). A) Numbers indicate amino acid position. A single subunit Rossmann-fold domain or domain I is indicated in yellow and the β-barrel domain or domain II is indicated in orange (Aoki *et al.*, 2009). Antigenic regions in VP7 are indicated by horizontal double-direction arrows (Zeller *et al.*, 2012). Hydrophobic domains (H1, H2) indicated in light blue. Affected residue is indicated in red sphere. **B)** Ribbon representation of a VP7 single subunit in yellow (Rossmann-fold domain, domain I) and orange (β-barrel domain, domain II) and residue affected as a red sphere. From PDB entry 3FMG (Aoki *et al.*, 2009).

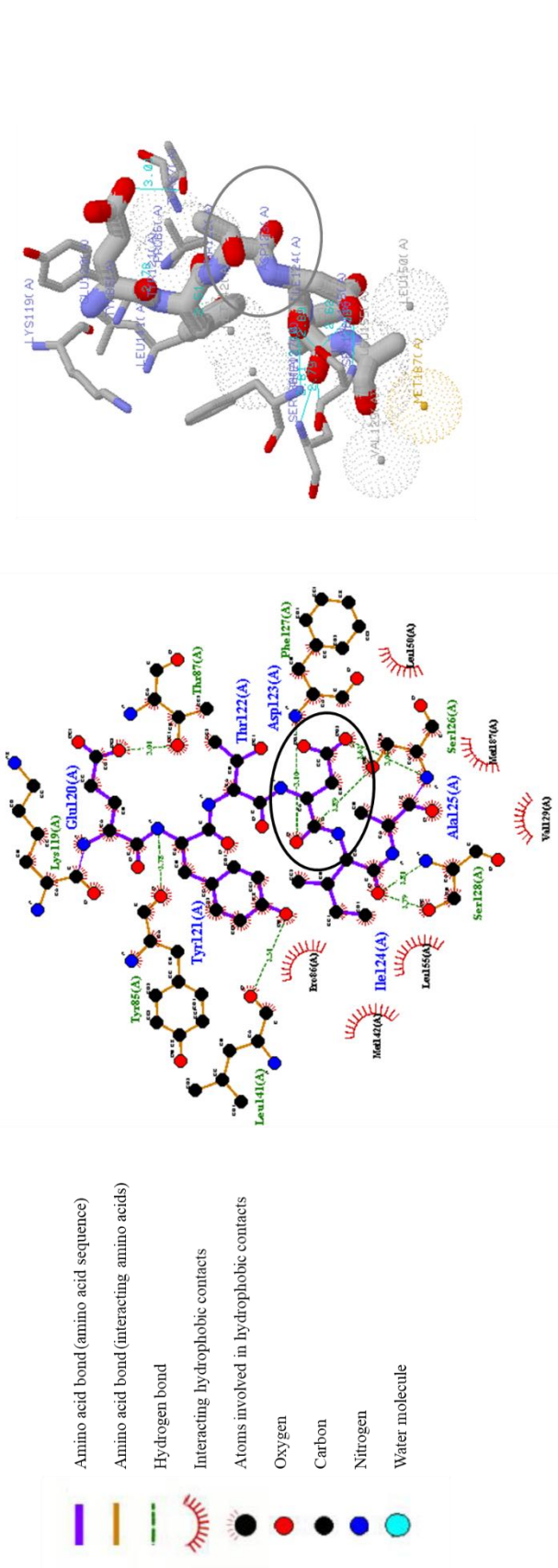

Fig. 4.8. Molecular schematic of residues in VP7 that interact with amino acid 123. Chain structure and 3D structure shown: Amino acid circled in black and grey respectively.

Gene segment 6, encoding VP6

In gene segment 6, one synonymous mutation G>A at nucleotide position 654 led to a silent amino acid substitution L218L (Table 4.5, Fig. 4.9) located in the β-roll region of VP6 domain H (Fig. 4.11). It was the same synonymous mutation previously identified in vaccine material (Mitchell, Lui, *et al.*, unpublished) and in stool it was common to two infants. No non-synonymous SNPs were identified in gene segment 6 in vaccine material or virus from stool. The silent amino acid substitution L218L was previously detected in vaccine material at frequencies up to 15% (Mitchell, Lui, *et al.*, unpublished). In stool, it was detected at similar frequency within the second week after dose 1 (individual J) and at lower frequency within the first week (individual M) (Table 4.5, Fig. 4.10). Molecular modelling of VP6 (Fig. 4.12) was performed following the Protein Data Bank Bos VP6 structure (PDB entry 1QHD). This analysis showed that leucine (L) 218 was predicted to form two hydrogen bonds with phenylalanine (F) 285 and one with valine (V) 330, the first one near a VP4 interaction site and the second one within the H domain. These interactions will be maintained in Rotarix® and in stool of two vaccine recipients as they presented the same amino acid change L218L.

Table 4. 5. Single nucleotide polymorphism loci identified in stool of individuals B-M for viral segment encoding VP6. Nucleotide (nt) original, nucleotide position in GenBank reference JX943613. Nucleotide change. Amino acid (aa) change. Vaccine frequency (%), frequency of SNP in Rotarix® previously (Mitchell, Lui, *et al.*, unpublished). Vaccine recently, if SNP loci identified in Rotarix® control within these sequencing runs. Individuals, individuals in whose stool the SNP has been identified. Timepoints, timepoints where SNP has been identified. Faecal frequency (%), frequency range in which the SNP has been identified. Underlined nucleotides, consensus identity. Nucleotides or amino acids in red, found in WT G1P[8] (GenBank reference JN887819). Amino acids in black bold, amino acid change. Amino acids in red bold, possible reversion to WT strain. [1] Identified in vaccine material at the NIBSC (Mitchell, Lui, *et al.*, unpublished). Shaded in blue, loci present in ≥2 infants. Marked in purple, loci present in ≥2 infants.

nt original	nt change	aa change	Individuals	Timepoints	Faecal frequency (%)
654	G>A	L218L[1]	J, M	1(day13)//1(day5)	12.7-16.6//5.4-5.7

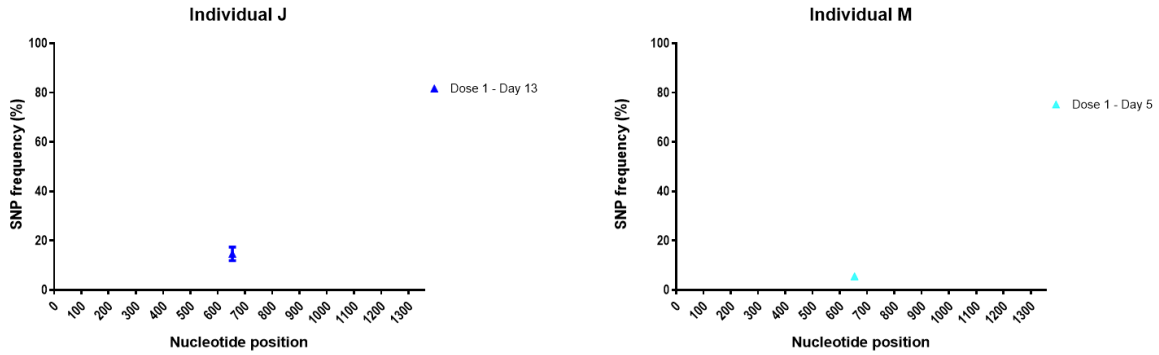

Fig. 4.9. Frequency of SNP loci over rotavirus genome segment 6 (VP6) in stool from infants J, M. Percentage of reads containing each SNP for each nucleotide position at several timepoints after dose 1 (blue triangles); error bars for triplicates shown. All days in reference to dose 1. Nucleotide position refers to full length coding sequence (JN887819).

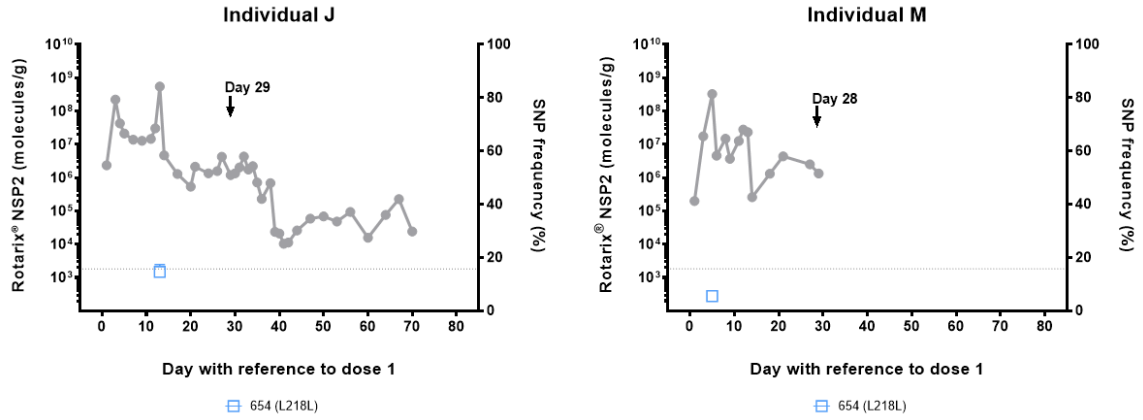

Fig. 4.10. Frequency of SNP loci identified in rotavirus genome segment 6 (VP6) over timepoints tested in stool from infants J, M. Vaccine genome copy number indicated on the left Y axis for reference and in grey on the graphs. Frequency of SNP loci indicated in right Y axis. SNP loci identified in stool from each infant described in key; error bars for triplicates shown. Dotted lines: Upper limit of SNP frequency in vaccine material for a particular SNP (key). Day: Day of dose 1. Day by black arrow: Day of dose 2. All days in reference to dose 1.

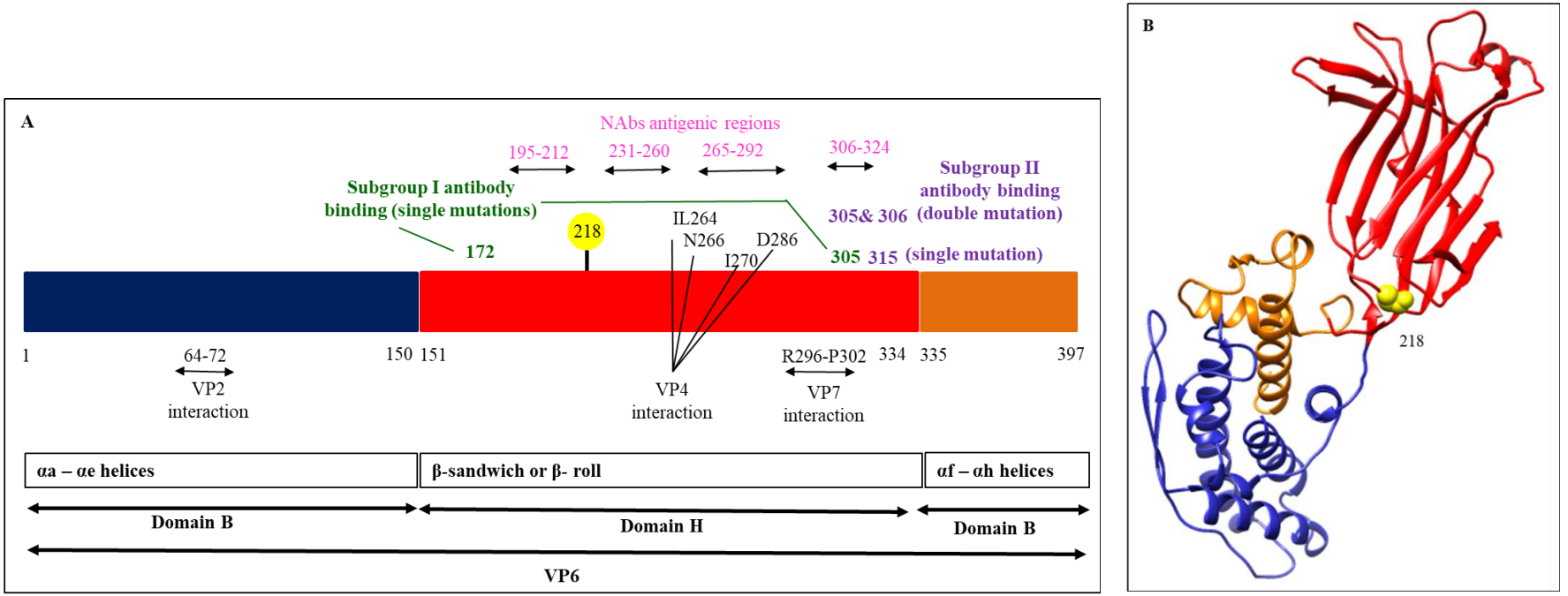

Fig. 4.11. A) Schematic of VP6 primary amino acid sequence and B) Atomic model of the VP6 inner capsid protein, highlighting the non-synonymous amino acid substitution originating from SNP loci identified in stool of ≥2 infants (J, M). A) Numbers indicate amino acid position. A single subunit B domain, eight α-helices, is indicated in dark blue and the H domain, β-barrel sandwich or β-roll, is indicated in red (Mathieu *et al.*, 2001). Regions interacting with VP4, VP7 and VP2 are indicated (Mathieu *et al.*, 2001; McClain *et al.*, 2010). Antigenic regions in VP6 are indicated in green for subgroup I and purple for subgroup II (Mathieu *et al.*, 2001). Quaternary antigenic regions for VP6-specific NAbs are indicated in pink (Aiyegbo *et al.*, 2013, 2014). Affected residue is indicated in yellow sphere. **B)** Ribbon representation of a VP6 single subunit in dark blue and orange (domain B, α-helices) and red (domain H, β-sandwich) and residue affected as a yellow sphere. From PDB entry 1QHD (Mathieu *et al.*, 2001).

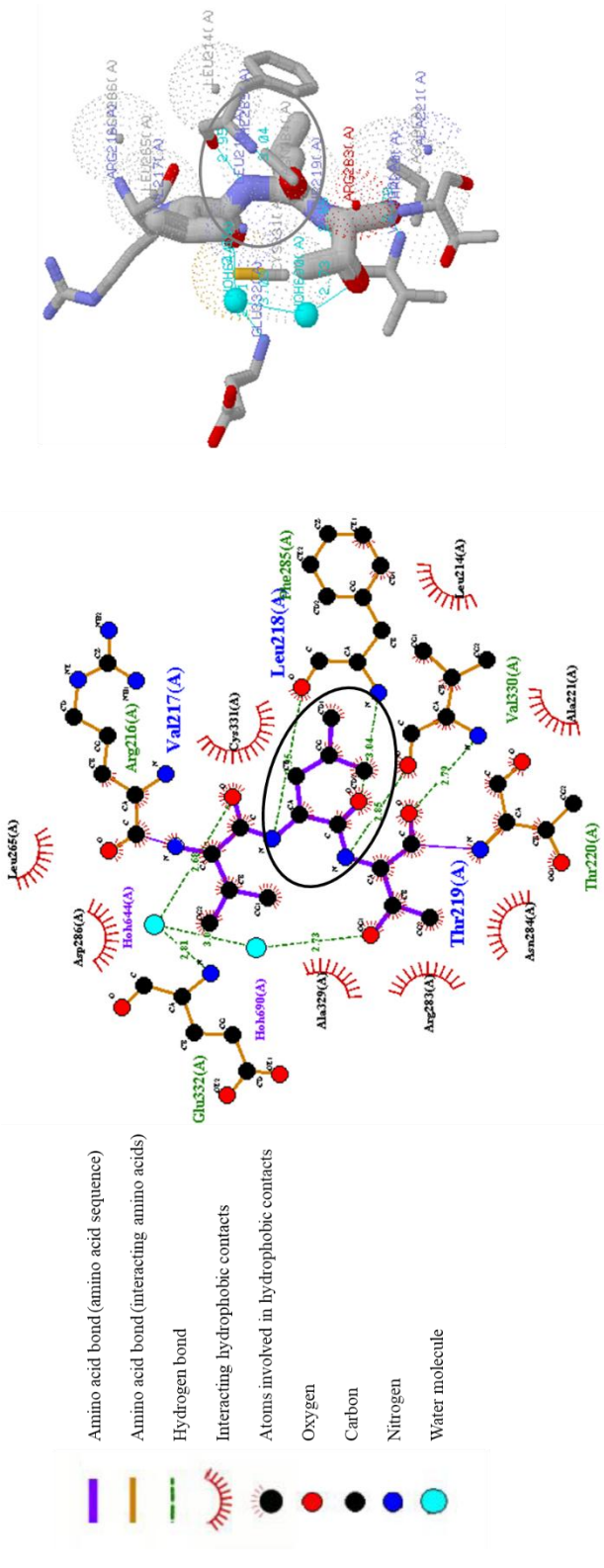

Fig. 4.12. Molecular schematic of residues in VP6 that interact with amino acid 218. Chain structure and 3D structure shown: Amino acid circled in black and grey respectively.

Gene segment 10, encoding NSP4

In the gene encoding NSP4, a total of 34 SNP loci were identified: 8 synonymous and 27 non-synonymous, with one reversion to WT (Table 4.6, Fig. 4.13). None of them was observed in vaccine material at the NIBSC (Mitchell, Lui, *et al.*, unpublished) or when tested in Rotarix® vaccine material used as control for this project. From the 27 non-synonymous novel SNP loci, 21 diverged from virus in vaccine material, human WT G1P[8] sequence (GenBank reference JN887818) and human WT consensus.

Mutation G150T leading to amino acid substitution A37-S and mutation T546C leading to amino acid substitution S169P diverged from virus in vaccine material and human WT consensus. Mutation T175C leading to amino acid substitution I45T diverged from virus in vaccine material and converged towards virus in human WT G1P[8] sequence (GenBank reference JN887818) and human WT consensus. One pair of contiguous SNP loci affecting amino acids 45 (T175C and A176G leading to I45T) was identified in six infants.

Twenty-four SNP loci were particular to one infant each. Of those, several non-synonymous mutations were identified in the viroporin domain of NSP4 (Fig. 4.15 A): mutations leading to amino acid changes H47P (non-conservative, positively charged to aromatic), I68S (non-conservative, hydrophobic to polar uncharged) and T74M (non-conservative, polar uncharged to hydrophobic). They were identified in continuous shedders or shedders between doses and at frequencies <20% in early or late timepoints. Nucleotide position 445 and mutation T>C led to non-conservative amino acid substitution I135T in the enterotoxin domain (Fig. 4.15, B) in individual I at low frequency (<2%) over a week after dose 1 (day 9). Molecular modelling of NSP4 at this position (Fig. 4.16) was performed following the Protein Data Bank human NSP4 structure (PDB entry 3MIW). This analysis showed that isoleucine (I) 135 was predicted to form an intramolecular hydrogen bond. Some of its atoms also present hydrophobic contacts with other atoms in nearby residues within the chain (leucine 134, threonine 136 or histidine 131). Nucleotide position 453 and mutation C>A, led to non-conservative amino acid substitution P138T, a hypervariable region in the amphipathic α-helix coiled coil domain, in individual J at low frequency (<6%) after dose 2 (day 27). Four SNP loci were common to two infants, such as locus at nucleotide position 183, mutation

A>G, leading to non-conservative amino acid substitution K48E in individuals J and I within two weeks of dose 1 at low frequencies (<15%). Mutation at nucleotide position 195, mutation C>T, led to non-conservative amino acid substitution P52S in individuals J and C at low frequencies (<10%) in early timepoints. Amino acid change K163R was identified in two infants from low to high frequencies (>50%) at early and late timepoints.

To focus data analysis, SNP loci common to ≥3 infants were considered: they were located within the hydrophobic H2 domain of the protein (Fig. 4.15 A). Because the complete structure of NPS4 is not resolved yet, these molecular interactions were not modelled for NSP4. Nucleotide position 139, mutation T>C, leading to non-conservative amino acid substitution F33S, was detected at low frequency in one infant (individual M) and frequencies higher after dose 2 than after dose 1 in two infants (individuals B, J) (Table 4.6 Fig. 4.14). This change from a hydrophobic to a polar amino acid might disturb the hydrophobicity and stability of NSP4 anchoring in the membrane. Nucleotide position 150, mutation G>A, leading to non-conservative amino acid substitution A37T, or mutation G>T, leading to non-conservative amino acid substitution A37S was detected at low frequencies (<16%) in stool from two infants (individuals C, M) after both doses and after dose 1. Nucleotide position 153, mutation T>C, leading to non-conservative amino acid substitution S38P, was detected stool from five infants at low frequency (individuals J, L), 50% (individual M) and very high frequency (individual E) after dose 1 and in stool from individual B from >60% after dose 1 to low frequency after dose 2.

Nucleotide position 175, mutation T>C, leading to non-conservative amino acid substitution I45T, was detected in stool of seven infants (Table 4.6 Fig. 4.14): at low frequency after dose 1 (individuals C, D, E, L, M), from low after dose 1 to 31% after dose 2 (individual F), and from 35% to low after dose 1 (individual J). Nucleotide position 176, mutation A>G, leading to conservative amino acid substitution I45M, was detected in five infants at low frequency (individuals B, D, M), 35% (individual L), low to >60% after dose 2 (individual F) and >84% after dose 2 (individual C). Positions 175 and 176 mutating as described above, led to non-conservative amino acid substitution I45T, which has been detected in five infants (C, D, F, L, M) along their vaccination period at the frequencies described

above. Nucleotide position 178, mutation T>C, leading to non-conservative amino acid substitution L46S, was detected at low frequencies in individuals C, L, and M.

Table 4. 6. Single nucleotide polymorphism loci identified in stool of individuals B-M for viral segment encoding NSP4. Nucleotide (nt) original, nucleotide position in GenBank reference JX943607. Nucleotide+12, nucleotide position from A in first codon encoding the first methionine (41 nucleotide shift when aligned to WT GenBank reference JN887809). Nucleotide change. Amino acid (aa) change. Vaccine frequency (%), frequency of SNP in Rotarix® previously (Mitchell, Lui, *et al.*, unpublished). Vaccine recently, if SNP loci identified in Rotarix® control within these sequencing runs. Individuals, individuals in whose stool the SNP has been identified. Timepoints, timepoints where SNP has been identified. Faecal frequency (%), frequency range in which the SNP has been identified. Underlined nucleotides, consensus identity. Nucleotides or amino acids in red, found in WT G1P[8] (GenBank reference JN887814). Amino acids in black bold, amino acid change. Amino acids in red bold, possible reversion to WT strain. Shaded in blue, loci present in ≥2 infants. Marked in purple, loci present in ≥3 infants.

nt original	nt+41	nt change	aa change	Individuals	Timepoints	Faecal frequency (%)
55	96	G>A	D19**N**	C	1(day34)	2.3-4.0
59	100	C>T	T20**I**	D	1(day8)	35.1-37.5
83	124	C>A	P28**H**	B	2(days32, 44)	1.5-4.3
98	139	T>C	F33**S**	J, M, B	4(days13, 27, 38, 67)//1(day13)//3(days19, 32, 44)	7.9-61.8//10.4-11.4//18.3-100.0
103	144	T>G	Y35**D**	J	4(days13, 17, 38, 67)	5.0-80.7
109	150	G>A	A37**T**	C	2(days9, 34)	4.7-15.6
109	150	G>T	A37**S**	M	1(day13)	3.0-4.1
112	153	T>C	S38**P**	J, M, B, L, E	1(day13)//1(day13)//2(days19, 32)//1(day15)//1(day35)	4.4-5.4//39.8-41.5//3.4-62.8//14.3-15.3 //100.0-100.0
117	158	T>C	V39V	B	2(days32, 44)	1.0-3.7
119	160	T>A	L40**Q**	D	1(day8)	2.2-2.6
121	162	A>G	T41**A**	K	1(day4)	1.6-2.6
131	172	T>G	F44**C**	M, L	1(day13)//1(day15)	4.9-5.5//11.9-12.2
134	175	T>C	I45**T**	J, D, F, M, L, E, C	2(days13, 27)//1(day8)//2(day7, 41) //1(day13)//1(day15)//1(day6)//2(days9, 34)	4.6-36.1//2.3-2.8//8.1-38.6//1.2-11.9//19.3-22.0//4.5-5.3//1.1-4.9
135	176	A>G	I45**M**	D, F, M, B, L, C	1(day8)//3(day7, 30, 41)//1(day13) //1(day19)//1(day15)//2(days9, 34)	4.0-4.1//1.2-71.9//2.7-3.6//2.8-3.8 //35.0-36.4//1.3-85.4

134 & 135	175 & 176	T>C & A>G	I45**T**	D, F, M, L, C		
137	178	T>C	L46**S**	M, L, C	1(day13)//1(day15)//2(days9, 34)	13.2-14.8//7.1-7.4//5.6-10.5
140	181	A>C	H47**P**	J	2(days13, 27)	1.4-4.7
142	183	A>G	K48**E**	J, I	1(day13)//1(day9)	3.5-4.1//7.9-12.9
154	195	C>T	P52**S**	J, C	1(day13)//1(day9)	8.9-8.9//8.6-9.0
203	244	T>G	I68**S**	C	1(day9)	2.7-3.0
213	254	T>C	C71C	J	2(days13, 38)	1.0-12.9
221	262	C>T	T74**M**	B	1(day32)	1.1-1.5
222	263	G>A	T74T	J	2(days38, 67)	2.1-17.4
279	320	C>T	D93D	J	1(day13)	1.8-2.0
354	395	T>C	T118T	J	1(day67)	8.0-17.1
404	445	T>C	I135**T**	I	1(day9)	1.2-2.0
412	453	C>A	P138**T**	J	1(day27)	3.1-5.8
462	503	A>G	K154K	J	2(days27, 38)	7.5-48.3
480	521	G>A	E160E	J	1(day67)	3.1-4.1
488	529	A>G	K163**R**	J, F	1(day27)//2(day7, 41)	3.5-9.1//27.5-55.1
505	546	T>C	S169**P**	J	1(day67)	1.1-4.2
507	548	A>G	S169S	B	1(day44)	1.1-4.4

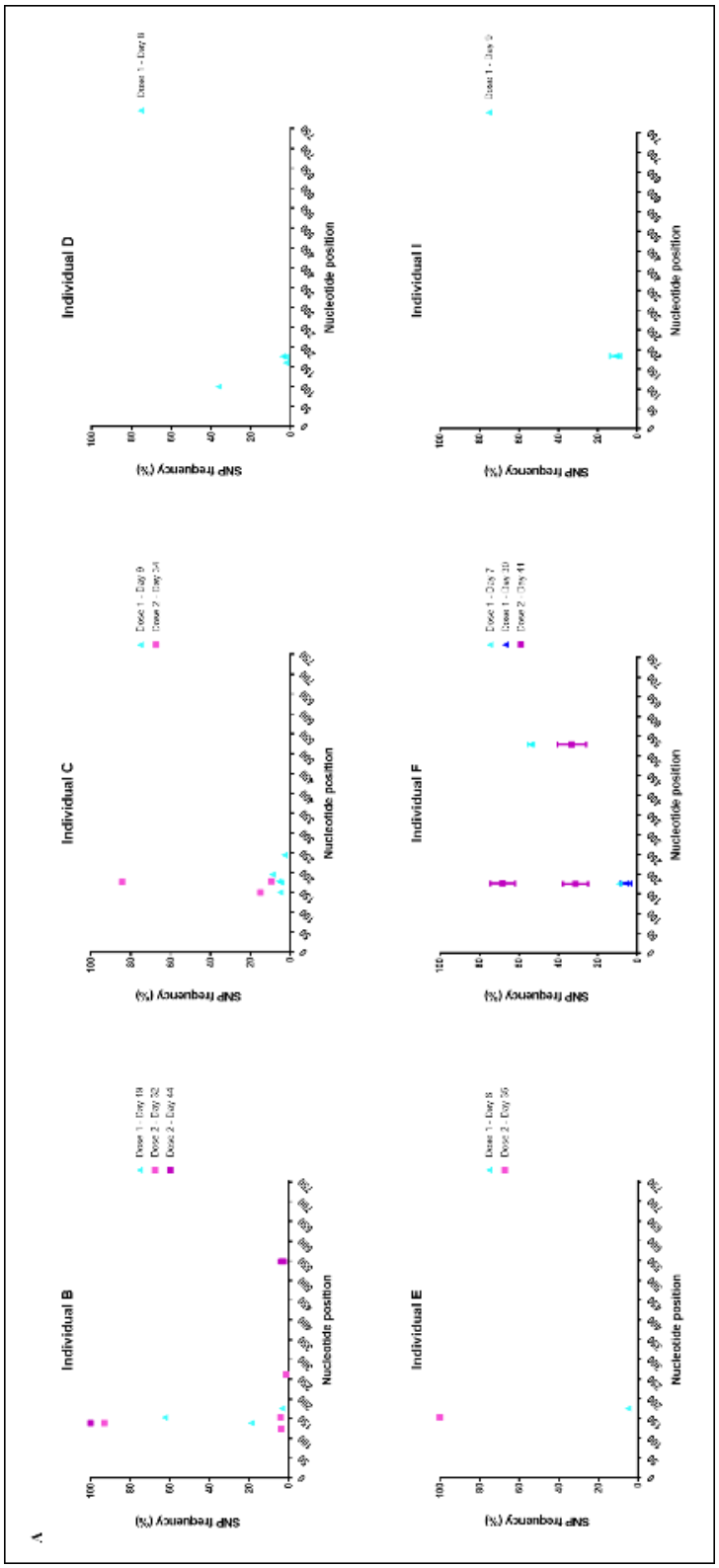

Fig. 4.13. Frequency of SNP loci over rotavirus genome segment 10 (NSP4) in stool from A) infants B-F, I; and B) infants J-M. Percentage of reads containing each SNP frequency for each nucleotide position at several timepoints after dose 1 (blue triangles) and dose 2 (pink squares); error bars for triplicates shown. All days in reference to dose 1. Nucleotide position refers to full length coding sequence

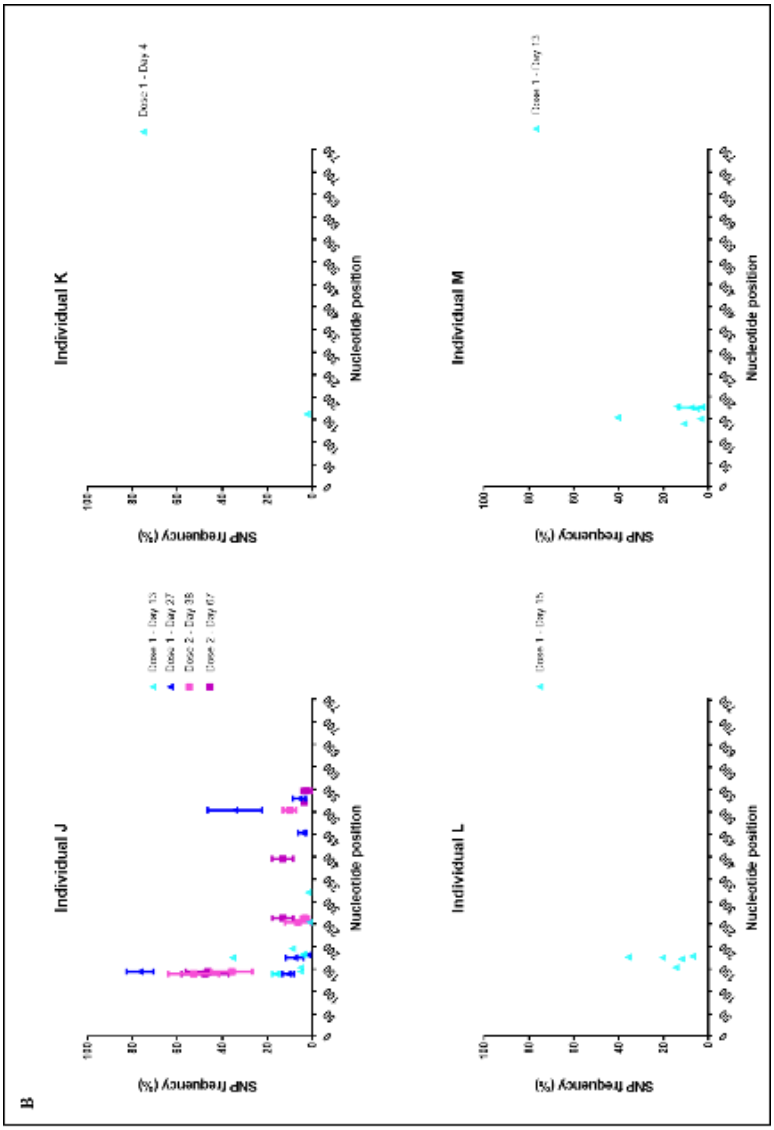
B
Individual J
Individual K
Individual L
Individual M
SNP frequency (%)
Nucleotide position

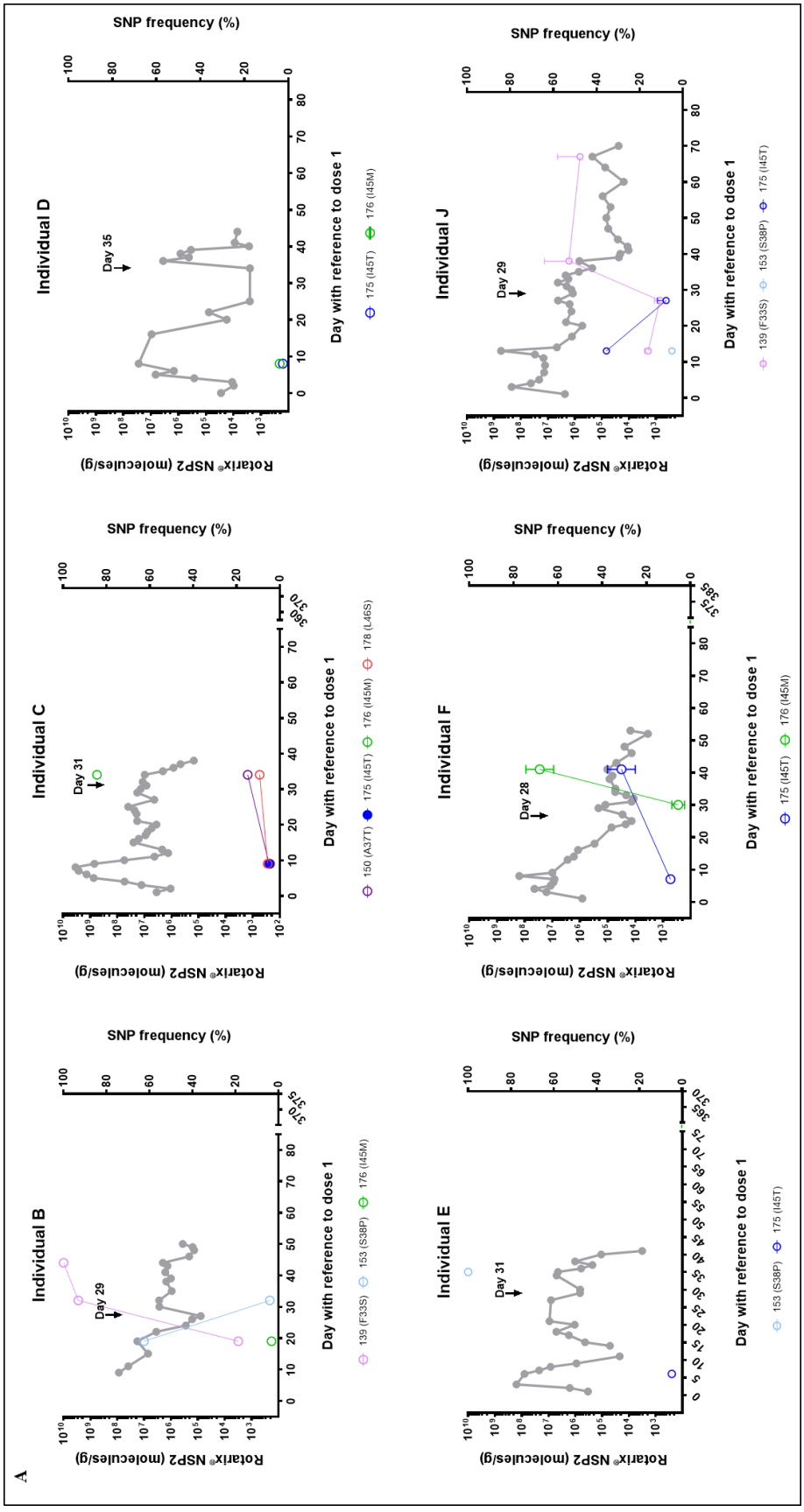

Fig. 4.14. Frequency of SNP loci identified in rotavirus genome segment 10 (NSP4) over timepoints tested in stool from A) infants B-F, J; and B) infants L, M. Vaccine genome copy number indicated on the left Y axis for reference and in grey on the graphs. Frequency of SNP loci indicated in right Y axis. SNP loci identified in stool from each infant described in key; error bars for triplicates shown. Dotted lines: Upper limit of SNP frequency in vaccine material for a particular SNP (key). Day: Day of dose 1. Day by black arrow: Day of dose 2. All days in reference to dose 1.

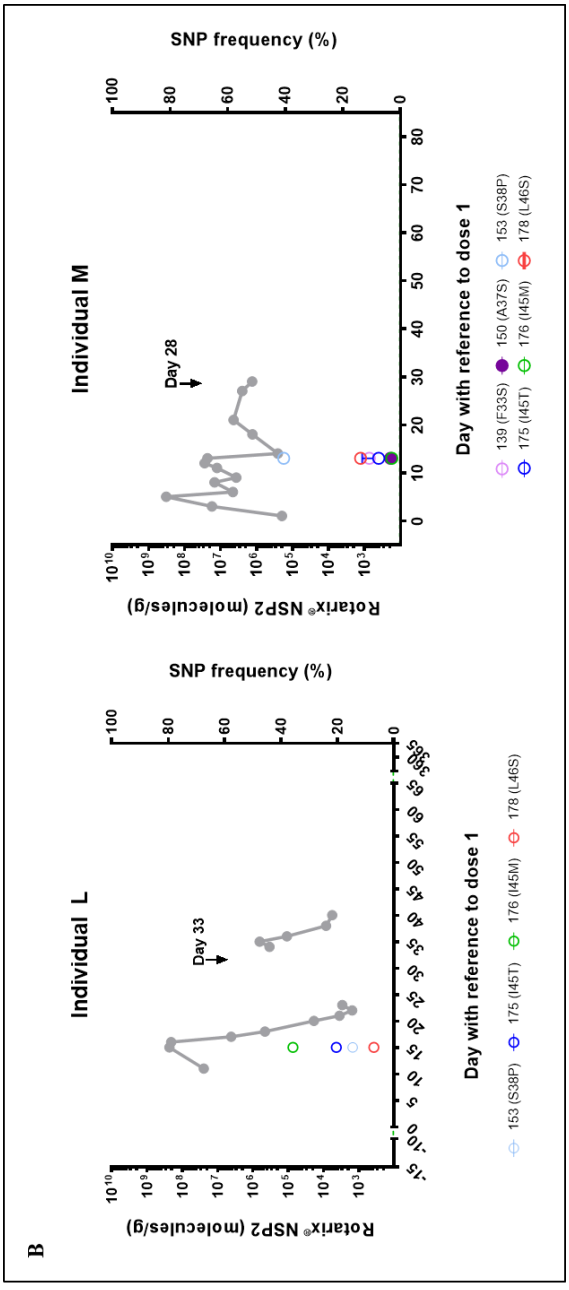
B
Individual L
Day 33
SNP frequency (%)
Rotarix® NSP2 (molecules/g)
Day with reference to dose 1
153 (S38P)
175 (I45T)
176 (I45M)
178 (L46S)
Individual M
Day 28
SNP frequency (%)
Rotarix® NSP2 (molecules/g)
Day with reference to dose 1
139 (F33S)
150 (A37S)
153 (S38P)
175 (I45T)
176 (I45M)
178 (L46S)

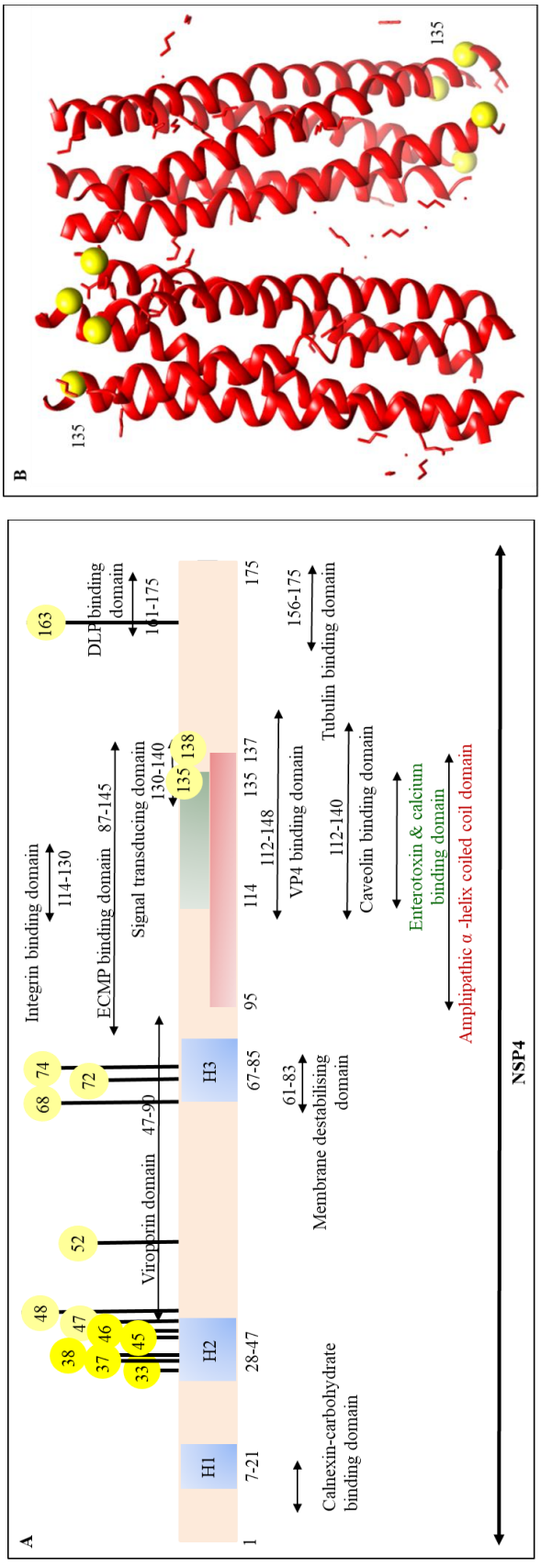

Fig. 4.15. A) Schematic of NSP4 primary amino acid sequence and B) Atomic model of the NSP4 enterotoxin, highlighting the non-synonymous amino acid substitutions originating from SNP loci identified in stool of ≥3 infants (B-M). A) Numbers indicate amino acid position. Enterotoxin domain indicated in green and amphipathic α-helix coiled coil domain indicated in red (Tsugawa, Tatsumi and Tsutsumi, 2014). Hydrophobic domains (H1, H2, H3) indicated in light blue. Affected residues are indicated as yellow spheres (intense yellow when identified in ≥3 infants, lighter yellow when identified in one or two infants within the viroporin domain, enterotoxin domain, hypervariable region or DLP-binding domain). **B)** Ribbon representation of the NSP4$_{95\text{-}137}$ oligomerization domain indicated in red. Only one residue affected by a non-synonymous mutation in one infant indicated in yellow in this domain. From PDB entry 3MIW (Chacko *et al.*, 2012).

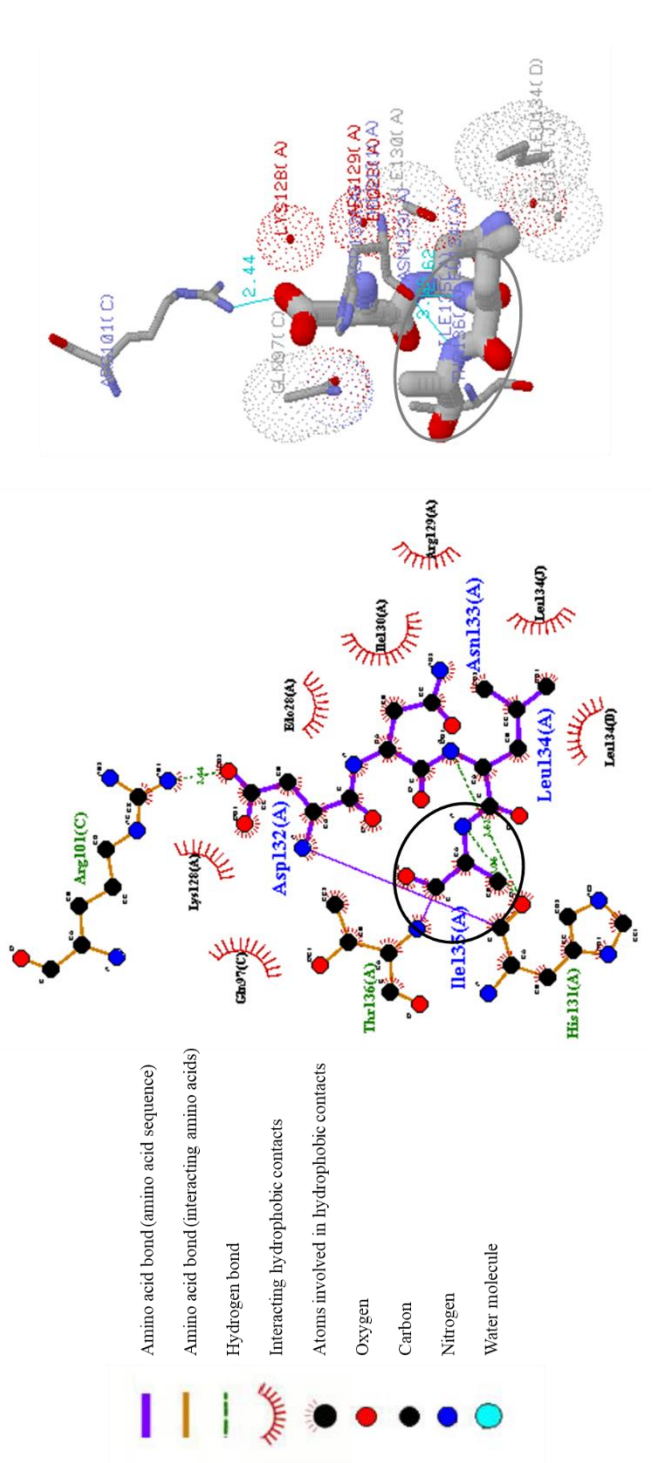

Fig. 4.16. Molecular schematic of residues in NSP4 that interact with amino acid 135. Chain structure and 3D structure shown: Amino acid circled in black and grey respectively.

Concluding remarks

Mutations identified in all four segments did not directly increase with time. The majority increased after dose 1 (and some also after dose 2) and later decreased or were not detected by the end of the vaccination period. Others, particularly in gene segments 4 and 10 of individual J, were dominant or fixed by the end of the vaccination period. Most of the mutations identified in stool of vaccine recipients diverged from the WT consensus. However, in one mutation in VP4 (leading to K368R) and another one in NSP4 (leading to I45T) the dominant sequence converged towards the WT consensus.

4.5 Discussion

The combined viral load and sequencing data on rotavirus indicate that vaccine virus can be detected in stool samples and that it is shed throughout the vaccination period (Chapter 3), supporting the hypothesis that vaccine-derived variants arise as a result of replication following vaccination. Previous studies assessed RV genetic stability in naturally infected infants by Sanger sequencing (Flores, Sears, *et al.*, 1988) and in cell culture (Tsugawa and Tsutsumi, 2016). Genetic stability of porcine RVs in pigs (Blackhall, Fuentes and Magnusson, 1996) and murine RVs in mice (Tsugawa, Tatsumi and Tsutsumi, 2014) have also been studied. A recent study at the NIBSC assessed the genetic stability of Rotarix® during manufacture (Mitchell, Lui, *et al.*, unpublished). This study uses a unique set of samples to elucidate the genetic variants arising as vaccine virus replicated in the gut of vaccine recipients as a measure of genetic stability in the population and is the first of its kind. The study of SNPs throughout replication in the host in comparison to vaccine material allows to study the genetic changes that may have contributed to attenuation and to further adaptation in the host.

In previous vaccine stability studies (Mitchell, Lui, *et al.*, unpublished), SNP loci were detected in all structural proteins and in one non-structural protein, NSP1. One triallelic mutation that was previously observed in vaccine material in gene segment 4 at low frequency was not detected in stool: nucleotide position 797, mutation A>C, leading to non-conservative amino acid substitution Y266S. The other allele (nucleotide substitution A>G, leading to amino acid substitution Y>C)

was detected in stool of individual H at an early timepoint and low frequency. The A>C allele may have been present at a frequency <1% detection threshold.

In stool from the 12 infants of this cohort, variants previously observed in vaccine material (Mitchell, Lui, *et al.*, unpublished) increased in frequency after replication in the gut, some of them achieving transient dominance or fixation by the latest timepoints studied. Novel variants arose as a result of replication in the gut, usually at low frequencies but some increasing to transient dominance or fixation as well. The gene segments characterised encoded proteins VP4, VP7, VP6 and NSP4, due to their importance in viral entry, immunogenicity and virulence. Single nucleotide polymorphism loci resulted in both synonymous and non-synonymous mutations leading to silent, conservative or non-conservative amino acid changes. To focus data analysis, only SNP loci common to ≥3 (gene segments 4 and 10) or ≥2 (gene segments 9 and 6) infants have been considered. Mapping of sequence changes to known or predicted amino acid structure and immune dominant domains was performed where possible.

Gene segment 4, encoding VP4

Mutations detected in VP4 that were previously observed in vaccine material (Mitchell, Lui, *et al.*, unpublished) were non-synonymous and appeared at similar or higher frequency in stool. One of them appeared in the hemagglutinin VP8* domain: amino acid substitution D252N. VP8* can act as a viral hemagglutinin (Weiner *et al.*, 1978; Yeung *et al.*, 1987; López and Arias, 2004) and the cleavage sites for trypsin are in the linker region, targeting mono-basic arginine (R) at amino acid positions 231, 241 and 247 (Arias *et al.*, 1996; Crawford *et al.*, 2001). The conformation stabilising effect of the salt bridges formed between D252 and neighbouring positively charged residues (arginines) will be lost as the D252N substitution abrogates the existing negative charge. The D252N substitution was detected at similar frequencies in vaccine material, and its location nearby the linker region implies a selective preference for conformational flexibility in this region.

A cluster of mutations was detected in the VP5* subunit between amino acids 363 and 388, pointing towards there being a hotspot region for variation at the start of the putative fusion domain of the virus (amino acids 384 to 401), which is a hydrophobic region (Mackow *et al.*, 1988; Dormitzer *et al.*, 2004; Trask *et al.*, 2010).

Changes in amino acids N363S and M364V/I were previously detected in the USA in WT isolates passaged in MA104 and Vero cell culture (Esona *et al.*, 2010). As conservative substitutions of polar uncharged and hydrophobic amino acids respectively, they may improve the ability to penetrate the cell since frequencies were higher than in vaccine early after dose 1 and in one continuous shedder (individual J) the mutation persists at frequencies up to 50% by the end of the vaccination period.

Mutation at amino acid 368 from K>R is present in a known WT RV G1P[8] strain (GenBank reference number JN887809), which suggests that a consistent and very high frequency in stool with respect to vaccine material comprise a complete reversion to WT sequence (e.g. individual J). Sanger sequencing that generated the original Rotarix® sequence (GenBank reference numbers JX943604-JX943614) (Gautam *et al.*, 2014) may have not detected the G allele if it was approximately 30%, but as it was 50-60%, it was unlikely it was undetected. In the case of other continuous shedders and shedders between doses, the frequency of this mutation after dose 2 appears to be proportionally equivalent to after dose 1, except for individual B, who maintained a very high frequency. It appears as if the immune response of individuals B and J, who presented low RV-specific copro-IgA (Chapter 5), was not strong enough to prevent the vaccine virus from replicating and generating this variant, suggesting it may be relevant for rotavirus vaccine persistence in the GI tract. In the case of early responders (who controlled virus between doses), only one infant (individual L) showed this mutation after dose 2 (when its RV-specific copro-IgA levels are medium). This amino acid change has also been identified in an immunocompromised infant in Germany (Andreas Mas Marques, personal communication, 2019). It appears as if the infection advantage gained in cell culture is maintained *in vivo*, especially in those individuals with a less robust or later immune response.

Changes in amino acids 385 and 388 are known to be related to neutralisation and attenuation of the virus (Kapikian, Hoshino and Chanock, 2001; Tsugawa and Tsutsumi, 2016). The non-conservative substitution at amino acid 385 (Y>H) is located between amino acids 384 and 386 of epitope region 5-1 (Zeller *et al.*, 2012) (Fig 4.9). In stool of this cohort, it was found at low frequencies similar to vaccine except in individual J, a continuous shedder in whose stool this mutation was

identified at high frequency (>80%) late after dose 1 but was decreased to 50% by the end of the vaccination period. Changes at this residue have previously been identified in several studies: in un-passaged 89-12 Rotarix® precursor, WTs and consensus as asparagine (N) and in Rotarix® candidate passaged 33 times as tyrosine (Y) in the USA (Ward *et al.*, 2006); in natural human strains passaged in cell culture MA104 and Vero cells in the USA (Esona *et al.*, 2010), in a mouse RV strain passaged in mice, changing from glutamic acid (E) to lysine (K) in Japan (Tsugawa, Tatsumi and Tsutsumi, 2014); in AGMK cells passaged with WT RVA G1P[8] as D385H/N in Japan (Tsugawa and Tsutsumi, 2016); and in an immunocompromised infant in Germany as Y385D (Andreas Mas Marques, personal communication, 2019). This non-conservative Y385H substitution could affect the fusion domain and attenuation of the virus and further affect epitope region 5-1, and it appears as if the change may be relevant in children with a weak/delayed immune response.

The conservative substitution at amino acid I388L is located in epitope region 5-1 (Zeller *et al.*, 2012) (Fig. 4.3). It was found at low frequency in the cohort except for individual C, who presented this change at >60% frequency early after dose 1 and individual M who presented >4% within the second week after dose 1. This amino acid change at 388 was previously identified in the USA in WT isolates passaged in cell culture MA104 and Vero cells (Esona *et al.*, 2010) and in an immunocompromised infant in Germany (Andreas Mas Marques, personal communication, 2019). Due to its conservative nature, it appears as if this amino acid substitution may not have a large impact on protein structure or immunogenicity.

The hyper-variation hotspot at amino acids 363 to 388 may alter the fusion capabilities of the virus (Mackow *et al.*, 1988; Gorziglia, Larralde and Ward, 1990; Burke, Bridger and Desselberger, 1994). It appears as if this cluster was generated *in vitro* when passaging the Rotarix® vaccine candidate in Vero cells and was maintained *in vivo* despite higher selection pressure as it provided an advantage to cell penetration and therefore infection. Areas of high mutability such as the proposed hotspot do not significantly modify protein structure and function and this region may be a result of the genetic robustness (Lauring, Frydman and Andino, 2013) by which rotavirus generates genetic diversity, leading to a not very different but potentially more advantageous phenotype *in vivo*.

Other mutations previously observed in vaccine material were I470T and Y479H. The change from a hydrophobic to a polar or to a positively charged amino acid might have effects in protein structure and the ability to fold and penetrate the cell. These changes appear at low frequency, except for I470T in individual F with high frequency after dose 1 but decreasing to low frequency after dose 2. A substitution at amino acid 470 was previously identified in mouse RV passaged in cell culture (Tsugawa, Tatsumi and Tsutsumi, 2014) and it appears less relevant than other mutations in the previous cluster.

Three novel mutations were identified in VP4 that were common to at least three infants: two in the VP8* subunit and one in the VP5* domains. Mutation leading to P114T in epitope region 8-3 (Zeller *et al.*, 2012) was detected at approximately 70% in individual M after dose 1, at >50% in individual C after dose 2 and fluctuating from 20% to 50% in individual J from after dose 1 through to after dose 2. Substitution P114T was previously identified in surveillance of clinical samples as vaccine-derived variant at Public Health England (PHE) by David J. Allen (Desselberger, 2017a) and at the NIBSC within this project (Preliminary data in Appendix II). First detection within the second week after dose 1 followed by high or consistent frequencies throughout the vaccination period suggest P114T might provide an advantage potentially in terms of evasion of the host immune response in individuals with high viral loads and low RV-specific copro-IgA levels.

Substitution F167L, located in the VP8* subunit, was detected in five individuals, in most of them at high or very high frequency after each dose or both. While the hydrophobicity of the amino acid is maintained, the leucine interactions may be key to binding sialic acids and the hemagglutinin function of the VP8* region. The leucine allele is present in a known human WT RVA G1P[8] strain (GenBank reference number JN887809) and may constitute a reversion to WT phenotype. This change was previously identified in several studies: in the USA as mentioned previously (Ward *et al.*, 2006; Esona *et al.*, 2010), in circulating RV strains from Belgian infants (Zeller *et al.*, 2017), in infants with suspected Rotarix®-derived severe gastroenteritis in Japan (Sakon, Miyamoto and Komano, 2017) and in an immunocompromised infant in Germany (Andreas Mas Marques, personal communication, 2019). High frequencies in infants with low RV-specific copro-IgA

suggest this revertant to wild type variant may potentially infect naïve and immunocompromised individuals.

Non-conservative amino acid substitution D477G in the VP5* subunit was identified at low frequencies in vaccine recipients. Conservative amino acid substitution N477S was previously observed in an isolate that could be cultured in the absence of trypsin, with slower proteolysis kinetics, but maintaining replication (Trask *et al.*, 2013). The change from an aspartic acid (D) at 477 in Rotarix® and consensus to a glycine (G) in vaccinees does not seem to provide a structural change favouring replication kinetics *in vivo*.

Gene segment 9, encoding VP7

One mutation detected in stool of two infants in VP7 was previously observed in vaccine material (Mitchell, Lui, *et al.*, unpublished): conservative S123N in epitope region 7-1a (Zeller *et al.*, 2012), an immunodominant region believed to be a target for NAbs (Aoki *et al.*, 2009). Moreover, it was previously found in stool from infected infants in Malawi (Jere *et al.*, 2018). In stool, it was detected at similar and higher frequencies than in vaccine material. Targeting of certain epitopes by the host immune system may drive mutation that favours immune escape of the virus. Alterations in this epitope region may affect the ability to evade antibodies, as reported previously for VP7 (Iturriza-Gómara *et al.*, 2001).

Gene segment 6, encoding VP6

One SNP locus was identified in stool of two infants in VP6 and previously detected in vaccine material: silent substitution L218L in the β-roll region of VP6 domain H. Its location in the protein is unrelated to VP2, VP7 or VP4 interaction and it is not located in a known antigenic region (Mathieu *et al.*, 2001; McClain *et al.*, 2010) nor within the quaternary epitope region in the transcriptional pore against which VP6-specific intracellular NAbs are directed (Aiyegbo *et al.*, 2013, 2014). This substitution may impact trimerization as it is located in the β-roll region of domain H (López *et al.*, 1994; Affranchino and González, 1997), although because it is silent, it suggests maintenance of a hydrophobic residue in a hydrophobic, conserved region (Mathieu *et al.*, 2001).

Gene segment 10, encoding NSP4

None of the mutations detected in NSP4 were previously observed in vaccine material and most of them were particular to one or two infants. Some SNP loci were located in the viroporin domain (amino acids 47 to 90) (Hyser *et al.*, 2010). Amino acid substitution K48E located in the penta-lysine domain (Hyser *et al.*, 2010) may affect transmembrane insertion and viroporin activity. It was previously observed in mice as K48I: the isoleucine was present in a limited-virulence tissue culture-attenuated murine RV strain (Angel *et al.*, 1998). NSP4 functions as enterotoxin (Estes and Kapikian, 2007; Rajasekaran *et al.*, 2008) and one of the SNP loci identified, leading to non-conservative amino acid substitution I135T, was located within its diarrhoea-mediating domain (amino acids 114 to 135 of NSP4) (Ball *et al.*, 1996; Ousingsawat *et al.*, 2011). Although the complete crystal structure of NSP4 has not been resolved yet, the oligomerisation domains (containing the enterotoxin domain) have been described (Bowman *et al.*, 2000; Chacko *et al.*, 2012; Kumar *et al.*, 2018). Modelling of amino acid 135 has shown a change from a hydrophobic (isoleucine) to a polar uncharged (threonine) amino acid, potentially affecting structure and enterotoxin function. Another mutation led to P138T, located within amino acids 131 to 140 which are considered a hypervariable region related to altered pathogenesis in cell culture of porcine RVs (Zhang *et al.*, 1998) and murine RVs (Angel *et al.*, 1998). Amino acid substitution P138T was previously observed in a porcine OSU RV mutant as P138S, losing ability to induce diarrhoea in neonatal mice (Zhang *et al.*, 1998). This change from an aromatic to a polar amino acid, as in the porcine study, might lead to an effect the ability to mobilise intracellular calcium. Amino acid change K163R in the DLP-binding domain was observed before in wildtype E2 genotypes of NPS4 (Srivastava *et al.*, 2015) with respect to DS-1 strain E2 genotype. The C-terminal region is relevant for multimerization (Rajasekaran *et al.*, 2008) and this change may provide an advantage *in vivo* as it was detected at >50% frequency late in the vaccination period in one of the continuous shedders (individual F).

Mutation leading to amino acid change F33S increased to >50% in a continuous shedder (individual J) and to fixation in another infant (individual B) who shed between doses and after dose 2. This change potentially disturbing the

hydrophobicity and stability of NSP4 anchoring in the membrane may provide an infection advantage in certain vaccine recipients.

Those SNP loci identified in at least three infants were non-synonymous mutations located in the H2 hydrophobic domain, located traversing the endoplasmic reticulum (ER) membrane and functioning as a signal sequence (Hu *et al.*, 2012), with residues 1-23 within the ER lumen and residues 44 to 715 in the cytoplasm (Parr *et al.*, 2006). Although identified at low frequency in stool of two infants only (individuals C, M), amino acid substitution at site 37 was previously observed in mice as a change from valine (V) to alanine (A), considered key for enterotoxin activity *in vivo* in mice (Tsugawa, Tatsumi and Tsutsumi, 2014). It was also identified in circulating RV strains in Belgium (Zeller *et al.*, 2017) and detected as A37S in a vaccine-derived RV in Japan (Sakon, Miyamoto and Komano, 2017). This change from a hydrophobic to a polar amino acid might affect the stability of the H2 domain and virulence *in vivo* as it appeared to have increased frequency late in stool from individual C.

Change S38P was identified at low frequency in some infants and at >40% and >60% in two individuals within the second week after dose 2. A substitution at amino acid 38 was previously detected in MA104 cell culture as a change from a serine (S) to phenylalanine (F) (polar to hydrophobic) (Tsugawa, Tatsumi and Tsutsumi, 2014) and in a tissue culture-attenuated mice strain as amino acid substitution S38F (polar to hydrophobic) (Angel *et al.*, 1998). This change S38P from a polar to a cyclical amino acid might affect protein structure, signal sequence and exposure of that residue, although it appears not to persist.

Substitution I45T was identified at low frequency except for two infants (F, J): although both are continuous shedders, in individual F it increased from <10% within the first week after dose 1 to approximately 30% ten days after dose 2, and in individual J it decreased 40% to <10% after dose 1. An amino acid change at position 45 was previously observed in the Rotarix® vaccine candidate 89-12 as a change from T45A in symptomatic and asymptomatic patients (Ward, Mason, *et al.*, 1997), as T45A in AGMK cells passaged with WT G1P[8] (Tsugawa and Tsutsumi, 2016) and in murine strains as T45M (Angel *et al.*, 1998). The change I45T from a hydrophobic to a polar amino acid might affect stability of NSP4 cytoplasmic domain and it appeared to be selected in one of the infants at a late timepoint.

Mutation leading to substitution I45M was identified at low frequency except for three infants (individuals L, C, F). The very high frequencies in stool of individuals C and F after dose 2 suggest this mutation is selected in some hosts where replication is prolonged and immune response low. This amino acid change was previously detected in murine strains (Angel *et al.*, 1998) and in an immunocompromised child (Andreas Mas Marques, personal communication, 2019). This maintenance of a hydrophobic amino acid might have affected stability of the cytoplasmic domain and provide an advantage to infection/spread within susceptible hosts.

Amino acid change L46S was identified at low frequency in vaccine recipients and it was observed previously detected in circulating RV strains in Belgium (Zeller *et al.*, 2017). This change from a hydrophobic to a polar amino acid might have contributed to stabilising the cytoplasmic domain.

Concluding remarks

As an RNA virus vaccine, Rotarix® exists as a quasispecies: a heterogeneous viral population. When a human monovalent G1P[8] strain was passaged *in vitro*, pressure to balance viral fitness and adapt to cells arose, resulting in accumulation of mutations and potential gain of attenuation in the original host. When administered at high dose in the original host, it replicated *in vivo* existing as a viral quasispecies now under increased selection pressure. The viable quasispecies continued to replicate and positively selected previous and/or novel variants resulting in structural or functional phenotypic changes that may have allowed improved infection, replication or escape from host immunity. These changes were selected at the quasispecies level and were not necessarily present in the same virion, so different virions may result in different phenotypes. Molecular evolution of a quasispecies can lead to transient dominance or fixation of alleles in the viral population, although population fitness takes priority over variants of high fitness and the quasispecies can supress those variants if they may disturb the mutation-selection balance (Andino and Domingo, 2015). Therefore, it was key to identify the genomic loci prone to mutation in the host and compare them to the ones previously identified in vaccine material, highly stable across independent bulks and fills (Mitchell, Lui, *et al.*, unpublished).

Changes in the outer capsid proteins VP7 and VP4 may result in functional differences in viral entry affecting receptor binding, trypsin cleavage sites and the fusion domain, as well as regions key for neutralisation. From the changes resulting from potential cell culture adaptation of the vaccine with increased frequency in vaccinees, a reversion to WT phenotype in the fusion domain is selected to very high frequency, suggesting it facilitates infection *in vivo*. The novel changes in the spike protein resulting from replication in the host appeared at high and very high frequency and may comprise variants with pathogenic capability. If they are immunodominant epitopes, they may lead to escape mutants. The inner capsid protein, VP6, has been found to maintain a silent mutation in an area unrelated to intracellular neutralization at similar levels to vaccine material in vaccine recipients, highlighting the importance of its structural conservation. Since no SNP loci were identified in NSP4 in vaccine material, it appears that NSP4 is stable and not crucial for *in vitro* viral adaptation. However, NSP4 appears to be potentially relevant for infection and further replication in infants.

Although synonymous mutations that are innocuous *in vitro* may have a large impact on the ability to infect and replicate *in vivo* —they may affect viral RNA secondary structure and/or codon-pair usage, increase immunomodulatory RNA regions and/or lead to codons that following a single nt substitution may result in stop codons, all of these potentially affecting viral fitness (Klitting *et al.*, 2018)—, the synonymous mutation leading to silent amino acid substitution L218L in VP6 appears not to affect quasispecies viability. Most of the common SNPs identified in this cohort were non-synonymous in genes encoding VP4, VP7 and NSP4. Genes encoding viral surface epitopes, flexible within the protein structure, tend to present non-synonymous mutations that allow for diversity that results in a neutral effect in a competent host but may be advantageous in an immunocompromised host (Lauring, Frydman and Andino, 2013). This antigenic variation in VP4 and VP7 may be unrelated to immune selection (Sánchez *et al.*, 2003) and it may represent mutational robustness (Lauring, Frydman and Andino, 2013). The variants previously observed in vaccine material (Mitchell, Lui, *et al.*, unpublished) identified at higher frequency in stool of vaccine recipients appear to have been a dominant minority in cell culture that was re-selected in the original host as a strategy to override the initial low fitness in infants. However, as the vaccine virus adapted in infants, only a few of them were

still selected. Revertant mutations might have been selected as a means of compensating the low fitness provided by attenuating mutations when replicating in the original host. Novel mutations appear to be a result of virus-host adaptation throughout replication in infants. All these mutations, whether in structural or non-structural proteins, may have an effect on cell tropism and host range (Domingo, Sheldon and Perales, 2012).

Data showed that SNPs previously identified in vaccine material were detected at similar or higher frequencies in vaccine recipients and that novel SNPs were introduced during viral replication. Some mutations identified at high frequency immediately after vaccination decreased their frequency later after dose 1, with immune pressure potentially forcing their disappearance or negative selection of those mutations being replaced by others providing better viral fitness. SNP loci maintained at a low frequency may represent minority variants that are emerging. Other SNPs appearing after a certain time at low frequency and then becoming undetectable in the population, potentially represent a minor variant that emerges and is then not selected within the viral population. SNPs emerging before dose 2 and staying at a similar frequency after could be driven by immune pressure to persist and suggested relevance in immunogenicity or pathogenesis. The changes that increased in frequency over time and those that appeared at very high frequency by the end of the vaccination period were detected in profiles where vaccine virus had not been cleared after first dose, infants with a low RV-specific copro-IgA response (Chapter 5). Most of the mutations that appear to be fixed by the end of the vaccination period were those previously observed in vaccine material, as well as two novel mutations, suggesting that the vaccine virus may acquire lasting changes while transiting the GI tract of certain infants.

In this cohort, the SNPs identified did not increase in number as the vaccine virus replicated in infants who controlled shedding early. In continuous shedders or shedders between doses, the quasispecies diversity increased by late timepoints presenting some novel variants signifying adaptation and further evolution within the host. However, except in three infants, viral loads were undetectable by the latest timepoints tested. In infants shedding vaccine virus by the latest timepoints, these vaccine-derived variants may pose a risk if transmitted horizontally in the population, as observed previously in several studies for rotavirus (Payne *et al.*,

2010; Rivera *et al.*, 2011; Kaneko *et al.*, 2017; Miura *et al.*, 2017; Sakon, Miyamoto and Komano, 2017) and rabies (Faber *et al.*, 2005). Herd immunity as well as the opportunity to evolve molecularly and become pathogenic both stem from this horizontal transmission.

No health-related data on vaccine recipients or susceptible contacts was provided in this study, so it was assumed they were asymptomatic shedders of vaccine virus. It appears then that attenuation was maintained in the original host and the virus was stable within the population of vaccinees. Novel variants may have arisen due to adaptation to human cells or, since they have been detected late in the vaccination period and previously observed in passaged vaccine virus (Ward *et al.*, 2006; Esona *et al.*, 2010), WT strain clinical surveillance (Desselberger, 2017a; Zeller *et al.*, 2017), vaccine-derived (Sakon, Miyamoto and Komano, 2017) and immunocompromised infants (Andreas Mas Marques, personal communication, 2019), may have appeared as immune escape mutants or receptor binding enhancer mutations.

To understand whether the replicating virus containing novel variants may be virulent, further studies engineering these variants into rotavirus would have to be performed in an animal model such as mice. Alternatively, since heterogeneity of rotavirus replication has previously been observed in human intestinal enteroids (HIEs) from different patients (Saxena *et al.*, 2016), these HIEs may be an appropriate model to test these mutations. A series of individual and combined variant tests would be required to study multifactorial pathogenesis: individual variants at low frequency may be sufficient to have a pathogenic effect (Bull, 2015), and so may be several variants in infection complementation. Since the establishment in 2017 of a helper-virus-free reverse genetics system to study rotavirus (Kanai et al., 2017), the mutations that led to relevant amino acid changes in VP4, VP7 and NSP4 could be engineered singly or in combination to study pathogenicity *in vivo*. Of interest, novel mutations resulting in substitutions P114T, F167L and D477G and strong revertant K368R in VP4, mutation leading to substitution S123N in VP7 and mutations leading to substitutions K48E, I35T and P138T, as well as F33S, A37T, S38P, I45T, I45M and L46S in NSP4. If any of these variants alone or in combination increase virulence/pathogenicity, methods for their control should be developed, maybe by increasing vaccine production yields to relieve vaccine virus

pressure. If they favour attenuation, they may be incorporated in vaccine candidates by genetic engineering as previously tested for a live rabies vaccine (Nakagawa *et al.*, 2017).

Although sampling bias and limit of detection may have influenced the variants detected, particularly those present at lower frequencies, the longitudinal nature of the study allowed observation of trends, increased knowledge about variant regions of the virus and about behaviour of vaccine virus in transit through the gut. Biological and technical replicates added confidence to the results. Overall, SNP frequency data from triplicates was consistent. A few exceptions of inconsistent frequency for some SNPs were detected, probably due to sampling bias and increased difficulty in efficient amplification of the longest gene segments. A limitation of this study was the low success obtaining amplicons for some of the genes at some timepoints, especially VP6 and VP7 at late timepoints (Table 4.1). This may be due to VP7 and VP6 being gene segments difficult to amplify at timepoints of low viral load, but in the case of high viral load timepoints, variability of primer binding regions and potential SNPs in them may have been responsible for low-intensity RT-PCR bands.

The results on vaccine virus sequence variation while replicating in the host suggest that variants previously detected in vaccine material (Mitchell, Lui, *et al.*, unpublished) were generated in cell culture and then either lost or selected and maintained in infants. Vaccine-derived novel variants arising as a result of adaptation to the host, together with vaccine variants maintained at high frequency by the end of the vaccination period may pose a risk to immunocompromised infants or immunocompromised contacts of vaccine recipients. As the antibody at site of infection, faecally-derived IgA (copro-IgA) may also reveal information on the ability of an infant to control a rotavirus infection. With the detailed profiling from this cohort, an association of copro-IgA with shed virus may now be possible (Chapter 5).

Chapter 5: Antibody-mediated mucosal immunogenicity to human monovalent G1P[8] RV vaccine in a cohort of vaccinated infants in the UK

5.1 Introduction

The immune response in rotavirus-infected individuals triggers interferons and an 'antiviral state' in a primary infection (Chapter, 1 section 1.6.1). In a secondary infection, the immune response is mediated mainly via secretory IgA in the duodenum, either by neutralising anti-VP4 or anti-VP7 antibodies (heterotypic immunity) or by non-neutralising anti-VP6 intracellular antibodies that block viral transcription (Chapter 1, section 1.6.2). Increases of >1:200 and >1:800 in RV-specific IgA and IgG titres in serum respectively, and increases of ≥20 arbitrary units (U)/mL as performed by Bernstein (Bernstein, 1998) or ≥4-fold in RV-specific serum IgA titre have been considered to provide protective immunity against infection and disease in natural rotavirus infection (Coulson *et al.*, 1992; Matson *et al.*, 1993; O'Ryan *et al.*, 1994; Velázquez *et al.*, 1996, 2000; Cheuvart *et al.*, 2014). While serum IgA appears to be a long-lasting marker of protection, copro-IgA appears to be a more accurate marker in the short-term at high levels in the population (Coulson *et al.*, 1990, 1992; Matson *et al.*, 1993; Clarke and Desselberger, 2015). Animal studies in mice indicate that copro-IgA, a good surrogate marker of duodenal IgA, is the most accurate marker of protection (Feng *et al.*, 1994; Burns *et al.*, 1995), likely due to its direct proximity to the site of viral replication.

Studies on correlates of protection after rotavirus vaccination have indicated that seroconversion rate correlated with efficacy at a population level and was associated with a decrease in RV disease (Chapter 1, section 1.16). Apart from homotypic protection, neutralising anti-VP7 and anti-VP4 serum antibodies may also provide heterotypic protection (Johansen and Svensson, 1997; Angel, Franco and

Greenberg, 2012; Clarke and Desselberger, 2015) and further heterotypic protection may be generated after vaccination due to non-neutralising, protective anti-VP6 antibodies. Transcytosed secretory anti-VP6 IgA might be responsible for viral "expulsion" and inhibition of transcription in rotavirus infection (Thouvenin *et al.*, 2001; Feng *et al.*, 2002; Aiyegbo *et al.*, 2013, 2014).

Rotavirus-specific copro-IgA shedding is expected in stool of Rotarix® vaccine recipients, as it has been detected in previous studies (Chapter 1, section 1.16). Clinical trials have assessed immunogenicity by RV-specific IgA seroconversion, RV-specific IgG seroconversion and by vaccine-specific NAbs (O'Ryan, 2007). These studies assessed a timepoint after dose 1 and another timepoint two months after dose 2. Later studies have used a similar approach or a small number of timepoints expanding the first two years after vaccination for clinical evaluation (Chapter 1, section 1.16). However, none covered multiple timepoints following vaccination and testing IgA at the site of infection.

In studies regarding the mode of feeding and immunogenicity, breastfed children were found to present lower IgA levels in stool following Rotarix® vaccination (Bautista-Marquez *et al.*, 2016). IgA acquired through breastmilk may interfere with infection by the vaccine virus, lowering replication and impairing mounting an immune response as robust as in non-breastfed infants, who present higher shedding after Rotarix® vaccination.

In the absence of serum material, which can only be retrieved by invasive approaches, a discrete study on faecal RV-specific copro-IgA levels in vaccine recipients would inform on the levels of RV-specific IgA in the duodenum, the most relevant site for virus neutralisation in the lumen and for intracellular "expulsion". This study, expanding from dose 1 to dose 2 and after, would help to elucidate differences in short-term mucosal response between individuals. This type of study would also contribute to better understand the relationship between virus shedding load and duration in relation to IgA-mediated mucosal immunity.

5.2 Aims

The first aim of the work presented in this chapter was to produce a detailed longitudinal pattern of anti-RV copro-IgA from infants vaccinated with Rotarix® in this UK cohort to understand the anti-RV mucosal immune response. The second aim

was to determine the relationship between Rotarix® faecal shedding and anti-RV copro-IgA.

5.3 Experimental methodology

To address anti-RV copro-IgA, the same cohort of infants described in Chapter 3 was sampled, using stool material from the pre-vaccination period through to approximately a month after dose 2 and, for some, after-a-year. Materials and methods are detailed in Chapter 2 and Appendix I. Faecal samples were processed and stored until used (Chapter 2, sections 2.1.9 & 2.2.1). Some samples were of low volume due to stooling patterns and this was reflected in the analysis. To maximise the information obtained from this limited resource, and to allow for the study in Chapter 4, the reproducibility of data in this chapter was addressed by quantifying total and specific anti-RV copro-IgA levels across technical duplicates from material extracted from a single faecal suspension. Relative quantification of anti-RV copro-IgA has been reported previously (Macartney and Offit, 2000). Total IgA was measured with a commercial kit and specific IgA was quantified as a trend and measured using a total IgA standard. Samples collected at times pre-, during and post-vaccination regimen were tested in an assay to measure total copro-IgA and another assay to measure specific anti-RV copro-IgA (Chapter 2, section 2.2.9).

5.4 Results

5.4.1 Sample set

Obtaining samples from equivalent timepoints across the cohort was not possible due to the nature and collection of the material. Where low amounts of stool were available, priority was assigned to Rotarix® faecal shedding quantification throughout the sample collection and to NGS of specific timepoints from each infant, based on their shedding profiles. Therefore, for IgA testing, samples from 11 infants were assayed at pre-vaccination, samples from 12 infants after dose 1 and dose 2 and samples from eight infants after a year. For one individual, the sample available at pre-vaccination was only sufficient to quantify shedding.

5.4.2 Preliminary data

Preliminary data was obtained using the total IgA in-house assay followed by the specific anti-RV IgA in-house assay using the original total purified human secretory IgA standard (Bio-Rad, PHP133, batch 290415) (Chapter 2, section 2.2.9.3). Sample from one individual was tested to evaluate the conditions of the assay parameters: Blocking concentration, dilution buffer concentration, concentrations of coating and detection antibodies, standard dynamic range and stool dilutions for total and specific IgA.

Data from one infant (M) (Fig. 5.1) throughout the vaccination period showed fluctuation in specific IgA from day 11, increasing until day 18, followed by lower levels. Total IgA was high at day 12, maintained by day 18 and decreasing after. This profile suggested IgA levels peaked around day 18, when viral loads (Fig. 5.1) are still high but beginning to drop (Chapter 3, Fig. 3.4 C).

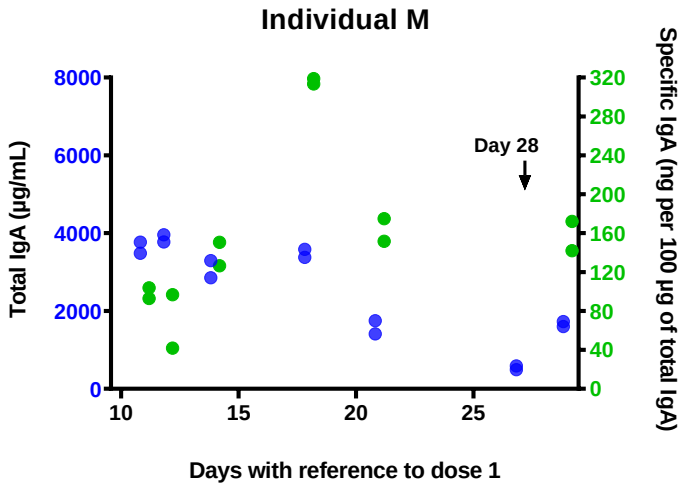

Fig. 5.1. Preliminary total and specific anti-RV copro-IgA concentration in one infant (M). Quantitation of total and specific IgA by direct sandwich ELISA shown in the left and right Y axes respectively. The X axis shows days with respect to dose 1. Day 0: Day of dose 1. Black arrow: Day of dose 2. Blue dots: Total IgA. Green dots: Specific IgA. Days shown in blue and green (slightly separated to avoid superimposed dots): 11, 12, 14, 18, 21 and 29. Day shown in blue only: 27.

The readout from the sandwich ELISA for total IgA was in µg/mL (or µg/g when related to stool; the range of the original standard being from 2 to 0.05 µg/mL), with specific IgA normalised to total IgA concentration in 1g (1mL) of stool. As an example: Individual M, on day 21 after dose 1, presented a total IgA level of 3481

µg/mL and a RV-specific IgA amount of 15 µg/mL. Therefore, 15/3481= 0.0043 µg of RV-specific IgA per 1 µg of total IgA, or 430 ng of RV-specific IgA per 100 µg of total IgA.

5.4.3 Optimisation of different batches of human secretory IgA

The total and specific IgA assays worked with the purified human IgA standard (Bio-Rad product PHP133, batch 290415) in the range of 2-0.1 µg/mL (Fig. 5.2. A). The stool suspensions were tested in dilutions 1/7500 for total IgA and 1/100 for RV-specific IgA. When these conditions were performed with a new batch of the standard (batch 020615), no dynamic range could be obtained, with the OD saturated at high amounts (OD>2.3) for all dilutions of the standard, despite low background (OD≤0.1) (Fig 5.2. B).

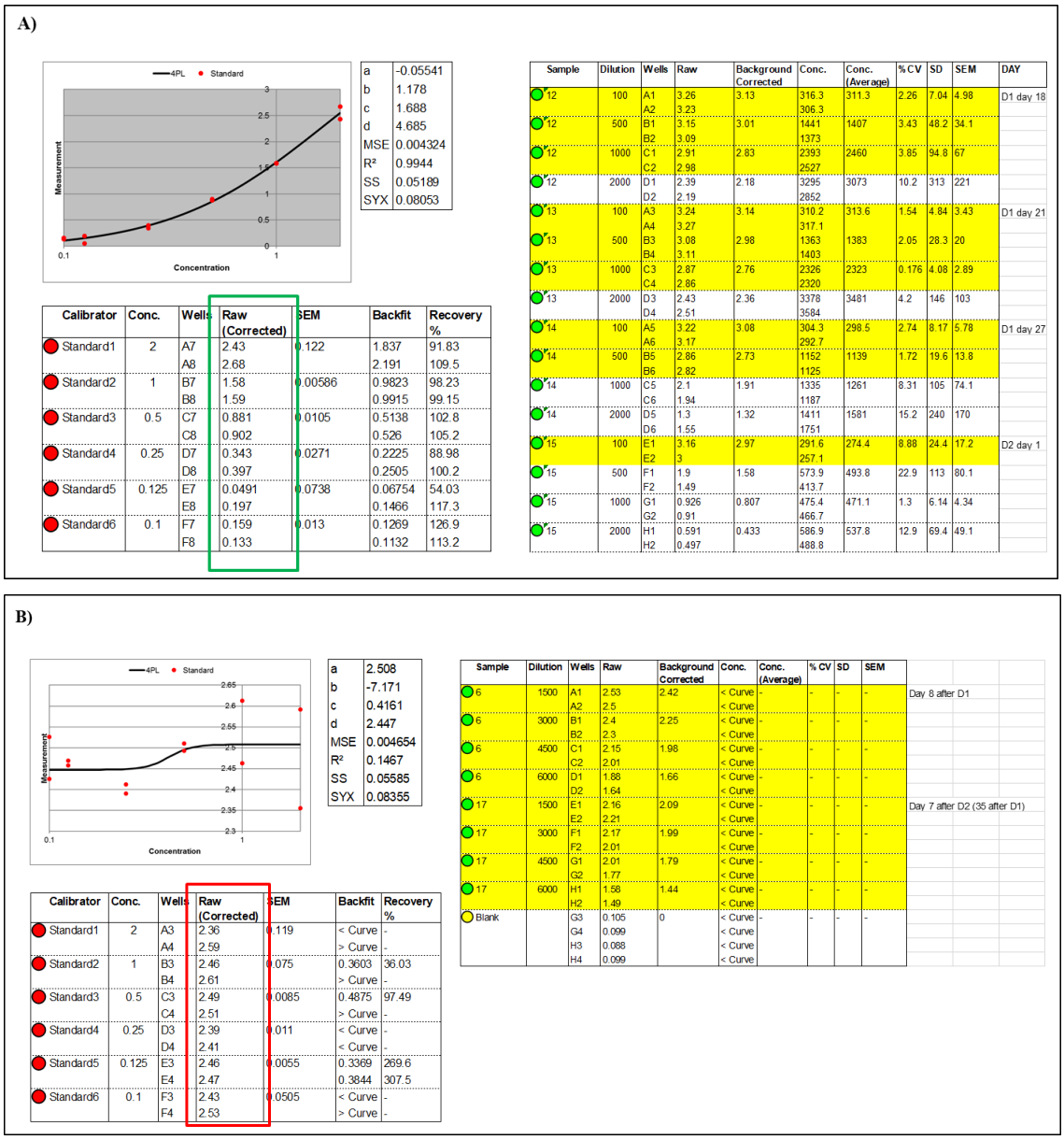

Calibrator	Conc.	Wells	Raw (Corrected)	SEM	Backfit	Recovery %
Standard1	2	A7	2.43	0.122	1.837	91.83
		A8	2.68		2.191	109.5
Standard2	1	B7	1.58	0.00586	0.9823	98.23
		B8	1.59		0.9915	99.15
Standard3	0.5	C7	0.881	0.0105	0.5138	102.8
		C8	0.902		0.526	105.2
Standard4	0.25	D7	0.343	0.0271	0.2225	88.98
		D8	0.397		0.2505	100.2
Standard5	0.125	E7	0.0491	0.0738	0.06754	54.03
		E8	0.197		0.1466	117.3
Standard6	0.1	F7	0.159	0.013	0.1269	126.9
		F8	0.133		0.1132	113.2

Sample	Dilution	Wells	Raw	Background Corrected	Conc.	Conc. (Average)	% CV	SD	SEM	DAY
12	100	A1	3.26	3.13	316.3	311.3	2.26	7.04	4.98	D1 day 18
		A2	3.23		306.3					
12	500	B1	3.15	3.01	1441	1407	3.43	48.2	34.1	
		B2	3.09		1373					
12	1000	C1	2.91	2.83	2393	2460	3.85	94.8	67	
		C2	2.98		2527					
12	2000	D1	2.39	2.18	3295	3073	10.2	313	221	
		D2	2.19		2852					
13	100	A3	3.24	3.14	310.2	313.6	1.54	4.84	3.43	D1 day 21
		A4	3.27		317.1					
13	500	B3	3.08	2.98	1363	1383	2.05	28.3	20	
		B4	3.11		1403					
13	1000	C3	2.87	2.76	2326	2323	0.176	4.08	2.89	
		C4	2.86		2320					
13	2000	D3	2.43	2.36	3378	3481	4.2	146	103	
		D4	2.51		3584					
14	100	A5	3.22	3.08	304.3	298.5	2.74	8.17	5.78	D1 day 27
		A6	3.17		292.7					
14	500	B5	2.86	2.73	1152	1139	1.72	19.6	13.8	
		B6	2.82		1125					
14	1000	C5	2.1	1.91	1335	1261	8.31	105	74.1	
		C6	1.94		1187					
14	2000	D5	1.3	1.32	1411	1581	15.2	240	170	
		D6	1.55		1751					
15	100	E1	3.16	2.97	291.6	274.4	8.88	24.4	17.2	D2 day 1
		E2	3		257.1					
15	500	F1	1.9	1.58	573.9	493.8	22.9	113	80.1	
		F2	1.49		413.7					
15	1000	G1	0.926	0.807	475.4	471.1	1.3	6.14	4.34	
		G2	0.91		466.7					
15	2000	H1	0.591	0.433	586.9	537.8	12.9	69.4	49.1	
		H2	0.497		488.8					

Calibrator	Conc.	Wells	Raw (Corrected)	SEM	Backfit	Recovery %
Standard1	2	A3	2.36	0.119	< Curve	-
		A4	2.59		> Curve	-
Standard2	1	B3	2.46	0.075	0.3603	36.03
		B4	2.61		> Curve	-
Standard3	0.5	C3	2.49	0.0085	0.4875	97.49
		C4	2.51		> Curve	-
Standard4	0.25	D3	2.39	0.011	< Curve	-
		D4	2.41		< Curve	-
Standard5	0.125	E3	2.46	0.0055	0.3369	269.6
		E4	2.47		0.3844	307.5
Standard6	0.1	F3	2.43	0.0505	< Curve	-
		F4	2.53		> Curve	-

Sample	Dilution	Wells	Raw	Background Corrected	Conc.	Conc. (Average)	% CV	SD	SEM	
6	1500	A1	2.53	2.42	< Curve	-	-	-	-	Day 8 after D1
		A2	2.5		< Curve					
6	3000	B1	2.4	2.25	< Curve	-	-	-	-	
		B2	2.3		< Curve					
6	4500	C1	2.15	1.98	< Curve	-	-	-	-	
		C2	2.01		< Curve					
6	6000	D1	1.88	1.66	< Curve	-	-	-	-	
		D2	1.64		< Curve					
17	1500	E1	2.16	2.09	< Curve	-	-	-	-	Day 7 after D2 (35 after D1)
		E2	2.21		< Curve					
17	3000	F1	2.17	1.99	< Curve	-	-	-	-	
		F2	2.01		< Curve					
17	4500	G1	2.01	1.79	< Curve	-	-	-	-	
		G2	1.77		< Curve					
17	6000	H1	1.58	1.44	< Curve	-	-	-	-	
		H2	1.49		< Curve					
Blank		G3	0.105	0	< Curve	-	-	-	-	
		G4	0.099		< Curve					
		H3	0.088		< Curve					
		H4	0.099		< Curve					

Fig. 5.2. A) Total human secretory IgA standard and stool samples from individual M, using the standard from Bio-Rad PHP133 batch 290415 and B) batch 060215. Dynamic range of the standard squared in green (batch 290415) or red (060215) box. Yellow highlighting indicates samples outside the range.

A series of modifications were performed to identify the cause of the poor dynamic range (Table 5.1). Washing buffer was changed to a stronger concentration; manual washing rather than a plate washer was introduced to ensure thorough washing; and the blocking agent was changed such that it contained 3% BSA to reduce the background. The dilution buffer was also changed to 3% BSA in PBS for consistency. The originally adapted protocol worked well, as the only changes implemented were BSA in the blocking and dilution buffers. The issue was most

likely related to the human secretory IgA standard. Two different and new batches from Bio-Rad (batches 020615 and 170516), one from Sigma (product I1010, batch SLBP7516V) and one from Invivogen (product ctrl-ga, batch GAC-36-01) were tested. None of these standards resulted in a dynamic range modelling the first batch (290415). In order to elucidate if the issue was related to the dilutions or the material itself, more material of the original batch (kindly provided by M. Iturriza Gómara and A. Pulawska-Czub) was tested and the dynamic range modelled that previously observed for batch 290415. The manufacturer was contacted: they explained that the source of human secretory IgA (which is purified from human colostrum by size-exclusion fractionation and ion-exchange chromatography; Bio-Rad PHP133 datasheet) from which they generated the original batch was exhausted, so the material would not be identical. Therefore, the original batch was kept for future quantification of specific anti-RV copro-IgA levels.

Table 5.1. Materials and reagents tested and modified to optimise the total IgA sandwich ELISA. ✓, worked; ✖, did not work.

Material or reagent	Modification	Effect
Plates	Nunc to COSTAR (hi-binding)	✓
Plate reader	Two different models	✓
PBS	Freshly prepared centrally at the NIBSC under quality system	✓
pH coating buffer	9.6 correct	✓
TMB	Within date, in good condition	✓
Stop solution	Within date, in good condition	✓
Washes	Plate washer *vs* manual washing 0.05% Tween20 in PBS *vs* 0.1% Tween20 in PBS	✓
Blocking	3% or 5% milk or BSA in PBS → 3% BSA	✓
Dilution buffer	1% or 3% milk or BSA in PBS → 3% BSA	✓
Coating antibody rabbit αhIgA	Batch, several dilutions → 1/4000 (original)	✓
Detection antibody goat αhIgA:HRP	Batch, several dilutions → 1/6000 (original)	✓
Standard human secretory IgA	Tested batch, dilutions and manufacturer Four different batches from Bio-Rad: Two ✖, one worked ✓ Two from other manufacturers (Invivogen, Sigma) ✖	✖

To test total IgA, four kits were considered: ThermoFisher Scientific IgA human uncoated ELISA kit (product 88-50600-22, range 1.6-100 ng/mL), an Abcam kit (product ab196263, range 0.78-50 ng/mL), Sigma SIgA ELISA (product SE 120114, range 0-200 µg/dL) and Salimetrics® Salivary Secretory IgA indirect enzyme immunoassay (product 1-1602-5, range 12.5-3000 µg/mL). The Salimetrics® Salivary Secretory IgA indirect enzyme immunoassay kit was selected as it had

previously worked well with stool samples (Miren Iturriza Gómara, personal communication). This kit provided a salivary secretory IgA (sIgA) standard with specific sensitivity of 12.5 µg/mL. The expected range of sIgA in saliva (93.2-974.03 µg/mL) is lower than in stool (520-2040 µg/mL). The Salimetrics® standard was tested using the direct sandwich ELISA and the original working standard was tested using the Salimetrics® competitive ELISA to establish assay comparability. The total copro-IgA levels would be measured using the competitive ELISA and RV-specific copro-IgA using the sandwich ELISA together with the original total working standard. The Salimetrics® assay detected stool samples for the dilutions indicated in the protocol and yielded a final standard dynamic range from 12.5-3000 µg/mL, as expected from the manufacturer's specifications. However, the original working standard tested in the Salimetrics® assay did not work due to the differences in protocol. The same was true for the standard from the Salimetrics® kit when tested in the sandwich ELISA for total IgA: they were not comparable.

In summary, the Salimetrics® kit was used to measure total IgA in the range of 12.5-3000 µg/mL and specific anti-RV IgA was measured using the in-house specific sandwich assay and quantifying with the original working standard for total IgA in the range of 2.5 to 0.1 µg/mL, with a LoD of 0.503 OD (no samples with OD>0.503 were plotted). The relative abundance is indicated as a ratio or trend of specific to total IgA.

5.4.4 Total copro-IgA

Total copro-IgA levels in this cohort were detected in the range of 173.5-16,250 µg/g of stool, a wider range than previously observed (Martin, 2000; Scholtens *et al.*, 2008). Although the pattern of total IgA detection varied across the cohort, all infants presented detectable levels throughout the timepoints tested from pre-vaccination to after dose 1 and 2 (Figs. 5.3. A & B). Highest total IgA levels usually followed a decrease in vaccine virus shedding after each vaccine dose (Figs. 3.4. A-D), with levels fluctuating during the rest of the period.

All 12 infants presented detectable total copro-IgA levels after dose 1, with three recruits (25%) presenting highest levels at days 2-9, five recruits (41.6%) at days 12-16 and four recruits (33.3%) at days 20-29, and a median day of highest total IgA of day 14. Although the pattern of total IgA detection varied across the cohort,

all infants presented detectable levels throughout the timepoints tested after dose 1 and 2. Interestingly, individuals E and C presented timepoints with very low total IgA levels immediately after dose 1. After dose 2, seven recruits (58.3%) presented highest IgA at days 30-38, two recruits (16.7%) at days 41-47 and three recruits (25%) at days 54-57. Individual H presented some timepoints with very low total IgA levels after dose 2. All the eight recruits for whom an after-a-year sample was available presented detectable total IgA levels.

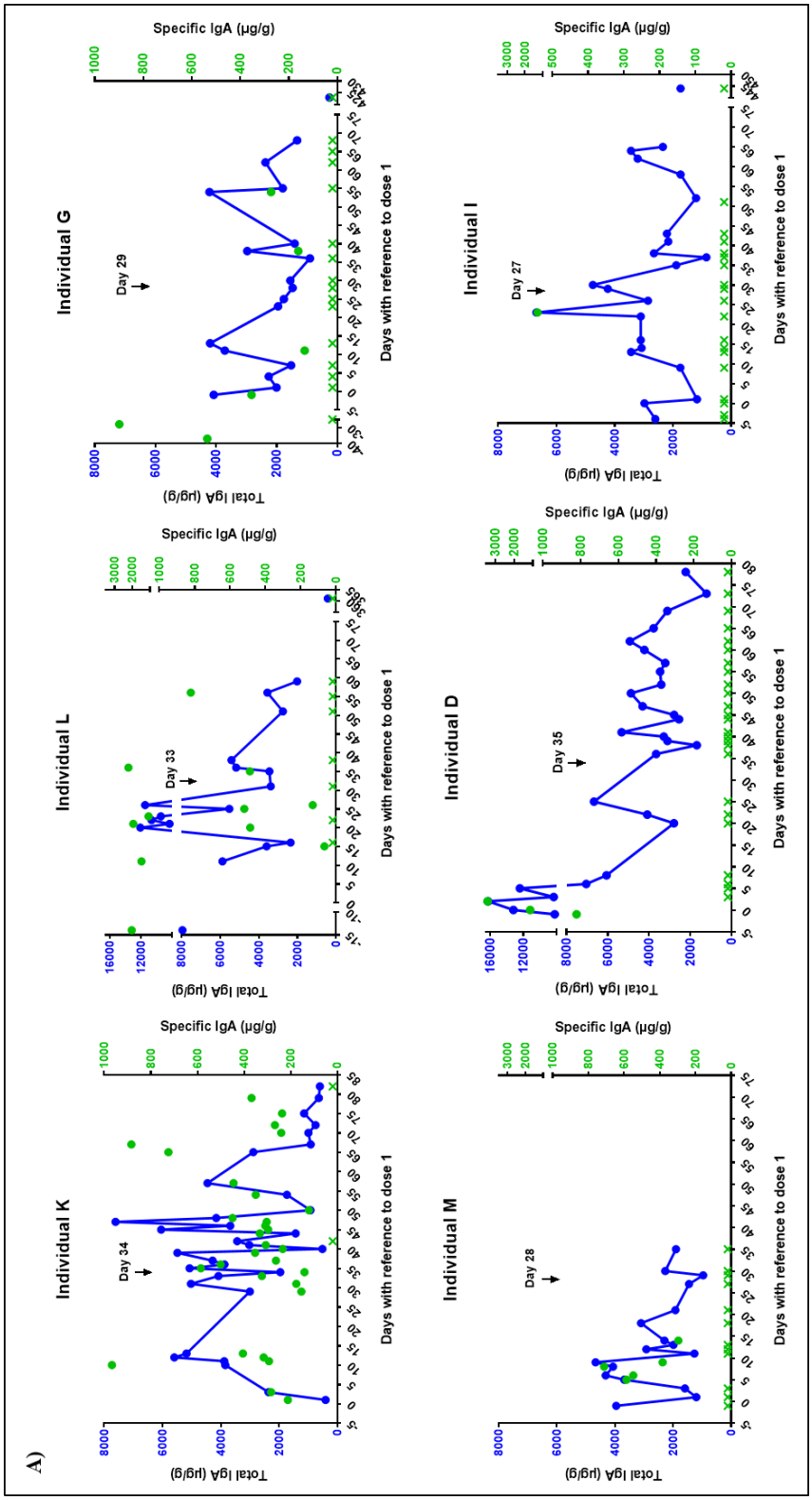

Fig. 5.3. Total and specific anti-RV copro-IgA concentration in A) individuals K, L, G, M, D and I and B) individuals H, B, E, C, J and F. Quantitation of total and specific IgA by indirect competitive and direct ELISA shown in left (limit of detection (LoD)=12.5 µg/mL or µg/g) and right (LoD=0.503 OD) Y axes respectively. The X axis shows days with respect to dose 1. Day 0: Day of dose 1. Black arrow: Day of dose 2. Blue datapoints: Total IgA. Green datapoints: Specific IgA. Timepoints at which samples which were tested but whose levels were below the LoD are shown as crosses.

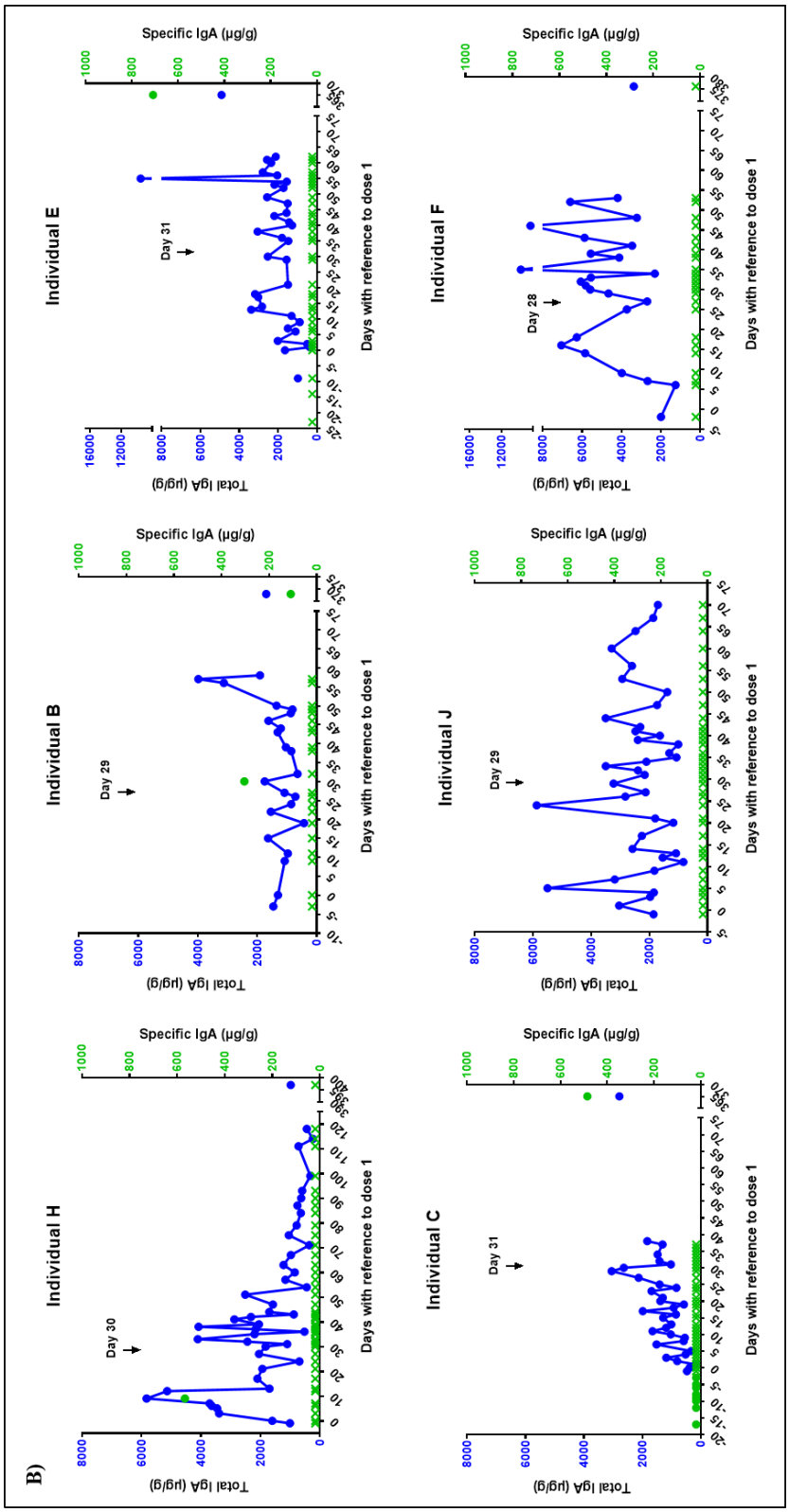
B)
Individual E
Day 31
Individual F
Day 28
Individual B
Day 29
Individual J
Day 29
Individual H
Day 30
Individual C
Day 31
Specific IgA (µg/g)
Total IgA (µg/g)
Days with reference to dose 1

5.4.5 Specific anti-RV copro-IgA

Specific anti-RV copro-IgA levels in this cohort were detected in the range of 67.17-3420.18 µg/g as readout using the total IgA standard (Figs. 5.3. A & B). Only positives based on the limit of detection established in the assay were considered. Furthermore, as a relative trend of specific IgA with respect to total IgA, detectable RV-specific copro-IgA levels ranged from 100 ng of RV-specific IgA per µg of total IgA to nearly 10,000 ng of RV-specific IgA per µg of total IgA (Figs. 5.4. A-C).

At pre-vaccination, three of 11 infants tested (D, G, L) were positive for anti-RV cIgA and all three of them had been breastfed. The other three breastfed infants (E, F, H) were negative for anti-RV cIgA at pre-vaccination. After dose 1, seven of the 12 infants tested (D, G, H, I, K, L, M) were positive for anti-RV cIgA and after dose 2, four of the 12 were positive (B, G, L, K). A year later, three of the 8 infants tested (B, C, E) were positive for anti-RV cIgA. By the period(s) where RV-specific copro-IgA was detected, one infant (D) was positive at pre-vaccination and after dose 1, two infants (G, L) were positive at pre-vaccination and after both doses, one infant (K) was positive after both doses, three infants (H, I, M) were positive only after dose 1, one infant (B) was positive only after dose 2, two infants (C, E) were positive after a year and two infants (F, J) presented no IgA.

Throughout the two to three months after dose 1, two infants presented spread RV- specific copro-IgA levels (K, L), three infants presented three to six curtailed (D, M) or protracted (G) RV- specific copro-IgA levels, another three infants (B, H, I) presented early (individual H), expected (individual I) or late (individual B) copro-IgA detection at a single timepoint, and four infants presented undetectable specific copro-IgA levels (C, E, F, J).

Individuals K and L presented a sustained RV-specific copro-IgA response after dose 1 and dose 2, with undetectable shedding after each dose (Fig. 5.4 A). They were mix-fed and breastfed respectively, and individual L provided no samples around the period of first vaccination (Chapter 2, Table 2.13), and presented highest detectable RV-specific IgA levels after dose 2. One infant (G) presented their highest RV-specific IgA levels at day 28 pre-vaccination (pre-vaccination sample tested) (Fig. 5.4. B). Just before dose 1, RV-specific IgA levels were still high, followed by lower RV-specific IgA levels that increased after dose 2.

Three infants presented their highest RV-specific IgA levels after dose 1 at days 2-10 (D, H, M) (Fig. 5.4 B). Individual D presented high RV-specific IgA levels pre-vaccination and very high levels immediately after dose 1, with undetectable levels thereafter. Individual H presented high RV-specific IgA levels following dose 1 immediately before shedding became undetectable. Individual M presented high (up to 1000 ng RV-specific IgA per 100 µg total IgA) and very high (>1000 ng RV-specific IgA per 100 µg total IgA) RV-specific IgA levels after dose 1. Another infant (I), for whom no shed virus was detectable after dose 1, presented highest RV-specific IgA levels after dose 1 at day 23, a week after viral loads were no longer detected (Fig 5.4 B; overimposed dots on this graph is a coincidence of the axes used across this set of data). Individual B presented their highest RV-specific IgA levels right after dose 2, with undetectable viral loads 25 days after dose 2 (Fig. 5.4 B) and positive RV-specific IgA levels a year after vaccination.

Two infants (C, E) presented their highest RV-specific IgA levels a year after vaccination without any RV-specific IgA levels having been detected previously (Fig 5.4. C). Individual C presented detectable viral loads for the number of samples provided and no shedding a year after vaccination. Individual E, however, presented undetectable viral loads around day 13 after dose 1 without any RV-specific IgA levels detected in that period and low total IgA levels throughout (Fig. 5.3. B), only increasing late after dose 2, when viral loads were undetectable. Another two infants (F, J) presented no RV-specific IgA levels at all, and their vaccine virus shedding was continuous and not controlled for the period of observation (Fig 5.4. C), including an after-a-year sample for individual F. Total IgA levels for these infants were higher than those of individuals C and E (Fig. 5.3. B). Individual F may have controlled infection at a few timepoints later than the last samples provided. Individual J, however, failed to control infection by the end of the vaccination period, since viral loads were not fully controlled after 70 days from dose 1.

Specific anti-RV copro-IgA data showed that children who presented sustained detectable levels of RV-specific copro-IgA shed vaccine virus for short periods of time with viral loads plummeting after peak RV-specific copro-IgA (K, L, H, I). In contrast, the other children who presented undetectable RV-specific copro-IgA had sustained shedding after both doses (C, E, F, J).

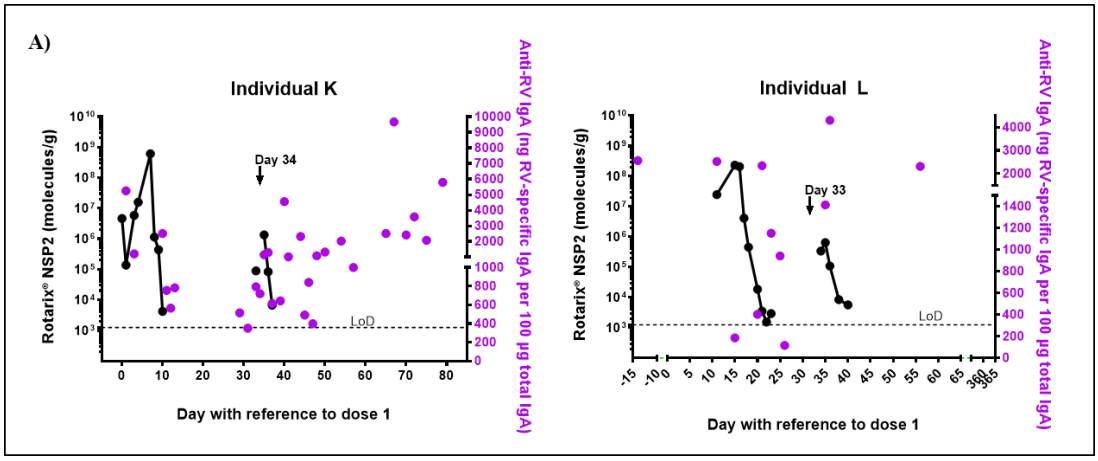

Fig. 5.4. Rotavirus vaccine RNA viral loads and anti-RV copro-IgA trend in A) individuals K and L; B) individuals B, D, G, H, I and M; and C) individuals C, E, F and J. Quantitation of rotavirus vaccine genome copy numbers by RT-qPCR: NSP2 gene copy numbers are shown in the left Y axis, limit of detection (LoD)= 1.25×10^3 copies/g; black dotted line. Trend of specific IgA expressed as ng of RV-specific IgA per 100 µg of total IgA: Shown in the right Y axis (LoD=0.503 OD). The X axis shows days with respect to dose 1. Day 0: Day of dose 1. Black arrow: Day of dose 2. Black dots and lines: Rotavirus RNA (only positives shown). Purple dots: Specific IgA trend (only positives shown). Green dots: Specific IgA (as µg/g of stool).

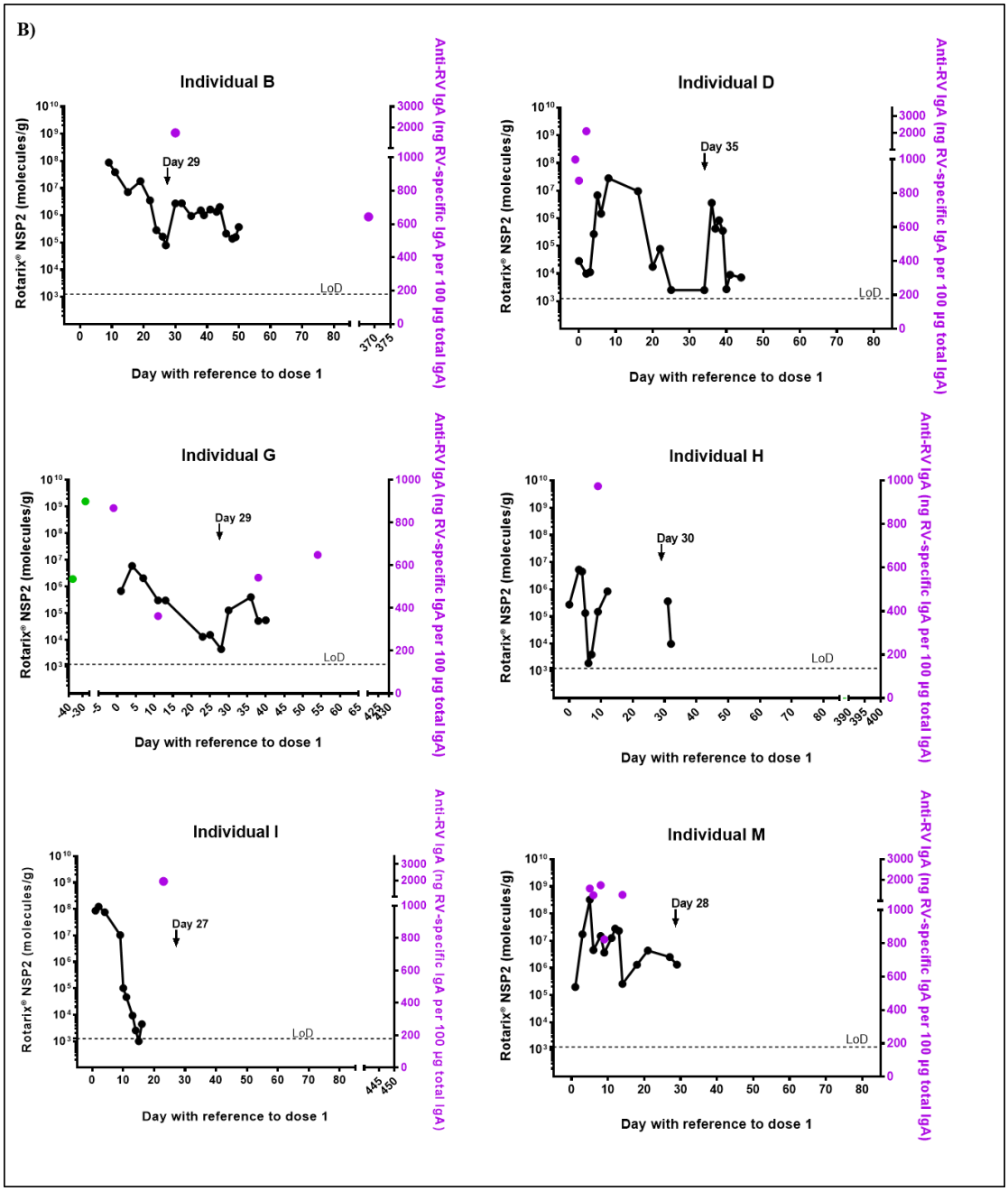
B)
Individual B
Day 29
LoD
Individual D
Day 35
LoD
Individual G
Day 29
LoD
Individual H
Day 30
LoD
Individual I
Day 27
LoD
Individual M
Day 28
LoD
Rotarix® NSP2 (molecules/g)
Anti-RV IgA (ng RV-specific IgA per 100 µg total IgA)
Day with reference to dose 1

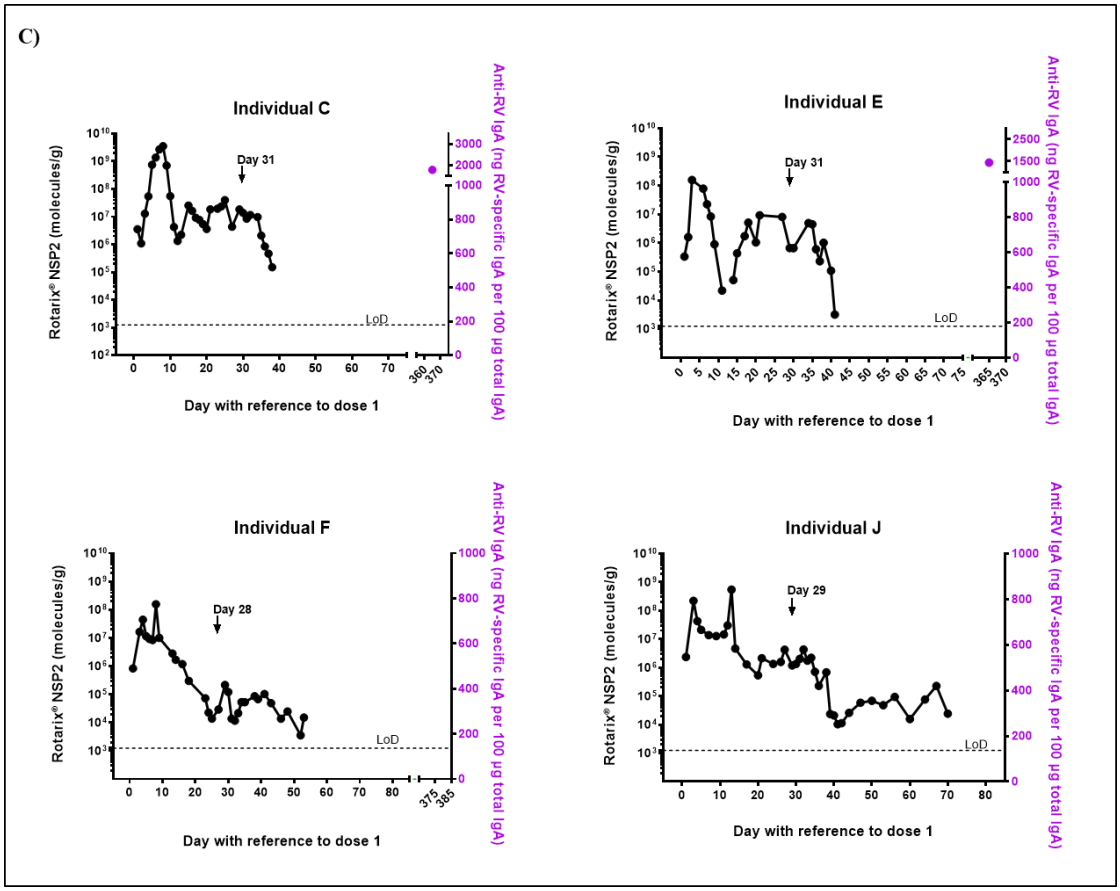

5.4.6 Rotarix® RNA faecal shedding and specific anti-RV copro-IgA

All the infants presented different profiles of shedding with respect to copro-IgA responses. High levels of RV-specific copro-IgA (>900 ng of RV-specific copro-IgA with respect to 100 µg of total copro-IgA) were detected among infants who controlled shedding rapidly (n=3; I, K, L; Fig. 5.4 A & B), as well as among shedders between doses (n=4; B, D, G, M; Fig. 5.4 B) and in the after-a-year sample of those who presented poor response after vaccination (n=2; C, E; Fig. 5.4 C). It was also observed that levels of RV-specific copro-IgA were poor or undetectable after vaccination among infants with high and/or protracted viral loads (n=5; C, D, E, F and J; Figs. 5.4 B & C).

5.4.7 Rotarix® RNA faecal shedding, specific anti-RV copro-IgA and vaccine and vaccine-derived variants in stool

Data on viral shedding and RV-specific copro-IgA was assessed against genetic stability data to identify any variants that may have had an impact on viral replication and the immune response against Rotarix®. Regarding gene segment 4 (encoding the rotavirus spike protein VP4), individuals K and L, who presented highest levels of copro-IgA and rapidly stopped shedding after both doses, presented a vaccine variant at high frequency (leading to amino acid change K368R) that was undetectable or present at lower frequency after dose 2. Individual L also presented a novel variant (leading to amino acid change F167L) at very high frequency after dose 1 that was not detected after dose 2.

Individual D, with undetectable RV-specific IgA from a few days after dose 1 and with protracted shedding until after dose 2 presented the same vaccine variant (resulting in K368R) and another (resulting in N363S) at high frequency after dose 1 but at lower frequency after dose 2. Individuals H, M and I, with a strong immune response and lack of shedding after dose 1 or soon after dose 2, presented the same variant (resulting in K368R) again at high frequency after dose 1 but undetectable after dose 2. Individual M also presented a novel variant (leading to P114T) at high frequency after dose 1.

Individual B, however, with a strong response but shedding between doses, presented that vaccine variant resulting in K368R at high frequency still after dose 2 and another vaccine variant (resulting in M364I) that increased from dose 1 to after dose 2. Individual E appeared to suppress the variant resulting in K368R after dose 2 but a novel variant (resulting in F167L) was present at high frequency after dose 2, suggesting it may have been responsible for the increase in viral loads. Similarly, individual C, with a poor response and high amounts of shedding, presented the variant resulting in K368R and the novel variant resulting in F167L at high frequency after both doses, in addition to two other vaccine variants that decreased (resulting in I388L) and increased (resulting in N363S) and another novel variant (leading to P114T) in common with individual M and detected after dose 2.

Individual F, continuous shedder with undetectable RV-specific copro-IgA response, presented the vaccine variant resulting in K368R and another vaccine

variant leading to I470T decreasing in frequency from after dose 1 to after dose 2 and the previously mentioned novel variant leading to F167L after dose 1, but undetectable after dose 2. Individual J presented the vaccine variant most common among infants (leading to K368R) at very high frequencies after dose 1 and dose 2 plus several other vaccine variants that fluctuated in frequency and were around 50% after dose 2 (leading to Y385H and M364V) and a novel variant that also fluctuated and was around the same frequency late after dose 2 (leading to P114T).

Variants detected in genes 9 and 6 (encoding VP7 and VP6 respectively) were detected early at low and 50% frequency in two infants, and early at low frequency in two infants, respectively. Regarding gene segment 10 (encoding the rotavirus enterotoxin NSP4), only variants resulting in F33S, S38P and I45M were detected at high frequency after the second dose in a continuous shedder and late responder (individuals J and B), in a late responder (individual E) and in continuous shedders (individuals C and J), respectively.

5.5 Discussion

In previous studies, RV-specific copro-IgA did not correlate with infection or illness in challenged adults (Ward *et al.*, 1989). However, copro-conversion had been detected in newborns, infants vaccinated with RotaShield® and adults fed filtrated stool (Bernstein, Ziegler and Ward, 1986; Losonsky *et al.*, 1988; Losonsky and Reymann, 1990). RV-specific copro-IgA was detected in approximately 77% of symptomatic infants (Hoshino *et al.*, 1985; Hjelt *et al.*, 1986; Grimwood *et al.*, 1988). Moreover, RV-specific copro-IgA was found to be predictive of duodenal RV-specific IgA one and four months after infection (although the four month detection may have been due to reinfection) (Grimwood *et al.*, 1988; Coulson *et al.*, 1992) and of neutralizing copro-antibodies in infants (Coulson 1992). Regardless of their shedding status (shedders or non-shedders), infected infants presented a ≥4-fold increase in RV-specific copro-IgA one month after infection (Matson *et al.*, 1993). There was an inverse correlation with infection rate when RV-specific copro-IgA was ≥80 U/mL and with disease when it was ≥20 U/mL (Matson *et al.*, 1993). A high proportion of infants (>90%) were found to be re-infected (Coulson *et al.*, 1992; Matson *et al.*, 1993), with 38% of them showing persistent increases in copro-IgA

levels defined as "plateaus" of neutralising activity (Coulson *et al.*, 1992). These "plateaus" were associated with higher infection although asymptomatic and usually occurred in infants with younger sibling or who attended nursery. The RV-specific copro-IgA response in asymptomatic individuals and non-shedders was found to be intermittent (Coulson *et al.*, 1990, 1992). Coulson and colleagues suggested that frequent infection generated an anamnestic duodenal IgA plateau (Coulson *et al.*, 1992). Fluctuations previously observed were also related to transient diarrhoea (in the presence or absence of shedding) (Grimwood *et al.*, 1988). Later, extended excretion was associated with intermittent RV-specific copro-IgA (Richardson *et al.*, 1998).

The peak of RV-specific copro-IgA was found to be at days 11-21 or between two and four weeks after infection in adults and infants (Grimwood *et al.*, 1988; Bernstein, McNeal, *et al.*, 1989; Richardson *et al.*, 1998). RV-specific copro-IgA declined or was found to be stable from two to seven months after infection (Hjelt *et al.*, 1986; Grimwood *et al.*, 1988; Matson *et al.*, 1993) and was detectable up to 9-12 months after infection and at 13.5-fold higher than baseline in adults (Bernstein, McNeal, *et al.*, 1989). In infants, RV-specific copro-IgA was detectable from up to 18 and 26 months after infection (Coulson *et al.*, 1990, 1992).

RV-specific copro-IgA as a predictor of neutralising copro-antibodies in the duodenum and copro-conversion were considered the most sensitive measure of immune response at the site of infection (Grimwood *et al.*, 1988; Coulson and Masendycz, 1990; Coulson *et al.*, 1990). It was estimated then that there was a 200% increased risk of protection prediction underestimation when using RV-specific serum IgA (Coulson *et al.*, 1990).

In some clinical trials, immunogenicity was measured as stool RV-specific IgA at pre-immunization and days 4, 7, 14 and 21 post-vaccination and resulted in significant increases (Bernstein, 1998). However, in most clinical trials, immunogenicity was measured in terms of RV-specific IgA seroconversion after dose 1, at two months and one year after vaccination or similarly, taking into account a titre increase of ≥20 units/mL or ≥4-fold in >60-90% of infants (depending on study settings) after dose 2 (Bernstein, 1998; Vesikari, Karvonen, Korhonen, *et al.*, 2004; Dennehy *et al.*, 2005; Phua *et al.*, 2005; Salinas *et al.*, 2005; Ruiz-Palacios *et al.*, 2007). This may be due to the detection consistency of RV-specific serum IgA at

days pre-vaccination, 14 and 21 post-vaccination than RV-specific copro-IgA. Moreover, until 2015, no other specimens but serum had been identified as correlates of protection or considered in regulatory decision-making (Powell *et al.*, 2015). A recent study on IgA response to rotavirus in infants vaccinated with Rotarix® in the UK observed a 50% seroconversion one week after each dose (Parker, 2019). A higher percentage of seroconversion may be detected at the time of peak seroconversion, three to four week after each dose. Efficacy was tested in terms of prevention of RVGE from after the second dose to two weeks, one year or more than a year later compared to placebo group (Dennehy *et al.*, 2005; Phua *et al.*, 2005; Ruiz-Palacios *et al.*, 2007) or weekly when a diarrhoea episode occurred and up to a year after vaccination (Salinas *et al.*, 2005).

Some of the original questions about how long RV-specific copro-IgA persists, if it correlates with protection against infection or RVGE and the titres needed to achieve protection have been answered in the past in natural infections. However, no such studies have been performed on infants vaccinated with Rotarix®, a live-attenuated vaccine that was considered to elicit asymptomatic infection in clinical trials. This is the first study to assess longitudinally and in a nearly exhaustive and comprehensive manner the levels of RV-specific copro-IgA in infants vaccinated with Rotarix® within the first two to three months after vaccination (as well as after a year since dose 1, where sample available) to assess the immune response at the site of infection.

In all 12 infants studied in this cohort, total copro-IgA was detected in a pattern of fluctuating levels, with total IgA coinciding with the viral shedding profile as amounts of total IgA were high when viral loads appeared undetectable in all infants overall. The RV-specific IgA response, however, did not present a clear correspondence or correlation. In some infants (individuals I, H, M), dose 1 appeared to be enough to generate a response that would eventually result in viral elimination from stool. In the profile of individual H, although no RV-specific IgA levels were detected after dose 2, shedding rapidly stopped (Chapter 3, Fig. 3.4 B), suggesting immunity generated after dose 1 was enough to impair lasting replication of the vaccine virus. For individual M, the high and very high RV-specific IgA levels after dose 1 signified a strong or very strong immune response that was potentially enough to eliminate viral shedding after dose 2. In the case of individual I, it appears that

immunity generated after dose 1 was sufficient to impair shedding after dose 2. Similarly, in individual D, a strong specific copro-IgA response after dose 1 appeared enough to eventually eliminate virus in stool. It appears as if maternal IgA from breastfeeding did not interfere with infection and replication, and no strong immune response was generated afterwards as infection lasted from dose 1 through to dose 2 and beyond. However, shedding data, despite being protracted after dose 1, indicated shedding decrease to undetectable levels after dose 2 (Chapter 3, Fig. 3.4 C). Hence, it is possible that RV-specific IgA levels were below the assay's limit of detection or that sample storage might have caused non uniform degradation across samples.

Interestingly, in those infants who presented a sustained and upward trend of RV-specific IgA response throughout the vaccination period (individuals K, L, G), dose 2 appeared to exert a booster effect as expected, allowing fast elimination of vaccine virus. If individual L experienced any illness, it did not appear to impair replication of vaccine virus and specific local immune response to it. In individual G's profile, although maternal IgA might have partly neutralised vaccine virus, it appears as if this infant was infected and Rotarix® replicated after dose 1 and dose 2, generating an immune response that allowed detectable levels after dose 1 and increased levels after dose 2, with an overall good immune response. By contrast, in another infant, dose 2 appeared necessary to generate a strong specific copro-IgA response (individual B). Although shedding increased from late after dose 1 to immediately after dose 2, it appears as if immunity after dose 2 was required to stop shedding after dose 2. Their detectable RV-specific IgA levels one year after vaccination suggested that if they came across a WT rotavirus there was no shedding and a specific response was mounted.

In two infants (individuals C, E), although the two doses did not appear to eliminate shedding or to generate a strong immune response, infants were protected against rotavirus infection in the long-term (a year later). In the case of individual C, although the number of samples provided were not enough to draw a firm conclusion, the clear downward trend in viral loads suggests that eventually control of infection after dose 2 would have been observed if sample collection had continued. A very high specific response was detected a year later in the absence of shedding, suggesting immunity against rotavirus was elicited after vaccination,

probably at levels below the assay's limit of detection during the period studied and/or at higher levels after collection stopped. For individual E, It is possible that a vaccine-derived variant arose around day 13 (such as that leading to amino acid change F167L; Chapter 4) and was responsible for the continued shedding during the latest days after dose 1 and before dose 2, with dose 2 acting as a booster that helped eliminate shedding. Their (individual E) low total IgA levels suggested RV-specific IgA levels may have been low and undetectable for the two-month period after vaccinations. Total IgA was only high after viral loads were undetectable and although no RV-specific IgA was detected then, it may have been low but enough to have stopped viral replication. The after-a-year sample being positive and high for RV-specific IgA levels in the absence of shedding suggests this individual acquired immunity against rotavirus after vaccination. This may be due to recovery from a potential IgA deficiency, to a subclinical recent re-infection stimulating their response or to the development of an immune response following continuous replication of vaccine virus at low levels (below the limit of detection of the assay).

In another two infants (F, J), however, vaccination clearly did not prevent long-term shedding nor generate a strong immune response in the first months after vaccination. The continuous and slowly decreasing shedding suggested there may have been an underlying immunodeficiency that prevented rapid clearing of the virus in stool. If they generated an immune response, they may be late responders and vaccine and vaccine-derived variants at high frequency throughout their vaccination periods may have influenced the delay in mounting an immune response (Chapter 4). They may also have controlled the disease by compensation mechanisms such as IgG (Istrate *et al.*, 2008), of slower generation than IgA.

The small number of individuals and inconsistent positive timepoints for RV-specific IgA in this cohort did not allow the comparison of RV-specific IgA levels in breastfed (n=6) versus mixed-fed (n=5) infants from a population point of view. Individuals who presented detectable strong and sustained RV-specific IgA responses (K, L) were mixed-fed and breastfed respectively. Similarly, those who presented strong responses (individuals B, G, H, I and M) were both mixed-fed and breastfed, similar to those individuals who presented poor or undetectable responses (D, E, F and J). The only formula-fed infant (individual C) also presented a poor immune response throughout the two-month period after vaccination.

Although RV-specific copro-IgA and shedding levels were different throughout the cohort, it was clear that a RV-specific response was present at detectable levels when shedding was undetectable and vice versa, undetectable RV-specific copro-IgA levels corresponded to lasting shedding. In early studies, although symptomatic infection was associated with lower RV-specific copro-IgA levels, it was found to be unrelated to viral shedding by electron microscopy or ELISA (Coulson *et al.*, 1992). We have considered these infants asymptomatic, although they may have experienced diarrhoea where a dip in viral load occurred, and it did not appear that low viral loads generated low IgA, since all infants presented high viral loads at some point after vaccination. Moreover, although detectable RV-specific copro-IgA before dose 1 in some infants appeared to be of maternal breastmilk origin (individuals G, D) and may have had an impact on the infants' mucosal IgA responses, breastfeeding did not appear to prevent vaccine virus shedding or influence the timepoints or amounts of RV-specific IgA detection, unlike previously reported in a larger cohort (Bautista-Marquez *et al.*, 2016).

Individuals who could eliminate shedding and presented a strong response also presented fewer variants and at lower frequency than those who shed continuously and presented an undetectable or poor immune response. These results suggested the local IgA response of infants with sustained shedding and poor or absent RV-specific copro-IgA levels was not fast enough to prevent the vaccine virus from reaching the replication stage at which variants have become transiently dominant or fixed.

These results illustrate the differences in immunogenicity at the level of RV-specific copro-IgA generated by the vaccine in different infants and suggest that, except in those with a poor or delayed immune response, Rotarix® generates a mucosal response sufficient to elicit a fast and effective response in the long-term (within the two-month vaccination period and a year later), in some cases already after one dose. No comments can be made regarding protection against severe diarrhoea as no data was provided on health status in the first months after vaccination or a year later. However, since Rotarix® is known to have a high protective efficacy against severe RVGE in developed settings, it appears that most of these infants (excluding the continuous shedders without information on the after-a-year response) would be protected against rotavirus diarrhoea. The continuous

shedders with low total IgA and low or absent RV-specific IgA may be protected through compensation mechanisms by IgG (Istrate *et al.*, 2008). Multiple intestinal host factors may be responsible for these differences in RV-specific copro-IgA fluctuating patterns.

The horizontal transmission of these vaccine viruses from the infants who eliminated shedding and presented a RV-specific copro-IgA response would likely contribute to herd immunity in the general population. However, transmission of variants that provide an advantage to infection, replication, pathogenicity, virulence or immune escape, mostly present and/or maintained at high frequency in continuous shedders, may pose a risk of vaccine-derived gastroenteritis if transmitted to susceptible contacts.

Despite the lack of direct quantitative comparability between total and RV-specific IgA, the relative proportion was maintained and indicated the trends in poor or strong RV-specific copro-IgA responses in this cohort. The generation of a RV-specific IgA standard (non-existent at present) would enable absolute quantification and comparison across laboratories. Moreover, due the nature of faecal samples regarding storage (and hence protein degradation) and low homogeneity, together with the variable amounts of true RV-specific IgA, positive results were detected at differing timepoints across infants. This intrinsic variation and inconsistency of detection would complicate the establishment of copro-IgA as an alternative correlate of protection to serum IgA. The identification of key predictive timepoints and standardised titre cut-off would contribute to further understanding peak time of rotavirus incidence and hence vaccine failure and improvement of vaccine scheduling across populations in different settings (Bennett *et al.*, 2017), as well as serve as an immunogenicity measure in future trials for next generation live-attenuated or non-replicative rotavirus vaccines.

This study is the first of its kind and has contributed to the knowledge about mucosal immunity against rotavirus in vaccine recipients, with a novel focus relating data on the early RV-specific copro-IgA response and viral shedding. The results confirm the generation of immunity against rotavirus in immunocompetent infants after two vaccine doses and provide finer detail on the different shedding profiles and the variety of immune responses. Faecal collection has proven to yield useful data

showing that detection of RV-specific IgA appears to be associated with elimination of shedding at an individual level.

Chapter 6: Conclusions

The overall findings in this thesis assessing vaccine virus shedding and genetic stability as well as RV-specific copro-IgA levels in this cohort constitute a novel and unique set of data that has contributed to a better understanding of the individual responses to vaccination and of vaccine virus evolution during replication in the host. The research implications of these results as well future directions are discussed here.

The aim of the work presented in this thesis was to assess the genetic stability of Rotarix® vaccine virus following replication in vaccinees in relation to their faecal viral loads and RV-specific IgA response. Previous studies have focused on minimal and cross-sectional timepoints to assess RV vaccine shedding and copro-conversion (Bernstein, 1998; Vesikari, Karvonen, Korhonen, *et al.*, 2004; Dennehy *et al.*, 2005; Phua *et al.*, 2005; Salinas *et al.*, 2005; Ruiz-Palacios *et al.*, 2007), so little is known about the dynamics of infection and immunity at the site of infection around the time of vaccinations. Moreover, deemed safe but without knowledge about the mutations that confer attenuation and with a potential to alter its virulence through mutation in the host, Rotarix® has only been characterised for genetic stability by the manufacturer using Sanger sequencing and recently at the NIBSC using NGS (Mitchell, Lui, *et al.*, unpublished). Characterisation of Rotarix® genetic stability in the population of vaccine recipients had not been performed to date. The introduction of Rotarix® in the NIP may generate vaccine variants of high frequency, revertants and novel variants while replicating in vaccinated infants and generating an intestinal IgA response to infection, and those variants may result in vaccine instability in vaccine recipients. The ready access to a cohort of vaccinated infants and a collection of longitudinal samples from before vaccination through to beyond the completion of the vaccine dose schedule generated data that provided a detailed assessment of the three parameters and added considerably to the knowledge of Rotarix® shedding and stability in vaccine recipients as well as to their RV-specific faecal IgA response.

In this detailed longitudinal study of Rotarix® shedding and RV-specific copro-IgA response following vaccination, none of the infants in the cohort appeared to have encountered rotavirus before vaccination as shown by the absence of vaccine

or WT rotavirus shedding —pre-vaccination RV-specific copro-IgA is likely of maternal breastmilk origin—, as expected in a high-income country where rotavirus is not known to circulate all year round (Kapikian *et al.*, 1976; Cook *et al.*, 1990). Overall, high and sustained shedding suggested active replication of Rotarix® in all vaccinees and it was clear that infants with detectable RV-specific copro-IgA levels controlled viral shedding more rapidly. The viral load range in this cohort was lower than in WT infection (Kang *et al.*, 2004; Kaplon *et al.*, 2015), as expected for a live-attenuated vaccine which would replicate asymptomatically, and similar to previously reported viral loads for Rotarix® in stool of vaccine recipients elsewhere (Hsieh *et al.*, 2014; Mijatovic-Rustempasic *et al.*, 2017). The detection of shedding in all or almost all (11/12) infants after dose 1 and dose 2, in contrast to previous studies that detected a higher proportion of infants shedding after dose 1 than after dose 2 (Bernstein, 1998; Vesikari, Karvonen, Korhonen, *et al.*, 2004; Dennehy *et al.*, 2005; Phua *et al.*, 2005; Salinas *et al.*, 2005; Ruiz-Palacios *et al.*, 2007; Hsieh *et al.*, 2014; Mijatovic-Rustempasic *et al.*, 2017), maybe due to a higher vaccine take in this cohort or due to reduced sampling frequency or larger cohorts used in previous studies. In accordance with previous studies, shedding was significantly higher after dose 1 than after dose 2, confirming vaccine take after dose 1 and a booster effect with vaccine take after dose 2. Among the cohort, total IgA was detected at fluctuating levels corresponding to shedding profiles, with high levels when viral loads were undetectable and vice versa, coinciding with shedding control. The granularity of this study allowed further detail regarding peak shedding, detecting two windows of peak shedding time: one during the first week and another one during the second week after dose 1, with most of the infants presenting early peak shedding also controlling shedding earlier than those with peak shedding during the second week. Although commencement of shedding was similar to previous reports (Bernstein, 1998; De Vos *et al.*, 2004; Dennehy *et al.*, 2005; Phua *et al.*, 2005; Salinas *et al.*, 2005; Ruiz-Palacios *et al.*, 2007; Hsieh *et al.*, 2014; Mijatovic-Rustempasic *et al.*, 2017; Pollock, 2018), duration was longer in three infants (up to 70 days after dose 1 in one of them), highlighting the valuable data obtained by a longitudinal study of this kind and indicating shedding duration depends on host immune status and other susceptibility factors.

Four distinct profiles of Rotarix® faecal shedding were observed. Those who presented shedding control with high RV-specific copro-IgA after the first dose as well as those who presented an early response with high RV-specific copro-IgA after the first dose, shedding control after dose 1 and low shedding after dose 2 appeared to mount an immune response to the two-dose vaccination regime that was robust enough to control shedding following dose 1 (those with specific IgA at a few timepoints) or with a booster effect by increasing RV-specific copro-IgA following dose 2 (those with specific IgA spread across timepoints). Although the assay to quantify total copro-IgA was not comparable to the assay used for RV-specific copro-IgA quantification, the relation could still be expressed as a trend that showed variable RV-specific copro-IgA in each infant. However, the generation of a rotavirus-specific IgA standard at the NIBSC would allow for harmonisation of assay data. If generated from copro-IgA, stool samples from a large cohort of infected and/or vaccinated infants would be collected weekly (Coulson et al., 1990), prepared as a faecal suspension and purified for anti-VP4/VP7/VP6 using filtration methods or magnetic beads. Units of protection would have to be established in a faecal suspension matrix and would need to be commutable. The generation of such a standard would contribute to better understanding of vaccine failure, comparison of results obtained in different studies and could be used as an immunogenicity measure in future rotavirus vaccine trials.

Regarding the other shedding profiles, late responders did not control shedding between doses and only after dose 2 the catch-up effect of the vaccine appeared to elicit an immune response, in some cases inferred from cessation of shedding as RV-specific copro-IgA was undetectable for most of them following dose 2 or both doses. Most of the infants were early or late responders, as expected in a high-income country, with infants controlling shedding either after dose 1 or immediately after dose 2. The continuous shedders, however, presented a delayed immune response based on a lack of viral load detection in the after-a-year samples after high viral loads in the absence of shedding control or detectable RV-specific copro-IgA following vaccination. The late responders and continuous shedders were previously identified in Malawi at lower proportions, where low shedders were most abundant (Pollock, 2018) and are expected to be a lower proportion in high-income settings. Any vaccinated infants shedding vaccine virus may potentially contribute to

horizontal transmission of Rotarix® vaccine or vaccine-derived variants, especially the continuous shedders who have vaccine virus replicating for longer. Suspected cases of symptomatic horizontal transmission of Rotarix® have been reported since 2005 but without full confirmation (Chapter 3, Discussion) and a few cases of asymptomatic transmission leading to indirect protection were reported in the Dominican Republic (Rivera *et al.*, 2011). Profiles of rotavirus vaccine shedding would be better understood if more studies were performed in different populations, potentially shedding light onto the proportions of types of shedders or non-shedders. Studies to clarify the potential for transmission to other strata of the population who are healthy but susceptible or immunocompromised would be unethical. Therefore, retrospective studies when such cases are reported are key. Parental information and awareness on hygiene practices when taking care of an infant vaccinated with a live-attenuated vaccine that is shed in stool should be encouraged to avoid transmission to susceptible contacts.

The differences observed in vaccine uptake and shedding duration in this cohort point towards varying susceptibilities to G1P[8] RV infection and differences in the immune responses within the cohort. No health or genetic data was provided, hence analysis in those respects was not possible. Similar studies in other cohorts in the UK with permission to test secretor status would shed light onto this susceptibility factor in this region, as has been assessed in Nicaragua and Malawi recently (Bucardo *et al.*, 2018; Pollock *et al.*, 2018). Interestingly, in this cohort, breastfeeding did not appear to be an obvious factor influencing shedding duration or RV-specific copro-IgA levels in any of the breastfed infants as opposed to a larger cohort where a reduction in shedding and RV-specific serum IgA was observed in breastfed infants (Bautista-Marquez *et al.*, 2016), probably due to the difference in size and the geography of cohorts, and supporting the hypothesis that breastfeeding does not reduce immunogenicity at an individual level. Another factor believed to be related to rotavirus susceptibility is the microbiome. Correlations between certain genera or between microbiota richness and Rotarix® shedding has been observed recently in India (Parker, Praharaj, *et al.*, 2018). Studying the microbiome (down to genus level) of Rotarix® vaccinees in this small cohort would contribute to better understanding this complex susceptibility factor. Samples from this cohort are

currently in use for such study at the NIBSC as a collaboration with Dr Gregory C. A. Amos in the Bacteriology Department.

A year after first vaccine dose, the fact that none of the infants presented vaccine rotavirus or all-RVA shedding suggested that if they had re-encountered rotavirus, very likely during their first year after vaccination, they were able to clear it rapidly. This was supported by data from those infants who presented detectable RV-specific copro-IgA levels a year after first dose, suggesting that whether they had controlled shedding after the two-dose regime or not, they were protected against rotavirus infection a year later. The limit of detection of the assays may have influenced results for those timepoints where amounts of virus or copro-IgA were very low and were considered negative, potentially impairing detection of low shedding and/or low RV-specific IgA responses.

Regarding these, it remains unclear whether the RV-specific IgA antibodies (anti-VP4, anti-VP7 and anti-VP6) in stool of infants have neutralising capacity and whether human anti-VP6 antibodies in stool of infants are able to block intracellular transcription as it has been reported for recombinant antibodies (Aiyegbo *et al.*, 2013). Anti-VP6 antibodies have also been reported to be protective in mice (Burns *et al.*, 1996; Corthésy *et al.*, 2006; Lappalainen *et al.*, 2014, 2015; Maffey *et al.*, 2016). Testing stool from the infants in this cohort who presented rapid viral load control and high pre-vaccination RV-specific copro-IgA, likely maternal from breastmilk, would be of highest interest to detect any anti-VP6 copro-IgA that may provide protection in humans. Samples from this cohort have been sent to Dr Sarah L. Caddy at the MRC in Cambridge and will be assayed using the two following working systems. On the one hand, electroporation of MA104 or Vero cells with anti-VP6/VP4/VP7 copro-IgA purified from stool (by filtration or using magnetic beads) will be used to test neutralisation of intracellular infection with WT G1P[8]. On the other hand, DLPs and TLPs of WT and vaccine G1P[8] strain will be incubated *in vitro* with anti-VP6 copro-IgA from stool (crude faecal suspension), followed by another incubation with dNTPs and tested by RT-qPCR to study whether transcription pockets would be blocked by these antibodies (Aiyegbo *et al.*, 2013), which could be further assayed to study *in vivo* protection in mice.

The work described in this thesis also aimed to assess the genetic stability of a rotavirus live-attenuated vaccine in a cohort of vaccine recipients. Whole genome

RNA sequencing may have allowed studying all the rotavirus gene segments in an economic and time-efficient manner. However, in the case of RNA from vaccine recipients in this cohort, low viral loads ($\leq 10^6$ viral copies/g) did not allow such approach (Appendix II). Another approach using segment-specific RT-PCR prior to DNA library preparation was used instead. Due to limited extraction volumes, amplification was only possible from four segments (Appendix II, section 8.2.1.2). Characterisation of gene segments encoding VP4, VP7, VP6 and NSP4 was prioritised as these viral proteins are involved in viral entry, immunogenicity and virulence. Next generation sequencing of Rotarix® genes encoding VP4, VP7, VP6 and NSP4 generated an extensive set of data and common SNPs were selected for analysis. However, SNPs particular to each infant could be investigated further.

At key timepoints of Rotarix® shedding, variants previously detected at low frequency in vaccine material (Mitchell, Lui, *et al.*, unpublished) were detected at high frequency in stool, some becoming transiently dominant or fixed by the latest timepoints, suggesting low level SNPs in cell culture adaptation of the Rotarix® vaccine candidate were selected *in vivo* in the immunised host. Other variants arose as a result of Rotarix® replication in vaccine recipients, some increasing to high frequencies by the end of the period observed. From the changes identified in the VP7 and VP4 encoding genes affecting receptor binding, trypsin cleavage, membrane fusion and neutralisation (the latter potentially enabling immune escape), the consistency and high frequency of a VP4 vaccine variant revertant to wild type that may enhance *in vivo* replication and of two VP4 vaccine-derived variants with immunodominant potential emphasised the relevance of the spike protein in infection and immune selection, despite the possibility of mutations being a result of mutational robustness and maintenance of fitness in the quasispecies. The synonymous mutation identified in VP6 highlighted the importance of its structural conservation *in vivo*. Moreover, mutations identified in the NSP4 encoding gene highlighted the importance of this protein in *in vivo* infection.

The data in this study suggested that some mutations generated during vaccine manufacture were re-selected *in vivo* if their adaptation resulted in a replication advantage, and other appeared to arise as a result of adaptation in the host. Although the vaccine virus appeared stable in the cohort with very few consistent and high-frequency mutations, changes that appeared fixed by the end of

the vaccination period suggested that Rotarix® may acquire lasting changes while replicating in some susceptible infants. While vaccine shedding and transmission may result in herd immunity of other individuals in contact with vaccine recipients, changes detected at the end of the vaccination period, as those observed in some continuous shedders, if transmitted horizontally to susceptible healthy individuals or to immunocompromised contacts, may contribute to vaccine derived RVGE. The mutations that increased in frequency over the vaccination period and those detected at very high frequency by the end of the vaccination period were identified in profiles where virus shedding had not ceased after dose 1, which corresponded with infants with low RV-specific copro-IgA levels. This data suggested that those infants who cannot control viral replication fast enough develop a weak RV-specific duodenal IgA response and are more prone to shed variants with pathogenic potential since they had a longer window of time to evolve within the host and become transiently dominant or fixed. In contrast, most infants exhibited a strong RV-specific copro-IgA response and controlled shedding, and thus appeared less likely to transmit vaccine or vaccine-derived variants and more likely to be protected later. Although late responders and continuous shedders presented variants at high frequency by the end of the vaccination period tested, the number of SNPs did not increase with time in infants who controlled shedding early. It appeared that attenuation in the infant cohort of asymptomatic shedders and Rotarix® genetic stability were maintained, suggesting this rotavirus vaccine is safe and unlikely to become pathogenic in vaccine recipients, as has been reported extensively for the live attenuated oral poliovirus vaccine (Cann *et al.*, 1984; Minor, 1993; Chumakov, 1999; Kew *et al.*, 2005; Burns *et al.*, 2014; Famulare *et al.*, 2016) and less so for others: e.g. HIV-1, mumps or varicella zoster virus vaccines (Berkhout *et al.*, 1999; Morfopoulou *et al.*, 2017; Willis *et al.*, 2017).

A relevant perspective to address the biological relevance of the genetic variants identified in vaccinees and their potential for horizontal transmission would be to assess and quantify any infectious vaccine-derived rotavirus in stool of vaccine recipients. For this, one approach would consist of performing nuclease digestion to destroy any non-encapsidated viral RNA, followed by RT and qPCR after viral RNA extraction. Another approach would consist of inoculating susceptible cell lines to recover infectious virus. Although technically challenging due to stool containing

high bacterial loads and likely other infectious viruses, these methods are used to recover enteroviruses such as poliovirus from stool samples and sewage (Majumdar *et al.*, 2018). The recovery of infectious rotavirus would shed light on the viability of the identified mutations as well as providing information about reversion when reintroduced in cell culture.

Following the identification of SNP loci and their corresponding amino acid changes in Rotarix® shed in stool of vaccine recipients, a reverse genetics system would be necessary to define the phenotype of these changes individually or in combination (Chapter 4, concluding remarks). This work could be performed in collaboration with Dr Gabriel I. Parra at the FDA, who has a working reverse genetics system kindly available (Dr Nicola J. Rose, personal communication). After generation of these engineered viruses as previously described and reviewed (Desselberger, 2017b; Kanai *et al.*, 2017), an animal model or human intestinal enteroids would be an appropriate system to test their host-restriction (effect of secretor status, cell differentiation stages, etc.), pathogenicity, virulence, attenuation or immunogenicity (Saxena *et al.*, 2016). Further studying whether specific sequence changes in the vaccine virus may elicit a stronger or weaker local IgA response would require a large sample size and the use of an animal or gut model. If the impact of the changes identified in Chapter 4 is elucidated, they could be used in the generation of a novel rotavirus live attenuated vaccine, as seen before for live rabies vaccine using one attenuating mutation (Nakagawa *et al.*, 2017) or tried unsuccessfully with stabilising mutations for oral poliovirus vaccines (Macadam *et al.*, 2006).

Apart from the effect in genetic variation of a live attenuated vaccine after introduction in infants, studying the effect of vaccine introduction in the environment would shed light onto emerging strains, as new types might appear that avoid immunity directed at the vaccine virus. Differences in circulating RV strains after vaccine introduction have been reported, with little evidence of this being caused by selective pressure (Leshem *et al.*, 2014; Markkula *et al.*, 2017). An increase in G2P[4] after vaccine introduction in countries who used Rotarix® has been reported, although G1P[8] was also a prevalent strain (Leshem *et al.*, 2014). Similarly, in countries that introduced RotaTeq® (containing G2), G1P[8] and G2P[4] were also prevalent, with G1P[8] slightly more prevalent (Leshem *et al.*, 2014). In countries

with little rotavirus vaccination, G2P[4] was also a predominant strain in recent years (Leshem *et al.*, 2014). In more recent studies in Australia, in areas where Rotarix® was introduced there was a shift in strains detected in RVGE hospitalised infants towards previous or novel circulating types (G3, G9, G12) which were also detected in countries with different levels of coverage (Roczo-Farkas *et al.*, 2018). Taken together, these differences may be due to natural variation during the seasons, to vaccine-induced immune pressure or to low effectiveness cross-protecting against certain strains.

An added perspective to this project would aim to characterise the circulating vaccine and WT RV strains using environmental sewage samples from before and after implementation of the immunisation programme, from across the UK. A collection of already concentrated sewage samples and unconcentrated raw sewage are available from the poliovirus group at the NIBSC (Appendix IV, Table 8.4.1). The concentrated sewage samples would be used to extract nucleic acids as described in Chapter 2 (Roche kit adapted method) and run VP6-pan-rotavirus qPCRs for samples before the introduction of rotavirus vaccination in the UK (available from 2004 and 2011). Samples from after vaccine introduction (available from 2015 and 2016) would be used to run the NSP2-vaccine-specific qPCR to quantify vaccine virus circulating into the environment. In order to assess whether the population differs across time periods, standard PCR typing would be performed with specific primers for G1-G4, G8, G9, G10 and G12 types; and P[4], P[6] and P[8] types, as well as RV-specific NGS using similar methods to those employed in this thesis. Raw sewage would be spiked with known amounts of Rotarix® to establish the limit of detection for qPCR as well as for genotyping and sequencing. In order to retrieve RV viral particles from sewage, a capture assay consisting of magnetic beads coated with protein G and anti-rotavirus-VP6 antibody would be performed. This (unpublished) protocol was kindly made available by Dr Khuzwayo C. Jere and Prof Miren Iturriza Gómara, University of Liverpool and would be used to quantify live rotavirus in sewage.

Finally, regarding the adventitious virus contained in Rotarix®, PCV1, transient passage through the gastrointestinal tract of vaccinated infants without replication was evidenced by the low viral loads detected briefly and at lower amounts than in vaccine material after each dose, similarly to a recent report in the

USA (Mijatovic-Rustempasic *et al.*, 2017). Following PCV1 viral load testing in this small cohort, sequencing of PCV1 DNA in stool from vaccine recipients was also performed at the NIBSC (Mitchell, Botas-Perez, *et al.*, unpublished) and it will inform on whether any sequence changes arose throughout the brief period of virus passing through the gut of vaccinated infants. Regarding any potential infectivity of PCV1, PCV1 from Rotarix® or from stool of vaccinees would be used in a range of cell lines to test any productive infection. Vaccine-unrelated purified PCV1 and animal cells would be used as controls for known productive infection: African green monkey kidney (WHO Vero cells; interferon-deficient (Desmyter, Melnick and Rawls, 1968; Chew *et al.*, 2009)), porcine kidney (PK-15 cells; and reported to support PCV1 replication (McClenahan, Krause and Uhlenhaut, 2011)) and swine testis (ST cells; reported to support PCV1 replication (McClenahan, Krause and Uhlenhaut, 2011)). Viral loads would be measured in the previous cell lines and potential infectivity assessed. Materials are available at the NIBSC to perform these studies.

In summary, this is the first study to have quantified in detail the longitudinal shedding of Rotarix® in vaccine recipients, as well as to assess the genetic stability of a rotavirus live-attenuated vaccine in vaccinees and to measure their RV-specific copro-IgA response. It has contributed to a more granular understanding of rotavirus replication defining clear shedding profiles, identifying shedding control in infants with detectable RV-specific copro-IgA response and a higher number of vaccine and vaccine-derived variants in infants with shedding of long duration and an absent or weak RV-specific copro-IgA response. This study has identified relevant regions in VP4, VP7 and NSP4 prone to variation in infants, as well as a region in VP6 key for structural conservation. Overall, Rotarix® appeared to be stable within the cohort of vaccinees, eliciting a RV-specific copro-IgA response, controlling shedding following replication and decreasing frequency of vaccine and vaccine-derived variants by the end of the vaccination period. This study has contributed to laying the groundwork for future studies to define shedding profiles in different populations of vaccinees, to pinpoint the role and RV-specific copro-IgA antibody types, to elucidate the phenotype of the vaccine and novel variants identified in vaccinated infants and to characterise the attenuating mutations in Rotarix®.

References

Abbas, A. M. A. and Denton, M. D. (1987) 'An outbreak of rotavirus infection in a geriatric hospital', *Journal of Hospital Infection*, 9(1), pp. 76–80.

Abeid, K. A. *et al.* (2016) 'Monovalent Rotavirus Vaccine Effectiveness and Impact on Rotavirus Hospitalizations in Zanzibar, Tanzania: Data From the First 3 Years After Introduction', *Journal of Infectious Diseases*, 215(2), pp. 183–191.

Abid, I. *et al.* (2007) 'Detection and characterization of human group C rotavirus in the pediatric population of Barcelona, Spain', *Journal of Clinical Virology*, 38(1), pp. 78–82.

Abou-Nader, A. J. *et al.* (2018) 'Global rotavirus vaccine introductions and coverage: 2006–2016', *Human Vaccines and Immunotherapeutics*, 14(9), pp. 2281–2296.

Adams, W. R. and Kraft, L. M. (1963) 'Epizootic diarrhea of infant mice: indentification of the etiologic agent', *Science*, 141(3578), pp. 359–60.

Affranchino, J. L. and González, S. A. (1997) 'Deletion mapping of functional domains in the rotavirus capsid protein VP6', *Journal of General Virology*, 78(8), pp. 1949–1955.

Aggarwal, R., Sentz, J. and Miller, M. A. (2007) 'Role of zinc administration in prevention of childhood diarrhea and respiratory illnesses: a meta-analysis', *Pediatrics*, 119(6), pp. 1120–1130.

Aiyegbo, M. S. *et al.* (2013) 'Human rotavirus VP6-specific antibodies mediate intracellular neutralization by binding to a quaternary structure in the transcriptional pore.', *PloS one*, 8(5), p. e61101.

Aiyegbo, M. S. *et al.* (2014) 'Differential accessibility of a rotavirus VP6 epitope in trimers comprising type I, II, or III channels as revealed by binding of a human rotavirus VP6-specific antibody.', *Journal of Virology*, 88(1), pp. 469–476.

Alfajaro, M. M. and Cho, K. O. (2014) 'Evidences and consequences of extra-intestinal spread of rotaviruses in humans and animals', *Virus Disease*, 25(2), pp. 186–194.

Ali, A. *et al.* (2015) 'Impact of withholding breastfeeding at the time of vaccination on the immunogenicity of oral rotavirus vaccine - A randomized trial', *PLoS one*, 10(6), pp. 1–12.

Allan, G. *et al.* (2012) 'Discovery and evolving history of two genetically related but phenotypically different viruses, porcine circoviruses 1 and 2', *Virus Research*, 164(1–2), pp. 4–9.

Allen, S. J. *et al.* (2011) 'Probiotics for treating acute infectious diarrhoea', *Cochrane Database of Systematic Reviews*, 11, pp. 1–128.

Anderson, E. J. (2008) 'Rotavirus vaccines: viral shedding and risk of transmission', *The Lancet Infectious Diseases*, 8(10), pp. 642–649.

Anderson, E. J. *et al.* (2012) 'Rotavirus in adults requiring hospitalization', *Journal of Infection*, 64(1), pp. 89–95.

Anderson, E. J. and Weber, S. G. (2004) 'Rotavirus infection in adults', *The Lancet. Infectious diseases*, 4(2), pp. 91–9.

Anderson, E. L. *et al.* (1986) 'Evaluation of rhesus rotavirus vaccine (MMU 18006) in infants and young children', *Journal of Infectious Diseases*, 153(5), pp. 823–831.

Andino, R. and Domingo, E. (2015) 'Viral quasispecies', *Virology*, pp. 46–51.

Andrews, S. (2010) *FastQC: a quality control tool for high throughput sequence data.* Available at: http://www.bioinformatics.babraham.ac.uk/projects/fastqc (Accessed: 18 May 2019).

Angel, J. *et al.* (1998) 'Studies of the role for NSP4 in the pathogenesis of homologous murine rotavirus diarrhea', *The Journal of Infectious Diseases*, 177(2), pp. 455–458.

Angel, J., Franco, M. A. and Greenberg, H. B. (2007) 'Rotavirus vaccines: recent developments and future considerations', *Nature Reviews Microbiology*, 5(7), pp. 529–39.

Angel, J., Franco, M. A. and Greenberg, H. B. (2012) 'Rotavirus immune responses and correlates of protection', *Current Opinion in Virology*, 2(4), pp. 419–425.

Angel, J., Steele, A. D. and Franco, M. A. (2014) 'Correlates of protection for rotavirus vaccines: possible alternative trial endpoints, opportunities, and challenges', *Human Vaccines and Immunotherapeutics*, 10(12), pp. 3659–71.

Ansari, S. A., Springthorpe, V. S. and Sattar, S. A. (1991) 'Survival and vehicular spread of human rotaviruses: possible relation to seasonality of outbreaks.', *Reviews of Infectious Diseases*, 13(3), pp. 448–61.

Aoki, S. T. *et al.* (2009) 'Structure of rotavirus outer-layer protein VP7 bound with a neutralizing Fab.', *Science*, 324(5933), pp. 1444–1447.

Appaiahgari, M. B. *et al.* (2014) 'Transplacental rotavirus IgG interferes with immune response to live oral rotavirus vaccine ORV-116E in Indian infants', *Vaccine*, 32(6), pp. 651–656.

Arana, A. *et al.* (2019) 'Molecular epidemiology of G12 rotavirus strains during eight consecutive epidemic seasons in the Basque Country (North of Spain), 2010–2018', *Infection, Genetics and Evolution*, 71, pp. 67–75.

Arias, C. F. *et al.* (1996) 'Trypsin activation pathway of rotavirus infectivity.', *Journal of Virology*, 70(9), pp. 5832–9.

Arnold, M. M. (2016) 'The rotavirus interferon antagonist NSP1: many targets, many questions', *Journal of Virology*, 90(March), p. JVI.03068-15. doi: 10.1128/JVI.03068-15.

Arnold, M. M., Barro, M. and Patton, J. T. (2013) 'Rotavirus NSP1 Mediates Degradation of Interferon Regulatory Factors through Targeting of the Dimerization Domain', *Journal of Virology*, 87(17), pp. 9813–9821.

Arnold, M. M. and Patton, J. T. (2011) 'Diversity of Interferon Antagonist Activities Mediated by NSP1 Proteins of Different Rotavirus Strains', *Journal of Virology*, 85(5), pp. 1970–1979. doi: 10.1128/jvi.01801-10.

Asensi, M. T., Martınez-Costa, C. and Buesa, J. (2006) 'Anti-rotavirus antibodies in human milk: quantification and neutralizing activity', *Journal of Pediatric Gastroenterology and Nutrition*, 42(May), pp. 560–567.

Atchison, C. J. *et al.* (2016) 'Rapid declines in age group-specific rotavirus infection and acute gastroenteritis among vaccinated and unvaccinated individuals within 1 year of rotavirus vaccine introduction in England and Wales', *Journal of Infectious Diseases*, 213(2), pp. 243–249.

Ayala-Breton, C. *et al.* (2009) 'Analysis of the Kinetics of Transcription and Replication of the Rotavirus Genome by RNA Interference', *Journal of Virology*, 83(17), pp. 8819–8831.

Azevedo, M. P. *et al.* (2013) 'Human rotavirus virus-like particle vaccines evaluated in a neonatal gnotobiotic pig model of human rotavirus disease', *Expert Review of Vaccines*, 12(2), pp. 169–181.

Azevedo, M. S. P. *et al.* (2004) 'Magnitude of Serum and Intestinal Antibody Responses Induced by Sequential Replicating and Nonreplicating Rotavirus Vaccines in Gnotobiotic Pigs and Correlation with Protection', *Clinical and Vaccine Immunology*, 11(1), pp. 12–20.

Azim, T. *et al.* (1999) 'Immune response of children who develop persistent diarrhea following rotavirus infection.', *Clinical and Diagnostic Laboratory Immunology*, 6(5), pp. 690–5.

Ball, J. M. *et al.* (1996) 'Age-dependent diarrhea induced by a rotaviral nonstructural glycoprotein.', *Science*, 272(5258), pp. 101–104.

Ballotti, S. and De Martino, M. (2007) 'Rotavirus Infections and Development of Type 1 Diabetes: An Evasive Conundrum', *Journal of Pediatric Gastroenterology and Nutrition*, 45(2), pp. 147–156.

Bányai, K. *et al.* (2017) 'Candidate new rotavirus species in Schreiber's bats, Serbia', *Infection, Genetics and Evolution*, 48, pp. 19–26.

Bar-Zeev, N. *et al.* (2018) 'Impact of monovalent rotavirus vaccine on diarrhoea-associated post-neonatal infant mortality in rural communities in Malawi: a population-based birth cohort study', *The Lancet Global Health*, 6(9), pp. e1036–e1044.

Barbé, L. *et al.* (2018) 'Histo-blood group antigen-binding specificities of human rotaviruses are associated with gastroenteritis but not with in vitro infection', *Nature Scientific Reports*, 8(1), pp. 1–14.

Barman, P. *et al.* (2004) 'Sequencing and sequence analysis of VP7 and NSP5 genes reveal emergence of a new genotype of bovine group B rotaviruses in India.', *Journal of Clinical Microbiology*, 42(6), pp. 2816–8.

Barnes, G. L. and Townley, R. R. (1973) 'Duodenal mucosal damage in 31 infants with gastroenteritis.', *Archives of Disease in Childhood*, 48(5), pp. 343–349.

Barro, M. and Patton, J. T. (2007) 'Rotavirus NSP1 Inhibits Expression of Type I Interferon by Antagonizing the Function of Interferon Regulatory Factors IRF3, IRF5, and IRF7', *Journal of Virology*, 81(9), pp. 4473–4481.

Bautista-Marquez, A. *et al.* (2016) 'Breastfeeding linked to the reduction of both rotavirus shedding and IgA levels after Rotarix® immunization in Mexican infants', *Vaccine*, 34(44), pp. 5284–5289.

Baylis, S. A. *et al.* (2011) 'Analysis of porcine circovirus type 1 detected in Rotarix vaccine.', *Vaccine*, 29(4), pp. 690–7.

Beach, N. M. *et al.* (2011) 'Productive infection of human hepatocellular carcinoma cells by porcine circovirus type 1', *Vaccine*, 29(43), pp. 7303–7306.

Beck, A. S. *et al.* (2018) 'Analysis By Deep Sequencing of Discontinued Neurotropic Yellow Fever Vaccine Strains', *Nature Scientific Reports*, 8(1), pp. 1–12.

Becker-Dreps, S. *et al.* (2015) 'Rotavirus-specific IgG antibodies from mothers' serum may inhibit infant immune responses to the pentavalent rotavirus vaccine', *Pediatric Infectious Disease Journal*, 34(1), pp. 115–116.

Bennett, A. *et al.* (2017) 'Estimating the incidence of rotavirus infection in children from India and Malawi from serial anti-rotavirus IgA titres', *PloS one*, 12(12), pp. 1–14.

Bennett, A. *et al.* (2018) 'Direct and possible indirect effects of vaccination on rotavirus hospitalisations among children in Malawi four years after programmatic introduction', *Vaccine*, 36(47), pp. 7142–7148.

Bennett, A. *et al.* (2019) 'Infrequent transmission of monovalent human rotavirus vaccine virus to household contacts of vaccinated infants in Malawi.', *The Journal of Infectious Diseases*, 11, pp. 1730–1734.

Bennett, A., Bar-Zeev, N. and Cunliffe, N. A. (2016) 'Measuring indirect effects of rotavirus vaccine in low income countries', *Vaccine*. The Authors, 34(37), pp. 4351–4353.

Bentes, G. A. *et al.* (2018) 'Cynomolgus monkeys (Macaca fascicularis) as an experimental infection model for human group a rotavirus', *Viruses*, 10(7), pp. 1–14.

Berkhout, B. *et al.* (1999) 'Genetic instability of live, attenuated human immunodeficiency virus type 1 vaccine strains', *Journal of Virology*, 73(2), pp. 1138–1145.

Bernstein, D. (1998) 'Safety and immunogenicity of live, attenuated human rotavirus vaccine 89-12', *Vaccine*, 16(4), pp. 381–387.

Bernstein, D. I., McNeal, M. M., *et al.* (1989) 'Induction and persistence of local rotavirus antibodies in relation to serum antibodies', *Journal of Medical Virology*, 28(2), pp. 90–95.

Bernstein, D. I., Kacica, M. A., *et al.* (1989) 'Local and systemic antibody response to rotavirus WC3 vaccine in adult volunteers', *Antiviral Research*. Elsevier, 12(5–6), pp. 293–300.

Bernstein, D. I. *et al.* (1990) 'Evaluation of WC3 Rotavirus Vaccine and Correlates of Protection in Healthy Infants', *Journal of Infectious Diseases*, 162(5), pp. 1055–1062.

Bernstein, D. I. *et al.* (1999) 'Efficacy of live, attenuated, human rotavirus vaccine 89-12 in infants: a randomised placebo-controlled trial.', *The Lancet*, 354(9175), pp. 287–290.

Bernstein, D. I., Ziegler, J. M. and Ward, R. L. (1986) 'Rotavirus fecal IgA antibody response in adults challenged with human rotavirus.', *Journal of Medical Virology*, 20(4), pp. 297–304.

Bertolotti-Ciarlet, A. *et al.* (2003) 'Immunogenicity and protective efficacy of rotavirus 2/6-virus-like particles produced by a dual baculovirus expression vector and administered intramuscularly, intranasally, or orally to mice', *Vaccine*, 21(25–26), pp. 3885–3900.

Bhan, M. K. *et al.* (1993) 'Protection Conferred by Neonatal Rotavirus Infection against Subsequent Rotavirus Diarrhea', *Journal of Infectious Diseases*, 168(2), pp. 282–287.

Bhan, M. K. *et al.* (2014) 'Team science and the creation of a novel rotavirus

vaccine in India: A new framework for vaccine development', *The Lancet*, 383(9935), pp. 2180–2183.

Bhandari, N., Rongsen-Chandola, T., Bavdekar, A., John, J., Antony, K., Taneja, S., Goyal, N., Kawade, A., Kang, G., Rathore, S. S., Juvekar, S., Muliyil, J., Arya, A., Shaikh, H., Abraham, V., Vrati, S., Proschan, M., Kohberger, R., Thiry, G., Glass, R., Greenberg, Harry B., *et al.* (2014) 'Efficacy of a monovalent human-bovine (116E) rotavirus vaccine in Indian children in the second year of life', *Vaccine*, 32(S1), pp. 110–116.

Bhandari, N., Rongsen-Chandola, T., Bavdekar, A., John, J., Antony, K., Taneja, S., Goyal, N., Kawade, A., Kang, G., Rathore, S. S., Juvekar, S., Muliyil, J., Arya, A., Shaikh, H., Abraham, V., Vrati, S., Proschan, M., Kohberger, R., Thiry, G., Glass, R., Greenberg, Harry B, *et al.* (2014) 'Efficacy of a monovalent human-bovine (116E) rotavirus vaccine in Indian infants: a randomised, double-blind, placebo-controlled trial.', *The Lancet*, 383(9935), pp. 2136–43.

BharatBiotech (2018) *About ROTAVAC®*, *Bharat Biotech*. Available at: https://bharatbiotech.com/rotavac.html (Accessed: 26 November 2018).

Bialowas, S. *et al.* (2016) 'Rotavirus and serotonin cross-talk in diarrhoea', *PLoS one*, 11(7), pp. 1–25.

Bidzhieva, B. *et al.* (2014) 'Deep sequencing approach for genetic stability evaluation of influenza A viruses', *Journal of Virological Methods*, 199, pp. 68–75.

Bilenko, N. *et al.* (2008) 'Partial breastfeeding protects Bedouin infants from infection and morbidity: prospective cohort study.', *Asia Pacific Journal of Clinical Nutrition*, 17(2), pp. 243–9.

Bines, J. E. *et al.* (2004) 'Acute intussusception in infants and children as an adverse event following immunization: Case definition and guidelines of data collection, analysis, and presentation', *Vaccine*, 22(5–6), pp. 569–574.

Bines, J. E. *et al.* (2015) 'Safety and immunogenicity of RV3-BB human neonatal rotavirus vaccine administered at birth or in infancy: a randomised, double-blind, placebo-controlled trial', *The Lancet Infectious Diseases*, 15(12), pp. 1389–1397.

Bines, J. E. *et al.* (2018) 'Human Neonatal Rotavirus Vaccine (RV3-BB) to Target Rotavirus from Birth', *New England Journal of Medicine*, 378(8), pp. 719–730.

Bishop, R. F. *et al.* (1973) 'Virus particles in epithelial cells of duodenal mucosa from children with acute non-bacterial gastroenteritis.', *The Lancet*, 2(7841), pp. 1281–3.

Bishop, R. F. *et al.* (1983) 'Clinical Immunity after Neonatal Rotavirus Infection', *New England Journal of Medicine*, 309(2), pp. 72–76.

Blackhall, J., Fuentes, A. and Magnusson, G. (1996) 'Genetic stability of a porcine rotavirus RNA segment during repeated plaque isolation', *Virology*, 225(1), pp. 181–190.

Blutt, S. E. *et al.* (2002) 'Early Response to Rotavirus Infection Involves Massive B Cell Activation', *The Journal of Immunology*, 168(11), pp. 5716–5721.

Blutt, S. E. *et al.* (2007) 'Rotavirus antigenemia in children is associated with

viremia.', *PLoS Medicine*, 4(4), p. e121.
Blutt, S. E. *et al.* (2012) 'IgA is important for clearance and critical for protection from rotavirus infection.', *Mucosal Immunology*, 5(6), pp. 712–9.
Bolger, A. M., Lohse, M. and Usadel, B. (2014) 'Trimmomatic: a flexible trimmer for Illumina sequence data', *Bioinformatics*, 30(15), pp. 2114–2120.
Bolivar, R. *et al.* (1978) 'Rotavirus in travelers' diarrhea: study of an adult student population in Mexico', *Journal of Infectious Diseases*, 137(3), pp. 324–327.
Boom, J. *et al.* (2012) 'Symptomatic Infection and Detection of Vaccine and Vaccine- Reassortant Rotavirus Strains in 5 Children: A Case Series', *Journal of Infectious Diseases*, 206(8), pp. 1275–1279.
Boshuizen, J. A. *et al.* (2004) 'Rotavirus Enterotoxin NSP4 Binds to the Extracellular Matrix Proteins Laminin-beta3 and Fibronectin', *Journal of Virology*, 78(18), pp. 10045–10053.
Bowen, M. D. and Payne, D. C. (2012) 'Rotavirus vaccine-derived shedding and viral reassortants', *Expert Review of Vaccines*, 11(11), pp. 1311–1314.
Bowman, G. D. *et al.* (2000) 'Crystal structure of the oligomerization domain of NSP4 from rotavirus reveals a core metal-binding site', *Journal of Molecular Biology*, 304(5), pp. 861–871.
Braeckman, T. *et al.* (2012) 'Effectiveness of rotavirus vaccination in prevention of hospital admissions for rotavirus gastroenteritis among young children in Belgium: Case-control study', *BMJ*, 345(7872), pp. 1–13.
BroadInstitute & GitHub (2018) *Picard Tools*, *Broad Institute, GitHub repository*. Available at: http://broadinstitute.github.io/picard/ (Accessed: 22 November 2018).
Bucardo, F. *et al.* (2018) 'The Lewis A phenotype is a restriction factor for Rotateq and Rotarix vaccine-take in Nicaraguan children', *Nature Scientific Reports*, 8(1), pp. 1–8.
Bucardo, F. *et al.* (2019) 'Histo-blood group antigens and rotavirus vaccine shedding in Nicaraguan infants', *Nature Scientific Reports*, 9(1), p. 10764.
Bull, J. J. (2015) 'Evolutionary reversion of live viral vaccines: Can genetic engineering subdue it?', *Virus Evolution*, 1(1), p. vev005.
Burke, B., Bridger, J. C. and Desselberger, U. (1994) 'Temporal correlation between a single amino acid change in the VP4 of a porcine rotavirus and a marked change in pathogenicity.', *Virology*, 202, pp. 754–759.
Burns, C. C. *et al.* (2014) 'Vaccine-derived polioviruses', *Journal of Infectious Diseases*, 210(Suppl 1), pp. S283–S293.
Burns, J. W. *et al.* (1995) 'Analysis of Homologous Rotavirus Infection in the Mouse Model', *Virology*, 207(1), pp. 143–153.
Burns, J. W. *et al.* (1996) 'Protective effect of rotavirus VP6-specific IgA monoclonal antibodies that lack neutralizing activity.', *Science*, 272(5258), pp. 104–7.
Butz, A. M. *et al.* (1993) 'Prevalence of rotavirus on high-risk fomites in day-care facilities', *Pediatrics*, 92(2), pp. 202–205.
Cacho, N. T. and Lawrence, R. M. (2017) 'Innate immunity and breast milk',

Frontiers in Immunology, 8(584), pp. 1–10.

Candy, D. C. A. (2007) 'Rotavirus Infection: A Systemic Illness?', *PLoS Medicine*, 4(4), p. e117.

Cann, A. *et al.* (1984) 'Reversion to neurovirulence of the live-attenuated Sabin type 3 oral poliovirus vaccine', *Nucleic Acids Research*, 12(20), pp. 7787–92.

Carey, M. E. (2017) *Currently available vaccines and introduction status., Bill and Melinda Gates Foundation. Journalist workshop.* Available at: http://rotacouncil.org/wp-content/uploads/2017/05/Singapore-Slides-Carey-Final.pdf (Accessed: 22 July 2019).

Caulfield, L. E. *et al.* (2004) 'Undernutrition as an underlying cause of child deaths associated with diarrhea, pneumonia, malaria, and measles.', *The American Journal of Clinical Nutrition*, 80(1), pp. 193–8.

CDC (2018) *Rotavirus vaccination: What everyone should know.*, *Centers for Disease Control*. Available at: https://www.cdc.gov/vaccines/vpd/rotavirus/public/index.html (Accessed: 22 November 2018).

Centers for Disease and Control (CDC) (2011) 'Notes From the Field: Outbreaks of Rotavirus Gastroenteritis Among Elderly Adults in Two Retirement Communities — Illinois, 2011', *Morbidity and Mortality Weekly Report*, 60(42), pp. 1456–58.

Centres for Disease Control (CDC) (1999) 'Withdrawal of Rotavirus Vaccine Recommendation', *MMWR. Morbidity and Mortality Weekly Report.*, 48(43), p. 1007.

Chacko, A. R. *et al.* (2012) 'A new pentameric structure of rotavirus NSP4 revealed by molecular replacement', *Acta Crystallographica Section D: Biological Crystallography*, 68(1), pp. 57–61.

Chan, J. *et al.* (2011) 'Maternal antibodies to rotavirus: Could they interfere with live rotavirus vaccines in developing countries?', *Vaccine*. Elsevier Ltd, 29(6), pp. 1242–1247.

Chang, J. T. *et al.* (2010) 'Ovine rotavirus strain LLR-85-based bovine rotavirus candidate vaccines: Construction, characterization and immunogenicity evaluation', *Veterinary Microbiology*, 146(1–2), pp. 35–43.

Chang, K. *et al.* (1999) 'Dual infection of gnotobiotic calves with bovine strains of group A and porcine-like group C rotaviruses influences pathogenesis of the group C rotavirus', *Journal of Virology*, 73(11), pp. 9284–9293.

Changotra, H. and Vij, A. (2017) 'Rotavirus virus- like particles (RV- VLPs) vaccines:An update', *Reviews in Medical Virology*, 27(August), p. e1954.

Chasey, D. and Banks, J. (1986) 'Replication of atypical ovine rotavirus in small intestine and cell culture', *Journal of General Virology*, 67(3), pp. 567–576.

Chasey, D., Bridger, J. and McCrae, M. (1986) 'A New Type of Atypical Rotavirus in Pigs', *Archives of Virology*, 89, pp. 235–243.

Chattha, K. S. *et al.* (2013) 'Probiotics and colostrum/milk differentially affect neonatal humoral immune responses to oral rotavirus vaccine', *Vaccine*, 31(15), pp. 1916–1923.

Chege, G. K. *et al.* (2005) 'Experimental infection of non-human primates

with a human rotavirus isolate', *Vaccine*, 23(12), pp. 1522–1528.

Chen, D. *et al.* (1999) 'Rotavirus open cores catalyze 5'-capping and methylation of exogenous RNA: Evidence that VP3 is a methyltransferase', *Virology*, 265(1), pp. 120–130.

Chen, J. Z. *et al.* (2009) 'Molecular interactions in rotavirus assembly and uncoating seen by high-resolution cryo-EM', *Proceedings of the National Academy of Sciences*, 106(26), pp. 10644–10648.

Chen, M. Y. *et al.* (2017) 'Rotavirus specific maternal antibodies and immune response to RV3-BB neonatal rotavirus vaccine in New Zealand', *Human Vaccines and Immunotherapeutics*, 13(5), pp. 1126–1135.

Chen, S. C. *et al.* (1997) 'Protective immunity induced by rotavirus DNA vaccines', *Vaccine*, 15(8), pp. 899–902.

Cheuvart, B. *et al.* (2014) 'Association of serum anti-rotavirus immunoglobulin A antibody seropositivity and protection against severe rotavirus gastroenteritis', *Human Vaccines & Immunotherapeutics*, 10(2), pp. 505–511.

Chew, T. *et al.* (2009) 'Characterization of the interferon regulatory factor 3-mediated antiviral response in a cell line deficient for IFN production.', *Molecular immunology*, 46(3), pp. 393–9.

Chiba, S. *et al.* (1986) 'Protective effect of naturally acquired homotypic and heterotypic rotavirus antibodies.', *The Lancet*, 2(8504), pp. 417–21.

Chilengi, R. *et al.* (2016) 'Association of maternal immunity with rotavirus vaccine immunogenicity in Zambian Infants', *PLoS one*, 11(3), pp. 1–12.

Ching, P. *et al.* (2000) 'Childhood mortality impact and costs of integrating vitamin A supplementation into immunization campaigns', *American Journal of Public Health*, 90(10), pp. 1526–1529.

Chitambar, S. *et al.* (2011) 'Occurrence of group B rotavirus infections in the outbreaks of acute gastroenteritis from Western India', *Indian Journal of Medical Research*, 134(September), pp. 399–400.

Chizhikov, V. and Patton, J. T. (2000) 'A four-nucleotide translation enhancer in the 3'-terminal consensus sequence of the nonpolyadenylated mRNAs of rotavirus', *RNA*, 6(6), pp. 814–825.

Cho, M.-K. *et al.* (2013) 'Full genomic analysis of a human rotavirus G1P[8] strain isolated in South Korea.', *Journal of Medical Virology*, 85(1), pp. 157–70.

Choi, A. H. *et al.* (1999) 'Antibody-independent protection against rotavirus infection of mice stimulated by intranasal immunization with chimeric VP4 or VP6 protein.', *Journal of Virology*, 73(9), pp. 7574–81.

Chomczynski, P. and Sacchi, N. (1987) 'Single-Step Method of RNA Isolation by Acid Guanidinium Thiocyanate–Phenol–Chloroform Extraction', *Analytical Biochemistry*, 162(1), pp. 156–159.

Chomczynski, P. and Sacchi, N. (2006) 'The single-step method of RNA isolation by acid guanidinium thiocyanate-phenol-chloroform extraction: Twenty-something years on.', *Nature Protocols*, 1(2), pp. 581–585.

Chow, C. M., Leung, A. K. and Hon, K. L. (2010) 'Acute gastroenteritis: from guidelines to real life.', *Clinical and Experimental Gastroenterology*, 3, pp. 97–112.

Chumakov, K. M. (1999) ‘Molecular consistency monitoring of oral poliovirus vaccine and other live viral vaccines.’, *Developments in Biological Standardization*, 100, pp. 67–74.

Ciarlet, M. and Schödel, F. (2009) ‘Development of a rotavirus vaccine: Clinical safety, immunogenicity, and efficacy of the pentavalent rotavirus vaccine, RotaTeq®’, *Vaccine*, 27(Supplement 6), pp. 72–81.

Clark, H. F. *et al.* (1986) ‘Immune response of infants and children to low-passage bovine rotavirus (strain WC3).’, *American Journal of Diseases of Children*, 140(4), pp. 350–6.

Clark, H. F. *et al.* (1988) ‘Protective effect of WC3 vaccine against rotavirus diarrhea in infants during a predominantly serotype 1 rotavirus season’, *Journal of Infectious Diseases*, 158(3), pp. 570–587.

Clark, H. F. *et al.* (2004) ‘Safety, efficacy, and immunogenicity of a live, quadrivalent human-bovine reassortant rotavirus vaccine in healthy infants’, *The Journal of Pediatrics*, 144(2), pp. 184–190.

Clark, H. F. *et al.* (2006) ‘The New Pentavalent Rotavirus Vaccine Composed of Bovine(Strain WC3)-Human Rotavirus Reassortants’, *The Pediatric Infectious Disease Journal*, 25(7), pp. 577–583.

Clark, H. F., Borian, F. E. and Plotkin, S. A. (1990) ‘Immune protection of infants against rotavirus gastroenteritis by a serotype 1 reassortant of bovine rotavirus WC3’, *Journal of Infectious Diseases*, 161(6), pp. 1099–1104.

Clarke, E. and Desselberger, U. (2015) ‘Correlates of protection against human rotavirus disease and the factors influencing protection in low-income settings’, *Mucosal Immunology*, 8(1), pp. 1–17.

Clements-Mann, M. Lou *et al.* (1999) ‘Safety and immunogenicity of live attenuated human-bovine (UK) reassortant rotavirus vaccines with VP7-specificity for serotypes 1, 2, 3 or 4 in adults, children and infants’, *Vaccine*, 17(20–21), pp. 2715–2725.

Clements-Mann, M. Lou *et al.* (2001) ‘Safety and immunogenicity of live attenuated quadrivalent human-bovine (UK) reassortant rotavirus vaccine administered with childhood vaccines to infants’, *Vaccine*, 19(32), pp. 4676–4684.

Clinicaltrials.gov (2012) *Safety and Immunogenicity Assessment of Rotavin-M1 in Vietnamese Children (Rotavin-M1)., NIH. US National Library of Medicine.* Available at: https://clinicaltrials.gov/ct2/show/NCT01502969 (Accessed: 22 November 2018).

Clinicaltrials.gov (2013) *A Phase 1 Dose Escalation Study to Examine the Safety of the P2-VP8 Rotavirus Vaccine*. Available at: https://clinicaltrials.gov/ct2/show/NCT01764256?cond=rotavirus+P2+VP8&rank=2 (Accessed: 22 July 2019).

Clinicaltrials.gov (2014) *Phase I/II Descending Age Study of P2VP8 Subunit Parenteral Rotavirus Vaccine in Healthy Toddlers and Infants*. Available at: https://clinicaltrials.gov/ct2/show/results/NCT02109484 (Accessed: 22 July 2019).

Clinicaltrials.gov (2016a) *A Dose-escalating Study to Evaluate the Immunogenicity and Safety of Rotavin-M1 Vaccine in Healthy Infants.* Available at: https://clinicaltrials.gov/ct2/show/NCT01377571 (Accessed: 22 November 2018).

Clinicaltrials.gov (2016b) *Safety and Immunogenicity Study of Trivalent P2-*

VP8 Subunit Rotavirus Vaccine in Adults, Toddlers and Infants. Available at: https://clinicaltrials.gov/ct2/show/NCT02646891?cond=rotavirus+P2+VP8&rank=4 (Accessed: 22 July 2019).

Clinicaltrials.gov (2016c) *Safety Study of a Rotavirus Vaccine (Rotavin-M1) Among Healthy Adults.* Available at: https://clinicaltrials.gov/ct2/show/NCT01375907 (Accessed: 22 November 2018).

Clinicaltrials.gov (2018) *Phase III Study of Liquid Formulation of ROTAVIN*. Available at: https://clinicaltrials.gov/ct2/show/NCT03703336 (Accessed: 22 July 2019).

Clinicaltrials.gov (2019) *A Trial to Assess the Safety, Immunogenicity and Efficacy of a Trivalent Rotavirus P2-VP8 Subunit Vaccine in Prevention of Severe Rotavirus Gastroenteritis in Healthy Infants in Africa and India*. Available at: https://clinicaltrials.gov/ct2/show/NCT04010448?cond=rotavirus+P2+VP8&rank=1 (Accessed: 22 July 2019).

Coldiron, M. E. *et al.* (2018) 'Safety of a heat-stable rotavirus vaccine among children in Niger: Data from a phase 3, randomized, double-blind, placebo-controlled trial', *Vaccine*, 36(25), pp. 3674–3680.

Colgate, E. R. *et al.* (2016) 'Delayed Dosing of Oral Rotavirus Vaccine Demonstrates Decreased Risk of Rotavirus Gastroenteritis Associated With Serum Zinc: A Randomized Controlled Trial', *Clinical Infectious Diseases*, 63(5), pp. 634–641.

Collins, P. J. *et al.* (2008) 'Molecular characterization of equine rotavirus in Ireland', *Journal of Clinical Microbiology*, 46(10), pp. 3346–3354.

Collins, P. J., Martella, V. and O'Shea, H. (2008) 'Detection and Characterization of Group C Rotaviruses in Asymptomatic Piglets in Ireland □', *Journal of Clinical M*, 46(9), pp. 2973–2979.

Cook, N. *et al.* (2004) 'The zoonotic potential of rotavirus', *Journal of Infection*, 48(4), pp. 289–302.

Cook, S. M. *et al.* (1990) 'Global seasonality of rotavirus infections.', *Bulletin of the World Health Organization*, 68(2), pp. 171–7.

Cortey, M. and Segalés, J. (2012) 'Low levels of diversity among genomes of Porcine circovirus type 1 (PCV1) points to differential adaptive selection between Porcine circoviruses.', *Virology*, 422(2), pp. 161–4.

Corthésy, B. *et al.* (2006) 'Rotavirus anti-VP6 secretory immunoglobulin A contributes to protection via intracellular neutralization but not via immune exclusion.', *Journal of Virology*, 80(21), pp. 10692–9.

Coulson, B. S. *et al.* (1990) 'Comparison of rotavirus immunoglobulin A coproconversion with other indices of rotavirus infection in a longitudinal study in childhood.', *Journal of Clinical Microbiology*, 28(6), pp. 1367–74.

Coulson, B. S. *et al.* (1992) 'Role of coproantibody in clinical protection of children during reinfection with rotavirus.', *Journal of Clinical Microbiology*, 30(7), pp. 1678–84.

Coulson, B. S., Londrigan, S. L. and Lee, D. J. (1997) 'Rotavirus contains integrin ligand sequences and a disintegrin-like domain that are implicated in virus entry into cells', *Proceedings of the National Academy of Sciences*, 94(10), pp. 5389–5394.

Coulson, B. S. and Masendycz, P. J. (1990) 'Measurement of rotavirus-neutralizing coproantibody in children by fluorescent focus reduction

assay', *Journal of Clinical Microbiology*, 28(7), pp. 1652–1654.
Cowley, D. *et al.* (2017) 'Rotavirus shedding following administration of RV3-BB human neonatal rotavirus vaccine', *Human Vaccines and Immunotherapeutics*, 13(8), pp. 1908–1915.
Crawford, S. E. *et al.* (2001) 'Trypsin cleavage stabilizes the rotavirus VP4 spike.', *Journal of Virology*, 75(13), pp. 6052–61.
Crawford, S. E. *et al.* (2017) 'Rotavirus infection', *Nature Reviews Disease Primers*, 3, p. 17083.
Crawford, S. E. and Desselberger, U. (2016) 'Lipid droplets form complexes with viroplasms and are crucial for rotavirus replication.', *Current Opinion in Virology*, 19, pp. 11–15.
Crotty, S., Cameron, C. E. and Andino, R. (2001) 'RNA virus error catastrophe: Direct molecular test by using ribavirin', *Proceedings of the National Academy of Sciences*, 98(12), pp. 6895–6900.
Cubitt, W. and Holzel, H. (1980) 'An outbreak of rotavirus infection in a long-stay ward of a geriatric hospital', *Journal of Clinical Pathology*, 33, pp. 306–308.
Curns, A. T. *et al.* (2010) 'Reduction in Acute Gastroenteritis Hospitalizations among US Children After Introduction of Rotavirus Vaccine: Analysis of Hospital Discharge Data from 18 US States', *The Journal of Infectious Diseases*, 201(11), pp. 1617–1624.
Danchin, M. *et al.* (2013) 'Phase I trial of RV3-BB rotavirus vaccine: A human neonatal rotavirus vaccine', *Vaccine*, 31(23), pp. 2610–2616.
Dang, D. *et al.* (2012) 'A dose-escalation safety and immunogenicity study of a new live attenuated human rotavirus vaccine (Rotavin-M1) in Vietnamese children.', *Vaccine*, 30(Suppl 1), pp. 114–121.
Das, B. K. *et al.* (1994) 'Characterization of rotavirus strains from newborns in New Delhi, India', *Journal of Clinical Microbiology*, 32(7), pp. 1820–1822.
Das, S. K. *et al.* (2017) 'Long-term impact of changing childhood malnutrition on rotavirus diarrhoea: Two decades of adjusted association with climate and socio-demographic factors from urban Bangladesh', *PLoS one*, 12(9), pp. 1–12.
Data Protection Act 1998. (1998) *Lesiglation.gov.uk.* Available at: http://www.lesgislation.gov.uk/ukpga/1998/29/contents (Accessed: 7 August 2018).
David, R. L. and Kirk, M. D. (2014) 'Rotavirus gastroenteritis hospitalisations following introduction of vaccination, Canberra', *Communicable Diseases Intelligence Quarterly Rerport*, 38(1), pp. E3-8.
Davidson, G. P. and Barnes, G. L. (1979) 'Structural and Functional Abnormalities of the Small Intestine in Infants and Young Children With Rotavirus Enteritis', *Acta Pædiatrica Scandinavia*, 68(3), pp. 181–186.
Davis, K. A. and Patton, J. T. (2017) 'Shutdown of interferon signaling by a viral-hijacked E3 ubiquitin ligase', *Microbial Cell*, 4(11), pp. 387–389.
Deen, J. *et al.* (2017) 'Improving rotavirus vaccine coverage : Can newer-generation and locally produced vaccines help ?', 5515(December).
Dennehy, P. H. *et al.* (2005) 'Comparative evaluation of safety and

immunogenicity of two dosages of an oral live attenuated human rotavirus vaccine.', *The Pediatric Infectious Disease Journal*, 24(6), pp. 481–488.

Depledge, D. P. *et al.* (2014) 'Deep sequencing of viral genomes provides insight into the evolution and pathogenesis of varicella zoster virus and its vaccine in humans', *Molecular Biology and Evolution*, 31(2), pp. 397–409.

Desmyter, J., Melnick, J. L. and Rawls, W. E. (1968) 'Defectiveness of interferon production and of rubella virus interference in a line of African green monkey kidney cells (Vero).', *Journal of Virology*, 2(10), pp. 955–61.

Desselberger, U. *et al.* (2013) 'Further characterisation of rotavirus cores: Ss(+)RNAs can be packaged in vitro but packaging lacks sequence specificity', *Virus Research*, 178(2), pp. 252–263.

Desselberger, U. (2014) 'Rotaviruses', *Virus Research*, 190, pp. 75–96.

Desselberger, U. (2017a) '7th European rotavirus biology conference, Cork/Ireland, 18–21 June 2017', *Virus Research*, 240(September), pp. 197–199.

Desselberger, U. (2017b) 'Reverse genetics of rotavirus.', *Proceedings of the National Academy of Sciences of the United States of America*, 114(9), pp. 2106–2108.

Desselberger, U. and Huppertz, H. I. (2011) 'Immune responses to rotavirus infection and vaccination and associated correlates of protection', *Journal of Infectious Diseases*, 203(2), pp. 188–195.

Dickman, K. G. *et al.* (2000) 'Rotavirus alters paracellular permeability and energy metabolism in Caco-2 cells.', *American Journal of Physiology Gastrointestinal and Liver Physiology*, 279(4), pp. G757-66.

Ding, S. *et al.* (2018) 'Rotavirus VP3 targets MAVS for degradation to inhibit type III interferon expression in intestinal epithelial cells', *eLife*, 7, p. e39494.

Doan, Y. H. *et al.* (2016) 'Genetic analysis of human rotavirus C: The appearance of Indian-Bangladeshi strain in Far East Asian countries', *Infection, Genetics and Evolution*, 41, pp. 160–173.

Dolcino, M. *et al.* (2013) 'A subset of anti-rotavirus antibodies directed against the viral protein VP7 predicts the onset of celiac disease and induces typical features of the disease in the intestinal epithelial cell line T84', *Immunologic Research*, 56(2–3), pp. 465–476.

Domingo, E., Sheldon, J. and Perales, C. (2012) 'Viral quasispecies evolution', *Microbiology and Molecular Biology Reviews*, 76(2), pp. 159–216.

Dominguez-Bello, M. G. *et al.* (2010) 'Delivery mode shapes the acquisition and structure of the initial microbiota across multiple body habitats in newborns', *PNAS USA*, 107(26), pp. 11971–5.

Donato, C. M. *et al.* (2012) 'Identification of Strains of RotaTeq Rotavirus Vaccine in Infants With Gastroenteritis Following Routine Vaccination', *The Journal of Infectious Diseases*, 206(3), pp. 377–383.

Donker, N. C., Boniface, K. and Kirkwood, C. D. (2011) 'Phylogenetic analysis of rotavirus A NSP2 gene sequences and evidence of intragenic recombination', *Infection, Genetics and Evolution*, 11(7),

pp. 1602–1607.

Donker, N. C. and Kirkwood, C. D. (2012) 'Selection and evolutionary analysis in the nonstructural protein NSP2 of rotavirus A', *Infection, Genetics and Evolution*, 12(7), pp. 1355–1361.

Dormitzer, P. R. *et al.* (2004) 'Structural rearrangements in the membrane penetration protein of a non-enveloped virus.', *Nature*, 430(7003), pp. 1053–1058.

Dubin, G. *et al.* (2013) 'Investigation of a regulatory agency enquiry into potential porcine circovirus type 1 contamination of the human rotavirus vaccine, Rotarix: approach and outcome.', *Human Vaccines & Immunotherapeutics*, 9(11), pp. 2398–408.

Dzidic, M. *et al.* (2018) 'Gut Microbiota and Mucosal Immunity in the Neonate', *Medical Sciences*, 6(56), pp. 1–23.

Eiden, J. J. *et al.* (1991) 'Detection of animal and human group B rotaviruses in fecal specimens by polymerase chain reaction', *Journal of Clinical Microbiology*, 29(3), pp. 539–543.

Eigen, M. and Schuster, P. (1977) 'The hypercycle. A principle of natural self-organization. Part A: Emergence of the hypercycle.', *Die Naturwissenschaften*, 64(11), pp. 541–65.

EMA (2006) *RotaTeq®, international nonproprietary (INN)-human rotavirus, live attenuated vaccine, Scientific Discussion, Evaluation of Medicines for Human Use, European Public Assessment Reports (EPAR).*

EMA (2008) *Rotarix®, international nonproprietary (INN)-human rotavirus, live attenuated vaccine, scientific discussion, evaluation of medicines for human use, European public assessment reports (EPAR).* Available at: https://www.ema.europa.eu/documents/ scientific-discussion/rotarix-epar-scientific-discussion_en.pdf.

EMA (2010) *European Medicines Agency confirms positive benefit-risk balance of Rotarix*. Available at: https://www.ema.europa.eu/en /documents/press-release/european-medicines-agency-confirms-positive-benefit-risk-balance-rotarix_en.pdf (Accessed: 30 July 2019).

Esona, M. D. *et al.* (2010) 'Molecular characterization of human rotavirus vaccine strain CDC-9 during sequential passages in Vero cells', *Human Vaccines*, 6(3), p. pii: 10409.

Espinoza, F. *et al.* (1997) 'Rotavirus infections in young Nicaraguan children.', *The Pediatric infectious disease journal*, 16(6), pp. 564–71.

Estes, M. K. (2001) 'Rotaviruses and their replication', in Knipe, D. M. and Howley, P. M. (eds) *Fields Virology*. Philadelphia: Lippincoot Williams & Wilkins, pp. 1747–1785.

Estes, M. K. and Greenberg, H. B. (2013) 'Rotaviruses', in Knipe, D. M. et al. (eds) *Fields Virology*. 6th edn. Philadelphia, pp. 1347-1400.

Estes, M. K. and Kapikian, A. Z. (2007) 'Rotaviruses and their replication', in Knipe, D. M. et al. (eds) *Fields Virology*. 5th edn. Philadelphia: Lippincoot Williams & Wilkins, pp. 1917–1974.

Estrozi, L. F. *et al.* (2013) 'Location of the dsRNA-dependent polymerase, VP1, in rotavirus particles', *Journal of Molecular Biology*, 425(1), pp. 124–132.

Eydelloth, R. S. *et al.* (1984) 'Kinetics of viral replication and local and

systemic immune responses in experimental rotavirus infection', *Journal of Virology*, 50(3), pp. 947–950.

Faber, M. *et al.* (2005) 'A single amino acid change in rabies virus glycoprotein increases virus spread and enhances virus pathogenicity.', *Journal of Virology*, 79(22), pp. 14141–14148.

Falcone, E. *et al.* (2015) 'Molecular characterization of avian rotaviruses circulating in Italian poultry flocks.', *Avian Pathology*, 44(6), pp. 509–15.

Famulare, M. *et al.* (2016) 'Sabin vaccine reversion in the field: a comprehensive analysis of Sabin-like poliovirus isolates in Nigeria.', *Journal of Virology*, 90(1), pp. 317–331.

Fedorowicz, Z., Va, J. and Carter, B. (2011) 'Antiemetics for reducing vomiting related to acute gastroenteritis in children and adolescents', *Cochrane Database of Systematic Reviews*, (9), pp. 1–74.

Feng, N. *et al.* (1994) 'Comparison of Mucosal and Systemic Humoral Immune Responses and Subsequent Protection in Mice Orally Inoculated with a Homologous or a Heterologous Rotavirus', *The Journal of Virology*, 68(12), pp. 7766–7773.

Feng, N. *et al.* (2002) 'Inhibition of rotavirus replication by a non-neutralizing, rotavirus VP6-specific IgA mAb.', *The Journal of Clinical Investigation*, 109(9), pp. 1203–13.

Finkbeiner, S. R. *et al.* (2012) 'Stem cell-derived human intestinal organoids as an infection model for rotaviruses.', *mBio*, 3(4), pp. e00159-12.

Fix, A. D. *et al.* (2015) 'Safety and immunogenicity of a parenterally administered rotavirus VP8 subunit vaccine in healthy adults', *Vaccine*, 33(31), pp. 3766–3772.

Flores, J., Sears, J., *et al.* (1988) 'Genetic stability of rotaviruses recovered from asymptomatic neonatal infections.', *Journal of Virology*, 62(12), pp. 4778–81.

Flores, J., Daoud, G., *et al.* (1988) 'Reactogenicity and antigenicity of rhesus rotavirus vaccine (MMU-18006) in newborn infants in Venezuela', *Pediatric Infectious Disease Journal*, 7(11), pp. 776–780.

Flores, J. *et al.* (1989) 'Reactions to and antigenicity of two human-rhesus rotavirus reassortant vaccine candidates of serotypes 1 and 2 in Venezuelan infants', *Journal of Clinical Microbiology*, 27(3), pp. 512–518.

Franco, M. A., Angel, J. and Greenberg, H. B. (2006) 'Immunity and correlates of protection for rotavirus vaccines.', *Vaccine*, 24(15), pp. 2718–31.

Franco, M. A. and Greenberg, H. B. (1999) 'Immunity to Rotavirus Infection in Mice', *The Journal of Infectious Diseases*, 179(Suppl 3), pp. 466–469.

Franco, M. A., Tin, C. and Greenberg, H. B. (1997) 'CD8+ T cells can mediate almost complete short-term and partial long-term immunity to rotavirus in mice', *Journal of Virology*, 71(5), pp. 4165–4170.

Fu, C. *et al.* (2007) 'Effectiveness of Lanzhou lamb rotavirus vaccine against rotavirus gastroenteritis requiring hospitalization: a matched case-control study.', *Vaccine*, 25(52), pp. 8756–61.

Fu, C., Tate, J. E. and Jiang, B. (2010) 'Effectiveness of Lanzhou lamb rotavirus vaccine against hospitalized gastroenteritis: further analysis

and update.', *Human Vaccines*, 6(11), p. 953.

Gastañaduy, P. A. *et al.* (2013) 'Gastroenteritis hospitalizations in older children and adults in the United States before and after implementation of infant rotavirus vaccination', *Journal of the American Medical Association*, 310(8), pp. 851–853.

Gautam, R. *et al.* (2014) 'Real-time RT-PCR assays to differentiate wild-type group A rotavirus strains from Rotarix® and RotaTeq® vaccine strains in stool samples.', *Human Vaccines & Immunotherapeutics*, 10(3), pp. 767–777.

Gautam, R. *et al.* (2016) 'One-step multiplex real-time RT-PCR assay for detecting and genotyping wild-type group A rotavirus strains and vaccine strains (Rotarix® and RotaTeq®) in stool samples.', *Peer Journal*, 4, p. e1560.

Georges-Courbot, M. *et al.* (1991) 'Evaluation of the efficacy of a low-passage bovine rotavirus (strain WC3) vaccine in children in Central Africa', *Research in Virology*, 142(2), pp. 405–411.

Ghosh, S. *et al.* (2006) 'Molecular characterization of a porcine Group A rotavirus strain with G12 genotype specificity', *Archives of Virology*, 151(7), pp. 1329–1344.

Gilliland, S. M. *et al.* (2012) 'Investigation of porcine circovirus contamination in human vaccines.', *Biologicals*, 40(4), pp. 270–7.

Gladstone, B. P. *et al.* (2011) 'Protective effect of natural rotavirus infection in an Indian birth cohort.', *The New England Journal of Medicine*, 365(4), pp. 337–46.

Glass, R. I. *et al.* (1991) 'Immune response to rotavirus vaccines among breast-fed and nonbreast-fed children', in Mestecky, J., Blair, C., and Ogra, P. L. (eds) *Immunology of Milk and the Neonate. Advances in Experimental Medicine and Biology*. Boston, MA: Springer, pp. 249–54.

Glass, R. I. *et al.* (2005) 'Development of Candidate Rotavirus Vaccines Derived from Neonatal Strains in India', *The Journal of Infectious Diseases*, 192(s1), pp. S30–S35.

Gómez-Rial, J. *et al.* (2019a) 'Further considerations on rotavirus vaccination and seizure-related hospitalization rates', *Infection and Drug Resistance*, 12, pp. 989–991.

Gómez-Rial, J. *et al.* (2019b) 'Rotavirus infection beyond the gut', *Infection and Drug Resistance*, 12, pp. 55–64.

Gonzalez-Ochoa, G. *et al.* (2017) 'Modulation of rotavirus severe gastroenteritis by the combination of probiotics and prebiotics', *Archives of Microbiology*, 199(7), pp. 953–961.

Gonzalez, A. M. *et al.* (2003) 'Rotavirus-Specific B Cells Induced by Recent Infection in Adults and Children Predominantly Express the Intestinal Homing Receptor α4β7', *Virology*, 305(1), pp. 93–105.

Gorziglia, M., Larralde, G. and Ward, R. L. (1990) 'Neutralization epitopes on rotavirus SA11 4fM outer capsid proteins.', *Journal of Virology*, 64(9), pp. 4534–4539.

Gothefors, L. *et al.* (1989) 'Prolonged Efficacy of Rhesus Rotavirus Vaccine in Swedish Children', *Journal of Infectious Diseases*, 159(4), pp. 753–757.

Gov.uk (2014) *Successful start to rotavirus vaccination programme.*, *Gov.uk*.

Available at: https://www.gov.uk/government/news/successful-start-to-rotavirus-vaccination-programme (Accessed: 7 August 2018).

Gov.uk (2018a) *Routine childhood immunisation schedule.*, *Gov.uk*. Available at: https://www.gov.uk/government/publications/routine-childhood-immunisation-schedule (Accessed: 7 August 2018).

Gov.uk (2018b) *The complete routine immunisation schedule*, *Gov.uk*. Available at: https://www.gov.uk/government/publications/routine-childhood-immunisation-schedule (Accessed: 7 August 2018).

Graff, J. W. *et al.* (2007) 'Zinc-binding domain of rotavirus NSP1 is required for proteasome-dependent degradation of IRF3 and autoregulatory NSP1 stability', *Journal of General Virology*, 88(2), pp. 613–620.

Graff, J. W., Ettayebi, K. and Hardy, M. E. (2009) 'Rotavirus NSP1 inhibits NFκB activation by inducing proteasome-dependent degradation of β-TrCP: A novel mechanism of IFN antagonism', *PLoS Pathogens*, 5(1).

Green, K. Y. *et al.* (1990) 'Homotypic and heterotypic epitope-specific antibody responses in adult and infant rotavirus vaccinees: Implications for vaccine development', *Journal of Infectious Diseases*, 161(4), pp. 667–679.

Green, K. Y. and Kapikian, A. Z. (1992) 'Identification of VP7 epitopes associated with protection against human rotavirus illness or shedding in volunteers.', *Journal of Virology*, 66(1), pp. 548–53.

Greenberg, H. B. and Estes, M. K. (2009) 'Rotaviruses: from pathogenesis to vaccination.', *Gastroenterology*, 136(6), pp. 1939–51.

Gregorio, G. V., Dans, L. F. and Silvestre, M. A. (2011) 'Early versus delayed refeeding for children with acute diarrhoea', *Cochrane Database Systematic Reviews*, 7(2), pp. 721–757.

Griffin, D. D. *et al.* (2002) 'Characterization of Nontypeable Rotavirus Strains from the United States: Identification of a New Rotavirus Reassortant (P2A[6],G12) and Rare P3[9] Strains Related to Bovine Rotaviruses', *Virology*, 294(2), pp. 256–269.

Grimwood, K. *et al.* (1983) 'Spread of rotavirus within families: a community based study', *British Medical Journal*, 287(August), pp. 575–577.

Grimwood, K. *et al.* (1988) 'Comparison of serum and mucosal antibody responses following severe acute rotavirus gastroenteritis in young children', *Journal of Clinical Microbiology*, 26(4), pp. 732–738.

Groome, M. J. *et al.* (2014) 'Effect of breastfeeding on immunogenicity of oral live-attenuated human rotavirus vaccine: a randomized trial in HIV-uninfected infants in Soweto, South Africa', *Bulletin of the World Health Organization*, 92(4), pp. 238–245.

Groome, M. J. *et al.* (2017) 'Safety and immunogenicity of a parenteral P2-VP8-P[8] subunit rotavirus vaccine in toddlers and infants in South Africa: a randomised, double-blind, placebo-controlled trial', *The Lancet Infectious Diseases*, 17(8), pp. 843–853.

Gutierrez, M. *et al.* (2010) 'Different Rotavirus Strains Enter MA104 Cells through Different Endocytic Pathways: the Role of Clathrin-Mediated Endocytosis', *Journal of Virology*, 84(18), pp. 9161–9169.

Hagbom, M. *et al.* (2011) 'Rotavirus stimulates release of serotonin (5-HT) from human enterochromaffin cells and activates brain structures

involved in nausea and vomiting', *PLoS Pathogens*, 7(7), pp. 1–10.
Hagbom, M. *et al.* (2017) 'Ondansetron treatment reduces rotavirus symptoms—A randomized double-blinded placebo-controlled trial', *PLOS one*, 12(10), p. e0186824.
Hakim, M. S. *et al.* (2018) 'Basal interferon signaling and therapeutic use of interferons in controlling rotavirus infection in human intestinal cells and organoids.', *Nature Scientific Reports*, 8(1), p. 8341.
Halaihel, N. *et al.* (2002) 'Direct Inhibitory Effect of Rotavirus NSP4(114-135) Peptide on the Na+-D-Glucose Symporter of Rabbit Intestinal Brush Border Membrane', *Journal of Virology*, 74(20), pp. 9464–9470.
Han, H. H. *et al.* (2017) 'Serologic response to porcine circovirus type 1 (PCV1) in infants vaccinated with the human rotavirus vaccine, Rotarix™: a retrospective laboratory analysis', *Human Vaccines & Immunotherapeutics*, 13(1), pp. 237–244.
Hanley, K. A. (2011) 'The double-edged sword: how evolution can make or break a live-attenuated virus vaccine.', *Evolution: Education and Outreach*, 4(4), pp. 635–643.
Hanlon, P. *et al.* (1987) 'Trial of an attenuated bovine rotavirus vaccine (RIT 4237) in Gambian infants.', *The Lancet*, 1(8546), pp. 1342–5.
Harris, J. P. *et al.* (2007) 'Evaluating rotavirus vaccination in England and Wales', *Vaccine*, 25(20), pp. 3962–3970.
Harris, V. C. *et al.* (2017) 'Significant Correlation Between the Infant Gut Microbiome and Rotavirus Vaccine Response in Rural Ghana', *The Journal of Infectious Diseases*, 215(1), pp. 34–41.
Harris, V. C., Haak, B. W., *et al.* (2018) 'Effect of Antibiotic-Mediated Microbiome Modulation on Rotavirus Vaccine Immunogenicity: A Human, Randomized-Control Proof-of-Concept Trial.', *Cell Host & Microbe*. Elsevier, 24(2), pp. 197-207.e4.
Harris, V. C., Ali, A., *et al.* (2018) 'Rotavirus vaccine response correlates with the infant gut microbiota composition in Pakistan', *Gut Microbes*, 9(2), pp. 93–101.
Harvala, H. *et al.* (2014) 'Comparison of diagnostic clinical samples and environmental sampling for enterovirus and parechovirus surveillance in Scotland, 2010 to 2012', *Eurosurveillance*, 19(15), p. 20772.
Hattermann, K. *et al.* (2004) 'Infection studies on human cell lines with porcine circovirus type 1 and porcine circovirus type 2.', *Xenotransplantation*, 11(3), pp. 284–94.
Heiman, E. M. *et al.* (2008) 'Group A Human Rotavirus Genomics: Evidence that Gene Constellations Are Influenced by Viral Protein Interactions', *Journal of Virology*, 82(22), pp. 11106–11116.
Heinimäki, S. *et al.* (2018) 'Intradermal and intranasal immunizations with oligomeric middle layer rotavirus VP6 induce Th1, Th2 and Th17 T cell subsets and CD4+ T lymphocytes with cytotoxic potential', *Antiviral Research*. Elsevier, 157(May), pp. 1–8.
Hemming, M. *et al.* (2014) 'Rotavirus Antigenemia in Children is Associated With More Severe Clinical Manifestations of Acute Gastroenteritis', *The Pediatric Infectious Disease Journal*, 33(4), pp. 366–371.
Hemming, M. and Vesikari, T. (2012) 'Vaccine-derived human-bovine double reassortant rotavirus in infants with acute gastroenteritis',

Pediatric Infectious Disease Journal, 31(9), pp. 992–994.

Herrera, D. *et al.* (2013) 'Rotavirus specific plasma secretory immunoglobulin in children with acute gastroenteritis and children vaccinated with an attenuated human rotavirus vaccine', *Human Vaccines and Immunotherapeutics*, 9(11), pp. 2409–2417.

Herring, A. J. *et al.* (1982) 'Rapid diagnosis of rotavirus infection by direct detection of viral nucleic acid in silver-stained polyacrylamide gels', *Journal of Clinical Microbiology*, 16(3), pp. 473–477.

Herrmann, J. E. *et al.* (1996) 'Protection Against Rotavirus Infections By Dna Vaccination', *Journal of Infectious Diseases*, 174(Supplement 1), pp. S93–S97.

Hewish, M., Takada, Y. and Coulson, B. (2000) 'Integrins a2b1 and a4b1 can mediate SA11 rotavirus attachment and entry into cells', *Journal of Virology*, 74(1), pp. 228–236.

Hiramatsu, H. *et al.* (2018) 'Rotavirus vaccination can be performed without viral dissemination in the neonatal intensive care unit', *Journal of Infectious Diseases*, 217(4), pp. 589–596.

Hjelt, K. *et al.* (1986) 'Antibody response in serum and intestine in children up to six months after a naturally acquired rotavirus gastroenteritis', *Journal of Pediatric Gastroenterology and Nutrition*, 5, pp. 74–80.

Hjelt, K. *et al.* (1987) 'Protective effect of preexisting rotavirus-specific immunoglobulin A against naturally acquired rotavirus infection in children.', *Journal of Medical Virology*, 21(1), pp. 39–47.

Hjelt, K. and Grauballe, C. (1990) 'Protective levels of intestinal rotavirus antibodies.', *The Journal of Infectious Diseases*, 161(2), pp. 352–3.

Holmes, I. A. N. H. *et al.* (1975) 'Infantile Enteritis Viruses:Morphogenesis and Morphology', *Journal of Virology*, 16(4), pp. 937–943.

Honeyman, M. C. *et al.* (2000) 'Association between rotavirus infection and pancreatic islet autoimmunity in children at risk of developing type 1 diabetes.', *Diabetes*, 49(8), pp. 1319–24.

Honeyman, M. C. *et al.* (2014) 'Rotavirus Infection Induces Transient Pancreatic Involution and Hyperglycemia in Weanling Mice', *PLoS one*, 9(9), p. e106560.

Horie, Y. *et al.* (1999) 'Diarrhea induction by rotavirus NSP4 in the homologous mouse model system', *Virology*, 262(2), pp. 398–407.

Hoshino, Y. *et al.* (1985) 'Serotypic characterization of rotaviruses derived from asymptomatic human neonatal infections', *Journal of Clinical Microbiology*, 21(3), pp. 425–430.

Hoshino, Y. *et al.* (1995) 'Identification of Group A Rotavirus Genes Associated with Virulence of a Porcine Rotavirus and Host Range Restriction of a Human Rotavirus in the Gnotobiotic Piglet Model', *Virology*, 209(1), pp. 274–280.

Hoshino, Y. *et al.* (1997) 'Construction of four double gene substitution human x bovine rotavirus reassortant vaccine candidates: Each bears two outer capsid human rotavirus genes, one encoding P serotype 1A and the other encoding G serotype 1,2,3,4 specificity', *Journal of Medical Virology*, 51(4), pp. 319–325.

Howe, B. *et al.* (2010) *Rotarix® (Rotavirus vaccine, live oral): GSK's PCV1 Investigation.* Available at: https://slideplayer.com/slide/4539569/ (Accessed: 25 October 2018).

Hsieh, Y.-C. *et al.* (2014) 'Comparison of virus shedding after lived attenuated and pentavalent reassortant rotavirus vaccine', *Vaccine*, 32(10), pp. 1199–1204.

Hu, L. *et al.* (2012) 'Rotavirus non-structural proteins: structure and function.', *Current Opinion in Virology*, 2(4), pp. 380–388.

Human Tissue Act 2004 (2004) *Legislation.gov.uk*. Available at: http://www.lesgislation.gov.uk/ukpga/2004/30/pdfs/ukpga_20040030_en.pdf (Accessed: 7 August 2018).

Hundley, F. *et al.* (1987) 'Heterogeneity of Genome Rearrangements in Rotaviruses Isolated from a Chronically Infected Immunodeficient Child', *Journal of Virology*, 61(11), pp. 3365–3372.

Hung, T. *et al.* (1983) 'Rotavirus-like agent in adult non-bacterial diarrhoea in China.', *The Lancet*, 2(8358), pp. 1078–9.

Hung, T. *et al.* (1984) 'Waterborne outbreak of rotavirus diarrhoea in adults in China caused by a novel rotavirus.', *The Lancet*, 1(8387), pp. 1139–42.

Hungerford, D. *et al.* (2014) 'Ecological assessment of the direct and indirect effects of routine rotavirus vaccination in Merseyside, UK using data from multiple health systems: a study protocol', *BMJ Open*, 4(11), pp. e006161–e006161.

Hungerford, D. *et al.* (2016) 'In-season and out-of-season variation of rotavirus genotype distribution and age of infection across 12 European countries before the introduction of routine vaccination, 2007/08 to 2012/13', *Eurosurveillance*, 21(2).

Hungerford, D. *et al.* (2019) 'Impact of rotavirus vaccination on rotavirus genotype distribution and diversity in England, September 2006 to August 2016', *Eurosurveillance*, 24(6).

Hyser, J. M. *et al.* (2010) 'Rotavirus disrupts calcium homeostasis by NSP4 viroporin activity', *mBio*, 1(5), pp. 1–12.

Imai, M. *et al.* (1983) 'Capped and conserved terminal structures in human rotavirus genome double-stranded RNA segments.', *Journal of Virology*, 47(1), pp. 125–36.

Imbert-Marcille, B. M. *et al.* (2014) 'A FUT2 gene common polymorphism determines resistance to rotavirus a of the P[8] genotype', *Journal of Infectious Diseases*, 209(8), pp. 1227–1230.

Isakov, O. *et al.* (2015) 'Deep sequencing analysis of viral infection and evolution allows rapid and detailed characterization of viral mutant spectrum', *Bioinformatics*, 31(13), pp. 2141–2150.

Isanaka, S. *et al.* (2017) 'Efficacy of a Low-Cost, Heat-Stable Oral Rotavirus Vaccine in Niger', *New England Journal of Medicine*, 376(12), pp. 1121–1130.

Istrate, C. *et al.* (2008) 'Individuals with selective IgA deficiency resolve rotavirus disease and develop higher antibody titers (IgG, IgG1) than IgA competent individuals.', *Journal of Medical Virology*, 80(3), pp. 531–535.

Iturriza-Gómara, M. *et al.* (2000) 'Molecular epidemiology of human group A rotavirus infections in the United Kingdom between 1995 and 1998', *Journal of Clinical Microbiology*, 38(12), pp. 4394–4401.

Iturriza-Gómara, M. *et al.* (2001) 'Amino acid substitution within the VP7 protein of G2 rotavirus strains associated with failure to serotype',

Journal of Clinical Microbiology, 39(10), pp. 3796–3798.

Iturriza-Gómara, M. *et al.* (2008) 'Structured surveillance of infantile gastroenteritis in East Anglia, UK: Incidence of infection with common viral gastroenteric pathogens', *Epidemiology and Infection*, 136(1), pp. 23–33.

Iturriza-Gómara, M. *et al.* (2011) 'Rotavirus genotypes co-circulating in Europe between 2006 and 2009 as determined by EuroRotaNet, a pan-European collaborative strain surveillance network.', *Epidemiology and Infection*, 139(6), pp. 895–909.

Iturriza-Gómara, M. and Cunliffe, N. (2013) 'Rotavirus vaccine: a welcome addition to the immunisation schedule in the UK.', *BMJ*, 346, p. f2347.

Jaimes, M. C. *et al.* (2002) 'Frequencies of Virus-Specific CD4+ and CD8+ T Lymphocytes Secreting Gamma Interferon after Acute Natural Rotavirus Infection in Children and Adults', *Journal of Virology*, 76(10), pp. 4741–4749.

Jaques, S. *et al.* (2014) 'Slow uptake of rotavirus vaccination in UK neonatal units', *Archives of Disease in Childhood: Fetal and Neonatal Edition*, 99(3), p. F252.

Jaques, S. C. *et al.* (2015) 'Rotavirus immunisation in NICU: A 1-year experience in a uk tertiary neonatal surgical unit postvaccine introduction', *Archives of Disease in Childhood: Fetal and Neonatal Edition*, 100(2), pp. F186–F187.

Jayanthi, V. *et al.* (1989) 'Intestinal transit in healthy Southern Indian subjects and in patients with tropical sprue', *Gut*, 30(1), pp. 35–38.

Jayaram, H., Estes, M. K. and Prasad, B. V. V. (2004) 'Emerging themes in rotavirus cell entry, genome organization, transcription and replication.', *Virus Research*, 101(1), pp. 67–81.

Jenkins, G. M. *et al.* (2002) 'Rates of Molecular Evolution in RNA viruses: A Quantitative Phylogenetic Analysis', *Journal of Molecular Evolution*, (54), pp. 156–165.

Jeon, J. S. *et al.* (2016) 'Analysis of single nucleotide polymorphism among Varicella-Zoster Virus and identification of vaccine-specific sites', *Virology*, 496, pp. 277–286.

Jere, K. C. *et al.* (2011) 'Whole genome analysis of multiple rotavirus strains from a single stool specimen using sequence-independent amplification and 454(R) pyrosequencing reveals evidence of intergenotype genome segment recombination', *Infection, Genetics and Evolution*, 11(8), pp. 2072–2082.

Jere, K. C. *et al.* (2018) 'Emergence of double- and triple-gene reassortant G1P[8] rotaviruses possessing a DS-1-like backbone after rotavirus vaccine introduction in Malawi.', *Journal of Virology*, 92(3), pp. e01246-17.

Jiang, B. *et al.* (2003) 'Cytokines as mediators for or effectors against rotavirus disease in children.', *Clinical and Diagnostic Laboratory Immunology*, 10(6), pp. 995–1001.

Jiang, B., Gentsch, J. R. and Glass, R. I. (2002) 'The Role of Serum Antibodies in the Protection against Rotavirus Disease: An Overview', *Clinical Infectious Diseases*, 34(10), pp. 1351–1361.

Jiang, B., Gentsch, J. R. and Glass, R. I. (2008) 'Inactivated rotavirus

vaccines: A priority for accelerated vaccine development', *Vaccine*, 26(52), pp. 6754–6758.

Jiang, B., Wang, Y. and Glass, R. I. (2013) 'Does a monovalent inactivated human rotavirus vaccine induce heterotypic immunity? Evidence from animal studies', *Human Vaccines and Immunotherapeutics*, 9(8), pp. 1634–1637.

Joensuu, J. *et al.* (1997) 'Randomised placebo-controlled trial of rhesus-human reassortant rotavirus vaccine for prevention of severe rotavirus gastroenteritis', *The Lancet*, 350(9086), pp. 1205–1209.

Johansen, K. *et al.* (1999) 'Humoral and cell-mediated immune responses in humans to the NSP4 enterotoxin of rotavirus', *Journal of Medical Virology*, 59(3), pp. 369–377.

Johansen, K. and Svensson, L. (1997) 'Neutralization of rotavirus and recognition of immunologically important epitopes on VP4 and VP7 by human IgA', *Archives of Virology*, 142(7), pp. 1491–1498.

Jonesteller, C. L. *et al.* (2017) 'Effectiveness of rotavirus vaccination: A systematic review of the first decade of global postlicensure data, 2006-2016', *Clinical Infectious Diseases*, 65(5), pp. 840–850.

Joshi, M. S., Jare, V. M. and Gopalkrishna, V. (2017) 'Group C rotavirus infection in patients with acute gastroenteritis in outbreaks in western India between 2006 and 2014', *Epidemiology and Infection*, 145(2), pp. 310–315.

Kanai, Y. *et al.* (2017) 'Entirely plasmid-based reverse genetics system for rotaviruses.', *Proceedings of the National Academy of Sciences of the United States of America*, 114(9), pp. 2349–2354.

Kaneko, M. *et al.* (2017) 'Identification of vaccine-derived rotavirus strains in children with acute gastroenteritis in Japan, 2012-2015', *PLOS one*, 12(9), p. e0184067.

Kang, G. *et al.* (2004) 'Quantitation of group A rotavirus by real-time reverse-transcription-polymerase chain reaction: correlation with clinical severity in children in South India.', *Journal of Medical Virology*, 73(1), pp. 118–22.

Kapikian, A. Z. *et al.* (1976) 'Human Reovirus-like Agent as the Major Pathogen Associated with Winter Gastroenteritis in Hospitalized Infants and Young Children', *New England Journal of Medicine*, 294(18), pp. 965–972.

Kapikian, A. Z. *et al.* (1983) 'Oral administration of human rotavirus to volunteers: Induction of illness and correlates of resistance', *Journal of Infectious Diseases*, 147(1), pp. 95–106.

Kapikian, A. Z. *et al.* (2005) 'A Hexavalent Human Rotavirus–Bovine Rotavirus (UK) Reassortant Vaccine Designed for Use in Developing Countries and Delivered in a Schedule with the Potential to Eliminate the Risk of Intussusception', *The Journal of Infectious Diseases*, 192(s1), pp. S22–S29.

Kapikian, A. Z., Hoshino, Y. and Chanock, R. M. (2001) 'Rotaviruses', in Knipe, D. M. and Howley, P. M. (eds) *Fields Virology*. 4th edn. Philadelphia: Lippincoot Williams & Wilkins, pp. 1787–1883.

Kaplon, J. *et al.* (2015) 'Rotavirus vaccine virus shedding, viremia and clearance in infants with severe combined immune deficiency.', *The Pediatric Infectious Disease Journal*, 34(3), pp. 326–8.

Kearney, K. *et al.* (2004) 'Cell-line-induced mutation of the rotavirus genome alters expression of an IRF3-interacting protein', *The EMBO Journal*, 23(20), pp. 4072–4081.

Kelkar, S. D. and Zade, J. K. (2004) 'Group B rotaviruses similar to strain CAL-1, have been circulating in Western India since 1993', *Epidemiology and Infection*, 132(4), pp. 745–749.

Kew, O. M. *et al.* (2005) 'Vaccine-Derived Polioviruses and the Endgame Strategy for Global Polio Eradication', *Annual Review of Microbiology*, 59(1), pp. 587–635.

El Khoury, A. *et al.* (2014) 'Projecting the effectiveness of RotaTeq® against rotavirus-related hospitalizations and deaths in six Asian countries', *Human Vaccines*, 7(5), pp. 506–510.

Kirkwood, C. D. (2010) 'Genetic and antigenic diversity of human rotaviruses: potential impact on vaccination programs', *The Journal of Infectious Diseases*, 202(Supplement 1), pp. S43-48.

Klitting, R. *et al.* (2018) 'Exploratory re-encoding of yellow fever virus genome: new insights for the design of live-attenuated viruses', *Virus Evolution*, 4(2), pp. 1–17.

Komoto, S. *et al.* (2017) 'Reverse genetics system demonstrates that rotavirus non-structural protein NSP6 is not essential for viral replication in cell culture.', *Journal of Virology*, 9(21), p. pii: e00695-17.

Komoto, S. and Taniguchi, K. (2013) 'Genetic engineering of rotaviruses by reverse genetics', *Microbiology and Immunology*, 57(7), pp. 479–86.

Kovbasnjuk, O. *et al.* (2013) 'Human enteroids: preclinical models of non-inflammatory diarrhea', *Stem Cell Research & Therapy*, 4 Suppl 1(Suppl 1), p. S3.

Kuehn, B. M. (2010) 'FDA: Benefits of rotavirus vaccination outweigh potential contamination risk.', *Journal of the American Medical Association*, 304(1), pp. 30–31.

Kumar, D. *et al.* (2012) 'Use of PCR-based assays for the detection of the adventitious agent porcine circovirus type 1 (PCV1) in vaccines, and for confirming the identity of cell substrates and viruses used in vaccine production', *Journal of Virological Methods*, 179(1), pp. 201–211.

Kumar, S. *et al.* (2018) 'New tetrameric forms of the rotavirus NSP4 with antiparallel helices', *Archives of Virology*, 163(6), pp. 1531–1547.

Ladhani, S. N. and Ramsay, M. E. (2014) 'Timely immunisation of premature infants against rotavirus in the neonatal intensive care unit', *Archives of Disease in Childhood: Fetal and Neonatal Edition*, 99(6), pp. F445–F447.

Lahon, A. *et al.* (2013) 'Group B rotavirus infection in patients with acute gastroenteritis from India: 1994-1995 and 2004-2010', *Epidemiology and Infection*, 141(5), pp. 969–975.

Lal, M. and Jarrahian, C. (2017) 'Presentation matters : Buffers , packaging , and delivery devices for new , oral enteric vaccines for infants', *Human Vaccines & Immunotherapeutics*, 13(1), pp. 46–49.

Lanata, C. F. *et al.* (1989) 'Protection of peruvian children against rotavirus diarrhea of specific serotypes by one, two, or three doses of the rit 4237 attenuated bovine rotavirus vaccine', *Journal of Infectious Diseases*, 159(3), pp. 452–459.

Lanata, C. F. *et al.* (2013) 'Global Causes of Diarrheal Disease Mortality in Children <5 Years of Age: A Systematic Review', *PLoS one*, 8(9), p. e72788.

Lanz Uhde, F. *et al.* (2008) 'Prevalence of four enteropathogens in the faeces of young diarrhoeic dairy calves in Switzerland', *Veterinary Record*, 163(12), pp. 362–366.

Lappalainen, S. *et al.* (2014) 'Immune responses elicited against rotavirus middle layer protein VP6 inhibit viral replication in vitro and in vivo', *Human Vaccines and Immunotherapeutics*, 10(7), pp. 2039–2047.

Lappalainen, S. *et al.* (2015) 'Protection against live rotavirus challenge in mice induced by parenteral and mucosal delivery of VP6 subunit rotavirus vaccine', *Archives of Virology*, 160(8), pp. 2075–2078.

Lappalainen, S. *et al.* (2017) 'Rotavirus vaccination and infection induce VP6-specific IgA responses', *Journal of Medical Virology*, 89(2), pp. 239–245.

Laskowski, R. A. and Swindells, M. B. (2011) 'LigPlot+: Multiple ligand-protein interaction diagrams for drug discovery', *Journal of Chemical Information and Modeling*, 51(10), pp. 2778–2786.

Lauring, A. S. and Andino, R. (2010) 'Quasispecies theory and the behavior of RNA viruses', *PLoS Pathogens*, 6(7), pp. 1–8.

Lauring, A. S., Frydman, J. and Andino, R. (2013) 'The role of mutational robustness in RNA virus evolution.', *Nature Reviews Microbiology*, 11(5), pp. 327–336.

Lawton, J. A. *et al.* (1997) 'Three-dimensional structural analysis of recombinant rotavirus-like particles with intact and amino-terminal-deleted VP2: implications for the architecture of the VP2 capsid layer.', *Journal of Virology*, 71(10), pp. 7353–60.

Lazzerini, M. and Ronfani, L. (2012) 'Oral zinc for treating diarrhoea in children', *Cochrane Database of Systematic Reviews*, 6, pp. 1–107.

Le, L. T. *et al.* (2009) 'Development and characterization of candidate rotavirus vaccine strains derived from children with diarrhoea in Vietnam', *Vaccine*, 27(Suppl 5), pp. 130–138.

Lee, B. *et al.* (2018) 'Histo–Blood group antigen phenotype determines susceptibility to genotype-specific rotavirus infections and impacts measures of rotavirus vaccine efficacy', *Journal of Infectious Diseases*, 217(9), pp. 1399–1407.

Leitner, T. *et al.* (1993) 'Analysis of heterogeneous viral populations by direct DNA sequencing.', *BioTechniques*, 15(1), pp. 120–7.

Leong, Y. K. and Awang, A. (1990) 'Experimental Group A Rotaviral Infection in Cynomolgus Monkeys Raised on Formula Diet', *Microbiology and Immunology*, 34(2), pp. 153–162.

Leshem, E. *et al.* (2014) 'Distribution of rotavirus strains and strain-specific effectiveness of the rotavirus vaccine after its introduction: A systematic review and meta-analysis', *The Lancet Infectious Diseases*, 14(9), pp. 847–56.

Li, H. (2011) 'A statistical framework for SNP calling, mutation discovery, association mapping and population genetical parameter estimation from sequencing data', *Bioinformatics*, 27(21), pp. 2987–2993.

Li, H. and Durbin, R. (2009) 'Fast and accurate short read alignment with Burrows-Wheeler transform', *Bioinformatics*, 25(14), pp. 1754–1760.

Li, J. *et al.* (2019) 'Effectiveness of Lanzhou lamb rotavirus vaccine in preventing gastroenteritis among children younger than 5 years of age', *Vaccine*, 37(27), pp. 3611–3616.

Li, L. *et al.* (2010) 'Multiple diverse circoviruses infect farm animals and are commonly found in human and chimpanzee feces', *Journal of Virology*, 84(4), pp. 1674–82.

Linhares, A. C. *et al.* (2008) 'Efficacy and safety of an oral live attenuated human rotavirus vaccine against rotavirus gastroenteritis during the first 2 years of life in Latin American infants: a randomised, double-blind, placebo-controlled phase III study', *The Lancet*, 371, pp. 1181–89.

Liu, L. *et al.* (2014) 'Global, regional, and national causes of child mortality in 2000–13, with projections to inform post-2015 priorities: an updated systematic analysis', *The Lancet*, 385(9966), pp. 430–440.

Liu, Yang *et al.* (2012) 'Rotavirus VP8*: Phylogeny, Host Range, and Interaction with Histo-Blood Group Antigens', *Journal of Virology*, 86(18), pp. 9899–9910.

Lloyd, M. B. *et al.* (2010) 'Rotavirus Gastroenteritis and Seizures in Young Children', *Pediatric Neurology*. Elsevier Inc., 42(6), pp. 404–408.

López, S. *et al.* (1994) 'Mapping the subgroup epitopes of rotavirus protein VP6.', *Virology*, pp. 153–162.

López, S. and Arias, C. F. (2004) 'Multistep entry of rotavirus into cells: a Versaillesque dance.', *Trends in Microbiology*, 12(6), pp. 271–278.

Lopman, B. A. *et al.* (2011) 'Infant rotavirus vaccination may provide indirect protection to older children and adults in the United States.', *The Journal of Infectious Diseases*, 204(7), pp. 980–6.

Losonsky, G. *et al.* (1986) 'Safety, infectivity, transmissibility and immunogenicity ofrhesus rotavirus vaccine (MMU 18006) in infants.', *Pediatric Infectious Disease Journal*, 5(1), pp. 25–29.

Losonsky, G. A. *et al.* (1988) 'Systemic and mucosal immune responses to rhesus rotavirus vaccine MMU 18006', *Pediatric Infectious Disease Journal*, 7(6), pp. 388–93.

Losonsky, G. A. and Reymann, M. (1990) 'The immune response in primary asymptomatic and symptomatic rotavirus infection in newborn infants', *Journal of Infectious Diseases*, 161(2), pp. 330–332.

Lu, X. *et al.* (2008) 'Mechanism for Coordinated RNA Packaging and Genome Replication by Rotavirus Polymerase VP1', *Structure*, 16(11), pp. 1678–1688.

Luchs, A. and Sampaio Tavares Timenetsky, M. do C. (2016) 'Group A rotavirus gastroenteritis: post-vaccine era, genotypes and zoonotic transmission', *Einstein (São Paulo)*, 14(2), pp. 278–287.

Lundgren, O. *et al.* (2000) 'Role of the enteric nervous system in the fluid and electrolyte secretion of rotavirus diarrhea', *Science*, 287(5452), pp. 491–495.

Lundgren, O. and Svensson, L. (2001) 'Pathogenesis of Rotavirus diarrhea', *Microbes and Infection*, 3(13), pp. 1145–1156.

M'Rabet, L. *et al.* (2008) 'Breast-feeding and its role in early development of the immune system in infants: consequences for health later in life.', *The Journal of nutrition*, 138(9), pp. 1782S-1790S.

Ma, H. *et al.* (2011) 'Investigations of porcine circovirus type 1 (PCV1) in

vaccine-related and other cell lines.', *Vaccine*, 29(46), pp. 8429–37.
Macadam, A. J. *et al.* (2006) 'Rational Design of Genetically Stable, Live-Attenuated Poliovirus Vaccines of All Three Serotypes: Relevance to Poliomyelitis Eradication', *Journal of Virology*, 80(17), pp. 8653–8663.
Macartney, K. K. and Offit, P. A. (2000) 'Rotaviruses. Methods and Protocols.', in Gray, J. and Desselberger, U. (eds) *Methods in molecular medicine*. New Jersey: Humana Press, Inc., pp. 119–132.
Mackow, E. R. *et al.* (1988) 'The rhesus rotavirus gene encoding protein VP3: location of amino acids involved in homologous and heterologous rotavirus neutralization and identification of a putative fusion region.', *Proceedings of the National Academy of Sciences USA*, 85(3), pp. 645–649.
Madhi, S. A. *et al.* (2010) 'Effect of human rotavirus vaccine on severe diarrhea in African infants', *New England Journal of Medicine*, 362(4), pp. 289–298.
Madore, H. P. *et al.* (1992) 'Field Trial of Rhesus Rotavirus or Human-Rhesus Rotavirus Reassortant Vaccine of VP7 Serotype 3 or 1 Specificity in Infants', *Journal of Infectious Diseases*, 166(2), pp. 235–243.
Maffey, L. *et al.* (2016) 'Anti-VP6 VHH: An experimental treatment for rotavirus a-associated disease', *PLoS one*, 11(9), pp. 1–27.
Majid, L. *et al.* (2015) 'Deep sequencing for evaluation of genetic stability of influenza A/California/07/2009 (H1N1) vaccine viruses', *PLoS one*, 10(9), pp. 1–18.
Majumdar, M. *et al.* (2018) 'Isolation of Vaccine-Like Poliovirus Strains in Sewage Samples From the United Kingdom', *The Journal of Infectious Diseases*, 217(8), pp. 1222–1230.
Malherbe, H. and Harwin, R. (1963) 'The cytopathic effects of vervet monkey viruses.', *South African Medical Journal*, 37, pp. 407–11.
Malm, M. *et al.* (2017) 'Rotavirus capsid VP6 tubular and spherical nanostructures act as local adjuvants when co-delivered with norovirus VLPs', *Clinical and Experimental Immunology*, 189(3), pp. 331–341.
Mankertz, A. *et al.* (1997) 'Mapping and characterization of the origin of DNA replication of porcine circovirus', *Journal of Virology*, 71(3), pp. 2562–2566.
Mankertz, A. *et al.* (2003) 'New reporter gene-based replication assay reveals exchangeability of replication factors of porcine circovirus types 1 and 2.', *Journal of Virology*, 77(18), pp. 9885–93.
Mankertz, A. *et al.* (2004) 'Molecular biology of Porcine circovirus: analyses of gene expression and viral replication.', *Veterinary Microbiology*, 98(2), pp. 81–8.
Mankertz, A. (2012) 'Molecular interactions of porcine circoviruses type 1 and type 2 with its host', *Virus Research*, 164(1–2), pp. 54–60.
Mankertz, A. and Hillenbrand, B. (2001) 'Replication of porcine circovirus type 1 requires two proteins encoded by the viral rep gene', *Virology*, 279(2), pp. 429–438.
Mankertz, A. and Hillenbrand, B. (2002) 'Analysis of transcription of porcine circovirus type 1', *Journal of General Virology*, 83(Pt 11), pp. 2743–

2751.
Marionneau, S. *et al.* (2001) 'ABH and Lewis histo-blood group antigens, a model for the meaning of oligosaccharide diversity in the face of a changing world', *Biochimie*, 83(7), pp. 565–573.
Markkula, J. *et al.* (2017) 'Rotavirus epidemiology 5–6 years after universal rotavirus vaccination: persistent rotavirus activity in older children and elderly', *Infectious Diseases*, 49(5), pp. 388–395.
Marlow, R. *et al.* (2015) 'Assessing the impacts of the first year of rotavirus vaccination in the United Kingdom', *Eurosurveillance*, 20(48), p. 30077.
Marshall, J. A. *et al.* (1984) 'Virus and virus-like particles in the faeces of cats with and without diarrhoea.', *Australian Veterinary Journal*, 61(2), pp. 33–38.
Marshall, J. A. *et al.* (1987) 'Virus and virus-like particles in the faeces of cats with and without diarrhoea.', *Australian Veterinary Journal*, 64(4), pp. 100–105.
Martella, V. *et al.* (2010) 'Zoonotic aspects of rotaviruses', *Veterinary Microbiology*, 140(3–4), pp. 246–255.
Marthaler, D. *et al.* (2014) 'Widespread rotavirus H in domesticated pigs, United States', *Emerging Infectious Diseases*, 20(7), pp. 1195–1198.
Martin, M. (Hrsg) (2000) *Gastroenterologische Aspekte in der Naturheilkunde*. ISBN 3-930620-29-4; S.31.
Martínez-Laso, J. *et al.* (2009) 'Diversity of the G3 genes of human rotaviruses in isolates from Spain from 2004 to 2006: Cross-species transmission and inter-genotype recombination generates alleles', *Journal of General Virology*, 90(4), pp. 935–943.
Mathieu, M. *et al.* (2001) 'Atomic structure of the major capsid protein of rotavirus: implications for the architecture of the virion.', *The EMBO journal*, 20(7), pp. 1485–1497.
Matson, D. O. *et al.* (1993) 'Fecal Antibody Responses to Symptomatic and Asymptomatic Rotavirus Infections', *Journal of Infectious Diseases*, 167(3), pp. 577–583.
Matthijnssens, J., Ciarlet, M., Heiman, E., *et al.* (2008) 'Full genome-based classification of rotaviruses reveals a common origin between human Wa-like and porcine rotavirus strains and human DS-1-like and bovine rotavirus strains.', *Journal of Virology*, 82(7), pp. 3204–3219.
Matthijnssens, J., Ciarlet, M., Rahman, M., *et al.* (2008) 'Recommendations for the classification of group A rotaviruses using all 11 genomic RNA segments.', *Archives of Virology*, 153(8), pp. 1621–9.
Matthijnssens, J. *et al.* (2009) 'Rotavirus disease and vaccination: impact on genotype diversity.', *Future Microbiology*, 4(10), pp. 1303–16.
Matthijnssens, J. *et al.* (2010) 'Phylodynamic Analyses of Rotavirus Genotypes G9 and G12 Underscore Their Potential for Swift Global Spread', *Molecular Biology and Evolution*, 27(10), pp. 2431–2436.
Matthijnssens, J. *et al.* (2011) 'Uniformity of rotavirus strain nomenclature proposed by the Rotavirus Classification Working Group (RCWG).', *Archives of Virology*, 156(8), pp. 1397–413.
Matthijnssens, J. *et al.* (2012) 'VP6-sequence-based cutoff values as a criterion for rotavirus species demarcation', *Archives of Virology*, 157(6), pp. 1177–1182.

Mattion, N. M. *et al.* (1991) 'Expression of rotavirus proteins encoded by alternative open reading frames of genome segment 11', *Virology*, 181(1), pp. 295–304.

McClain, B. *et al.* (2010) 'X-ray crystal structure of the rotavirus inner capsid particle at 3.8 A resolution.', *Journal of molecular biology*, 397(2), pp. 587–599.

McClenahan, S. D., Krause, P. R. and Uhlenhaut, C. (2011) 'Molecular and infectivity studies of porcine circovirus in vaccines.', *Vaccine*, 29(29–30), pp. 4745–53.

McCowan, C. *et al.* (2018) 'A novel group A rotavirus associated with acute illness and hepatic necrosis in pigeons (Columba livia), in Australia', *PLoS one*, 13(9), pp. 1–16.

McDonald, S. M., Matthijnssens, J., *et al.* (2009) 'Evolutionary dynamics of human rotaviruses: balancing reassortment with preferred genome constellations.', *PLoS pathogens*, 5(10), p. e1000634.

McDonald, S. M., Aguayo, D., *et al.* (2009) 'Shared and Group-Specific Features of the Rotavirus RNA Polymerase Reveal Potential Determinants of Gene Reassortment Restriction', *Journal of Virology*, 83(12), pp. 6135–6148.

McDonald, S. M. *et al.* (2016) 'Reassortment in segmented RNA viruses: mechanisms and outcomes.', *Nature Reviews Microbiology*, 14(7), pp. 448–60.

McDonald, S. M. and Patton, J. T. (2011a) 'Assortment and packaging of the segmented rotavirus genome.', *Trends in Microbiology*, 19(3), pp. 136–44.

McDonald, S. M. and Patton, J. T. (2011b) 'Rotavirus VP2 Core Shell Regions Critical for Viral Polymerase Activation', *Journal of Virology*, 85(7), pp. 3095–3105.

McNeal, M. M. *et al.* (2005) 'Development of a Rotavirus-Shedding Model in Rhesus Macaques, Using a Homologous Wild-Type Rotavirus of a New P Genotype', *Journal of Virology*, 79(2), pp. 944–954.

McNeal, M. M. *et al.* (2006) 'Protection against rotavirus shedding after intranasal immunization of mice with a chimeric VP6 protein does not require intestinal IgA', *Virology*, 346(2), pp. 338–347.

Mebus, C. A. *et al.* (1969a) 'Calf diarrhea (Scours): reproduced with a virus from a field outbreak', *Research Bulletin: Bulletin of the Agricultural Experiment Station of Nebraska*, 233, pp. 1–16.

Mebus, C. A. *et al.* (1969b) 'Further studies on neonatal calf diarrhea virus.', *Proceedings, annual meeting of the United States Animal Health Association*, 73, pp. 97–9.

Meehan, B. M. *et al.* (1997) 'Sequence of porcine circovirus DNA: affinities with plant circoviruses.', *Journal of General Virology*, 78(1), pp. 221–227.

Meehan, B. M. *et al.* (1998) 'Characterization of novel circovirus DNAs associated with wasting syndromes in pigs.', *Journal of General Virology*, 79(Pt 9), pp. 2171–9.

MerckVaccines.com (2018) *Dosage and administration for RotaTeq®.*, *MerkVaccines.com*. Available at: https://www.merckvaccines.com/products/rotateq/dosage-and-administration/ (Accessed: 22 November 2018).

Mesa, M. C. *et al.* (2010) 'A TGF-β mediated regulatory mechanism modulates the T cell immune response to rotavirus in adults but not in children', *Virology*, 399(1), pp. 77–86.

Midthun, K. *et al.* (1985) 'Reassortant rotaviruses as potential live rotavirus vaccine candidates.', *Journal of Virology*, 53(3), pp. 949–954.

Mihalov-Kovács, E. *et al.* (2015) 'Candidate new rotavirus species in sheltered dogs, Hungary', *Emerging Infectious Diseases*, 21(4), pp. 660–663.

Mihatsch, W., Hoegel, J. and Pohlandt, F. (2006) 'Prebiotic oligosaccharides reduce stool viscosity and accelerate gastrointestinal transport in preterm infants', *Acta Paediatrica*, 95(7), pp. 843–848.

Mijatovic-Rustempasic, S. *et al.* (2017) 'Shedding of porcine circovirus type 1 DNA and rotavirus RNA by infants vaccinated with Rotarix®', *Human Vaccines & Immunotherapeutics*, 0(0), pp. 1–8.

Mikami, T. *et al.* (2004) 'An outbreak of gastroenteritis during school trip caused by serotype G2 group A rotavirus', *Journal of Medical Virology*, 73(3), pp. 460–464.

Minor, P. D. (1993) 'Attenuation and reversion of the Sabin vaccine strains of poliovirus.', *Developments in Biological Standardization*, 78, pp. 17–26.

Minor, P. D. (2015) 'Live attenuated vaccines: Historical successes and current challenges', *Virology*. Elsevier, 479–480, pp. 379–392.

Mitchell, J. L., Botas-Perez, L., *et al.* (no date) 'Shedding and genetic stability of PCV1 DNA in infants vaccinated with Rotarix® in the UK', *Unpublished*.

Mitchell, J. L., Lui, Y., *et al.* (no date) 'Stability assessment of two monovalent rotavirus vaccines by next generation sequencing.', *Unpublished*.

Miura, H. *et al.* (2017) 'Rotavirus vaccine strain transmission by vaccinated infants in the foster home.', *Journal of Medical Virology*, 89(1), pp. 79–84.

Mladenova, Z. *et al.* (2011) 'Genetic characterization of bulgarian rotavirus isolates and detection of rotavirus variants: challenges for the rotavirus vaccine program?', *Journal of Medical Virology*, 83(2), pp. 348–356.

De Mol, P. *et al.* (1986) 'Failure of live, attenuated oral rotavirus vaccine.', *The Lancet*, 2(8498), p. 108.

Molinari, B. L. D. *et al.* (2014) 'Species H Rotavirus Detected in Piglets with Diarrhoea, Brazil, 2012', *Emerging Infectious Diseases*, 20(6), pp. 1019–22.

Molto, Y. *et al.* (2011) 'Reduction of Diarrhea-associated Hospitalizations Among Children Aged < 5 Years in Panama Following the Introduction of Rotavirus Vaccine', *The Pediatric Infectious Disease Journal*, 30(1), pp. S16–S20.

Monnier, N. *et al.* (2006) 'High-resolution molecular and antigen structure of the VP8* core of a sialic acid-independent human rotavirus strain.', *Journal of Virology*, 80(3), pp. 1513–1523.

Moon, S.-S. *et al.* (2016) 'Prevaccination Rotavirus Serum IgG and IgA Are Associated With Lower Immunogenicity of Live, Oral Human Rotavirus Vaccine in South African Infants', *Clinical Infectious*

Diseases, 62(2), pp. 157–165.

Moon, S. *et al.* (2010) 'Inhibitory Effect of Breast Milk on Infectivity of Live Oral Rotavirus Vaccines', *Pediatric Infectious Disease*, 29(10), pp. 919–923.

Moon, S., Tate, J., *et al.* (2013) 'Differential Profiles and Inhibitory Effect on Rotavirus Vaccines of Nonantibody Components in Breast Milk From Mothers in Developing and Developed Countries', *Pediatric Infectious Disease*, 32(8), pp. 863–870.

Moon, S., Wang, Y., *et al.* (2013) 'Dose sparing and enhanced immunogenicity of inactivated rotavirus vaccine administered by skin vaccination using a microneedle patch', *Vaccine*, 31(34), pp. 3396–3402.

Morelli, M., Dennis, A. F. and Patton, J. T. (2015) 'Putative E3 ubiquitin ligase of human rotavirus inhibits NF-κB activation by using molecular mimicry to target β-TrCP', *mBio*, 6(1), pp. 1–13.

Morfopoulou, S. *et al.* (2017) 'Deep sequencing reveals persistence of cell-associated mumps vaccine virus in chronic encephalitis', *Acta Neuropathologica*, 133(1), pp. 139–147.

Mori, I. *et al.* (2002) 'Prolonged shedding of rotavirus in a geriatric inpatient', *Journal of Medical Virology*, 67(4), pp. 613–615.

Morrow, A. L. *et al.* (2005) 'Human-milk glycans that inhibit pathogen binding protect breast-feeding infants against infectious diarrhea.', *The Journal of Nutrition*, 135(5), pp. 1304–7.

Mossel, E. C. and Ramig, R. F. (2016) 'A Lymphatic Mechanism of Rotavirus Extraintestinal Spread in the Neonatal Mouse A Lymphatic Mechanism of Rotavirus Extraintestinal Spread in the Neonatal Mouse', *Journal of Virology*, 77(November 2003), pp. 2–7.

Moya, A., Holmes, E. C. and González-Candelas, F. (2004) 'The population genetics and evolutionary epidemiology of RNA viruses', *Nature Reviews Microbiology*, 2(4), pp. 279–288.

Mukhopadhya, I. *et al.* (2013) 'Rotavirus shedding in symptomatic and asymptomatic children using reverse transcription-quantitative PCR', *Journal of Medical Virology*, 85(9), pp. 1661–1668.

Murphy, B. R. *et al.* (2003) 'Reappraisal of the Association of Intussusception with the Licensed Live Rotavirus Vaccine Challenges Initial Conclusions', *The Journal of Infectious Diseases*, 187(8), pp. 1301–1308.

Murphy, T. V. *et al.* (2001) 'Intussusception among Infants Given an Oral Rotavirus Vaccine', *New England Journal of Medicine*, 344(8), pp. 564–572.

Mwila, K. *et al.* (2017) 'Contribution of Maternal Immunity to Decreased Rotavirus Vaccine Performance in Low- and Middle-Income Countries.', *Clinical and Vaccine Imunology*, 24(1), pp. e00405-16.

Nagavoshi, S. *et al.* (1980) 'Changes of the Rotavirus Concentration in Faeces During the Course of Acute Gastroenteritis as Determined by the Immune Adherence Hemmagglutination Test', *European Journal of Pediatrics*, 134, pp. 99–102.

Nair, N. *et al.* (2017) 'VP4- and VP7-specific antibodies mediate heterotypic immunity to rotavirus in humans.', *Science Translational Medicine*, 9(395), p. eaam5434.

Nakagawa, Keisuke *et al.* (2017) 'Generation of a novel live rabies vaccine strain with a high level of safety by introducing attenuating mutations in the nucleoprotein and glycoprotein', *Vaccine*. Elsevier Ltd, 35(42), pp. 5622–5628.

Nakagomi, O. *et al.* (1990) 'Molecular identification by RNA-RNA hybridization of a human rotavirus that is closely related to rotaviruses of feline and canine origin', *Journal of Clinical Microbiology*, 28(6), pp. 1198–1203.

Nakata, S. *et al.* (1987) 'Detection of antibody to group B adult diarrhea rotaviruses in humans', *Journal of Clinical Microbiology*, 25(5), pp. 812–818.

Naylor, C. *et al.* (2015) 'Environmental Enteropathy, Oral Vaccine Failure and Growth Faltering in Infants in Bangladesh', *EBioMedicine*, 2(11), pp. 1759–1766.

Newburg, D. S. *et al.* (1998) 'Role of human-milk lactadherin in protection against symptomatic rotavirus infection', *The Lancet*, 351(9110), pp. 1160–1164.

Newton, K. *et al.* (1997) 'Rotavirus nonstructural glycoprotein NSP4 alters plasma membrane permeability in mammalian cells', *Journal of Virology*, 71(12), pp. 9458–9465.

Nilsson, M. *et al.* (2002) 'Incidence and Genetic Diversity of Group C Rotavirus among Adults', *The Journal of Infectious Diseases*, 182(3), pp. 678–684.

Nordgren, J. *et al.* (2014) 'Both Lewis and Secretor Status Mediate Susceptibility to Rotavirus Infections in a Rotavirus Genotype–Dependent Manner', *Clinical Infectious Diseases*, 59(11), pp. 1567–1573.

O'Neal, C. M. *et al.* (1997) 'Rotavirus virus-like particles administered mucosally induce protective immunity.', *Journal of Virology*, 71(11), pp. 8707–17.

O'Ryan, M. (2007) 'Rotarix (RIX4414): an oral human rotavirus vaccine.', *Expert Review of Vaccines*, 6(1), pp. 11–9.

O'Ryan, M. L. *et al.* (1994) 'Anti-Rotavirus G Type-Specific and Isotype-Specific Antibodies in Children with Natural Rotavirus Infections', *Journal of Infectious Diseases*, 169(3), pp. 504–511.

Obert, G., Peiffer, I. and Servin, A. L. (2002) 'Rotavirus-Induced Structural and Functional Alterations in Tight Junctions of Polarized Intestinal Caco-2 Cell Monolayers', *Journal of Virology*, 74(10), pp. 4645–4651.

Offit, P. A. (1996) 'Host Factors Associated with Protection against Rotavirus Disease : The Skies Are Clearing', *The Journal of Infectious Diseases*, 174(Suppl 1), pp. 59–64.

ONS (2018) *Births in England and Wales., Office for National Statistics (ONS)*. Available at: https://www.ons.gov.uk/peoplepopulationandcommunity/birthsdeathsandmarriages/livebirths/bulletins/birthsummarytablesenglandandwales/2014-07-16 (Accessed: 18 June 2019).

Otto, P., Schulze, P. and Herbst, W. (1999) 'Demonstration of group C rotaviruses in fecal samples of diarrheic dogs in Germany', *Archives of Virology*, 144(12), pp. 2467–2473.

Ousingsawat, J. *et al.* (2011) 'Rotavirus toxin NSP4 induces diarrhea by activation of TMEM16A and inhibition of Na+ absorption', *Pflugers Archiv European Journal of Physiology*, 461(5), pp. 579–589.

Pai, C., Shahrabadi, M. and Ince, B. (1985) 'Rapid Diagnosis of Rotavirus Gastroenteritis by a Commercial Latex Agglutination Test', *Journal of Clinical Microbiology*, 22(5), pp. 846–850.

Pane, J. A., Webster, N. L. and Coulson, B. S. (2014) 'Rotavirus Activates Lymphocytes from Non-Obese Diabetic Mice by Triggering Toll-Like Receptor 7 Signaling and Interferon Production in Plasmacytoid Dendritic Cells', *PLoS Pathogens*, 10(3).

Pang, X. L. *et al.* (2004) 'Increased detection of rotavirus using a real time reverse transcription-polymerase chain reaction (RT-PCR) assay in stool specimens from children with diarrhea', *Journal of Medical Virology*, 72(3), pp. 496–501.

Pappenheimer, A. M. and Enders, J. F. (1947) 'An epidemic diarrheal disease of suckling mice. II. Inclusions in the intestinal epithelial cells', *Journal of Experimental Medicine*, 85(4), pp. 417–422.

Parashar, U. D. *et al.* (2003) 'Global illness and deaths caused by rotavirus disease in children', *Emerging Infectious Diseases*, 9(5), pp. 565–572.

Parashar, U. D. *et al.* (2006) 'Severe childhood diarrhea', *Emerging Infectious Diseases*, 12(2), pp. 304–306.

Parashar, U. D., Nelson, E. A. S. and Kang, G. (2013) 'Diagnosis, management, and prevention of rotavirus gastroenteritis in children.', *BMJ*, 347, p. f7204.

Parker, E. P. K. *et al.* (2014) 'Influence of enteric infections on response to oral poliovirus vaccine: A systematic review and meta-analysis', *Journal of Infectious Diseases*, 210(6), pp. 853–864.

Parker, E. P. K., Ramani, S., *et al.* (2018) 'Causes of impaired oral vaccine efficacy in developing countries', *Future Microbiology*, 13(1), pp. 97–118.

Parker, E. P. K., Praharaj, I., *et al.* (2018) 'Influence of the intestinal microbiota on the immunogenicity of oral rotavirus vaccine given to infants in south India', *Vaccine*, 36(2), pp. 264–272.

Parker, E. P. K. (2019) 'Faecal shedding of Rotarix® in vaccinees in the UK, RoVI study.', in *8th European Rotavirus Biology Meeting*. Riga.

Parr, R. D. *et al.* (2006) 'The Rotavirus Enterotoxin NSP4 Directly Interacts with the Caveolar Structural Protein Caveolin-1', *Journal of Virology*, 80(6), pp. 2842–2854.

Parra, G. I. *et al.* (2004) 'Evidence of rotavirus intragenic recombination between two sublineages of the same genotype', *Journal of General Virology*, 85(6), pp. 1713–1716.

Parwani, A. V., Lucchelli, A. and Saif, L. J. (1987) 'Identification of group B rotaviruses with short genome electropherotypes from adult cows with diarrhea', *Journal of Clinical Microbiology*, 34(5), pp. 1303–1305.

Patel, M. *et al.* (2009) 'Oral Rotavirus Vaccines: How Well Will They Work Where They Are Needed Most?', *Journal of Infectious Diseases*, 200(01), pp. 39–48.

Patel, M. *et al.* (2013) 'A systematic review of anti-rotavirus serum IgA antibody titer as a potential correlate of rotavirus vaccine efficacy', *Journal of Infectious Diseases*, 208(2), pp. 284–294.

Patel, M. M. *et al.* (2011) 'Real-world impact of rotavirus vaccination', *Pediatric Infectious Disease Journal*, 30(SUPPL. 1), pp. 1–5.

Patel, M. M. *et al.* (2012) 'Fulfilling the promise of rotavirus vaccines:how far have we come since licensure?', *The Lancet Infectious Diseases*, 12(7), pp. 561–570.

Patel, M., Steele, A. D. and Parashar, U. D. (2012) 'Influence of oral polio vaccines on performance of the monovalent and pentavalent rotavirus vaccines.', *Vaccine*, 30 Suppl 1, pp. A30-5.

Patel, N. C. *et al.* (2012) 'Chronic Rotavirus Infection in an Infant with Severe Combined Immunodeficiency: Successful Treatment by Hematopoietic Stem Cell Transplantation', *Clinical Immunology*, 142(3), pp. 399–401.

PATH (2018) *India-made rotavirus vaccine achieves World Health Organization prequalification.* Available at: https://www.path.org/media-center/india-made-rotavirus-vaccine-achieves-world-health-organization-prequalification/ (Accessed: 26 November 2018).

Patton, J. T. *et al.* (1996) 'cis-Acting Signals That Promote Genome Replication in Rotavirus mRNA', *Journal of Virology*, 70(6), pp. 3961–3971.

Patton, J. T. (2012) 'Rotavirus diversity and evolution in the post-vaccine world.', *Discovery Medicine*, 13(68), pp. 85–97.

Paul, A. (2002) 'RNA-dependent RNA polymerases, viruses, and RNA silencing', *Science*, 296(5571), pp. 1270–1273.

Paulke-Korinek, M. *et al.* (2011) 'Herd immunity after two years of the universal mass vaccination program against rotavirus gastroenteritis in Austria', *Vaccine*. Elsevier Ltd, 29(15), pp. 2791–2796.

Payne, D. C. *et al.* (2010) 'Sibling transmission of vaccine-derived rotavirus (RotaTeq) associated with rotavirus gastroenteritis.', *Pediatrics*, 125(2), pp. 438–441.

Payne, D. C. (2019) 'US experience with RV vaccination', in *6th European Expert Meeting on Rotavirus Vaccination*. Riga.

Pedley, S. *et al.* (1983) 'Molecular Characterization of Rotaviruses with Distinct Group Antigens', *Journal of General Virology*, 64(10), pp. 2093–2101.

Periz, J. *et al.* (2013) 'Rotavirus mRNAS are released by transcript-specific channels in the double-layered viral capsid', *Proceedings of the National Academy of Sciences*, 110(29), pp. 12042–12047.

Peter, G. *et al.* (2002) 'Intussusception, rotavirus, and oral vaccines: summary of a workshop', *Pediatrics*, 110(6), p. e67.

Peters, G. A. *et al.* (2012) 'The Attenuated Genotype of Varicella-Zoster Virus Includes an ORF0 Transitional Stop Codon Mutation', *Journal of Virology*, 86(19), pp. 10695–10703.

Petitpas, I. *et al.* (1998) 'Crystallization and preliminary X-Ray analysis of rotavirus protein VP6.', *Journal of Virology*, 72(9), pp. 7615–9.

Phan, T. G. *et al.* (2007) 'Evidence of Intragenic Recombination in G1 Rotavirus VP7 Genes', *Journal of Virology*, 81(18), pp. 10188–10194.

Phan, T. G. *et al.* (2016) 'Detection of a novel circovirus PCV3 in pigs with cardiac and multi-systemic inflammation.', *Virology journal*, 13(1), p. 184.

PHE (2014) ‘National rotavirus immunisation programme: preliminary data for England, October 2013 to September 2014.’, *Health Protection Report. Weekly Report.*, 8(41), pp. 1–6.

PHE (2015) ‘National rotavirus immunisation programme : preliminary data for England, February 2014 to July 2015.’, *Health Protection Report. Weekly Report.*, 9(30), pp. 2–7.

PHE (2016a) ‘National rotavirus immunisation programme update : preliminary vaccine coverage for England , August 2015 to January 2016.’, *Health Protection Report. Weekly Report.*, 10(8), pp. 8–11.

PHE (2016b) ‘National rotavirus immunisation programme update : preliminary vaccine coverage for England , February 2016 to July 2016’, *Health Protection Report. Weekly Report.*, 10(32), pp. 1–5.

Phillips, G. *et al.* (2010) ‘Asymptomatic rotavirus infections in England: Prevalence, characteristics, and risk factors’, *American Journal of Epidemiology*, 171(9), pp. 1023–1030.

Phua, K. B. *et al.* (2005) ‘Evaluation of RIX4414, a live, attenuated rotavirus vaccine, in a randomized, double-blind, placebo-controlled phase 2 trial involving 2464 Singaporean infants.’, *The Journal of Infectious Diseases*, 192(Suppl 1), pp. S6–S16.

Pichichero, M. E. (1990) ‘Effect of breast-feeding on oral rhesus rotavirus vaccine seroconversion: A metaanalysis’, *Journal of Infectious Diseases*, 162(3), pp. 753–755.

Pitzer, V. E. *et al.* (2011) ‘Modeling rotavirus strain dynamics in developed countries to understand the potential impact of vaccination on genotype distributions’, *Proceedings of the National Academy of Sciences*, 108(48), pp. 19353–19358.

Pollard, S. L. *et al.* (2015) ‘Estimating the herd immunity effect of rotavirus vaccine’, *Vaccine*, 33(32), pp. 3795–3800.

Pollock, L. *et al.* (2018) ‘Nonsecretor Histo–blood Group Antigen Phenotype Is Associated With Reduced Risk of Clinical Rotavirus Vaccine Failure in Malawian Infants’, *Clinical Infectious Diseases*, (December), pp. 1–7.

Pollock, L. E. (2018) *Predictors of vaccine viral replication, immune response and clinical protection following oral rotavirus vaccination in Malawian children.* University of Liverpool.

Pollock, L. E. (2019) ‘Faecal shedding of Rotarix® in vaccinees in Malawi (personal communication).’, in *8th European Biology Meeting*. Riga.

Pongsuwanna, Y. *et al.* (2002) ‘Detection of a human rotavirus with G12 and P[9] specificity in Thailand’, *Journal of Clinical Microbiology*, 40(4), pp. 1390–1394.

Poole, E. and Penny, S. M. (2018) ‘Pediatric Intussusception: The Cinnamon Bun Sign’, *Journal of Diagnostic Medical Sonography*, 34(4), pp. 275–280.

Potgieter, A. C. *et al.* (2009) ‘Improved strategies for sequence-independent amplification and sequencing of viral double-stranded RNA genomes.’, *The Journal of General Virology*, 90(Pt 6), pp. 1423–32.

Powell, M. *et al.* (2015) ‘Guidelines on Clinical Evaluation of Vaccines: Regulatory Expectations’, *World Health Organization - Draft*, (29 October), pp. 1–102.

Prasad, B. V and Chiu, W. (1994) ‘Structure of rotavirus.’, *Current Topics in*

Microbiology and Immunology, 185, pp. 9–29.

Prelog, M. *et al.* (2016) 'Universal mass vaccination against Rotavirus: indirect effects on Rotavirus infections in neonates and non-vaccinated small infants not eligible for vaccination.', *The Journal of Infectious Diseases*, 214(4), pp. 546–555.

Quintanar-Solares, M. *et al.* (2011) 'Impact of Rotavirus Vaccination on Diarrhea-related Hospitalizations Among Children < 5 Years of Age in Mexico', *The Pediatric Infectious Disease Journal*, 30(1), pp. S11–S15.

Rahman, M., Banik, S., *et al.* (2005) 'Detection and characterization of human group C rotaviruses in Bangladesh', *Journal of Clinical Microbiology*, 43(9), pp. 4460–4465.

Rahman, M., Matthijnssens, J., *et al.* (2005) 'Predominance of rotavirus G9 genotype in children hospitalized for rotavirus gastroenteritis in Belgium during 1999-2003', *Journal of Clinical Virology*, 33(1), pp. 1–6.

Rahman, M. *et al.* (2007) 'Evolutionary History and Global Spread of the Emerging G12 Human Rotaviruses', *Journal of Virology*, 81(5), pp. 2382–2390.

Rahman, M. *et al.* (2008) 'Emerging G9 rotavirus strains in the northwest of China', *Virus Research*, 137(1), pp. 157–162.

Rajasekaran, D. *et al.* (2008) 'The flexible C terminus of the rotavirus non-structural protein NSP4 is an important determinant of its biological properties', *Journal of General Virology*, 89(6), pp. 1485–1496.

Ramachandran, M. *et al.* (1998) 'Lack of maternal antibodies to P serotypes may predispose neonates to infections with unusual rotavirus strains', *Clinical and Diagnostic Laboratory Immunology*, 5(4), pp. 527–530.

Ramani, S., Sankaran, P., *et al.* (2010) 'Comparison of Viral Load and Duration of Virus Shedding in Symptomatic and Asymptomatic Neonatal Rotavirus Infections', *Journal of Medical Virology*, 82, pp. 1803–1807.

Ramani, S., Paul, A., *et al.* (2010) 'Rotavirus Antigenemia in Indian Children with Rotavirus Gastroenteritis and Asymptomatic Infections', *Clinical Infectious Diseases*, 51(11), pp. 1284–1289.

Ramig, R. F. (1997) 'Genetics of the Rotaviruses', *Annual Review of Microbiology*, 51(1), pp. 225–255.

Ranucci, C. S., Tagmyer, T. and Duncan, P. (2011) 'Adventitious Agent Risk Assessment Case Study: Evaluation of RotaTeq(R) for the Presence of Porcine Circovirus', *PDA Journal of Pharmaceutical Science and Technology*, 65(6), pp. 589–598.

Rathi, N. *et al.* (2018) 'A Phase III open-label, randomized, active controlled clinical study to assess safety, immunogenicity and lot-to-lot consistency of a bovine-human reassortant pentavalent rotavirus vaccine in Indian infants', *Vaccine*, 36(52), pp. 7943–7949.

RCWG (2018) *Rotavirus: List of accepted new genotypes., Rotavirus Classification Working Group (RCWG) KU Leuven Laboratory of Viral Metagenomics*. Available at: https://rega.kuleuven.be/cev/viralmetagenomics/virus-classification/rcwg (Accessed: 12 November 2018).

Rennels, M. B. (1996) 'Influence Of Breast-Feeding And Oral Poliovirus

Vaccine On The Immunogenicity And Efficacy Of Rotavirus Vaccines', *Journal of Infectious Diseases*, 174(Suppl 1), pp. S107–S111.

Rennels, M. B. *et al.* (1996) 'Safety and efficacy of high-dose rhesus-human reassortant rotavirus vaccines--report of the National Multicenter Trial. United States Rotavirus Vaccine Efficacy Group.', *Pediatrics*, 97(1), pp. 7–13.

Resch, T. K. *et al.* (2018) 'Inactivated rotavirus vaccine by parenteral administration induces mucosal immunity in mice', *Nature Scientific Reports*, 8(1), pp. 1–11.

Richardson, S. *et al.* (1998) 'Extended excretion of rotavirus after severe diarrhoea in young children', *The Lancet*, 351(9119), pp. 1844–1848.

Riemersma, K. K. *et al.* (2018) 'Chikungunya Virus Fidelity Variants Exhibit Differential Attenuation and Population Diversity in Cell Culture and Adult Mice', *Journal of Virology*, 93(3), pp. 1–19.

Rivera, L. *et al.* (2011) 'Horizontal transmission of a human rotavirus vaccine strain-A randomized, placebo-controlled study in twins', *Vaccine*, 29(51), pp. 9508–9513.

Rivero-Calle, I., Gómez-Rial, J. and Martinón-Torres, F. (2016) 'Systemic features of rotavirus infection.', *The Journal of Infection*, 72, pp. S98–S105.

Robinson, J. T. (2012) 'Integrated genomics viewer', *Nature Biotechnology*, 29(1), pp. 24–26.

Roczo-Farkas, S. *et al.* (2018) 'The impact of rotavirus vaccines on genotype diversity: A comprehensive analysis of 2 decades of australian surveillance data', *Journal of Infectious Diseases*, 218(4), pp. 546–554.

Rodger, S. M., Bishop, R. F. and Holmes, I. H. (1982) 'Detection of rotavirus-like agent associated with diarrhea in an infant', *Journal of Clinical Microbiology*, 16(4), pp. 724–726.

Rodríguez-Díaz, J. *et al.* (2017) 'Relevance of secretor status genotype and microbiota composition in susceptibility to rotavirus and norovirus infections in humans', *Scientific Reports*, 7(February), p. 45559.

Rodriguez, W. J. *et al.* (1979) 'Common exposure outbreak of gastroenteritis due to type 2 rotavirus with high secondary attack rate within families', *Journal of Infectious Diseases*, 140(3), pp. 353–357.

Rojas, O. L. *et al.* (2003) 'Human rotavirus specific T cells: Quantification by ELISPOT and expression of homing receptors on CD4+ T cells', *Virology*, 314(2), pp. 671–679.

Rongsen-Chandola, T. *et al.* (2014) 'Effect of withholding breastfeeding on the immune response to a live oral rotavirus vaccine in North Indian infants', *Vaccine*, 32(S1), pp. A134–A139.

Rose, J. *et al.* (2017) 'Health impact and cost-effectiveness of a domestically-produced rotavirus vaccine in India: A model based analysis', *PLoS one*, 12(11), pp. 1–16.

Rosen, B. I. *et al.* (1994) 'Serotypic differentiation of rotaviruses in field samples from diarrheic pigs by using nucleic acid probes specific for porcine VP4 and human and porcine VP7 genes', *Journal of Clinical Microbiology*, 32(2), pp. 311–317.

Rosenfeld, L. *et al.* (2017) 'Life-threatening systemic rotavirus infection after

vaccination in severe combined immunodeficiency (SCID)', *Pediatric Allergy and Immunology*, 28(8), pp. 841–843.

Rossignol, J.-F. and El-Gohary, Y. M. (2006) 'Nitazoxanide in the treatment of viral gastroenteritis: a randomized double-blind placebo-controlled clinical trial.', *Alimentary Pharmacology & Therapeutics*, 24(10), pp. 1423–30.

Rossignol, J. F. *et al.* (2006) 'Effect of nitazoxanide for treatment of severe rotavirus diarrhoea: randomised double-blind placebo-controlled trial', *The Lancet*, 368(9530), pp. 124–129.

RotaCouncil&ViewHubRV (2018) *Current Rotavirus Vaccine Introduction Map (as of August 2018)*. Available at: http://rotacouncil.org/vaccine-introduction/global-introduction-status/ (Accessed: 22 November 2018).

RotaCouncil (2018) *Rotavirus vaccines: Global introduction status.*, *RotaCouncil*. Available at: http://rotacouncil.org/vaccine-introduction /global-introduction-status/ (Accessed: 18 June 2019).

Ruiz-Palacios, G. M. *et al.* (2006) 'Safety and efficacy of an attenuated vaccine against severe rotavirus gastroenteritis.', *The New England Journal of Medicine*, 354(1), pp. 11–22.

Ruiz-Palacios, G. M. *et al.* (2007) 'Dose response and efficacy of a live, attenuated human rotavirus vaccine in Mexican infants.', *Pediatrics*, 120(2), pp. e253–e261.

Ryan, M. J. *et al.* (1997) 'Outbreaks of infectious intestinal disease in residential institutions in England and Wales 1992-1994', *Journal of Infection*, 34(1), pp. 49–54.

Saif, L. J. *et al.* (1980) 'Rotavirus-like, calicivirus-like, and 23-nm virus-like particles associated with diarrhea in young pigs.', *Journal of Clinical Microbiology*, 12(1), pp. 105–11.

Saif, L. J. *et al.* (1996) 'The gnotobiotic piglet as a model for studies of disease pathogenesis and immunity to human rotaviruses.', *Archives of virology. Supplementum*, 12, pp. 153–61.

Sakon, N., Miyamoto, R. and Komano, J. (2017) 'An infant with acute gastroenteritis caused by a secondary infection with a Rotarix-derived strain', *European Journal of Pediatrics*, 176(9), pp. 1275–1278.

Salas, A. *et al.* (2019) 'Impact of rotavirus vaccination on childhood hospitalizations for seizures: Heterologous or unforeseen direct vaccine effects?', *Vaccine*, 37(25), pp. 3362–3368.

Salinas, B. *et al.* (2005) 'Evaluation of safety, immunogenicity and efficacy of an attenuated rotavirus vaccine, RIX4414: a randomized, placebo-controlled trial in Latin American infants.', *The Pediatric Infectious Disease Journal*, 24(9), pp. 807–16.

Sánchez, G. *et al.* (2003) 'Evidence for quasispecies distributions in the human hepatitis A virus genome', *Virology*, 315(1), pp. 34–42.

Sanjuán, R. *et al.* (2010) 'Viral Mutation Rates', *Journal of Virology*, 84(19), pp. 9733–9748.

Santos, N. and Hoshino, Y. (2005) 'Global distribution of rotavirus serotypes/genotypes and its implication for the development and implementation of an effective rotavirus vaccine.', *Reviews in Medical Virology*, 15(1), pp. 29–56.

Santosham, M. *et al.* (1991) 'A Field Study of the Safety and Efficacy of Two

Candidate Rotavirus Vaccines in a Native American Population', *The Journal of Infectious Diseases*, 163(3), pp. 483–487.

Santosham, M. *et al.* (1997) 'Efficacy and safety of high-dose rhesus-human reassortant rotavirus vaccine in Native American populations', *Journal of Pediatrics*, 131(4), pp. 632–638.

Sarkar, T. *et al.* (2014) 'In silico study of potential autoimmune threats from rotavirus infection', *Computational Biology and Chemistry*, 51, pp. 51–56.

Sarker, S. A. *et al.* (2013) 'Anti-rotavirus protein reduces stool output in infants with diarrhea: A randomized placebo-controlled trial', *Gastroenterology*, 145(4), pp. 740–748.

Sato, T. and Clevers, H. (2013) 'Growing Self-Organizing Mini-Guts from a Single Intestinal Stem Cell: Mechanism and Applications', *Science*, 340(6137), pp. 1190–1194.

Saulsbury, F. T., Winkelstein, J. A. and Yolken, R. H. (1980) 'Chronic rotavirus infection in immunodeficiency', *The Journal of Pediatrics*, 97(1), pp. 61–65.

Saxena, K. *et al.* (2016) 'Human Intestinal Enteroids : a New Model To Study Human Rotavirus Infection , Host Restriction , and Pathophysiology', *Journal of Virology*, 90(1), pp. 43–56.

Saxena, K. *et al.* (2017) 'A paradox of transcriptional and functional innate interferon responses of human intestinal enteroids to enteric virus infection.', *Proceedings of the National Academy of Sciences USA*, 114(4), pp. E570–E579.

Sayle, R. and Milner-White, E. (1995) 'RasMol: Biomolecular graphics for all.', *Trends in Biochemical Sciences*, 20(9), pp. 374–376.

Scholtens, P. A. M. J. *et al.* (2008) 'Fecal Secretory Immunoglobulin A Is Increased in Healthy Infants Who Receive a Formula with Short-Chain Galacto-Oligosaccharides and Long-Chain Fructo-Oligosaccharides', *The Journal of Nutrition*, 138(6), pp. 1141–1147.

Sen, A. *et al.* (2009) 'IRF3 inhibition by rotavirus NSP1 is host cell and virus strain dependent but independent of NSP1 proteasomal degradation', *Journal of Virology*, 83(20), pp. 10322–10335.

Sen, A. *et al.* (2014) 'Rotavirus NSP1 protein inhibits interferon-mediated STAT1 activation', *Journal of Virology*, 88(1), pp. 41–53.

Sen, A. *et al.* (2019) 'Rotavirus infection induces both interferon (IFN) and inflammatory resistance by re-programming intestinal IFN receptor signaling.', *BioRxiv*. doi: 10.1101/702837.

Settembre, E. C. *et al.* (2011) 'Atomic model of an infectious rotavirus particle.', *The EMBO journal*, 30(2), pp. 408–16.

Shah, M. P. *et al.* (2018) 'Annual changes in rotavirus hospitalization rates before and after rotavirus vaccine implementation in the United States', *PLoS one*, 13(2), pp. 1–14.

Small, C. *et al.* (2007) 'Genome heterogeneity of SA11 rotavirus due to reassortment with "O" agent', *Virology*, 2(359), pp. 415–124.

Soares-Weiser, K. *et al.* (2012) 'Vaccines for preventing rotavirus diarrhoea: vaccines in use.', *The Cochrane Database of Systematic Reviews*, (11), p. CD008521.

Spence, J. R. *et al.* (2011) 'Directed differentiation of human pluripotent stem cells into intestinal tissue in vitro', *Nature*, 470(7332), pp. 105–109.

Srivastava, S. *et al.* (2015) 'Molecular characterization of the rotavirus enterotoxin NSP4 gene of strains causing diarrhoea in children aged 0-5 years in northern India', *Journal of Applied Pharmaceutical Science*, 5(11), pp. 43–49.

Staat, M. A. *et al.* (2011) 'Effectiveness of Pentavalent Rotavirus Vaccine Against Severe Disease', *Pediatrics*, 128(2), pp. e267–e275.

Steele, D. A., Kirkwood, C. D. and Ma, L.-F. (2018) *Next generation rotavirus vaccines, Bill and Melinda Gates Foundation. WHO product development for Vaccines Advisory Committe.* Available at: https://www.who.int/immunization/research/meetings_workshops/23_Steele_Rot_vaccines.pdf?ua=1 (Accessed: 22 July 2019).

Steffen, R. *et al.* (1999) 'Epidemiology, Etiology, and Impact of Traveler ' s Diarrhea in Jamaica', *Journal American Medical Association*, 281(9), pp. 811–817.

Stene, L. C. *et al.* (2006) 'Rotavirus infection frequency and risk of celiac disease autoimmunity in early childhood: A longitudinal study', *American Journal of Gastroenterology*, 101(10), pp. 2333–2340.

Stuker, G., Oshiro, L. S. and Schmidt, N. J. (1980) 'Antigenic Comparisons of Two New Rotaviruses from Rhesus Monkeys', *Journal of Clinical Microbiology*, 11(2), pp. 202–203.

Svensson, L., Sheshberadaran, H., Vesikari, T., *et al.* (1987) 'Immune Response to Rotavirus Polypeptides after Vaccination with Heterologous Rotavirus Vaccines (RIT 4237, RRV-1)', *Journal of General Virology*, 68(Pt 7), pp. 1993–1999.

Svensson, L., Sheshberadaran, H., Vene, S., *et al.* (1987) 'Serum antibody responses to individual viral polypeptides in human rotavirus infections', *Journal of General Virology*, 68(3), pp. 643–651.

Svensson, L. *et al.* (2016) *Viral Gastroenteritis. Molecular epidemiology and pathogenesis.* 1st edn. Elsevier.

Sykes, L. *et al.* (2012) 'The Th1:Th2 Dichotomy of Pregnancy and Preterm Labour', *Mediators of Inflammation*, 2012, pp. 1–12.

Tafazoli, F. *et al.* (2002) 'NSP4 Enterotoxin of Rotavirus Induces Paracellular Leakage in Polarized Epithelial Cells', *Journal of Virology*, 75(3), pp. 1540–1546.

Tam, C. C. and O'Brien, S. J. (2016) 'Economic cost of campylobacter, norovirus and rotavirus disease in the United Kingdom.', *PloS one*, 11(2), p. e0138526.

Tang, B. *et al.* (1997) 'Comparison of the rotavirus gene 6 from different species by sequence analysis and localization of subgroup-specific epitopes using site-directed mutagenesis', *Virology*, 237(1), pp. 89–96.

Taniguchi, K., Kojima, K. and Urasawa, S. (1996) 'Nondefective rotavirus mutants with an NSP1 gene which has a deletion of 500 nucleotides, including a cysteine-rich zinc finger motif- encoding region (nucleotides 156 to 248), or which has a nonsense codon at nucleotides 153-155', *Journal of virology*, 70(6), pp. 4125–4130.

Taniuchi, M. *et al.* (2016) 'Impact of enterovirus and other enteric pathogens on oral polio and rotavirus vaccine performance in Bangladeshi infants', *Vaccine*, 34(27), pp. 3068–3075.

Tate, J. E. *et al.* (2012) '2008 estimate of worldwide rotavirus-associated

mortality in children younger than 5 years before the introduction of universal rotavirus vaccination programmes: a systematic review and meta-analysis.', *The Lancet Infectious Diseases*, 12(2), pp. 136–141.

Tate, J. E. *et al.* (2013) 'Trends in National Rotavirus Activity Before and After Introduction of Rotavirus Vaccine into the National Immunization Program in the United States , 2000 to 2012', *The Pediatric Infectious Disease Journal*, 32(7), pp. 741–744.

Tate, J. E. *et al.* (2016) 'Global, regional, and national estimates of rotavirus mortality in children <5 years of age, 2000-2013.', *Clinical Infectious Diseases*, 62(Suppl 2), pp. S96–S105.

Tate, J. E. and Parashar, U. D. (2014) 'Rotavirus vaccines in routine use.', *Clinical Infectious Diseases*, 59(9), pp. 1291–301.

'The Caldicott Report.' (1999) *The journal of the Institute of Health Record Information and Management (IHRIM)*, 40(2), pp. 17–19. Available at: http://www.ncbi.nlm.nih.gov/pubmed/10538665 (Accessed: 7 August 2018).

Theil, K. W. *et al.* (1985) 'Porcine rotavirus-like virus (group B rotavirus): Characterization and pathogenicity for gnotobiotic pigs', *Journal of Clinical Microbiology*, 21(3), pp. 340–345.

Thomas, S. L. *et al.* (2017) 'Impact of the national rotavirus vaccination programme on acute gastroenteritis in England and associated costs averted.', *Vaccine*, 35(4), pp. 680–686.

Thouvenin, E. *et al.* (2001) 'Antibody inhibition of the transcriptase activity of the rotavirus DLP: a structural view', *Journal of Molecular Biology*, 307(1), pp. 161–172.

Thu, H. M. *et al.* (2017) 'Chicken Egg Yolk Antibodies (IgY) for Prophylaxis and Treatment of Rotavirus Diarrhea in Human and Animal Neonates: A Concise Review', *Korean Journal for Food Science of Animal Resources*, 37(1), pp. 1–9.

Tian, Y. *et al.* (1993) 'Genomic concatemerization/deletion in rotaviruses: a new mechanism for generating rapid genetic change of potential epidemiological importance.', *Journal of Virology*, 67(11), pp. 6625–32.

Tino De Franco, M. *et al.* (2013) 'Neutralizing activity and secretory IgA antibodies reactive with rotavirus SA-11 (serotype G3) in colostrum and milk from Brazilian women', *Paediatrics and International Child Health*, 33(2), pp. 102–107.

Tischer, I., Rasch, R. and Tochtermann, G. (1974) 'Characterization of papovavirus-and picornavirus-like particles in permanent pig kidney cell lines.', *Zentralblatt für Bakteriologie, Parasitenkunde, Infektionskrankheiten und Hygiene. Erste Abteilung Originale. Reihe A: Medizinische Mikrobiologie und Parasitologie*, 226(2), pp. 153–67.

Tombácz, K. *et al.* (2014) 'Lack of genetic diversity in newly sequenced porcine circovirus type 1 strains isolated 20 years apart.', *Genome Announcements*, 2(2), p. pii: e00156-14.

Torres-Medina, A. (1987) 'Isolation of an atypical rotavirus causing diarrhea in neonatal ferrets.', *Laboratory Animal Science*, 37(2), pp. 167–71.

Tortorici, A. M., Shapiro, B. A. and Patton, J. T. (2006) 'A base-specific recognition signal in the 5′ consensus sequence of rotavirus plus-

strand RNAs promotes replication of the double-stranded RNA genome segments', *RNA*, 12(1), pp. 133–146.

Trask, S. D. *et al.* (2010) 'A rotavirus spike protein conformational intermediate binds lipid bilayers.', *Journal of Virology*, 84(4), pp. 1764–1770.

Trask, S. D. *et al.* (2013) 'Mutations in the rotavirus spike protein VP4 reduce trypsin sensitivity but not viral spread', *Journal of General Virology*, 94(Pt_6), pp. 1296–1300.

Trask, S. D., McDonald, S. M. and Patton, J. T. (2012) 'Structural insights into the coupling of virion assembly and rotavirus replication.', *Nature Reviews Microbiology*, 10(3), pp. 165–77.

Treanor, J. J. *et al.* (1995) 'Evaluation of the protective efficacy of a serotype 1 bovine-human rotavirus reassortant vaccine in infants.', *The Pediatric Infectious Disease Journal*, 14(4), pp. 301–7.

Tsugawa, T., Tatsumi, M. and Tsutsumi, H. (2014) 'Virulence-associated genome mutations of murine rotavirus identified by alternating serial passages in mice and cell cultures.', *Journal of Virology*, 88(10), pp. 5543–5558.

Tsugawa, T. and Tsutsumi, H. (2016) 'Genomic changes detected after serial passages in cell culture of virulent human G1P[8] rotaviruses.', *Infection, Genetics and Evolution*, 45, pp. 6–10.

Tsunemitsu, H. *et al.* (1991) 'Isolation, characterization, and serial propagation of a bovine group C rotavirus in a monkey kidney cell line (MA104)', *Journal of Clinical Microbiology*, 29(11), pp. 2609–2613.

Tuanthap, S. *et al.* (2018) 'Porcine rotavirus C in pigs with gastroenteritis on Thai swine farms, 2011–2016', *Peer Journal*, 6, p. e4724.

Uhnoo, I. *et al.* (1988) 'Immunological aspects of interaction between rotavirus and the intestine in infancy.', *Immunology and Cell Biology*, 66(2), pp. 135–145.

Uhnoo, I., Olding-Stenkvist, E. and Kreuger, A. (1986) 'Clinical features of acute gastroenteritis associated with rotavirus, enteric adenoviruses, and bacteria', *Archives of Disease in Childhood*, 61(8), pp. 732–738.

Uzri, D. and Greenberg, H. B. (2013) 'Characterization of rotavirus RNAs that activate innate immune signaling through the RIG-I-like receptors', *PLoS ONE*, 8(7), pp. 1–14.

Vaccineresources.org (2016) *National RV introductions by geographic region: 81 countries**. Available at: http://www.vaccineresources.org/files/PATH-Worldwide-Rotavirus-Vaccine-Introduction-Map-EN-2016.05.01.pdf (Accessed: 22 November 2018).

Velázquez, F. R. *et al.* (1996) 'Rotavirus infections in infants as protection against subsequent infections', *The New England Journal of Medicine*, 335(14), pp. 1022–8.

Velázquez, F. R. *et al.* (2000) 'Serum antibody as a marker of protection against natural rotavirus infection and disease', *The Journal of Infectious Diseasesfectious diseases*, 182(6), pp. 1602–9.

Velázquez, R. F. *et al.* (2017) 'Efficacy, safety and effectiveness of licensed rotavirus vaccines: A systematic review and meta-analysis for Latin America and the Caribbean', *BMC Pediatrics*, 17(1), pp. 1–12.

Vende, P. *et al.* (2002) 'Efficient Translation of Rotavirus mRNA Requires Simultaneous Interaction of NSP3 with the Eukaryotic Translation Initiation Factor eIF4G and the mRNA 3' End', *Journal of Virology*, 74(15), pp. 7064–7071.

Vesikari, T. *et al.* (1983) 'Immunogenicity and safety of live oral attenuated bovine rotavirus vaccine strain RIT 4237 in adults and young children.', *The Lancet*, 2(8354), pp. 807–11.

Vesikari, T. *et al.* (1985) 'Clinical efficacy of the RIT 4237 live attenuated bovine rotavirus vaccine in infants vaccinated before a rotavirus epidemic', *The Journal of Pediatrics*, 107(2), pp. 189–194.

Vesikari, T. *et al.* (1986) 'A comparative trial of rhesus monkey (RRV-1) and bovine (RIT 4237) oral rotavirus vaccines in young children', *The Journal of Infectious Diseases*, 153(5), pp. 832–839.

Vesikari, T., Karvonen, A., Puustinen, L., *et al.* (2004) 'Efficacy of RIX4414 live attenuated human rotavirus vaccine in Finnish infants.', *The Pediatric infectious disease journal*, 23(10), pp. 937–943.

Vesikari, T., Karvonen, A., Korhonen, T., *et al.* (2004) 'Safety and immunogenicity of RIX4414 live attenuated human rotavirus vaccine in adults, toddlers and previously uninfected infants', *Vaccine*, 22(21), pp. 2836–2842.

Vesikari, T., Clark, H. F., *et al.* (2006) 'Effects of the potency and composition of the multivalent human-bovine (WC3) reassortant rotavirus vaccine on efficacy, safety and immunogenicity in healthy infants', *Vaccine*, 24(22), pp. 4821–4829.

Vesikari, T., Karvonen, A. V., *et al.* (2006) 'Safety, Efficacy, and Immunogenicity of 2 Doses of Bovine-Human (UK) and Rhesus–Rhesus-Human Rotavirus Reassortant Tetravalent Vaccines in Finnish Children', *The Journal of Infectious Diseases*, 194(3), pp. 370–376.

Vesikari, T., Matson, D. O., *et al.* (2006) 'Safety and Efficacy of a Pentavalent Human– Bovine (WC3) Reassortant Rotavirus Vaccine', *New England Journal of Medicine*, 354(1), pp. 23–33.

Vesikari, T. *et al.* (2007) 'Efficacy of human rotavirus vaccine against rotavirus gastroenteritis during the first 2 years of life in European infants: randomised, double-blind controlled study.', *The Lancet*, 370(9601), pp. 1757–63.

Vesikari, T. *et al.* (2009) 'RotaTeq®, a pentavalent rotavirus vaccine: Efficacy and safety among infants in Europe', *Vaccine*, 28(2), pp. 345–351.

Vesikari, T. (2012) 'Rotavirus vaccination: a concise review', *Clinical Microbiology and Infection*, 18, pp. 57–63.

Vesikari, T. (2015) 'Neonatal rotavirus vaccination making headway', *The Lancet Infectious Diseases*, 15(12), pp. 1362–1363.

Vesikari, T., Sarkkinen, H. and Mäki, M. (1981) 'Quantitative Aspects of Rotavirus Excretion in Childhood Diarrhoea', *Acta Pædiatrica*, 70(5), pp. 717–721.

Victoria, J. G. *et al.* (2010) 'Viral nucleic acids in live-attenuated vaccines: detection of minority variants and an adventitious virus.', *Journal of Virology*, 84(12), pp. 6033–6040.

ViewHubRV (2018a) *Rotavirus vaccines: #Children without Access.*, *ViewHub RV*. Available at: http://www.view-

hub.org/viz/ ?YXBwaWQ9MSZpbmRpY2F0b3JpZD0xNTc=# (Accessed: 18 June 2019).

ViewHubRV (2018b) *Rotavirus vaccines: Current vaccine Intro status.*, *ViewHub RV*. Available at: http://www.view-hub.org/viz/ ?YXBwaWQ9MSZpbmRpY2F0 (Accessed: 18 June 2019).

ViewHubRV (2018c) *Rotavirus vaccines: WUENIC (WHO/UNICEF Estimates of National Immunization Coverage) Coverage rates.*, *ViewHub RV*. Available at: http://www.view-hub.org/viz/ ?YXBwaWQ9MSZpbmRpY2F0b3JpZD0xNTc=# (Accessed: 18 June 2019).

Vignuzzi, M. *et al.* (2006) 'Quasispecies diversity determines pathogenesis through cooperative interactions in a viral population', *Nature*, 439(7074), pp. 344–348.

ViralZone (2008) *Circoviridae virion.*, *Swiss Institute of Bioinformatics (SIB)*. Available at: https://viralzone.expasy.org/11?outline=all_by_species (Accessed: 22 November 2018).

ViralZone (2013) *Rotavirus segmented linear dsRNA genome.*, *ViralZone, Swiss Institute of Bioinformatics (SIB)*. Available at: https://viralzone.expasy.org/107?outline=all_by_species (Accessed: 22 November 2018).

De Vos, B. *et al.* (2004) 'A rotavirus vaccine for prophylaxis of infants against rotavirus gastroenteritis.', *The Pediatric infectious disease journal*, 23(10 Suppl), pp. S179–S182.

Wakuda, M. *et al.* (2011) 'Porcine Rotavirus Closely Related to Novel Group of Human Rotaviruses', *Emerging Infectious Diseases*, 17(8), pp. 1491–93.

Wang, Y. *et al.* (2010) 'Inactivated rotavirus vaccine induces protective immunity in gnotobiotic piglets', *Vaccine*, 28(33), pp. 5432–5436.

Wang, Y. *et al.* (2016) 'Skin Vaccination against Rotavirus Using Microneedles: Proof of Concept in Gnotobiotic Piglets', *PLoS one*, 700, pp. 1–15.

Ward, R. L. *et al.* (1986) 'Human rotavirus studies in volunteers: determination of infectious dose and serological response to infection.', *The Journal of Infectious Diseases*, 154(5), pp. 871–80.

Ward, R. L. *et al.* (1989) 'Effects of antibody to rotavirus on protection of adults challenged with a human rotavirus.', *The Journal of Infectious Diseases*, 159(1), pp. 79–88.

Ward, R. L., Sander, D. S., *et al.* (1990) 'Effect of vaccination on serotype-specific antibody responses in Infants administered WC3 bovine rotavirus before or after a natural rotavirus infection', *Journal of Infectious Diseases*, 162(6), pp. 1298–1303.

Ward, R. L., Bernstein, D. I., *et al.* (1990) 'Protection of adults rechallenged with a human rotavirus', *Journal of Infectious Diseases*, 161(3), pp. 440–445.

Ward, R. L. (1996) 'Mechanisms Of Protection Against Rotavirus In Humans And Mice', *Journal of Infectious Diseases*, 174(Supplement 1), pp. S51–S58.

Ward, R. L., Mason, B. B., *et al.* (1997) 'Attenuation of a human rotavirus vaccine candidate did not correlate with mutations in the NSP4

protein gene.', *Journal of Virology*, 71(8), pp. 6267–70.

Ward, R. L., Knowlton, D. R., *et al.* (1997) 'Serologic Correlates of Immunity in a Tetravalent Reassortant Rotavirus Vaccine Trial', *The Journal of Infectious Diseases*, 176(3), pp. 570–577.

Ward, R. L. (2003) 'Possible mechanisms of protection elicited by candidate rotavirus vaccines as determined with the adult mouse model', *Viral Immunology*, 16(1), pp. 17–24.

Ward, R. L. *et al.* (2004) 'Rotavirus immunoglobulin a responses stimulated by each of 3 doses of a quadrivalent human/bovine reassortant rotavirus vaccine', *The Journal of Infectious Diseases*, 189(12), pp. 2290–2293.

Ward, R. L. *et al.* (2006) 'Reductions in cross-neutralizing antibody responses in infants after attenuation of the human rotavirus vaccine candidate 89-12.', *The Journal of Infectious Diseases*, 194(12), pp. 1729–1736.

Ward, R. L. (2008) 'Rotavirus vaccines : how they work or don ' t work', *Expert Reviews in Molecular Medicine*, 10(February), pp. 1–14.

Ward, R. L. and Bernstein, D. I. (1994) 'Protection against Rotavirus Disease after Natural Rotavirus Infection', *Journal of Infectious Diseases*, 169(4), pp. 900–904.

Ward, R. L. and McNeal, M. M. (2010) 'VP6: A Candidate Rotavirus Vaccine', *The Journal of Infectious Diseases*, 202(S1), pp. S101–S107.

Ward, R. L., McNeal, M. M. and Sheridan, J. F. (1990) 'Development of an adult mouse model for studies on protection against rotavirus.', *J. Virol.*, 64(10), pp. 5070–5075.

Waseem, M. and Rosenberg, H. (2008) 'Intussusception.', *Pediatric Emergency Care*, 24(11), pp. 793–800.

Watson, S. J. *et al.* (2013) 'Viral population analysis and minority-variant detection using short read next-generation sequencing', *Philosophical Transactions of the Royal Society B: Biological Sciences*, 368(1614), pp. 20120205–20120205.

Weclewicz, K. *et al.* (1993) 'The endoplasmic reticulum-associated VP7 of rotavirus is targeted to axons and dendrites in polarized neurons.', *Journal of Neurocytology*, 22(8), pp. 616–26.

Weclewicz, K., Svensson, L. and Kristensson, K. (1998) 'Targeting of endoplasmic reticulum-associated proteins to axons and dendrites in rotavirus-infected neurons', *Brain Research Bulletin*, 46(4), pp. 353–360.

Wegmann, T. G. *et al.* (1993) 'Bidirectional cytokine interactions in the maternal-fetal relationship: is successful pregnancy a Th2 phenomenon?', *Immunology Today*, 14(7), pp. 353–356.

Weiner, H. L. *et al.* (1978) 'Identification of the gene coding for the hemagglutinin of reovirus', *Virology*, 86(2), pp. 581–584.

Weiss, C. and Clark, H. (1985) 'Rapid Inactivation of Rotaviruses by Exposure to Acid Buffer or Acidic Gastric Juice', *Journal of General Virology*, 66, pp. 2725–2730.

Weitkamp, J.-H. *et al.* (2003) 'Infant and Adult Human B Cell Responses to Rotavirus Share Common Immunodominant Variable Gene Repertoires', *The Journal of Immunology*, 171(9), pp. 4680–4688.

Weitkamp, J.-H. *et al.* (2014) 'VH1-46 Is the Dominant Immunoglobulin Heavy Chain Gene Segment in Rotavirus-Specific Memory B Cells Expressing the Intestinal Homing Receptor 4 7', *The Journal of Immunology*, 174(6), pp. 3454–3460.

Wen, X. *et al.* (2012) 'Construction and characterization of human rotavirus recombinant VP8*subunit parenteral vaccine candidates', *Vaccine*, 30(43), pp. 6121–6126.

Wen, X. *et al.* (2015) 'Tandem truncated rotavirus VP8* subunit protein with T cell epitope as non-replicating parenteral vaccine is highly immunogenic', *Human Vaccines and Immunotherapeutics*, 11(10), pp. 2483–2489.

Wentz, M. J., Patton, J. T. and Ramig, R. F. (1996) 'The 3'-terminal consensus sequence of rotavirus mRNA is the minimal promoter of negative-strand RNA synthesis', *J Virol*, 70(11), pp. 7833–41.

Westerman, L. E. *et al.* (2005) 'Serum IgG mediates mucosal immunity against rotavirus infection', *PNAS USA*, 102(20), pp. 7268–7273.

White, L. J. *et al.* (2008) 'Rotavirus within day care centres in Oxfordshire, UK: Characterization of partial immunity', *Journal of the Royal Society Interface*, 5(29), pp. 1481–1490.

WHO (2003) *Guidelines for environmental surveillance of poliovirus circulation. WHO/V&B/03.03*. Geneva, Switzerland.

WHO (2004) *Polio laboratory manual. WHO/IVB/04.10*. Geneva, Switzerland.

WHO (2005) *The treatment of diarrhoea: A manual for physicians and other senior health workers*. 4th edn. Geneva, Switzerland.

WHO (2006) 'Conclusions and recommendations from the Immunization Strategic Advisory Group', *Weekly epidemiological record*, 81, pp. 2–11.

WHO (2009) 'Rotavirus vaccines: an update.', *Weekly epidemiological record*, 84(51–52), pp. 533–540.

WHO (2010) *Statement of the Global Advisory Committee on Vaccine Safety on Rotarix*. Available at: https://www.who.int/vaccine_safety/committee/topics/rotavirus/rotarix_statement_march_2010/en/ (Accessed: 30 July 2019).

WHO (2012) 'Poliomyelitis: intensification of the global eradication initiative.', in *Report by the Secretariat. EB132/17*. Geneva, Switzerland., pp. 1–4.

WHO (2013) 'Rotavirus vaccines. WHO position paper: January 2013 - Recommendations', *Vaccine*, 31(52), pp. 6170–6171.

WHO (2016) *Estimated rotavirus deaths for children under 5 years of age: 2013, 215000., WHO Immunization, Vaccines and Biologicals*. Available at: https://www.who.int/immunization/monitoring_surveillance/burden/estimates/rotavirus/en/ (Accessed: 18 June 2019).

Wikswo, M. E. *et al.* (2019) 'Evidence for Household Transmission of Rotavirus in the United States, 2011–2016', *Journal of the Pediatric Infectious Diseases Society*. doi: 10.1093/jpids/piz004.

Willis, E. *et al.* (2017) 'Herpes zoster vaccine live: A 10 year review of post-marketing safety experience.', *Vaccine*, 35(52), pp. 7231–7239.

Wolf, M., Vo, P. T. and Greenberg, H. B. (2011) 'Rhesus Rotavirus Entry into a Polarized Epithelium Is Endocytosis Dependent and Involves

Sequential VP4 Conformational Changes', *Journal of Virology*, 85(6), pp. 2492–2503.

Wright, P. F. *et al.* (1987) 'Candidate rotavirus vaccine (rhesus rotavirus strain) in children: an evaluation', *Pediatrics*, 80(4), pp. 473–480.

Yen, C., Armero Guardado, J. A., *et al.* (2011) 'Decline in Rotavirus Hospitalizations and Health Care Visits for Childhood Diarrhea Following Rotavirus Vaccination in El Salvador', *The Pediatric Infectious Disease Journal*, 30(1), pp. 6–10.

Yen, C., Jakob, K., *et al.* (2011) 'Detection of Fecal Shedding of Rotavirus Vaccine in Infants Following Their First Dose of Pentavalent Rotavirus Vaccine', *Vaccine*, 29(24), pp. 4151–4155.

Yen, C., Tate, J. E., *et al.* (2011) 'Rotavirus vaccines: update on global impact and future priorities.', *Human vaccines*, 7(12), pp. 1282–90.

Yeung, M. C. *et al.* (1987) 'Purification and characterization of the reovirus cell attachment protein sigma 1', 156(2), pp. 377–385.

Yin, N. *et al.* (2018) 'Neonatal rhesus monkeys as an animal model for rotavirus infection', *World Journal of Gastroenterology*, 24(45), pp. 5109–5119.

Yoder, J. D. *et al.* (2009) 'VP5* rearranges when rotavirus uncoats.', *Journal of Virology*, 83(21), pp. 11372–7.

Yuan, L. and Saif, L. J. (2002) 'Induction of mucosal immune responses and protection against enteric viruses: rotavirus infection of gnotobiotic pigs as a model', *Veterinary Immunology and Immunopathology*, 87(3), pp. 147–160.

Yung, C. F., Chong, C. Y. and Thoon, K. C. (2016) 'Age at First Rotavirus Vaccination and Risk of Intussusception in Infants: A Public Health Modeling Analysis', *Drug Safety*, 39(8), pp. 745–748.

Zade, J. K. *et al.* (2014) 'Bovine rotavirus pentavalent vaccine development in India', *Vaccine*, 32(S1), pp. A124–A128.

Zapata, J. C. *et al.* (2014) 'Genetic Variation In Vitro and In Vivo of an Attenuated Lassa Vaccine Candidate', *Journal of Virology*, 88(6), pp. 3058–3066.

Zárate, S. *et al.* (2000) 'The VP5 domain of VP4 can mediate attachment of rotaviruses to cells.', *Journal of Virology*, 74(2), pp. 593–9.

Zárate, S. *et al.* (2004) 'VP7 Mediates the Interaction of Rotaviruses with Integrin alphavbeta3 through a Novel Integrin-Binding Site', *Journal of Virology*, 78(20), pp. 10839–10847.

Zeller, M. *et al.* (2012) 'Genetic analyses reveal differences in the VP7 and VP4 antigenic epitopes between human rotaviruses circulating in Belgium and rotaviruses in Rotarix and RotaTeq.', *Journal of Clinical Microbiology*, 50(3), pp. 966–976.

Zeller, M. *et al.* (2015) 'Genome-wide evolutionary analyses of G1P[8] strains isolated before and after rotavirus vaccine introduction', *Genome Biology and Evolution*, 7(9), pp. 2473–2483.

Zeller, M. *et al.* (2017) 'Comparative analysis of the Rotarix™ vaccine strain and G1P[8] rotaviruses detected before and after vaccine introduction in Belgium.', *Peer Journal*, 5, p. e2733.

Zhang, M. *et al.* (1998) 'Mutations in rotavirus nonstructural glycoprotein NSP4 are associated with altered virus virulence', *Journal of Virology*, 72(5), pp. 3666–3672.

Zhen, S. *et al.* (2015) ‘Effectiveness of the live attenuated rotavirus vaccine produced by a domestic manufacturer in China studied using a population-based case – control design’, *Emerging Infectious Diseases*, 4(July), pp. 1–6.

Zlamy, M. *et al.* (2013) ‘The impact of Rotavirus mass vaccination on hospitalization rates, nosocomial Rotavirus gastroenteritis and secondary blood stream infections’, *BMC Infectious Diseases*, 13(112), pp. 1–10.

Appendix I: Faecal sample collection

Overall collection

The overall collection consisted of faecal samples from 12 infants born and vaccinated in around Hertfordshire, South East England, UK (Chapter 2, Table 2.13). Information on gender or health status was not provided. Information on year of birth not displayed to maintain anonymity. Infants received the first dose of Rotarix® at 8 weeks (10 infants) or 9 weeks (2 infants) of age, and the second dose at 12 weeks (9 infants) or 13 weeks (3 infants), spaced by a month (11 infants) or a month and a week (1 infant). Rotarix® batch numbers for dose 1 and dose 2 were not provided.

Individuals

Individual B

Table 8.1.1. Faecal sample aliquot collection for infant B. Number of aliquots collected per timepoint available before vaccination, after dose 1, after dose 2 and after a year.

	Day in reference to dose 1 (in ref. to dose 2)	No. of samples	No. of aliquots
Pre-vaccination	-6	1	1 at 332 mg
	-3	1	2 from 503 mg to 692 mg
Dose 1	0	1	3 from 450 mg to 919 mg
	9	1	4 from 332 mg to 478 mg
	11	1	5 from 485 mg to 659 mg
	15	1	2 from 379 mg to 389 mg
	19	2	7 from 348 mg to 787 mg
	22	2	6 from 395 mg to 802 mg
	24	1	4 from 472 mg to 770 mg
	26	1	2 from 432 mg to 537 mg
	27	1	2 from 519 mg to 576 mg
Dose 2	30 (1)	1	2 from 613 mg to 651 mg
	32 (3)	1	2 from 467 mg to 483 mg
	35 (6)	1	1 at 296 mg
	38 (9)	1	3 from 620 mg to 812 mg
	39 (10)	1	8 from 430 mg to 820 mg
	41 (12)	1	1 at 359 mg
	43 (14)	1	2 from 458 mg to 511 mg
	44 (15)	1	2 from 424 mg to 654 mg
	46 (17)	1	4 from 380 mg to 742 mg
	48 (19)	1	2 from 490 mg to 641 mg
	49 (20)	1	5 from 356 mg to 700 mg
	50 (21)	1	6 from 330 mg to 719 mg
	56 (27)	1	5 from 355 mg to 866 mg
	57 (28)	1	4 from 326 mg to 492 mg
	58 (29)	1	5 from 368 mg to 924 mg
After a year	368	2	30 from 265 mg to 962 mg

Individual C

Table 8.1.2. Faecal sample aliquot collection for infant C. Number of aliquots collected per timepoint available before vaccination, after dose 1, after dose 2 and after a year.

	Day in reference to dose 1 (in ref. to dose 2)	No. of samples	No. of aliquots
Pre-vaccination	-17	1	3 from 148 mg to 294 mg
	-12	1	22 from 242 mg to 822 mg
	-11	1	16 from 258 mg to 647 mg
	-10	1	29 from 221 mg to 957 mg
	-9	1	18 from 280 mg to 659 mg
	-8	1	15 from 275 mg to 1147 mg
	-6	1	20 from 394 mg to 844 mg
	-5	1	16 from 294 mg to 894 mg
	-3	1	23 from 259 mg to 679 mg
	-1	1	18 from 252 mg to 779 mg
Dose 1	0	1	19 from 204 mg to 684 mg
	1	1	18 from 225 mg to 796 mg
	2	1	23 from 206 mg to 589 mg
	3	1	20 from 360 mg to 745 mg
	4	1	17 from 374 mg to 720 mg
	5	1	15 from 321 mg to 656 mg
	6	1	20 from 223 mg to 578 mg
	7	1	17 from 247 mg to 694 mg
	8	1	25 from 229 mg to 790 mg
	9	1	27 from 325 mg to 902 mg
	10	1	29 from 283 mg to 846 mg
	11	1	11 from 329 mg to 803 mg
	12	1	14 from 286 mg to 569 mg
	13	1	19 from 317 mg to 727 mg
	15	1	19 from 352 mg to 918 mg
	16	1	5 from 276 mg to 623 mg
	17	1	27 from 289 mg to 924 mg
	18	1	7 from 311 mg to 975 mg
	19	1	18 from 179 mg to 798 mg
	20	1	11 from 552 mg to 1074 mg
	21	1	15 from 403 mg to 815 mg
	23	1	23 from 343 mg to 718 mg
	24	1	13 from 394 mg to 953 mg
	25	1	5 from 128 mg to 650 mg
	27	1	16 from 456 mg to 728 mg
	29	1	14 from 395 mg to 775 mg
	30	1	20 from 340 mg to 961 mg
Dose 2	31 (0)	1	20 from 431 mg to 803 mg
	32 (1)	1	27 from 359 mg to 887 mg
	34 (3)	1	13 from 423 mg to 766 mg
	35 (4)	1	13 from 356 mg to 649 mg
	36 (5)	1	10 from 363 mg to 631 mg
	37 (6)	1	28 from 336 mg to 848 mg
	38 (7)	1	16 from 484 mg to 746 mg
After a year	365	1	34 from 177 mg to 814 mg

Individual D

Table 8.1.3. Faecal sample aliquot collection for infant D. Number of aliquots collected per timepoint available before vaccination, after dose 1, after dose 2 and after a year.

	Day in reference to dose 1 (in ref. to dose 2)	No. of samples	No. of aliquots
Pre-vaccination	-2	2	2 from 164 mg to 175 mg
	-1	3	4 from 103 mg to 242 mg
Dose 1	0	1	4 from 102 mg to 330 mg
	1	2	3 from 49 mg to 291 mg
	2	1	5 from 123 mg to 358 mg
	3	1	5 from 172 mg to 329 mg
	4	1	1 at 114 mg
	5	1	3 from 225 mg to 400 mg
	6	1	5 from 76 mg to 338 mg
	8	1	6 from 114 mg to 426 mg
	16	1	1 at 685mg
	20	1	4 from 49 mg to 321 mg
	22	1	2 from 167 mg to 230 mg
	25	1	6 from 169 mg to 709 mg
	34	1	1 at 237 mg
Dose 2	36 (1)	1	6 from 281 mg to 594 mg
	37 (2)	1	2 from 257 mg to 363 mg
	38 (3)	1	2 from 221 mg to 237 mg
	39 (4)	1	5 from 165 mg to 509 mg
	40 (5)	1	7 from 217 mg to 638 mg
	41 (6)	1	5 from 281 mg to 415 mg
	44 (9)	1	13 from 153 mg to 761 mg
	45 (10)	1	2 from 185 mg to 289 mg
	47 (12)	1	3 from 240 mg to 295 mg
	50 (15)	1	13 from 203 mg to 566 mg
	52 (17)	1	5 from 160 mg to 436 mg
	55 (20)	1	2 from 234 mg to 274 mg
	57 (22)	1	7 from 255 mg to 533 mg
	60 (25)	1	7 from 223 mg to 507 mg
	62 (27)	1	7 from 218 mg to 409 mg
	65 (30)	1	11 from 246 mg to 623 mg
	69 (34)	1	7 from 281 mg to 530 mg
	73 (38)	1	8 from 241 mg to 501 mg
	78 (43)	1	5 from 268 mg to 391 mg

Individual E

Table 8.1.4. Faecal sample aliquot collection for infant E. Number of aliquots collected per timepoint available before vaccination, after dose 1, after dose 2 and after a year.

	Day in reference to dose 1 (in ref. to dose 2)	No. of samples	No. of aliquots
Pre-vaccination	-23	1	3 from 216 mg to 359 mg
	-14	1	2 from 212 mg to 232 mg
	-10	1	2 from 211 mg to 213 mg
	-9	1	3 from 147 mg to 252 mg
Dose 1	0	1	3 from 171 mg to 205 mg
	1	1	4 from 229 mg to 297 mg
	2	1	3 from 164 mg to 292 mg
	3	1	3 from 141 mg to 257 mg
	6	1	3 from 234 mg to 304 mg
	7	1	5 from 232 mg to 322 mg
	8	1	2 from 163 mg to 215 mg
	9	1	3 from 157 mg to 228 mg
	11	1	5 from 195 mg to 372 mg
	13	1	5 from 188 mg to 252 mg
	14	1	4 from 196 mg to 329 mg
	15	1	2 from 125 mg to 198 mg
	17	1	4 from 254 mg to 365 mg
	18	1	4 from 245 mg to 350 mg
	20	1	2 from 115 mg to 233 mg
	21	1	3 from 166 mg to 312 mg
	27	1	1 at 165 mg
	29	1	3 from 265 mg to 373 mg
	30	1	4 from 289 mg to 395 mg
Dose 2	34 (3)	1	1 at 214 mg
	35 (4)	1	5 from 130 mg to 450 mg
	36 (5)	1	4 from 230 mg to 335 mg
	37 (6)	1	2 from 284 mg to 340 mg
	38 (7)	1	3 from 125 mg to 229 mg
	40 (9)	1	4 from 288 mg to 335 mg
	41 (10)	1	4 from 235 mg to 442 mg
	43 (12)	1	4 from 203 mg to 377 mg
	44 (13)	1	3 from 254 mg to 310 mg
	47 (16)	1	3 from 369 mg to 709 mg
	49 (18)	1	3 from 303 mg to 305 mg
	51 (20)	1	2 from 180 mg to 194 mg
	52 (21)	1	3 from 234 mg to 354 mg
	53 (22)	1	5 from 280 mg to 436 mg
	54 (23)	1	4 from 307 mg to 416 mg
	55 (24)	1	4 from 154 mg to 291 mg
	56 (25)	1	3 from 174 mg to 403 mg
	57 (26)	1	4 from 211 mg to 418 mg
	60 (29)	1	6 from 299 mg to 614 mg
	61 (30)	1	7 from 318 mg to 433 mg
	62 (31)	1	3 from 309 mg to 482 mg
After a year	365	1	20 from 297 mg to 686 mg

Individual F

Table 8.1.5. Faecal sample aliquot collection for infant F. Number of aliquots collected per timepoint available before vaccination, after dose 1, after dose 2 and after a year.

	Day in reference to dose 1 (in ref. to dose 2)	No. of samples	No. of aliquots
Pre-vaccination	-2	1	2 from 324 mg to 397 mg
Dose 1	0	1	1 at 67 mg
	1	1	1 at 165 mg
	3	1	1 at 43 mg
	4	2	4 from 92 mg to 268 mg
	5	1	2 from 222 mg to 246 mg
	6	1	3 from 259 mg to 318 mg
	7	1	2 from 429 mg to 576 mg
	8	1	1 at 90 mg
	9	1	3 from 277 mg to 476 mg
	13	1	1 at 118 mg
	14	2	3 from 162 mg to 188 mg
	16	1	2 from 176 mg to 295 mg
	18	1	2 from 333 mg to 393 mg
	23	1	2 from 85 mg to 182 mg
	24	1	2 from 95 mg to 298 mg
	25	1	9 from 23 mg to 502 mg
	27	1	5 from 189 mg to 389 mg
Dose 2	29 (1)	1	3 from 193 mg to 286 mg
	30 (2)	1	3 from 143 mg to 348 mg
	31 (3)	2	13 from 221 mg to 731 mg
	32 (4)	3	13 from 279 mg to 511 mg
	33 (5)	1	6 from 233 mg to 340 mg
	34 (6)	2	3 from 265 mg to 305 mg
	35 (7)	2	4 from 150 mg to 500 mg
	38 (10)	1	5 from 256 mg to 365 mg
	39 (11)	1	9 from 47 mg to 466 mg
	41 (13)	2	9 from 188 mg to 524 mg
	43 (15)	2	8 from 202 mg to 623 mg
	46 (18)	1	3 from 345 mg to 447 mg
	48 (20)	2	15 from 238 mg to 570 mg
	52 (24)	1	5 from 312 mg to 630 mg
	53 (25)	1	6 from 333 mg to 425 mg
After a year	376	3	47 from 196 mg to 1014 mg

Individual G

Table 8.1.6. Faecal sample aliquot collection for infant G. Number of aliquots collected per timepoint available before vaccination, after dose 1, after dose 2 and after a year.

	Day in reference to dose 1 (in ref. to dose 2)	No. of samples	No. of aliquots
Pre-vaccination	-37	1	7 from 278 mg to 403 mg
	-28	1	6 from 315 mg to 617 mg
	-25	1	8 from 467 mg to 710 mg
	-1	1	6 from 432 mg to 740 mg
Dose 1	1	1	10 from 350 mg to 675 mg
	4	1	14 from 344 mg to 729 mg
	7	1	14 from 434 mg to 783 mg
	11	1	8 from 321 mg to 671 mg
	13	1	16 from 327 mg to 815 mg
	23	1	14 from 197 mg to 839 mg
	25	1	7 from 184 mg to 719 mg
	28	1	25 from 337 mg to 903 mg
Dose 2	30 (1)	1	6 from 387 mg to 659 mg
	36 (7)	1	21 from 272 mg to 871 mg
	38 (9)	1	14 from 341 mg to 845 mg
	40 (11)	1	27 from 175 mg to 839 mg
	51 (22)	1	2 from 255 mg to 317 mg
	54 (25)	1	8 from 343 mg to 566 mg
	55 (26)	1	23 from 201 mg to 799 mg
	62 (33)	1	12 from 268 mg to 888 mg
	65 (36)	1	25 from 157 mg to 871 mg
	68 (39)	1	11 from 195 mg to 772 mg
After a year	421	1	26 from 316 mg to 677 mg
	423	1	23 from 224 mg to 697 mg

Individual H

Table 8.1.7. Faecal sample aliquot collection for infant H. Number of aliquots collected per timepoint available before vaccination, after dose 1, after dose 2 and after a year.

	Day in reference to dose 1 (in ref. to dose 2)	No. of samples	No. of aliquots
Pre-vaccination	-1	1	7 from 253mg to 391 mg
Dose 1	0	1	4 from 196 mg to 423 mg
	3	1	4 from 225 mg to 373 mg
	4	1	1 at 73 mg
	5	1	4 from 158 mg to 385 mg
	6	1	8 from 118 mg to 308 mg
	7	1	5 from 144 mg to 258 mg
	9	1	3 from 173 mg to 355 mg
	12	1	2 from 243 mg to 323 mg
	13	1	2 from 142 mg to 181 mg
	17	1	2 from 135 mg to 158 mg
	21	1	4 from 199 mg to 294 mg
	24	1	3 from 247 mg to 276 mg
	27	1	8 from 194 mg to 522 mg
Dose 2	30 (0)	1	2 from 110 mg to 214 mg
	31 (1)	1	4 from 220 mg to 338 mg
	32 (2)	1	5 from 215 mg to 376 mg
	33 (3)	1	8 from 183 mg to 398 mg
	35 (5)	2	9 from 161 mg to 408 mg
	36 (6)	1	3 from 205 mg to 277 mg
	37 (7)	1	5 from 197 mg to 305 mg
	38 (8)	1	6 from 121 mg to 279 mg
	39 (9)	1	10 from 181 mg to 369 mg
	41 (11)	1	4 from 166 mg to 409 mg
	42 (12)	1	4 from 188 mg to 343 mg
	43 (13)	1	3 from 217 mg to 299 mg
	44 (14)	1	8 from 174 mg to 416 mg
	47 (17)	1	6 from 171 mg to 416 mg
	51 (21)	1	3 from 337 mg to 477 mg
	54 (24)	1	5 from 251 mg to 400 mg
	57 (27)	1	7 from 203 mg to 561 mg
	60 (30)	1	5 from 192 mg to 448 mg
	63 (33)	1	10 from 172 mg to 383 mg
	67 (37)	1	7 from 192 mg to 421 mg
	71 (41)	1	6 from 181 mg to 395 mg
	75 (45)	1	4 from 107 mg to 245 mg
	79 (49)	1	6 from 170 mg to 380 mg
	84 (54)	1	6 from 280 mg to 520 mg
	87 (57)	1	7 from 188 mg to 344 mg
	90 (60)	1	4 from 192 mg to 378 mg
	93 (63)	1	6 from 258 mg to 525 mg
	99 (69)	1	5 from 291 mg to 551 mg
	111 (81)	1	7 from 156 mg to 478 mg
	114 (84)	1	3 from 197 mg to 322 mg
	118 (88)	1	6 from 193 mg to 263 mg
After a year	396	1	7 from 256 mg to 444 mg
	397	1	20 from 211 mg to 568 mg

Individual I

Table 8.1.8. Faecal sample aliquot collection for infant I. Number of aliquots collected per timepoint available before vaccination, after dose 1, after dose 2 and after a year.

	Day in reference to dose 1 (in ref. to dose 2)	No. of samples	No. of aliquots
Pre-vaccination	-5	1	2 from 204 mg to 371 mg
	-4	1	4 from 76 mg to 186 mg
	-3	1	3 from 106 mg to 282 mg
	-1	1	3 from 84 mg to 232 mg
Dose 1	0	1	4 from 283 mg to 492 mg
	1	4	19 from 90 mg to 606 mg
	4	1	3 from 90 mg to 281 mg
	9	2	3 from 179 mg to 393 mg
	10	1	9 from 247 mg to 510 mg
	11	1	1 at 262 mg
	12	1	2 from 204 mg to 254 mg
	13	2	3 from 234 mg to 314 mg
	14	1	5 from 206 mg to 467 mg
	15	1	1 at 141 mg
	16	1	2 from 232 mg to 270 mg
	21	1	1 at 313 mg
	22	1	7 from 369 mg to 522 mg
	23	2	9 from 219 mg to 475 mg
	26	2	4 from 119 mg to 259 mg
Dose 2	27 (0)	1	1 at 267 mg
	29 (2)	1	3 from 221 mg to 424 mg
	30 (3)	2	9 from 218 mg to 688 mg
	32 (5)	1	1 at 284 mg
	35 (8)	2	9 from 119 mg to 503 mg
	37 (10)	1	8 from 230 mg to 624 mg
	38 (11)	1	7 from 396 mg to 610 mg
	39 (12)	1	1 at 93 mg
	41 (14)	2	6 from 150 mg to 412 mg
	43 (16)	2	9 from 141 mg to 500 mg
	46 (19)	1	1 at 270 mg
	47 (20)	1	3 from 101 mg to 273 mg
	49 (22)	1	1 at 217 mg
	50 (23)	1	1 at 318 mg
	51 (24)	1	2 from 212 mg to 324 mg
	52 (25)	1	3 from 233 mg to 290 mg
	55 (28)	1	2 from 66 mg to 285 mg
	56 (29)	1	1 at 219 mg
	58 (31)	1	3 from 254 mg to 405 mg
	60 (33)	1	1 at 492 mg
	61 (34)	1	1 at 68 mg
	62 (35)	1	2 from 360 mg to 421 mg
	63 (36)	1	2 from 181 mg to 190 mg
	64 (37)	2	5 from 116 mg to 430 mg
	65 (38)	1	4 from 252 mg to 288 mg
After a year	444	1	12 from 233 mg to 693 mg
	445	1	9 from 258 mg to 605 mg

Individual J

Table 8.1.9. Faecal sample aliquot collection for infant J. Number of aliquots collected per timepoint available before vaccination, after dose 1, after dose 2 and after a year.

	Day in reference to dose 1 (in ref. to dose 2)	No. of samples	No. of aliquots
Pre-vaccination	-1	1	8 from 202 mg to 738 mg
Dose 1	1	3	32 from 132 mg to 1010 mg
	3	1	8 from 263 mg to 512 mg
	4	1	5 from 318 mg to 833 mg
	5	1	10 from 291 mg to 516 mg
	7	1	8 from 200 mg to 888 mg
	9	1	10 from 216 mg to 679 mg
	11	1	6 from 246 mg to 610 mg
	12	1	6 from 293 mg to 605 mg
	13	1	10 from 302 mg to 688 mg
	14	1	8 from 241 mg to 584 mg
	17	1	7 from 274 mg to 619 mg
	20	1	5 from 245 mg to 536 mg
	21	1	10 from 187 mg to 601 mg
	24	1	13 from 237 mg to 977 mg
	26	1	4 from 309 mg to 742 mg
	27	1	6 from 186 mg to 502 mg
Dose 2	29 (0)	1	9 from 123 mg to 587 mg
	30 (1)	1	16 from 166 mg to 544 mg
	31 (2)	1	11 from 214 mg to 1380 mg
	32 (3)	1	5 from 440 mg to 1077 mg
	33 (4)	1	8 from 250 mg to 554 mg
	34 (5)	1	4 from 227 mg to 723 mg
	35 (6)	1	5 from 268 mg to 649 mg
	36 (7)	1	7 from 212 mg to 530 mg
	38 (9)	1	3 from 398 mg to 916 mg
	39 (10)	1	6 from 242 mg to 717 mg
	40 (11)	1	8 from 241 mg to 632 mg
	41 (12)	1	10 from 228 mg to 598 mg
	42 (13)	1	7 from 214 mg to 992 mg
	44 (15)	1	6 from 405 mg to 652 mg
	47 (18)	1	7 from 291 mg to 625 mg
	50 (21)	1	6 from 229 mg to 754 mg
	53 (24)	1	9 from 319 mg to 588 mg
	56 (27)	1	8 from 304 mg to 620 mg
	60 (31)	1	9 from 345 mg to 692 mg
	64 (35)	1	11 from 212 mg to 667 mg
	67 (38)	1	11 from 269 mg to 630 mg
	70 (41)	1	5 from 432 mg to 638 mg

Individual K

Table 8.1.10. Faecal sample aliquot collection for infant K. Number of aliquots collected per timepoint available before vaccination, after dose 1, after dose 2 and after a year.

	Day in reference to dose 1 (in ref. to dose 2)	No. of samples	No. of aliquots
Pre-vaccination	-1	1	2 from 169 mg to 290 mg
Dose 1	0	1	1 at 321 mg
	1	1	3 from 206 mg to 589 mg
	3	1	3 from 310 mg to 367 mg
	4	1	3 from 98 mg to 276 mg
	7	1	1 at 41 mg
	8	1	1 at 117 mg
	9	1	1 at 87 mg
	10	1	4 from 281 mg to 628 mg
	11	1	4 from 132 mg to 420 mg
	12	1	5 from 188 mg to 329 mg
	13	1	6 from 254 mg to 413 mg
	16	1	2 from 183 mg to 292 mg
	27	1	3 from 59 mg to 563 mg
	29	1	4 from 196 mg to 360 mg
	30	1	1 at 208 mg
	31	1	4 from 219 mg to 485 mg
	33	1	7 from 258 mg to 577 mg
Dose 2	34 (0)	1	3 from 216 mg to 606 mg
	35 (1)	1	3 from 154 mg to 250 mg
	36 (2)	1	4 from 95 mg to 420 mg
	37 (3)	1	5 from 234 mg to 467 mg
	38 (4)	1	1 at 197 mg
	39 (5)	1	5 from 301 mg to 457 mg
	40 (6)	1	8 from 262 mg to 596 mg
	41 (7)	1	8 from 212 mg to 543 mg
	42 (8)	1	6 from 277 mg to 553 mg
	44 (10)	1	5 from 223 mg to 625 mg
	45 (11)	1	5 from 287 mg to 574 mg
	46 (12)	1	12 from 325 mg to 594 mg
	47 (13)	1	7 from 386 mg to 612 mg
	48 (14)	1	10 from 278 mg to 514 mg
	50 (16)	1	8 from 290 mg to 441 mg
	54 (20)	1	4 from 328 mg to 519 mg
	57 (23)	1	15 from 301 mg to 588 mg
	65 (31)	1	5 from 228 mg to 559 mg
	67 (34)	1	10 from 235 mg to 755 mg
	70 (37)	1	10 from 275 mg to 628 mg
	72 (39)	1	10 from 305 mg to 674 mg
	75 (42)	1	12 from 236 mg to 665 mg
	79 (46)	1	7 from 262 mg to 476 mg
	82 (49)	1	8 from 388 mg to 799 mg

Individual L

Table 8.1.11. Faecal sample aliquot collection for infant L. Number of aliquots collected per timepoint available before vaccination, after dose 1, after dose 2 and after a year.

	Day in reference to dose 1 (in ref. to dose 2)	No. of samples	No. of aliquots
Pre-vaccination	-14	4	46 from 25 mg to 986 mg
Dose 1	11	1	2 from 225 mg to 233 mg
	15	2	6 from 33 mg to 290 mg
	16	1	4 from 178 mg to 298 mg
	17	1	2 from 53 mg to 324 mg
	18	1	1 at 167 mg
	20	1	3 from 134 mg to 254 mg
	21	1	5 from 280 mg to 456 mg
	22	1	6 from 117 mg to 744 mg
	23	1	5 from 269 mg to 481 mg
	25	1	2 from 188 mg to 283 mg
	26	1	9 from 230 mg to 528 mg
	31	1	2 from 224 mg to 238 mg
Dose 2	34 (1)	1	2 from 219 mg to 319 mg
	35 (2)	2	5 from 312 mg to 661 mg
	36 (3)	1	3 from 357 mg to 395 mg
	38 (5)	1	2 from 347 mg to 377 mg
	40 (7)	1	1 at 388 mg
	51 (18)	1	3 from 271 mg to 444 mg
	53 (20)	2	3 from 121 mg to 220 mg
	55 (22)	1	7 from 388 mg to 615 mg
	56 (23)	1	6 from 319 mg to 404 mg
	59 (36)	1	8 from 258 mg to 467 mg
	63 (30)	1	1 at 188mg
After a year	361	1	11 from 271 mg to 470 mg

Individual M

Table 8.1.12. Faecal sample aliquot collection for infant M. Number of aliquots collected per timepoint available before vaccination, after dose 1, after dose 2 and after a year.

	Day in reference to dose 1 (in ref. to dose 2)	No. of samples	No. of aliquots
Pre-vaccination	-1	1	7 from 280 mg to 646 mg
Dose 1	1	1	5 from 319 mg to 639 mg
	3	1	4 from 282 mg to 470 mg
	5	1	6 from 378 mg to 633 mg
	6	1	4 from 618 mg to 836 mg
	8	1	6 from 413 mg to 653 mg
	9	1	6 from 301 mg to 634 mg
	11	1	4 from 493 mg to 782 mg
	12	1	3 from 516 mg to 613 mg
	13	1	3 from 511mg to 740mg
	14	1	3 from 323 mg to 560 mg
	18	1	6 from 475 mg to 790 mg
	21	1	5 from 496 mg to 841 mg
	27	1	3 from 389 mg to 707 mg
Dose 2	29 (1)	1	3 from 456 mg to 578 mg
	30 (2)	1	5 from 424 mg to 704 mg
	35 (7)	1	4 from 387 mg to 818 mg

Appendix II: Preliminary data - Genetic stability of faecal rotavirus RNA in infants vaccinated with Rotarix®

8.2.1 Sequence-dependent amplification followed by Nextera® library prep

8.2.1.1 Introduction

The Nextera® XT DNA kit protocol would be used after specific gene segment RT-PCR. The transposomes with adaptors are combined with the DNA template, followed by tagmentation to fragment the DNA and addition of adapters (Fig. 8.2.1). Limited cycle PCR incorporates the sequencing primers and indices.

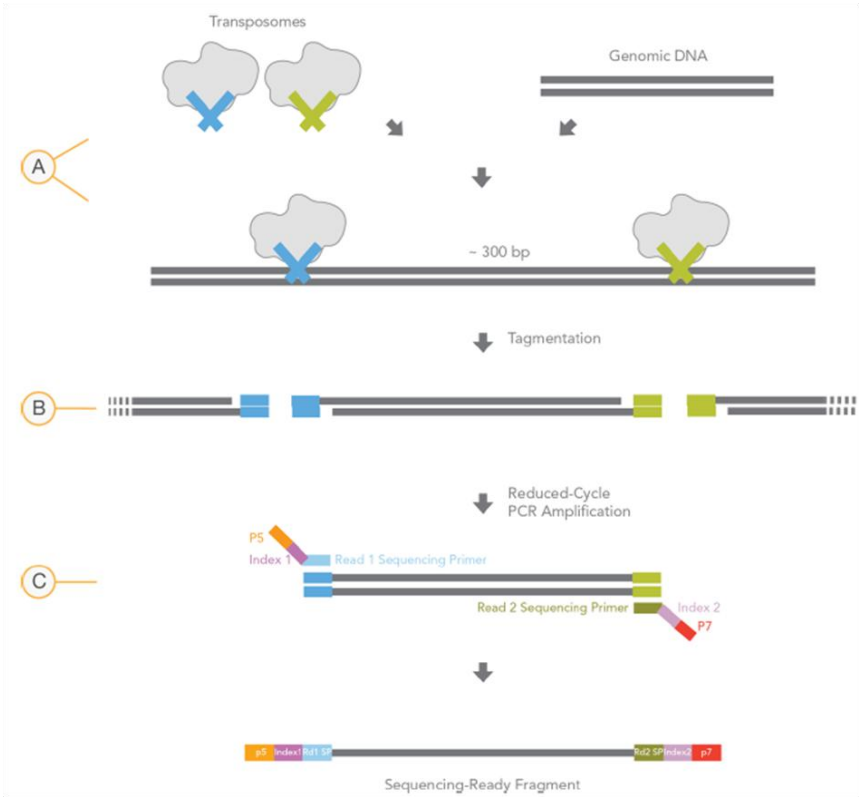

Fig. 8.2.1. An overview of the procedure for the Nextera® XT DNA Sample Preparation Guide. From the Nextera® XT DNA Sample Preparation Guide (#15031942, Illumina®).

Rotavirus vaccine material has been previously sequenced using this method (Mitchell, Lui, *et al.*, unpublished). Sequence-dependent amplification of rotavirus gene segments is a more time-consuming and expensive method than sequence independent amplification due to RT-PCR prior to library preparation. Although it may introduce errors from starting PCR and from PCR during library preparation, accounting for PCR errors such as marked duplicates, generates reliable and consistent data.

8.2.1.2 Experimental methodology and sample set

For a first assessment of the genetic stability of Rotarix®, we used faecal material from two infants (J and F) in the cohort previously described (Chapter 2 and Appendix I). Samples were aliquoted and stored until use (Chapter 2, section 2.1.9 and 2.2.1) and only samples of high quantity were used for this assessment. Timepoints of expected high viral loads were tested as three technical replicates from one single extract. Viral nucleic acids were extracted following the methods in Chapter 2, sections 2.2.3.1 and 2.2.3.3. To prepare for library generation with the Nextera® XT DNA kit, cDNA synthesis and PCR amplification were performed on extracted RNA (Chapter 2, section 2.2.4), pooled in equimolar amounts and purified following the methods in Chapter 2, section 2.2.6. Library preparation by fragmentation and tagging with adapters in a single reaction using Nextera® (Chapter 2, section 2.2.6), bioinformatic analysis (Chapter 2, section 2.2.7) and further data analysis (Chapter 2, section 2.2.8) were performed jointly with the NGS team.

The timepoints tested were equivalent or nearly equivalent in both infants: days 4, 9 and 24/25 (J/F) after dose 1 and days 2/3 (J/F) and 4 after dose 2. In order to assay three technical replicates, extraction volumes of 50 µl allowed the assessment of four gene segments: 12 µl were used in cDNA synthesis for each segment, so 48 µl from the extraction volume would be used to test four segments. Genetic characterization was performed on genes encoding VP3, VP4, VP6 and VP7 as these presented non-synonymous SNP loci variants and the highest frequency ranges in vaccine material (Mitchell, Lui, *et al.*, unpublished). Moreover, VP3, VP4 and VP7 were related to virulence in the gnotobiotic piglet (Hoshino *et al.*, 1995) and VP4, VP6 and VP7 were reported to undergo selection in cell culture and be targets

for neutralizing protective antibodies (Burns *et al.*, 1996; Feng *et al.*, 2002; Corthésy *et al.*, 2006; Nair *et al.*, 2017)**.**

8.2.1.3 Results and short discussion

Preliminary data from VLs in stool from two infants (J, F) was in the range of expected copy number in stool of vaccinated infants of 10^2-10^{10} copies/mL (Mijatovic-Rustempasic *et al.*, 2017). Viral loads were high after dose 1, while lower VLs appeared after dose 2. Preliminary data for viral segments VP3, VP4, VP6 and VP7 at several timepoints after dose 1 and dose 2 identified SNPs at a frequency of ≥1% (Table 8.2.1). Both individuals presented the highest number of SNPs against reference for gene segment 4 (encoding VP4) and they both presented more non-synonymous than synonymous SNPs for all four viral segments. All the potential reversions to wild type were previously identified in vaccine material (Mitchell, Lui, *et al.*, unpublished) except for one in segment 4. Frequencies in stool are similar to vaccine material, high (>50%) or very high (>90%).

Table 8.2.1. Single nucleotide polymorphisms identified in stool from two infants (J, F) for genes encoding VP3, VP4, VP6 and VP7 by Nextera®. Protein encoded by gene segment, infant, number of SNPs against reference (JX943611-JX943614), type of SNP, frequency and common SNPs. S, synonymous; NS, non-synonymous; previously identified in vaccine material; Rev. to WT (JN887809-10, (JN887818-19), reversion to wild type.

Prot. gene	Infant	SNPs against reference	S	NS	V	Rev. to WT	SNP frequency	Common SNPs	
VP3	Individual J	39	18	21	1	1	38 SNPs at <26%; 1 SNP at 43% (S)	2	NS; 1 in vaccine
	Individual F	56	25	31	1	0	All SNPs at <22%		
VP4	Individual J	86	30	57	9	1 (V)	80 SNPs at <50%; 6 SNPs at >50%/<97% (2S, 4NS)	13	3 S; 10 NS; 8 in vaccine (NS)
	Individual F	61	17	44	10	2 (1V)	56 SNPs at <50%; 5 SNPs at >51%/<99% (NS)		
VP6	Individual J	62	29	33	1	0	60 SNPs at <17%; 2 SNPs at >40%/>50% (S)	2	2 S; 2 NS; 1 in vaccine (S)
	Individual F	26	9	17	1	0	All SNPs at <6%		
VP7	Individual J	40	17	23	2	3 (V)	38 SNPs at <13%; 1 SNP at >14% (rev. to WT); 1 SNP at >55% (NS)	1	NS
	Individual F	34	12	22	1	0	All SNPs at <8%		

VP3. One SNP locus found in the VP3 encoding gene for individual J coincides with the SNP locus previously identified in vaccine material (Mitchell, Lui, *et al.*, unpublished): nucleotide change G1715A affecting amino acid R572K (Table 8.2.2). Most of the mutations in VP3 were synonymous and there were eight amino acid changes, two of them were previously observed in WT RV G1P[8] strain

(GenBank reference number JN887810): nucleotide change A1470G affecting amino acid I490M and nucleotide change C1838T affecting amino acid A613V. The viral segment encoding VP3 presented low frequency synonymous mutations and isolated high frequency mutations. Some SNP loci were consistent, like the first one, amino acid D27D, which was detected on day 24 after dose 1 and stayed at a similar frequency after the second dose was administered. Other SNP loci appeared after a certain time at low frequency and then disappeared after that, such as those affecting amino acid N729D. Further points were needed to assess reappearance (Chapter 4). Other SNPs increase and then are not detected later, such as amino acid L169L.

VP6, VP7. For VP6 and VP7, most mutations were synonymous and appeared at low frequencies and early timepoints (Table 8.2.3). Individual J presented one SNP locus in VP6 previously found in the vaccine material (Mitchell, Lui, *et al.*, unpublished) at low frequency: nucleotide change G654A leading to amino acid silent substitution L218L. The viral segment encoding VP7 presented five low frequency synonymous mutations and four non-synonymous low frequency mutations at early timepoints for both infants. There was a SNP locus affecting amino acid 123, with the non-synonymous mutation S123N increasing frequency in individual J to about 40%, potentially indicating the emergence of a mixed population.

Table 8.2.2. SNP loci in stool of individuals J and F for viral segment encoding VP3. % SNP frequency shown for each nucleotide (nt) and amino acid (aa) position at days 4, 9 and 24/25 after dose 1; and days 2/3, 4 and 21/NA after dose 2. aa changes in bold and possible reversions to a WT in red. [1] identified in vaccine by our group. Frequency range of SNPs in vaccine material shown where applicable. Shaded in red, loci present in two replicates; shaded in yellow, loci present in three replicates; and shaded in green, loci present in four replicates.

VP3		SNP frequency in stool (%)									
		After dose 1					After dose 2				
	Vac.	Day 4	Day 9		Day 24	Day 25	Day 2	Day 3	Day 4		Day 21
nt (aa)	Freq. (%)	F	J	F	J	F	J	F	J	F	J
T81C (D27D)					40.0		48.3		46.1		33.9
A114G (L38L)											4.4
A132G (L44L)							4.1		15.5		11.1
A415G (N139**D**)							1.7				
A463G (I155V)							7.2		3.0		
G507A (L169L)			1.1		22.3		7.3		10.4		
T666C (F222F)											3.9
A750G (R250R)		2.3									
T765C (D255D)									1.3		
T811C (Y271**H**)							2.3		3.4		
G990A (K330K)											5.9
A1104C (A368A)										8.4	
T1146C (V382V)						4.5					
C1171T (L391L)											14.9
A1470G (I490M)			2.5								
G1533A (L511L)		3.7									
T1542C (D514D)						13.7					
G1715A (R572K)[1]	4.9-7.7							5.0			
C1838T (A613V)						4.4					
T2052C (Y684Y)		1.5									
T2127C (P709P)									3.1		
A2185G (N729**D**)				3.6	1.5						
T2314C (S772**P**)											

Table 8.2.3. SNP loci in stool of individuals J and F for viral segments VP6 and VP7. % SNP frequency shown for each nucleotide (nt) and amino acid (aa) position in corresponding viral segment at days 4 and 9 after dose 1. aa changes in bold and possible reversions to a WT in red. [1] identified in vaccine by our group. Frequency range of SNPs in vaccine material shown where applicable. Shaded in red, loci present in two replicates; shaded in yellow, loci present in three replicates; and shaded in green, loci present in four replicates.

VP6		SNP freq. in stool (%)			
		After dose 1			
	Vac.	Day 4		Day 9	
nt (aa)	Freq. (%)	J	F	J	F
G85A (D29N)		2.1			
A247G (T83A)		0.9			
G484T (A162S)				7.2	
G654A (L218L)[1]	0-15.8	2.1		6.0	
G823A (A275T)		1.8			

VP7		SNP freq. in stool (%)			
		After dose 1			
	Vac.	Day 4		Day 9	
nt (aa)	Freq. (%)	J	F	J	F
C80T (T27**I**)			1.1		
G107A (R36K)					4.3
G162A (G54G)				12.5	
G368A (S123N)[1]	3.4-17	6.8		40.2	
C421T (L141L)			1.3		
T444C (L148L)		3.6			
G594T (L198L)			1.6		
T904C (Y302**H**)		1.8			
C918T (I306I)			2.3		

VP4. The VP4 encoding gene segment presented most of the SNP loci as non-synonymous mutations (Table 8.2.4). Most SNP loci identified in the vaccine virus were present in virus shed by both infants (Fig. 8.2.2). Most of the low frequency mutations occurred at one point in time and disappeared, not being selected or appearing as a minor variant not detected later. There was a non-synonymous novel mutation, changing amino acid 114 from P to T (P114T), and appearing in both infants after first dose first at low frequency and then at consistent high frequencies since day 25 after dose 1 (from a frequency of 34% to 78%).

The region covering nucleotides 1088 - 1409 (aa 363-470) may be a hotspot for variation as SNP loci were observed in stool at frequencies higher than in vaccine material. A number of the changes seen in the proposed hotspot were already present in the vaccine at a range of frequencies (from 1% to almost 60%). Most of these changes appeared at a frequency higher than 50% or at a very high frequency (>90%) and seemed to become transiently dominant or fixed over the vaccination period evaluated. Amino acid change K368R is of interest: it was present at about 50% in vaccine material and appeared in the stool at 99% to 100% after both doses in stool from both infants. It consists of potential reversion to a known WT RV G1P[8] strain (GenBank reference number JN887809) at nucleotide position 1103 and amino acid 368, that might alter the putative fusion domain of the virus (aa 384-404) (Mackow *et al.*, 1988; Dormitzer *et al.*, 2004; Trask *et al.*, 2010).

Two other variant amino acids, Y385H and I388L fell within the limits of the virus fusion domain and are believed to be related to neutralisation and attenuation of the virus (Kapikian, Hoshino and Chanock, 2001; Tsugawa and Tsutsumi, 2016), potentially affecting the fusion domain and attenuation. Other SNP loci appeared at high frequency and seemed fixed, such as nucleotide position C999T (amino acid P333P) in individual J, while the remaining SNP loci appeared at frequencies lower than 15%. VP4 presented a region prone to variation in both infants and in vaccine, as well as specific SNP loci to virus shed by each infant.

Table 8.2.4. SNP loci in stool of individuals J and F for viral segment VP4. % SNP frequency shown for each nucleotide (nt) and amino acid (aa) position at days 4, 9 and 24/25 after dose 1; and days 2/3, 4 and 21/NA after dose 2. aa changes in bold and possible reversions to a WT in red. [1] identified in vaccine by our group. Frequency range of SNPs in vaccine material shown where applicable. Shaded in blue, loci present in both infants; shaded in red, loci present in two replicates; shaded in yellow, loci present in three replicates; and shaded in green, loci present in four replicates.

VP4		SNP frequency in stool (%)										
		After dose 1						After dose 2				
		Day 4		Day 9		Day 24	Day 25	Day 2	Day 3	Day 4		Day 21
nt (aa)	Vac. Freq. (%)	J	F	J	F	J	F	J	F	J	F	J
G61A (E21K)			12.4									
A190G (I64V)											11.7	
C227A (P76Q)						1.8						
C331T (H111Y)			7.5									
C340A (P114T)				9.7		17.5	52.2	52.3	34.2	46.0	78.6	83.2
T499C (F167L)					98.4							
G547A (A183T)								2.0				10.5
T567C (S189S)								1.7		1.8		
A647G (N216S)				1.6								
G754A (D252N)[1]	13.8-16.6								11.0			
T807C (D269D)			1.7									
C998T (P333L)						1.8						
C999T (P333P)						9.6		49.0		44.6		71.7
A1088G (N363S)[1]	1.1-1.8	4.5	6.2	4.0								
A1090G (M364V)[1]	6.2-9.6	12.1	3.0	14.1		22.0		56.4		48.8		85.3
G1092A (M364I)[1]	4.1-5.9	22.4	25.7	24.0			9.6				13.2	
A1103G (K368R)[1]	53.9-59.3	95.3	99.3	99.6	100.0	99.9	100.0		70.4	100.0	99.8	100.0
A1113G (A371A)						1.7						
T1143C (G381G)			2.0									
G1148A (S383N)							7.4					
T1153C (Y385H)[1]	12.1-19.2	9.0		11.2	54.1	76.0		43.7		51.4		14.2
G1160A (S387N)								1.7				
A1162C (I388L)[1]	2.7-4.8	11.0	19.8	6.2								
A1362C (P454P)								1.4		1.7		
T1409C (I470T)[1]	6.3-10.4	9.8	2.3	4.6	42.9							
A1430G (D477G)		1.5										
T1435C (Y479H)[1]	2.4-5.2	1.3										
T1702A (S568T)								2.8				
C1893T (S627S)		1.3				2.5						
A2040G (V680V)			2.0									
T2283C (I761I)								1.6				

In VP4, there was a novel SNP locus identified at nucleotide position 340 (amino acid P114T; in VP8* epitope region 8-3 (Zeller *et al.*, 2012)) in both infants, but not in the in-house vaccine sequence (Fig. 8.2.2). SNP loci in the nucleotide region 1088-1409 were identified in both infants at higher frequency than in the in-house vaccine sequence. Some SNP loci affecting amino acids I388L and Y385H were identified in VP5* epitope region 5-1 (Zeller *et al.*, 2012) and others affecting amino acids N363S, M364V/M354I, I470T and K368R in the body of VP5* (putative fusion domain) (Fig. 8.2.3). Nucleotide position 1103 (K368R) appeared at 99-100% in stool and 50% in vaccine material.

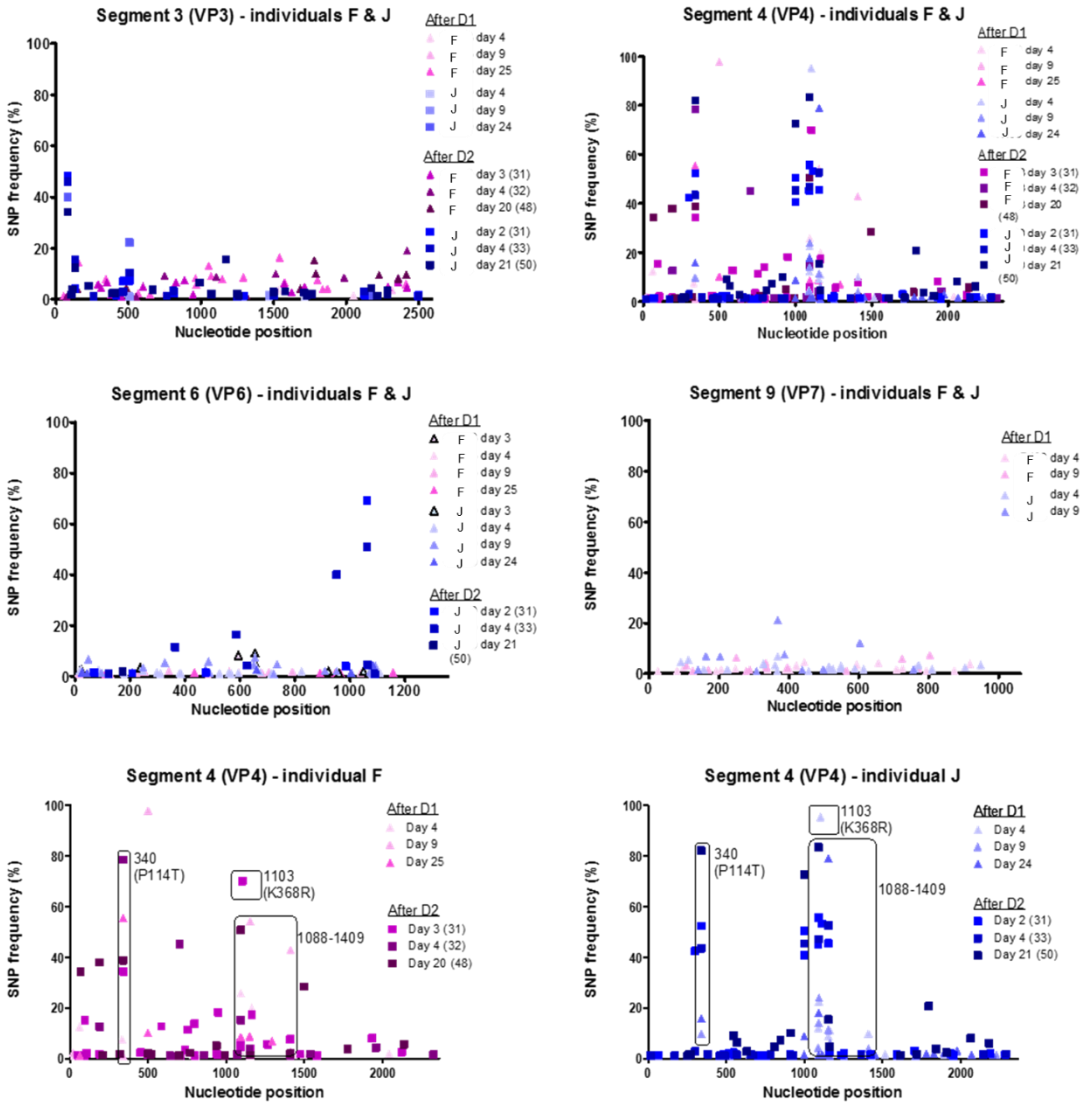

Fig. 8.2.2. SNP loci individuals J and F for viral segment VP4. SNP frequency (%) shown for each nucleotide (nt) position at several timepoints after dose 1 (blue/pink triangles) and dose 2 (blue/pink squares; day from dose 1 in brackets). SNP loci 340 (P114T), 1103 (K368R) and cluster 1088-1409 boxed. Nucleotide position refers to full length coding sequence (JN887809).

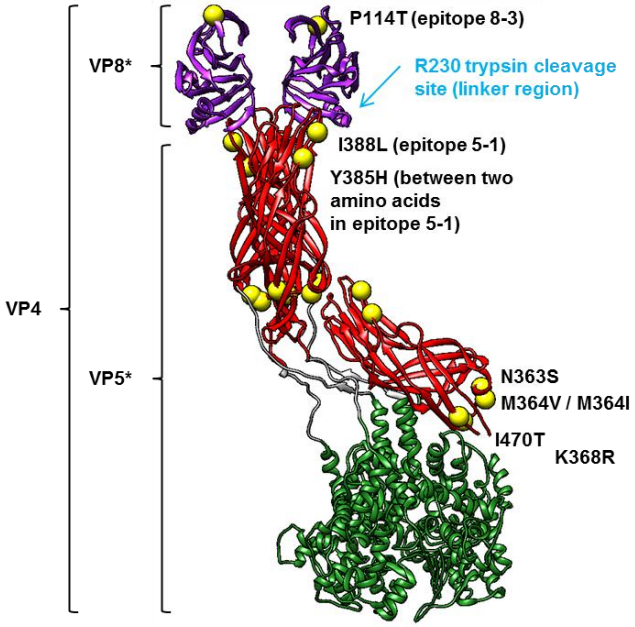

Fig. 8.2.3. Amino acid changes observed at high frequencies in VP4. VP8* subunit in purple, VP5* subunit in red (the antigen domains) and green (the foot domain), and SNP loci in yellow.

8.2.2 Sequence-independent amplification followed by RNA ScriptSeq® library prep

8.2.2.1 Introduction

The RNA ScriptSeq™ v2 kit protocol would be used for direct whole genome sequencing of all 11 rotavirus gene segments. The protocol starts by fragmenting RNA and then using random primers to perform cDNA synthesis, tagging the 5' end at the same time (Fig. 8.2.4). Terminal tagging oligonucleotides are used to tag the 5' end of the cDNA (now di-tagged), which is amplified by limited-cycle PCR using primers complimentary to tagging sequences that add adapters necessary to generate clusters. Illumina® indexes replace the reverse primer during PCR amplification to barcode samples if several of them are pooled in one run.

Few reports exist on RVA clinical samples sequenced using RNA ScriptSeq™ by direct sequencing (after generation of a dsDNA library from RNA starting material) of RNA with random hexamers (Jere *et al.*, 2018). RNA ScriptSeq™ has been previously used in clinical samples from RVA diarrhoeic

infants down to 10^2 copies/µL of qPCR reaction (Miren Iturriza Gómara and Khuzwayo C. Jere, personal communication, 2017).

Sequence-independent amplification of rotavirus gene segments is a less time-consuming method and would allow reducing costs of RT and PCR amplification. No errors from pre-library preparation PCR would be carried over to library preparation, although errors from the library preparation PCR are still possible.

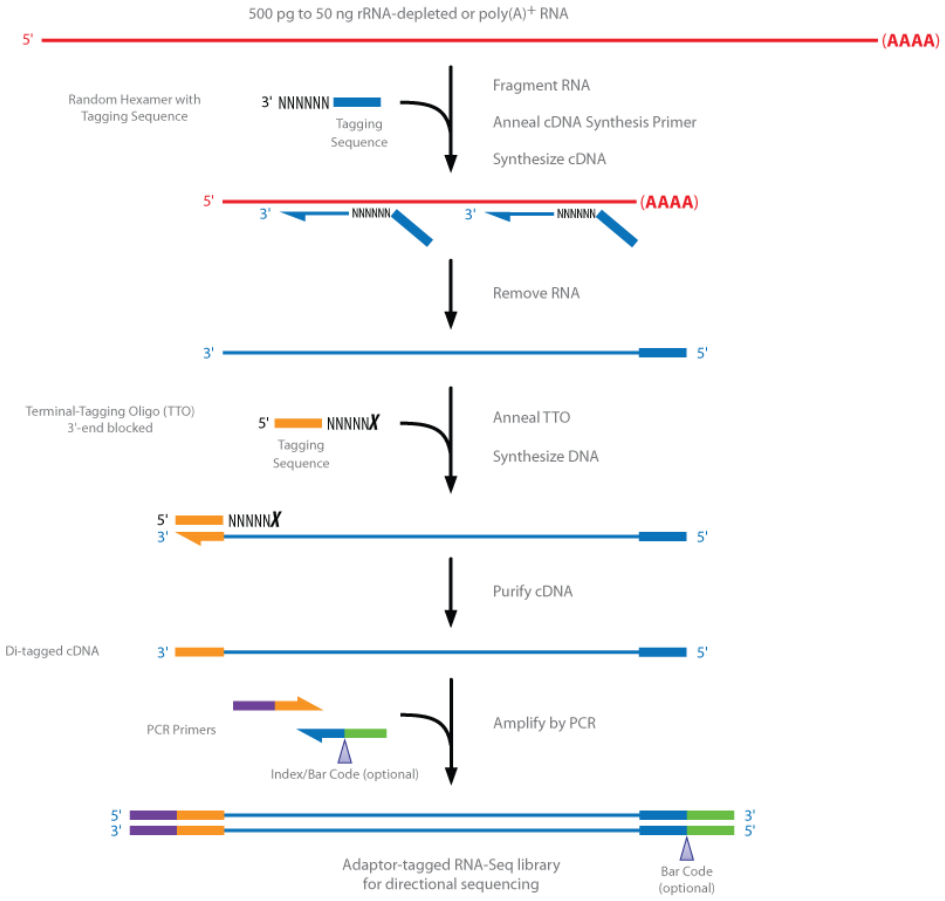

Fig. 8.2.4. An overview of the procedure for the ScriptSeq™ v2 RNA-Seq Library Preparation Kit. From the ScriptSeq™ v2 RNA-Seq Library Preparation Kit* manual (SSV21124, Epicentre®, an Illumina® company).

8.2.2.2 Experimental methodology and sample set

Vaccine material

Six independent PCV1-free Rotarix® virus harvest bulks were sequenced by sequence-dependent amplification by Dr Jane L. Mitchell. Vaccine material was

stored at -80ºC and viral RNA was extracted, reverse-transcribed, amplified and purified following the manufacturer's instructions (GSK's protocol made available to Dr Jane L. Mitchell). Library preparation using the Nextera® XT DNA kit (Chapter 2, section 2.2.6), bioinformatic analysis and further data analysis were performed by the NGS team and by Dr Jane L. Mitchell (not shown).

Six independent Rotarix® final fills were sequenced by sequence-independent amplification by Dr Jane L. Mitchell. Vaccine material was stored at 4ºC and viral RNA was extracted following the TriReagent® and chloroform method (Chapter 2, section 2.2.3.3). To prepare for library generation with the RNA ScriptSeq™ kit, extracted RNA was DNAse I-treated, purified using the Agencourt® AMPure XP system or Agencourt® RNA Clean XP system, and quantified by NSP2 cDNA synthesis (Chapter 2, section 2.2.4) and Rotarix® NSP2-specific qPCR (Chapter 2, section 2.2.5.1). Library preparation by unique terminal tagging using RNA ScriptSeq™ (see *Faecal Samples* within this section), bioinformatic analysis and further data analysis were performed by the NGS team and by Dr Jane L. Mitchell (not shown).

Faecal samples

For a sequence-independent assessment of the genetic stability of Rotarix® in vaccine recipients, faecal material from individual C in the cohort previously described was used (Chapter 2 and Appendix I). Samples were aliquoted and stored until use (Chapter 2, sections 2.1.9 and 2.2.1) and samples with sufficient surplus material in optimisations were used for this assessment. Viral nucleic acids were extracted following the methods in Chapter 2, sections 2.2.3.1 and as follows testing several methods:

Qiagen kit method. A volume of 140 µL of 10% faecal suspension (section 2.2.3.1) was used to extract total RNA following the modified QIAamp® Viral RNA Mini Kit's instructions. Wash AW1 consisted of 250 µL, followed by centrifugation at 13,200 × *g*' for 1 min. An additional DNase I treatment was performed as indicated by the manufacturer (15 min incubation at AT) after the AW1 wash. The next AW1 wash consisted again of 250 µL, followed by centrifugation at 13,200 × *g*' for 1 min. The rest of the method was performed as described by the manufacturer, eluting in a volume of 50 µL of RNAse/DNAse-free water and storing samples at -

80ºC. Quantification was performed using the Qubit® RNA High Sensitivity Assay kit following manufacturer instructions, followed by Rotarix® NSP2-specific qPCR (section 2.2.6.1).

Roche RNA kit method. A volume of 200 µL of 10% faecal suspension was used to extract total RNA using the High Pure RNA Isolation Kit, eluting in 50 µL RNAse-free water and storing samples at -80ºC. Quantification with Qubit® RNA High Sensitivity Assay kit was followed by Rotarix® NSP2-specific qPCR.

Potgieter's adapted method from faecal suspension. A volume of 200 µL of 10% faecal suspension was used to extract total RNA following a published method (Potgieter *et al.*, 2009) further adapted as described in section 2.2.1, resuspending in 50 µL of RNAse-free water and storing samples at -80ºC. Single-stranded RNA (ssRNA) and protein impurities were removed following the published method. Quantification with Qubit® RNA High Sensitivity Assay kit was followed by Rotarix® NSP2-specific qPCR.

Potgieter's adapted method from stool. This method was adapted and kindly shared by Dr Khuzwayo C. Jere at the University of Liverpool. An amount of 100 mg of faecal matter was used to extract total RNA as described in the previous paragraph but with different starting material, directly the faecal matter. Next, lithium chloride 2 M was used to precipitate ssRNA and protein impurities, incubating first for 20 min at AT followed by 16 h in an ice and water bath, at 4°C. The samples were treated with DNAse I (Sigma-Aldrich) as indicated by the manufacturer and purified using the magnetic bead Agencourt® AMPure XP system or Agencourt® RNA Clean XP system. Quantification with Qubit® RNA High Sensitivity Assay kit was followed by Rotarix® NSP2-specific qPCR.

Of the four methods tested, *Potgieter's adapted method from faecal suspension* was the optimal protocol when tested in vaccine material, spiked vaccine material and faecal material from an infant who supplied large amounts of sample, due to higher RNA yields.

To prepare for library generation with the RNA ScriptSeq™ kit, extracted RNA was cleaned from ssRNA, DNAse I-treated, purified and quantified (previous paragraphs and Chapter 2). The RNA ScriptSeq™ v2 library preparation kit was used to prepare the sequencing libraries from 500 pg to 50 ng of dsRNA extracted from faecal samples or 10% faecal suspensions and denaturing the dsRNA at 95°C

for 5 min before following the manufacturer's instructions. Library quantification was performed using Qubit® dsDNA HS Assay Kit. The size distribution was assessed on an Agilent High Sensitivity DNA chip, Agilent 2100 Bioanalyzer and Agilent 2100 Expert Software B.02.08 following the manufacturer's instructions. The libraries were sequenced on the MiSeq platform using the 2x 251 paired end v2 Flow cells. The sequence data generated was analysed by NGS team at the NIBSC. A similar workflow as the one described in the Nextera® XT DNA analysis was used to analyse the data generated with the RNA ScriptSeq™ v2 kit. The workflow used a Phred score cutoff of ≤Q30 and SNP loci were called if there was a mean coverage of aligned reads of ≥100, ≥50, ≥20 or ≥10 for each studied position at a mean frequency of ≥1%, ≥2%, ≥5% and ≥10% respectively, (frequency threshold selected dependent on read depth); and observed in ≥2 of 3 replicates. Further data analysis (Chapter 2, section 2.2.8) were performed by the NGS team and by me. Several extraction methods were tested:

University of Liverpool preliminary data: For samples of expected high shedding, Potgieter's adapted method from stool was used.

Primary preliminary data: Faecal samples from individual C, at day 7 after dose 1 (10^9 copies/mL of stool), day 7 after dose 2 (or day 38 after dose 1; 10^5 copies/mL of stool), day 7 after dose 2 diluted 1/10 (10^4 copies/mL of stool) and day 7 after dose 2 diluted 1/100 (10^3 copies/mL of stool) were extracted with the High Pure RNA Isolation Kit from Roche from faecal suspensions, the QIAamp® Viral RNA Mini Kit from Qiagen from faecal suspensions and Potgieter's adapted method from faecal suspensions and from stool (Chapter 2, section 2.2.4.3). Timepoints were tested as technical duplicates from a single faecal suspension.

Secondary preliminary data: Faecal samples from individual C, at day 7 after dose 1 (10^9 copies/mL of stool) and dilutions at different concentrations from 10^8 to 10^3 copies/mL of stool, at day 8 after dose 1 (10^9 copies/mL of stool) and at day 8 after dose 2 (or day 37 after dose 1; 10^5 copies/mL of stool) were tested in triplicate to pool plus another sample alone. They were extracted with Potgieter's adapted method from faecal suspensions (Chapter 2, section 2.2.4.3). The same was performed with the day 7 after dose 1 (10^9 copies/mL of stool) and dilutions at different concentrations from 10^8 to 10^3 copies/mL of stool tested in triplicate to pool

plus another sample alone cleaned up in parallel with the MinElute® Gel Extraction kit to identify the best purification method.

Tertiary preliminary data: Faecal sample suspensions (previous suspensions from -80°C plus suspensions made on the day) from individual C, at days 7, 8 10 and 15 after dose 1 were tested as three extractions from one single faecal suspension with Potgieter's adapted method from faecal suspensions (Chapter 2, section 2.2.4.3). Because RNA extracted from the mentioned faecal suspensions were detected in low amounts by Qubit® with respect to the fresh faecal suspensions, as well as by NSP2-specific qPCR, with 1-2 $\log_{10}$ variability (data not shown), faecal samples from all infants and several timepoints were extracted again as three extractions from one single faecal suspension, cleaned-up and quantified using the same methods as in the previous paragraphs to prepare for RNA ScriptSeq™ library generation (Table 8.2.5).

Table 8.2.5. List of individuals and timepoints prepared to test by RNA ScriptSeq™ library preparation. RNA was extracted using Potgieter's adapted method, cleaned-up with Agencourt® RNA Clean XP system and quantified by Qubit® RNA High Sensitivity Assay and Rotarix® NSP2-specific qPCR.

Individual	Time points
K	0, 1, 3, 4, 10, 33, 35, 36, 37
H	0, 3, 5, 9, 12, 31
L	15, 16, 20, 21, 34, 35, 36, 38
D	3, 6, 8, 16, 20, 36, 39
G	1, 4, 13, 30, 36, 40
J	1, 3, 9, 13, 14, 20, 24, 27, 29, 34, 36, 38, 56, 64, 67
F	4, 6, 7, 9, 14, 29, 30
C	4, 8, 10, 15, 12, 17, 20, 23, 25, 27, 30, 34, 37
I	1, 9, 11
M	1, 3, 5, 6, 8, 9, 12, 14, 18, 21, 29
B	9, 15, 19, 22, 24, 30, 32, 38, 46, 50
E	1, 3, 9, 15, 18, 21, 29, 30, 35, 37, 40

8.2.2.3 Results and short discussion

Vaccine material

Rotarix® sequencing of virus harvest bulks by sequence-dependent amplification identified 26 SNPs present at frequencies from 5% to over 60% frequency (Mitchell *et al.*, unpublished data), similarly to the original vaccine

sequence (Mitchell, Lui, *et al.*, unpublished). Most of them were identified in the viral segment encoding VP4. Rotarix® sequencing of final fills by RNA ScriptSeq™ identified a small amount of SNPs present at low frequency (<25%) (Mitchell *et al.*, unpublished data) with respect to the original vaccine sequence (Mitchell, Lui, *et al.*, unpublished). Only nucleotide position 1103 for segment 4 was detected at >50% frequency (Mitchell *et al.*, unpublished data). This mutation appeared in the original vaccine sequence at a similar frequency, detected at the NIBSC (Mitchell, Lui, *et al.*, unpublished).

Faecal samples

In this cohort, Rotarix®/rotavirus in stool of vaccinees was detected in the range of 10^3-10^9 copies/g of stool (Chapter 3), comparable to previous reports in the range of 10^2-10^{10} copies/mL of stool (Mijatovic-Rustempasic *et al.*, 2017).

University of Liverpool preliminary data: A first attempt to sequence all the viral segments was made using RNA ScriptSeq™ library preparation as sequencing strategy. When samples from this cohort were tested in parallel to clinical samples at the University of Liverpool, they were not detected by AGE and not sent for NGS (data now shown). Other attempts were performed at the NIBSC using adapted methods.

Primary preliminary data: The method that yielded consistent viral loads and samples detectable by Qubit® was Potgieter's adapted method from faecal suspensions, maintaining glycogen as a carrier (Table 8.2.6). Preliminary data for individual C, day 7 after dose 1 presented 10% mapping to Rotarix® and day 7 after dose 2 presented 2% mapping to vaccine sequence. Mean coverage was 200-400 per bp for sample from day 7 after dose 1 and lower than 100 reads per base for day 7 after dose 2. Glycogen as a carrier generated less SNPs than no carrier at all (Table 8.2.7). In total, there were eight SNPs against the reference, one synonymous and seven non-synonymous, as well as two reversions to wild type.

Secondary data: The method that yielded best results was the Agencourt® RNA Clean XP system, considering Qubit® quantification was very low for the gel extraction method. Coverage cut-offs for SNP calling of 10, 20, 50 and 100 reads were compared to the qPCR mean copies per 2 µL and it was observed that if those mean copies were below 10^2, there was less SNP calling the more stringent the

coverage cut-off was (Figure 8.2.5). Data from individual C at a cut-off of 10 reads presented SNPs for VP1, VP3, VP4, VP6, VP7, NSP1, NSP2 and NSP2 gene segments (data not shown). At a cut-off of 20 reads, data presented SNPs for VP1, VP2, VP3, VP4, VP6, VP7, NSP1, NSP2 and NSP4 segments (data not shown). At a cut-off of 50 reads, data presented SNPs for VP1, VP3, VP4, VP6, VP7, NSP1 and NSP3 segments (data not shown). At a cut-off of 100 reads, data presented SNPs for VP1, VP3, VP4 and NSP1 segments: VP4 presented five non-synonymous SNPs across the timepoints studied, four at frequencies >50% and one at a frequency lower than 30%. Three of the SNPs were previously detected in the vaccine, while two were novel in stool. Two were a mutation to wild type (one seen previously by Nextera® in vaccine material and stool from infants and the other one novel in stool and previously identified in stool by Nextera®). VP1 presented one novel synonymous SNP at a frequency lower than 70%. VP3 presented three SNPs, one at lower than 7% and two between 8 and 22%, with three amino acid changes and two to wild type, none seen before in vaccine material or stool. NSP1 presented another novel SNP at frequency lower than 20%. At less stringent cut-offs, most of the SNP loci are maintained and other ones arise. SNP loci detected in vaccine final fill material by RNA ScriptSeq™ (Mitchell *et al.*, unpublished data) that were also detected in stool of infants by the same sequencing method were in NSP2, NSP4, VP1, VP2, VP3, VP4 and VP6 (Table 8.2.8). It was decided that a copy number $\leq 10^3$ copies/2 µL qPCR reaction, which translated into $\leq 10^6$ copies/mL of stool, reduced the ability to call low frequencies of SNPs (Fig. 8.2.5).

Table 8.2.6. Optimisation of extraction methods for downstream RNA ScriptSeq™ library preparation. Extraction methods, use of carrier, timepoints of samples tested, expected viral loads, viral loads after extraction and after magnetic bead purification, as well as Qubit® dsRNA quantification are shown for individual C. VL, viral loads.

Extraction method	Carrier	Time point	Expected VL	VL after extraction	VL after AMPureXP beads purification	Qubit (ng/mL) (2uL)	Qubit original (ng/mL) (2uL)	Qubit (ng/mL) (10uL)	Qubit original (ng/mL) (10uL)
RocheRNAonly	NA	D1 day 7 (1/10)	E+009	3.46E+08	4.13E+08				
		D2 day 7 D1 day 38 (neat)	E+005	1.46E+04	1.46E+05				
QIAamp Viral RNA Mini Kit	No carrier	D1 day 7 (1/10)	E+009	5.07E+07	7.29E+07				
	AVE carrier	D1 day 7 (1/10)	E+009	9.32E+07	5.18E+07	34.2	3420		
	No carrier	D2 day 7 D1 day 38 (neat)	E+005	1.86E+04	2.23E+04				
	AVE carrier	D2 day 7 D1 day 38 (neat)	E+005	1.33E+04					
TriR/CHCl3 Potgieter's adapted method from faecal suspension	No carrier	D1 day 7 (1/10)	E+009	3.75E+09	5.88E+09			30.6	612
	Glycogen 0.05 µg/mL	D1 day 7 (1/10)	E+009	3.43E+09	6.62E+09			69.5	1390
	No carrier	D2 day 7 D1 day 38 (neat)	E+005	1.51E+05	3.39E+05				
	Glycogen 0.05 µg/mL	D2 day 7 D1 day 38 (neat)	E+005	9.97E+04	3.02E+05				
	Glycogen 0.05 µg/mL	D2 day 7 1/100 D1 day 38 (neat)	E+005	1.84E+06	4.94E+06				
TriR/CHCl3 Potgieter's adapted method from faecal matter	No carrier	D1 day 7 (1/10)	E+009	5.25E+08	3.91E+06	168	16800		
	Glycogen 0.05 µg/mL	D1 day 7 (1/10)	E+009	3.20E+09	2.38E+06	134	13400		
	No carrier	D2 day 7 D1 day 38 (neat)	E+005	2.40E+06	1.28E+09				
	Glycogen 0.05 µg/mL	D2 day 7 D1 day 38 (neat)	E+005	2.09E+06	6.92E+08				

Table 8.2.7. Single nucleotide polymorphisms detected during optimisation for downstream RNA ScriptSeq™ library preparation. Frequency of SNPs detected in stool of individual C, at day 7 after dose 1, with respect to SNPs previously detected in vaccine material. Amino acid change in bold, amino acid change to wild type in bold red, [1] mutation detected in vaccine bulks and fills (Mitchell, Lui, *et al.*, unpublished), * used in previous project (Mitchell, Lui, *et al.*, unpublished), light blue background for mutations detected in samples from other infants. aa, amino acid; NA, not applicable; nt, nucleotide.

Carrier	Segment encoding protein	Nt change (aa change)	SNP frequency in vaccine* (%)	SNP frequency in stool (%)
Glycogen 0.05 µg/mL	VP4	A1103G (K368**R**)[1]	53.9-59.3	99,40
No carrier	VP4	T499C (F167**L**)	NA	99,70
		A1088G (N363**S**)[1]	1.1-1.8	18,8
		A1103G (K368**R**)[1]	53.9-59.3	99,70
		A1162C (I388**L**)[1]	2.7-4.8	82,80
	VP3	A1000G (N334**D**)	NA	16,30
	VP1	A681C (I227I)	NA	75,90
	NSP1	G845A (C282**Y**) or (C282**H** if sequence for previous aa as in vaccine)	NA	19,30

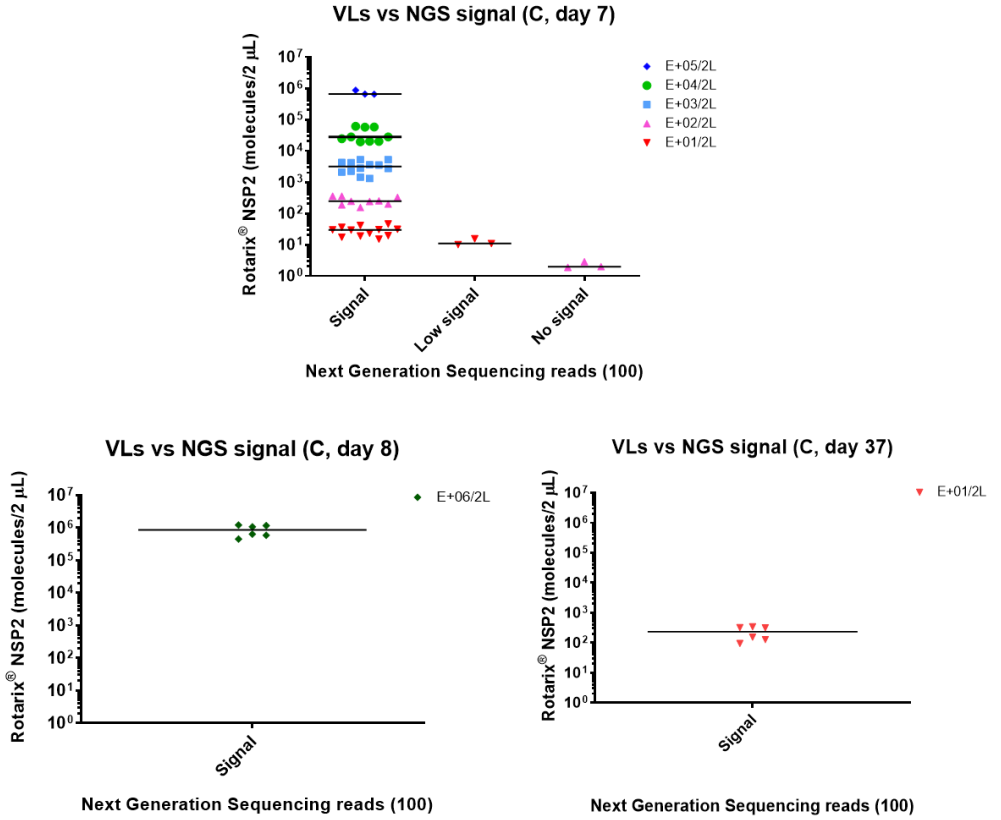

Fig. 8.2.5. Rotarix® copy number in stool of one infant (individual C) and RNA ScriptSeq™ next generation sequencing signal comparison. Rotarix® copy number is displayed on the Y axis and next generation (NGS) signal at coverage of 100 mean reads on the X axis. Top panel: Sample from an early timepoint (day 7 after dose 1) at original viral load plus a range of dilutions. Bottom left panel: Sample from an early timepoint (day 8 after dose 1). Bottom right panel: Sample from a late timepoint day 37 after dose 1).

Table 8.2.8. Single nucleotide polymorphisms detected by RNA ScriptSeq™ and Nextera® XT in vaccine material, as well as which of those were detected in stool of several infants by RNA ScriptSeq™ and Nextera® XT. Protein encoded by gene segment, nucleotide position, nucleotide change, SNPs detected by RNA ScriptSeq™ in vaccine material, which of those were detected by Nextera® XT in vaccine material, which were detected in stool of one infant (C) by RNA ScriptSeq™ and which were detected in stool of two infants (J, F) by Nextera® XT.

			RNA ScriptSeq™	Nextera® XT	RNA ScriptSeq™	Nextera® XT	
Encoded protein	**Nt position**	**Nt change**	**Vaccine material (final fills)**		**Individual C**	**Individual J**	**Individual F**
NSP1							
NSP2	108	T>C	Yes		Yes		
NSP3							
NSP4	475	T>C/A	Yes		Yes		
NSP5	447	T>C	Yes				
VP1	1106	T>C	Yes				
	1700	A>G/T	Yes		Yes		
	1767	A>G	Yes		Yes		
	2445	A>G	Yes		Yes		
	2892	T>C	Yes				
VP2	1587	A>G/T	Yes		Yes		
	2087	T>C/G	Yes		Yes		
VP3	399	T>C/G	Yes		Yes		
	1410	A>G	Yes		Yes		
	1715	G>A	Yes	Yes		Yes	Yes
VP4	754	G>A	Yes	Yes		Yes	Yes
	797	A>G	Yes	Yes		Yes	
	852	A>G	Yes				
	1090	A>G	Yes	Yes		Yes	Yes
	1103	A>G	Yes	Yes	Yes	Yes	Yes
	1153	T>C	Yes	Yes		Yes	Yes
	1409	T>C	Yes	Yes		Yes	Yes
VP6	147	A>G	Yes				
	192	T>C	Yes				
	654	G>A	Yes	Yes		Yes	Yes
	820	C>T	Yes				
	1131	T>C	Yes		Yes		
VP7	368	G>A	Yes	Yes		Yes	
	531	A>G	Yes				

Tertiary preliminary data: When two of seven plates were run, there was low frequency of successful library generation, low proportion of reads mapping to rotavirus and low sequencing depth for all the samples. A small number of samples of known high viral loads (individual C, day 8 after dose 1 repeats, with 10^9 copies/mL of stool; and individual L, day 15, with 10^8 copies/mL of stool) aligned to rotavirus, showing some level of duplication. It appeared as if other nucleic acid outcompeted or inhibited rotavirus, and/or small amounts of molecules participated in the sequencing reaction. Therefore, samples were re-cleaned with new LiCl, freshly extracted and comparable samples were used in parallel with new LiCl.

Faecal suspensions from individual C at 10 days before dose 1 were spiked with Rotarix® at 10^9 to 10^6 copies/mL of vaccine using previously used LiCl for the 10^9 copies/ml one and fresh LiCl for the rest. Read depth was too low to apply a threshold for variant calling of 100 reads. Only 0.04% of reads were assigned to viruses. No analysis of the bacterial complement was permitted to be performed by NIBSC HuMAC. The raw reads did not correlate with the number of reads mapping to the reference. The samples that were re-cleaned with LiCl, individual C day 8, individual L day 15 and individual D day 8, produced more library than the rest. It appeared there was systematic presence of bacterial ribosomal RNA outcompeting rotavirus, or a higher virus to contaminant ratio in the samples that produce informative library.

The high amounts of bacterial ssRNA with respect to dsRNA from rotavirus might have not been removed with the 2 M LiCl precipitation. The use of a bacterial ribosomal RNA removal kit, such as Ribo-Zero™, before RNA ScriptSeq™ library preparation might have contributed to obtaining cleaner rotavirus dsRNA for NGS. Due to small amounts of RNA extracted from stool, sometimes not detected by Qubit® and around the ng/µL concentration scale, far from the 1-5 µg needed for Ribo-Zero™ and just below the minimum 10^2 copies/µL of qPCR reaction needed for RNA ScriptSeq™ on clinical samples, this type of kit was not used for subsequent samples. This kit was discontinued on November the 2nd, 2018.

8.2.4 Genetic stability of faecal Rotarix® assessed by sequence-dependent vs sequence-independent methods

This preliminary data studying SNP loci in virus shed in stool of two/several vaccine recipients suggested that vaccine variants increase in frequency and that novel SNPs arise during viral replication in infants. A similar number of SNPs were called by RNA ScriptSeq™ and by Nextera® XT in vaccine material (Table 8.2.2.4) (Mitchell, Lui, *et al.*, unpublished). In stool, there were more SNPs called by Nextera® than by RNA ScriptSeq™ and those detected by RNA ScriptSeq™ were not as consistent within repeats and only identified at timepoints with very high viral loads (10^6-10^9 copies/g of stool), since other timepoints yielded very low RNA amounts mapping to RVA. The need to use a consistent method for library

preparation, the vaccine material sequencing work having been performed using Nextera® XT (Mitchell, Lui, *et al.*, unpublished), as well as the discontinuation of the RNA ScriptSeq™ enzyme were factors influencing the decision to perform RT-PCR and Nextera® XT library preparation on RNA extracted from stool.

Appendix III: Python script

In order to analyse sequencing data prepared with the Nextera® XT DNA Library Preparation kit v2 and processed by the NGS team at the NIBSC (Chapter 2, section 2.2.7.3), a Python script was set up (developed by Edward T. Mee) to sort output files by date, project, repeat, timepoint, infant and viral segment (script shown below), with the possibility of sorting by each parameter.

Input file: rota.calls.rotarix.together.may17.csv
Output file: rota.calls.rotarix.together.may17.csv_output_sorted
Python version: 2.7.15 (v2.7.15:ca079a3ea3, Apr 30 2018, 16:30:26) [MSC v.1500 64 bit (AMD64)]
Processed with: filterv5.py written by Ed Mee.
Script last modified: 24/05/2018 11:06
Processed by: lbotaspe
Processed at: 24/05/2018 14:35
Number of unique sample identifiers : 110
Parameters were:
Minimum coverage: 100
Maximum reference frequency: 0.99

****
Script:

```
#Written by ETM for LBP, May 2018

import csv
import pprint
import sys
import operator
import os
import time
import getpass

# Input files must be in csv format ['sample','chr','pos','ref','cov', 'R','A','C','G','T','pR','pA','pC','pG','pT'\]
# For .xlsx files open in Excel and save as .csv
input_file = sys.argv[1]

# could modify to automatically name the output_file with the input_file + e.g _output/
output_file = input_file+"_output"

# prompt the user to specify the desired coverage cutoff
cutoff = int(raw_input("Specify minimum coverage required:"))

#prompt the user to specify the desired reference cutoff
ref_frequency = float(raw_input("Specify maximum reference value (1 - SNP frequency):"))
```

```
# function to extract unique names to be used as the filenames for the sorted data
# based on separation of files by specific delimiter in the first column
# currently set to take the name from the first column and the second field delimited by '_'
def get_filenames(file_to_filter):
    # Open the sorted combined file
    with open (file_to_filter, 'r') as combined_file:

        csv2 = csv.reader(combined_file, delimiter = ',')
        # skip the header row
        csv2.next()

        # define new list for all (redundant) and unique names
        redundant = []
        unique = []
            # read through each line in the file
        for row in csv2:

            #define the entire first column as the sample
            sample = row[0]

            #split the sample fullname from the entry based on the delimiter '_'
            date, fullname, seqnumber, lane = sample.split('_')

            redundant.append(fullname)

        # check each entry in the redundant list....
        for entry in redundant:

            #.... against the unique list
            if entry in unique:
                #if it is already in the list then skip
                pass
            #otherwise add it to the list
            else:
                unique.append(entry)

    # return the unique list
    return unique



#function to take the final file names, open the results and write specific results to final output files.
def write_unique_to_file(unique_in):
    final_names = []
    templist = []
    for i in unique_in:

            final_names.append(i)

    # open the sorted output file
    with open (output_file+"_sorted.csv", 'r') as sorted_outfile:
            # define csv3 as the variable
            csv3 = csv.reader(sorted_outfile, delimiter=',')
```

```
        # for each row in this file
        for row in csv3:
            # add that entry to templist
            templist.append(row)

        # set counter to 0 to read through list of file names
        k = 0
        # iterate until the end of the list
        while k < len(final_names):
            # take each entry in final names
            final_name = final_names[k]

            # open a new file with a name corresponding the sample
            with open(final_name+".csv", 'wb') as final_file:

                # read in each line from the sorted_outfile / csv3 IF it contains a
string matching the final_name
                writer=csv.writer(final_file, delimiter=',', quotechar='"')
                # write the header row into the output file

writer.writerow(['sample','chr','pos','ref','cov','R','A','C','G','T','pR','pA','pC','pG','pT'])

                # set counter j to 0 to interate through the templist, i.e. all sorted
results
                j = 1
                # iterate until the end of the list
                while j < len(templist):

                    #############
                    entry = str(templist[j])
                    #print code
                    code = entry.split('_')[1]
                    #print code

                    if code == final_name:

                    # add each entry to the output file
                        writer.writerow(templist[j])
                    else:
                        pass
                    j +=1

            k += 1

#function to sort the final files by chr and position
def sort_files (input_file):

    with open (input_file+".csv", 'r') as f_in, open (input_file+"_sorted.csv", 'wb') as
f_out:

        # read in the unsorted data
        csv1 = csv.reader(f_in, delimiter=',')

        # skip the first row with the header
        csv1.next()
```

```
            #sort the remaining rows by column 3 (position)
            sort = sorted(csv1, key=lambda x: (str(x[1]), int(x[2])))

            writer=csv.writer(f_out, delimiter=',', quotechar='"')
            # write the header row into the output file

writer.writerow(['sample','chr','pos','ref','cov','R','A','C','G','T','pR','pA','pC','pG','pT'])
            # take each row in the sorted data and write it into the new file
            for row in sort:
               writer.writerow(row)

#function to write metadata including analysis paramaters to a separate file
def metafile (meta_out):

      # name the output file
      with open(meta_out+"_meta.tsv", 'w') as metadata:
            #specify the user-supplied input and output file names
         print >> metadata, "Input file: " +"\t" + input_file
         print >> metadata, "Output file: " +"\t" + output_file + "_sorted"

            #record details of the script, when it was modified, when it was run
         print >> metadata, "Python version: " +"\t" + sys.version
         print >> metadata, "Processed with: " +"\t" + os.path.basename(__file__) + "
written by Ed Mee."
         print >> metadata, "Script last modified: " +"\t" + time.strftime('%d/%m/%Y
%H:%M', time.gmtime(os.path.getmtime(__file__)))
         print >> metadata, "Processed by: " +"\t" + str(getpass.getuser())
         print >> metadata, "Processed at: " +"\t" + (time.strftime("%d/%m/%Y")
+"\t" +time.strftime("%H:%M"))

            # record the number of unique samples that were found in the input file and
the user-supplied parameters.
         print >> metadata, "Number of unique sample identifiers :" +"\t" +
str(len(file_names))
         print >> metadata, "Parameters were: \nMinimum coverage: " +"\t" +
str(cutoff) + "\nMaximum reference frequency: " +"\t" + str(ref_frequency)
         print >> metadata, "\n******************\nScript:"
         with open(__file__) as f:
               print >> metadata, '\n'.join(f.read().split('\n')[1:])

#function to delete intermediate files
def cleanup(tempfiles):

      for tempfile in tempfiles:
            os.remove(tempfile+".csv")

if __name__== '__main__':
   try:

      # open the spreadsheet with the raw data.
      with open (input_file, 'rb') as csvfile:

      # specify that the delimiter is a comman and do not treat commas inside quotes
as delimiters.
         reader = csv.reader (csvfile, delimiter = ',', quotechar = '"')
```

```
        next(reader,None)

        # Define a new array to hold the results. The header row will be same as in the input file, but can be altered if a different text is required.
        results = [['sample','chr','pos','ref','cov','R','A','C','G','T','pR','pA','pC','pG','pT']]

        # read one row at a time
        for row in reader:

            # skip any rows where the coverage is less than the user specified cutoff. Can be fixed if it will always be the same

            if int(row[4])<cutoff:
                pass

            # for all rows with coverage greater than the cutoff
            else:
                # check the pR value. If it is less than 0.99 then the result is kept
                if float(row[10])<=ref_frequency:
                    # the entire row is taken as a result
                    result = row [0:15]
                    #the row is added to the end of the results array
                    results.append(result)
                # if the pR value is > 0.99 then the row is ignored
                else:
                    pass

        # Create and open a new file with the name specified by the user
        with open (output_file+".csv", 'wb') as outfile:
            #define the new file as a csv
            writer=csv.writer(outfile, delimiter=',', quotechar='"')
            # for each row in the results array, write the row to the new file
            for r in results:
                writer.writerow(r)

        # Open the results file and create a new file with the suffix _sorted
        with open (output_file+"_sorted.csv", 'wb') as sorted_outfile, open (output_file+".csv", 'r') as unsorted:
            # read in the unsorted data
            csv1 = csv.reader(unsorted, delimiter=',')

            # skip the first row with the header
            csv1.next()
            #sort the remaining rows by column 3 (position)
            sort = sorted(csv1, key=lambda x: int(x[2]))

            writer=csv.writer(sorted_outfile, delimiter=',', quotechar='"')
            # write the header row into the output file

writer.writerow(['sample','chr','pos','ref','cov','R','A','C','G','T','pR','pA','pC','pG','pT'])
            # take each row in the sorted data and write it into the new file
            for row in sort:
                writer.writerow(row)
```

```
        #scan the sorted file to determine the unique names that will be used for the final sample files
        file_names = get_filenames(output_file+"_sorted.csv")

        # write each set of entries to a new file corresponding to the sample name
        write_unique_to_file(file_names)

        for name in file_names:
            sort_files (name)

        # call the metafile function
        metafile(output_file)

        cleanup(file_names)

    except IndexError:
        print "\n\n !! ERROR !! \nScript should contain exactly 3 arguments. \nUsage: python " + os.path.basename(__file__) + " input_file.csv output_file"

    except ValueError:
        print "\n\n !! ERROR !! \n\n Cutoff must be an integer. \n Maximum reference value must be 0 - 1"
```

Appendix VI: Sewage collection

Sewage samples from sewage plants in Beckton (London, Greater London), Dalmarnock (Glasgow, Scotland), Dunstable (Luton, Bedfordshire), Severn (Worcester) and Sheildhall (Glasgow) from before (2004/2005/2011) and after (2015/2016) the introduction of Rotarix® in the vaccination programme, were kindly provided by Dr Javier Martin and Dr Manasi Majumdar at the NIBSC (Table 8.4.1). These samples were concentrated using the two-phase separation method, following the 'Guidelines for environmental surveillance of poliovirus circulation' (WHO, 2003; Harvala *et al.*, 2014; Majumdar *et al.*, 2018). A litre of raw sewage from Roundhill (Stourbridge, UK; 16th December 2004) was kindly provided by Dr Dimitra Klapsa.

Table 8.4.1. Sewage sample collection. Samples collected in years 2004, 2005, 2011, 2015 and 2016 and several locations. *Beckton: 24h composite (1 sample every hour). All other sites: Grab (1 single take).

Sample no.	Code	Site	Date of collection
1		Dunstable (Luton, Bedfordshire)	30/09/2004
2		Dunstable	12/10/2004
3		Dunstable	07/12/2004
4		Dunstable	06/01/2005
5		Dunstable	15/02/2005
6		Dunstable	02/03/2005
7		Severn (Worcester, West Midlands)	22/01/2004
8		Severn	16/11/2004
9		Severn	11/11/2004
10		Severn	14/12/2004
11		Beckton (Docklands near London City Airport, London)*	28/01/2011
12	Env-15-001	Sheildhall (Glasgow)	21/01/2015
13	Env-15-002	Dalmarnock (Glasgow)	23/01/2015
14	Env-15-003	Sheildhall	26/02/2015
15	Env-15-004	Dalmarnock	26/02/2015
16	Env-15-008	Dalmarnock	30/04/2015
17	Env-15-009	Sheildhall	28/05/2015
18	Env-15-010	Dalmarnock	27/05/2015
19	Env-15-011	Sheildhall	24/06/2015
20	Env-15-012	Dalmarnock	26/06/2015
21	Env-15-013	Sheildhall	29/07/2015
22	Env-15-015	Sheildhall	28/08/2015
23	Env-15-018	Sheildhall	30/09/2015
24	Env-15-021	Dalmarnock	25/11/2015
25	Env-15-022	Sheildhall	25/11/2015
26	Env-16-004	Sheildhall	30/03/2016
27	Env-16-005	Dalmarnock	30/03/2016
28	Env-16-007	Dalmarnock	25/05/2016
29	Env-16-009	Dalmarnock	29/06/2016
30	Env-16-010	Beckton*	12/07/2016
31	Env-16-011	Sheildhall	27/07/2016
32	Env-16-012	Dalmarnock	27/07/2016
33	Env-16-014	Sheildhall	31/08/2016
34	Env-16-015	Dalmarnock	31/08/2016
35	Env-16-017	Dalmarnock	28/09/2016
36	Env-16-018	Beckton*	11/10/2016
37	Env-16-019	Dalmarnock	22/11/2016
38	Env-16-020	Beckton*	22/11/2016
39	Env-16-021	Dalmarnock	30/11/2016
40	Env-16-022	Beckton*	13/12/2016